PWA FR-4249
21 APRIL 1971
VOLUME III

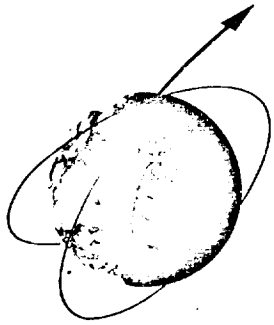

Space Shuttle Main Engine Definition (Phase B)

ENGINE DESIGN DEFINITION REPORT

VOLUME III

COMBUSTION DEVICES

MSFC-DRL-163, ITEM 30
DRD SE-275

Prepared Under Contract NAS8-26186 for
National Aeronautics and Space Administration
George C. Marshall Space Flight Center
Marshall Space Flight Center, Alabama 35812

Pratt & Whitney Aircraft DIVISION OF UNITED AIRCRAFT CORPORATION
FLORIDA RESEARCH AND DEVELOPMENT CENTER
BOX 2691, WEST PALM BEACH, FLORIDA 33402

12

Printed in the United States of America

CONTENTS

SECTION		PAGE
	INTRODUCTION	vii
I	MODULAR ENGINE POWERHEAD	I-1
	A. Introduction	I-1
	B. Description - Spherical Main Case Basic Engine Structure	I-1
II	PREBURNER INJECTOR	II-1
	A. Introduction	II-1
	B. Description	II-1
	1. Function	II-1
	2. Location	II-1
	3. Mechanical Description	II-1
	C. Requirements	II-12
	D. Substantiation	II-20
III	ENGINE MAIN CASE ASSEMBLY	III-1
	A. Main Case	III-1
	1. Introduction	III-1
	2. Description	III-2
	3. Requirements	III-11
	4. Substantiation	III-12
	5. Capability	III-12
	B. Main Case Centerbody Duct	III-13
	1. Introduction	III-13
	2. Description	III-14
	3. Design Requirements	III-17
	4. Capability	III-18
	5. Substantiation	III-18
	C. Preburner Combustion Chamber	III-20
	1. Introduction	III-20
	2. Description	III-20
	3. Requirements	III-29
	4. Capability	III-30
IV	MAIN CHAMBER INJECTOR	IV-1
	A. Introduction	IV-1
	B. Mechanical Description	IV-2
	1. Function	IV-2
	2. Configuration	IV-2
	C. Design Requirements	IV-15
	D. Capabilities	IV-18

CONTENTS (Continued)

SECTION			PAGE
	E.	Design Substantiation	IV-19
		1. Oxidizer Injection Elements	IV-19
		2. Injector Pattern	IV-22
		3. Spraybar Concept	IV-22
		4. Fuel Faceplate	IV-24
		5. Conical Face for Combustion Stability	IV-25
V	MAIN CHAMBER		V-1
	A.	Introduction	V-1
	B.	Description	V-1
		1. Transpiration Cooled Liner	V-1
		2. Outer Case	V-17
	C.	Requirements	V-20
	D.	Capability	V-23
		1. Transpiration Cooled Chamber	V-23
		2. Outer Case	V-24
	E.	Substantiation	V-24
		1. Transpiration- Cooled Liner	V-24
		2. Outer Case	V-32
		3. Coolant Distribution	V-32
		4. Impulse Comparison Testing	V-32
VI	TORCH IGNITERS		VI-1
	A.	Introduction	VI-1
	B.	Description	VI-1
	C.	Requirements	VI-6
	D.	Design Capability	VI-9
	E.	Design Substantiation	VI-10
VII	NOZZLES		VII-1
	A.	Nozzle Contour Design	VII-1
		1. Introduction	VII-1
		2. Description	VII-1
		3. Requirements	VII-5
		4. Design Substantiation	VII-5
		5. Design Capability	VII-5
	B.	Primary Nozzle	VII-5
		1. Introduction	VII-5
		2. Description	VII-6
		3. Requirements	VII-15
		4. Capability	VII-17
		5. Design Substantiation	VII-20

CONTENTS (Continued)

SECTION		PAGE
VIII	EXTENDIBLE NOZZLE	VIII-1
	A. Introduction	VIII-1
	B. Description	VIII-1
	1. Structural Analysis	VIII-11
	C. Requirements/Compliance	VIII-15
	D. Capability	VIII-18
	E. Substantiation	VIII-19
	1. Test Programs	VIII-19
	2. Fabrication Programs	VIII-22
	3. Extendible Nozzle Detail Parts Testing	VIII-23
IX	COMBUSTION STABILITY	IX-1

INTRODUCTION

The P&WA SSME combustion system design is based on components with demonstrated high performance to provide low development risk. These designs are the result of high pressure combustion and cooling experience involving over 300 tests and 23 injector configurations that have produced configurations with a specific impulse that exceeds the SSME requirements by 5 seconds.

The plug-in spherical engine main case with a single preburner provides a compact efficient structure which eliminates high pressure, external hot gas ducting. In addition, it provides a 24-inch long combustion gas path from the injector through a centerbody to the turbine inlets for complete mixing and uniform turbine inlet temperature. Both turbopump turbines discharge into the main case sphere at the same mixture ratio and flow through the main chamber injector for injection into the main chamber. Twenty-eight tests of the 250K, XLR129 powerhead engine main case have been conducted to date confirming design techniques. These tests were conducted with a preburner and fuel turbopump, for hot turbine verification testing and with the main chamber for impulse performance testing.

A fixed area preburner injector provides a uniform temperature profile and throttleability with stable combustion. This is achieved by the use of dual orifice self-atomizing liquid oxygen injection elements and a closely coupled preburner oxidizer valve ensuring good starting and shutdown characteristics.

A radial spraybar main chamber injector with a high element density of self-atomizing liquid oxygen injection elements is mechanically simple, lightweight, and provides high performance. Extensive testing since 1966 at the 10K, 50K, and 250K thrust sizes has demonstrated the durability and very high performance of this main chamber injector configuration.

Although instability problems are not expected, chamber wall absorption has been incorporated into both the preburner and main chamber design. The chambers will have the capability of easily incorporating additional damping if required.

A transpiration cooled main chamber provides safety and long life while meeting the specification performance with margin. During Phase B testing, the performance of a regeneratively cooled chamber is being evaluated. This testing will enable a factual trade decision to be made between the basic high performance of regenerative cooling and the ability to optimize nozzle combustion for high durability, and forgiveness of the transpiration cooled chamber.

Regeneratively cooled primary orbiter and booster nozzles provide low development risk. The designs are based upon proven design and fabrication techniques.

A dump-cooled, corrugated skin, two-position nozzle will provide low weight, long life and mechanical simplicity. Light weight is achieved by the use of low pressure coolant and simple gather forming construction. Fabrication techniques have been developed. Cooling has been demonstrated during RL10 chamber firings with a dump-cooled nozzle extension.

The P&WA SSME combustion system incorporated combustion component concepts evolved and developed during high chamber pressure 5K, 10K, 50K and 250K thrust chamber and engine test programs. This unique experience has been incorporated in analytical and design techniques that are the basis for the SSME, figure 1. The use of thoroughly tested hardware concepts in the SSME design will provide a low risk program that meets performance cost, and schedule requirements.

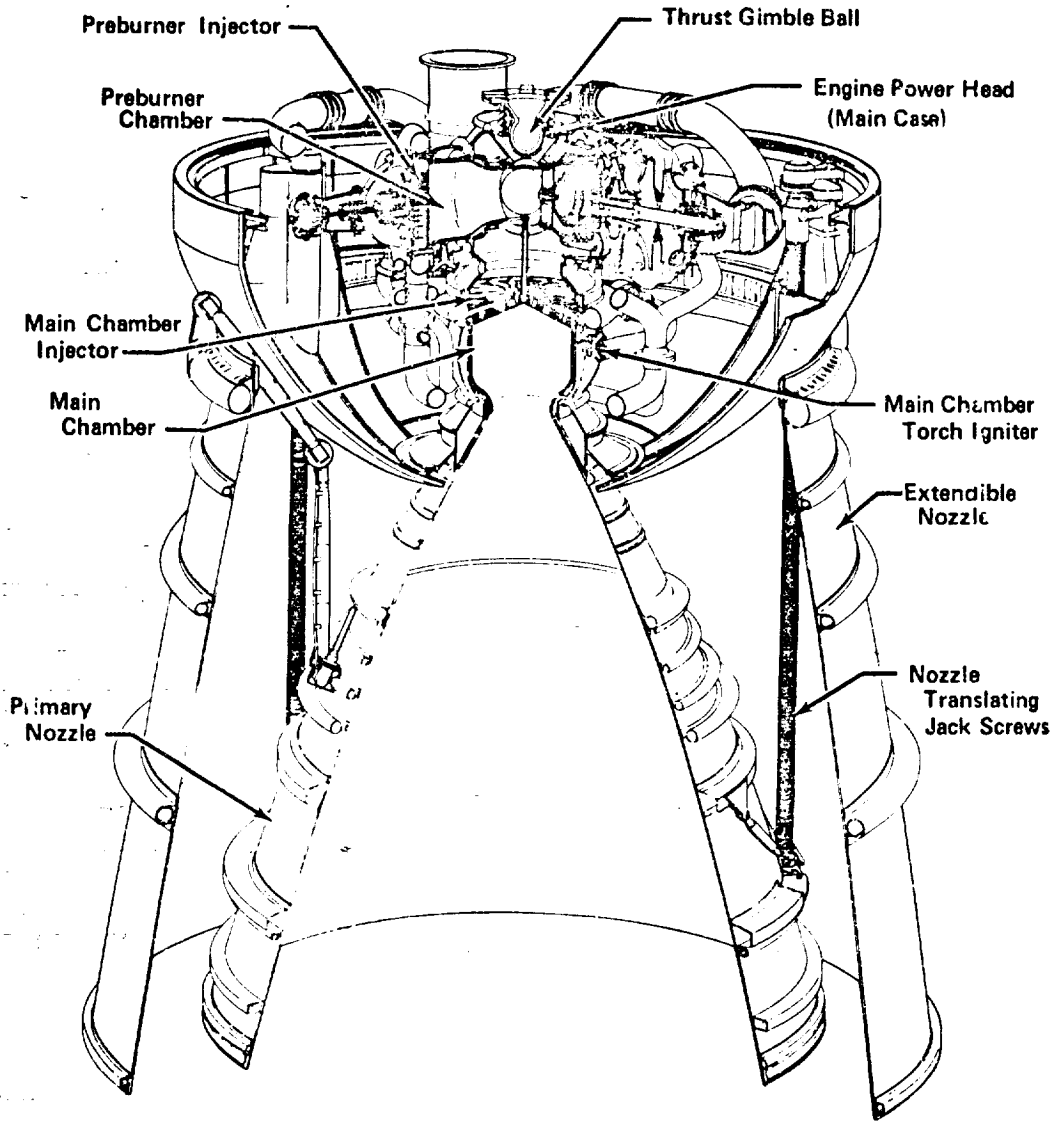

Figure 1. Pratt & Whitney Aircraft Space Shuttle Main Engine FD 52678

SECTION I
MODULAR ENGINE POWERHEAD

A. INTRODUCTION

The plug-in components, spherical main case concept for the single-preburner cycle engine provides the best arrangement and minimum weight for the SSME engine powerhead. It eliminates hot, high pressure, external ducting. It provides a single long combustion gas path through a centerbody to the turbine inlets. With internal ducting and plug-in components, the engine external arrangement is simplified and exceptional maintainability is provided. The entire spherical plug-in concept has been successfully demonstrated during more than 26 tests confirming design techniques. This demonstrated lowest risk design will meet the cost and time schedules of the SSME program. The spherical powerhead concept is shown in figure I-1.

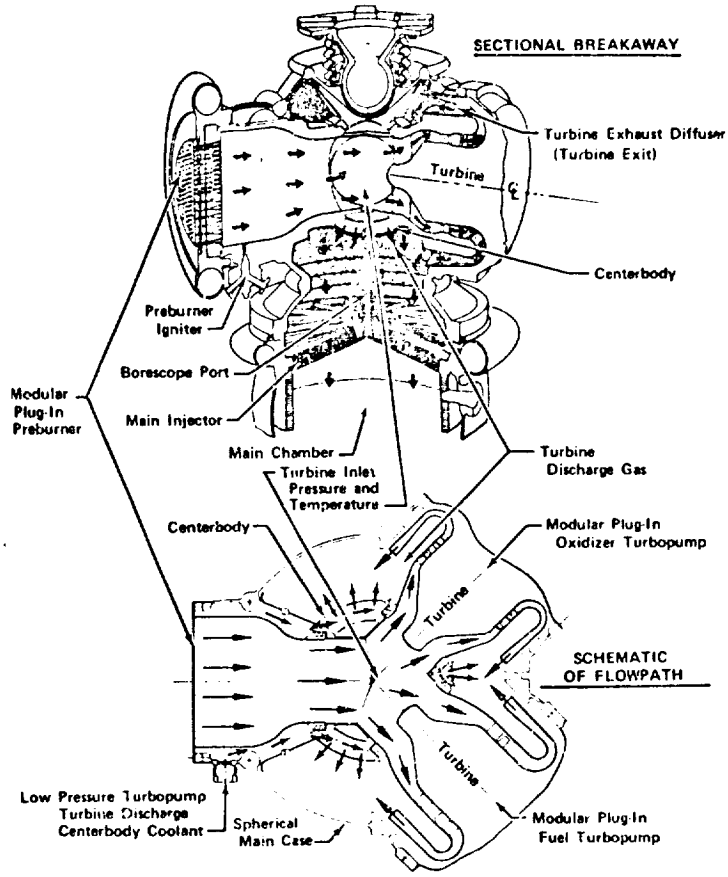

Figure I-1. Spherical Plug-In Main Case Design Eliminates External Hot Gas Ducts FD 52201

B. DESCRIPTION - SPHERICAL MAIN CASE BASIC ENGINE STRUCTURE

A spherical plug-in main case provides the basic engine structure. The gimbal, which transmits engine thrust, is contained in the main case. The requirements for bracketry to mount the high pressure turbopumps and the preburner are eliminated. External ducting is avoided by employing short

internal ducts. The preburner chamber and turbopump turbine inlets plug into a centerbody supported in the center of the main case. The preburner hot gases for turbine power flow directly through the centerbody to the pump turbine inlets, then is turned back into the main case outside the centerbody. Structural requirements are reduced on the preburner and turbine inlet hot gas ducting because the pressure differential across them is only the pressure differential through the turbine and not the differential to ambient. Turbine exhaust gases exit the main case at its base into the main chamber injector and main chamber.

All ducting is an integral part of the individual components, creating a compact duct system easy to maintain. These ducts have flow path heat shielding to reduce the temperature gradients in the cooled hot gas duct walls and the ends are free to slide with the dual piston ring seal for the differential coefficient of thermal expansion. The main case inner walls are shielded and cooled with a transpiration-cooled liner to allow higher working stresses for light weight and improved thermal compatibility between the case and the modular components.

- INTERSECTING SPHERES PROVIDE LIGHTWEIGHT MAIN CASE STRUCTURE

An intersecting sphere main case design was selected because of its structural efficiency as a pressure vessel and because the intersection planes are circular, minimizing stress discontinuities and providing for low-cost fabrication. Stiffening rings are provided at the sphere intersections to carry the shell load of the material that was removed. The deflections of the rings are matched to the free sphere deflection to minimize bending stresses and reduce the stresses to tangential tension loads.

- INTERNAL HOT GAS DUCTS ARE SIMPLE LIGHTWEIGHT CONFIGURATION

Internal ducts are better than external ducts because they eliminate major problems associated with thermal and dynamic growths experienced with external ducts. The use of slip joints with piston rings at the centerbody joints in the powerhead concept, allows the ducts room to grow due to high pressure and thermal growths without generating large loads. The powerhead configuration with the internal ducting is lighter and safer because the ducts carry only the pressure differential between turbine inlet and low pressure turbopump turbine discharge pressures, while external ducts must carry the total turbine inlet pressure. The internal ducts carry 35% to 40% of the differential pressure that the external ducts must carry, or 2100 versus 5500 psi. With internal joints, 2100°R leakage can be tolerated without hazard and there is no performance loss because the leakage still goes through the main chamber injector. Engine external leaks present hazards especially on hot high pressure lines and internal ducts provide for fewer external joints than required for other configurations. Lower risk and safety are additionally enhanced because a failure of any internal duct is contained within the powerhead and will result in a failsafe engine shutdown.

- SPHERICAL MAIN CASE PROVIDES COMPACT PACKAGING FOR SINGLE PREBURNER

The spherical powerhead permits easy incorporation of a single preburner and results in a longer combustion gas path to the turbine inlets. This is a positive factor in providing a good temperature profile at the turbine inlets. The single preburner requires less plumbing and associated hardware, and elimination of hot external ducting greatly simplifies the engine external arrangement. A fixed split from the preburner to the two main pump turbines is a natural benefit from using the single preburner. The turbulent turning of the hot gases in the centerbody provides added preburner flowpath mixing and lowers the temperature profile of the gases prior to entering the turbine inlet bullets. The centerbody outer surface provides an ideal location for reinjecting the low pressure pump turbine exhaust gases without disrupting the mass profile to the main chamber injector. A borescope hole on the bottom of the centerbody allows inspection of the preburner injector and parts in the hot gas flowpath without engine disassembly.

- SPHERICAL MAIN CASE PROVIDES ADEQUATE SPACE FOR FULL ANNULAR DIFFUSER AT TURBINE DISCHARGE

The spherical powerhead concept, in addition to affording structural, maintainability, and safety advantages, offers distinct flow system advantages. This concept allows space for each of the main pump turbines to have an efficient full annular diffuser for recovering static pressure from the turbine discharges. This space also forms an excellent plenum-mixing chamber where the main pump turbine exhaust gases and the low pressure pump turbine exhaust gases from the centerbody can be mixed by the swirling turbine discharges. Between this mixing chamber (main sphere area) and the main chamber injector, the main case has a local constriction that further enhances mixing of the gases prior to flowing through the main chamber injector. The hot gas flow system performance and pressure losses have been thoroughly analyzed during design and have been confirmed by extensively testing the XLR129 powerhead by water flow model tests for distortion and pressure loss measurements.

- MODULAR PLUG-IN ENGINE POWERHEAD CONFIGURATION CONFIRMED BY EXTENSIVE TESTING

Twenty-six tests of the XLR129 lightweight, spherical main case and of the plug-in components shown in figures I-2 and I-3 have confirmed the design techniques used for the SSME's powerhead design. These tests were run as a part of the XLR129 Reusable Rocket Engine Program at high chamber pressure with the preburner and spherical main case hot gas system to confirm their design, and with the preburner providing the hot combustion gases to drive the high pressure fuel turbopump mounted in the main case as shown in figures I-4 and I-5. The preburner and main case are currently being tested with a main chamber and nozzle during the Phase B stage combustion test program, graphic representation of which is shown in figures I-6 and I-7.

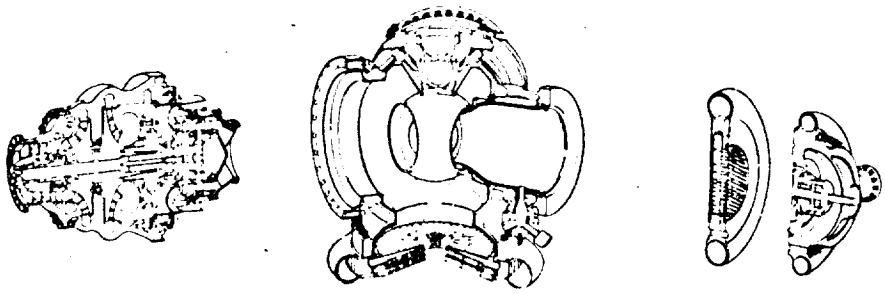

Figure I-2. Plug-In Concept FD 33179A

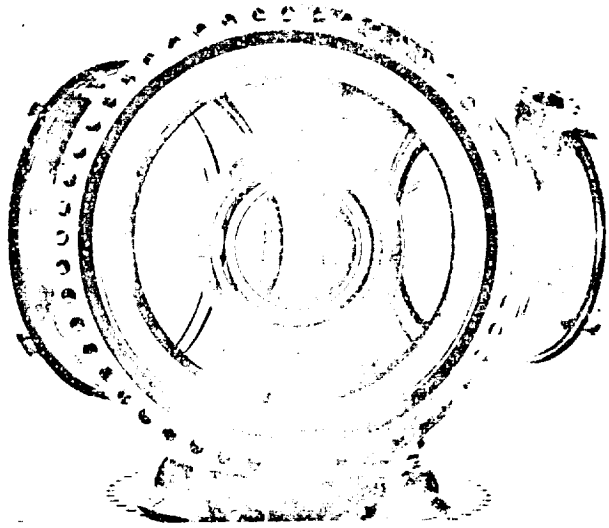

Figure I-3. Main Case With Cooling Liner and Centerbody Installed FD 42899

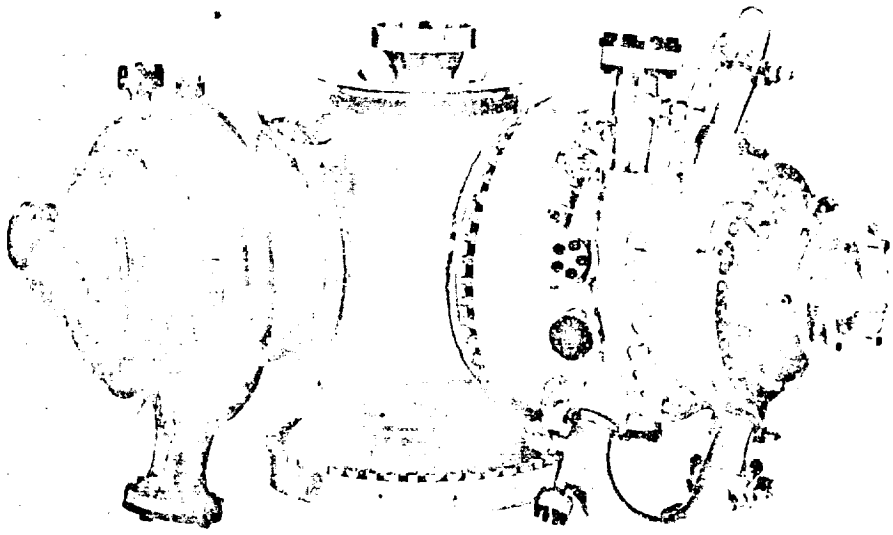

Figure I-4. XLR129 Main Case With Preburner and Fuel Turbopump Installed KFE 101219

Figure I-5. XLR129 Powerhead With Back-Pressure Plate Installed for Hot Turbine Fuel Turbopump Testing FE 99485

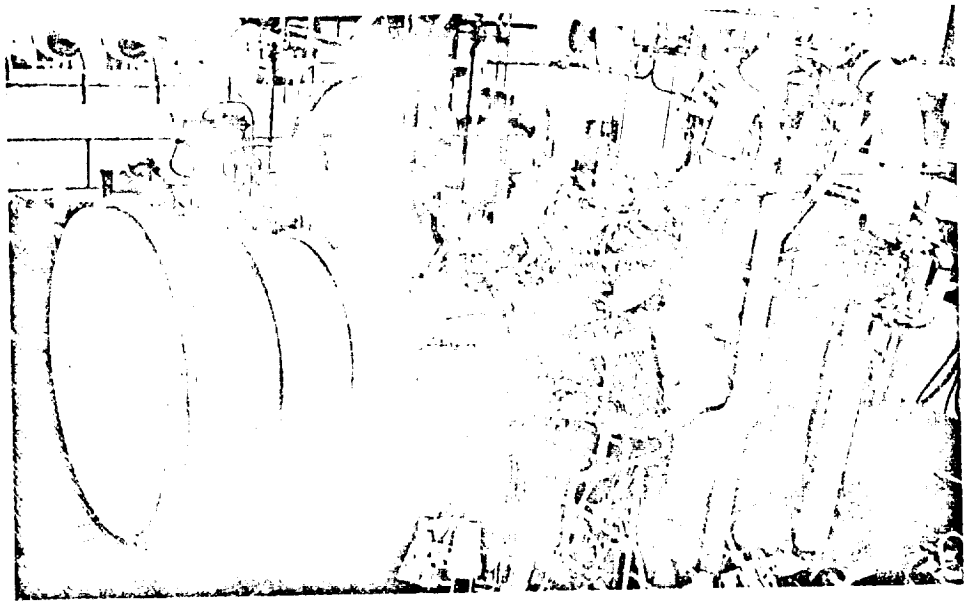

Figure I-6. Main Chamber and Nozzle With XLR129 Engine Main Case and Preburner Mounted in Test Stand for Impulse Performance Testing FE 106120

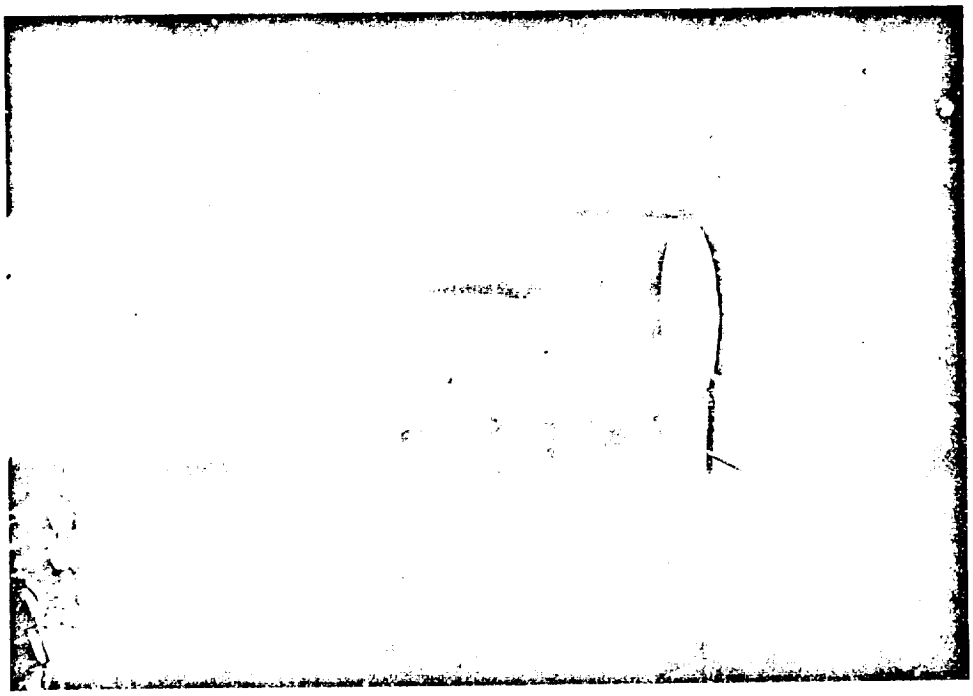

Figure I-7. Phase B 250K Stage Combustion Firing, XLR129 Powerhead Combustion System FE 106251-3

SECTION II
PREBURNER INJECTOR

A. INTRODUCTION

A fixed-area preburner injector has been selected for the SSME design. Eighty-eight hot firings using three generations of high pressure 250K preburner injectors has resulted in the development of a fixed-area preburner injector with good combustion temperature profile, stable combustion, and throttleability in excess of SSME requirements.

Two basic design features, which are the primary reasons for the successful performance of the fixed-area preburner injector are: (1) the injector uses self-atomizing dual orifice injector elements to provide very fine atomization of the liquid oxygen over the starting and operating range; (2) close-coupling of the oxidizer valve to the injector reduces the liquid oxygen volumes downstream of the shutoff valve to a minimum for good starting and shutdown characteristics.

B. DESCRIPTION

1. Function - THE PREBURNER INJECTOR IS BASIC BUILDING BLOCK OF ENGINE POWER SYSTEM

The preburner injector injects most of the engine fuel with sufficient liquid oxygen to provide the hot working fluid for driving the fuel and oxidizer high pressure turbopumps. Liquid oxygen and hydrogen are pumped to the preburner injector and controlled to the combustion temperature required by the engine cycle. Propellants are ignited by a spark-ignited torch igniter and burned in the preburner chamber duct. The hot gases resulting from this combustion are divided in a centerbody duct and directed to the two high pressure turbopump turbines. The turbopump turbines discharge into the common collection volume of the main case where the hot gases flow to the main chamber injector and are injected into the main chamber for combustion with the remainder of the liquid oxygen.

2. Location - PLUG-IN PREBURNER PROVIDES COMPACT POWERHEAD WITH MAINTENANCE ACCESSIBILITY

The injector is located between the preburner oxidizer valve and the preburner chamber segment of the main case. The centerline of the injector is perpendicular to the engine thrust axis, with the centerline lying on a common plane with that of the oxidizer and fuel turbopumps. This configuration allows ease of maintenance access and a compact package.

3. Mechanical Description - SSME PREBURNER INJECTOR IS A SCALED, DEMONSTRATED DESIGN

The preburner injector design for the SSME is based on a scaled design of the demonstrated 250K XLR129 perburner injector shown in figure II-1. Dual-orifice, tangential slot swirl injection elements with concentric fuel injection are used. Figure II-2 shows a cross-section of the SSME injector

design and details of the injection elements. The following description is numerically keyed to identify injector features:

Fuel is supplied to the circular fuel manifold (1) by the fuel system. The fuel flows through slots between bolt holes in the injector housing (2) into the manifold cavity (3) behind the faceplate (4), and is metered into the combustion chamber through concentric annuli (5), around each oxidizer element. A seal (6) is used between the faceplate and the preburner injector housing (7) to minimize fuel flow leakage between the faceplate and the housing. Liquid oxygen is supplied to the injector from the preburner oxidizer valve, which has flow provisions to deliver oxidizer to the primary (8) and secondary (9) manifolds. Oxidizer flow is injected into the combustion chamber through individual slot swirler elements (10). Each element has flow entries machined tengentially to the inner diameter of the tube; rectangular slots for the secondary flow (11) and circular holes for the primary flow (12). The element length is influenced by the heights of the fuel manifold (3), primary oxidizer manifold (8), and secondary oxidizer manifold (9), these heights are kept to a minimum consistent with low distribution losses and structural requirements. The turbine inlet temperature profile design goal for this preburner combustion system is 120 deg maximum.

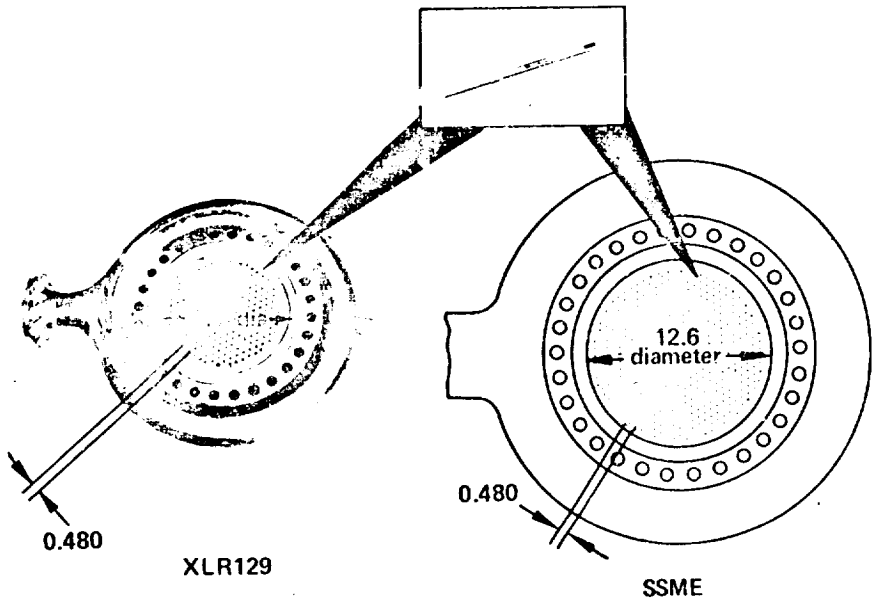

Figure II-1. SSME Preburner Injector Based on Demonstrated Technology FD 42229C

- DUAL-ORIFICE SLOT SWIRLER INJECTION ELEMENTS PROVIDES FINE ATOMIZATION FOR ENGINE OPERATION AND STARTING

Using the dual-orifice principle applied to the tangential swirl elements, a two-stage feature is achieved that allows mass flow to be varied maintaining high injection differential pressures with a reduced injection pressure penalty at a high flow condition. Because the liquid oxygen is essentially incompressible, the mass flow through a single orifice injection element varies directly as the square root of the pressure drop. A two-fold increase in flow would require a four-fold increase in the injection ΔP. Use of the dual-stage design

allows the maximum injection ΔP to be reduced to lower levels than possible with a single-orifice by changing the flow split over the throttling range. A momentum interchange occurs in the injection element tube between the high velocity flow from the small primary orifice slots to the lower velocity flow of the larger secondary orifice slots to provide for good atomization and stability throughout the start transient and throttling range.

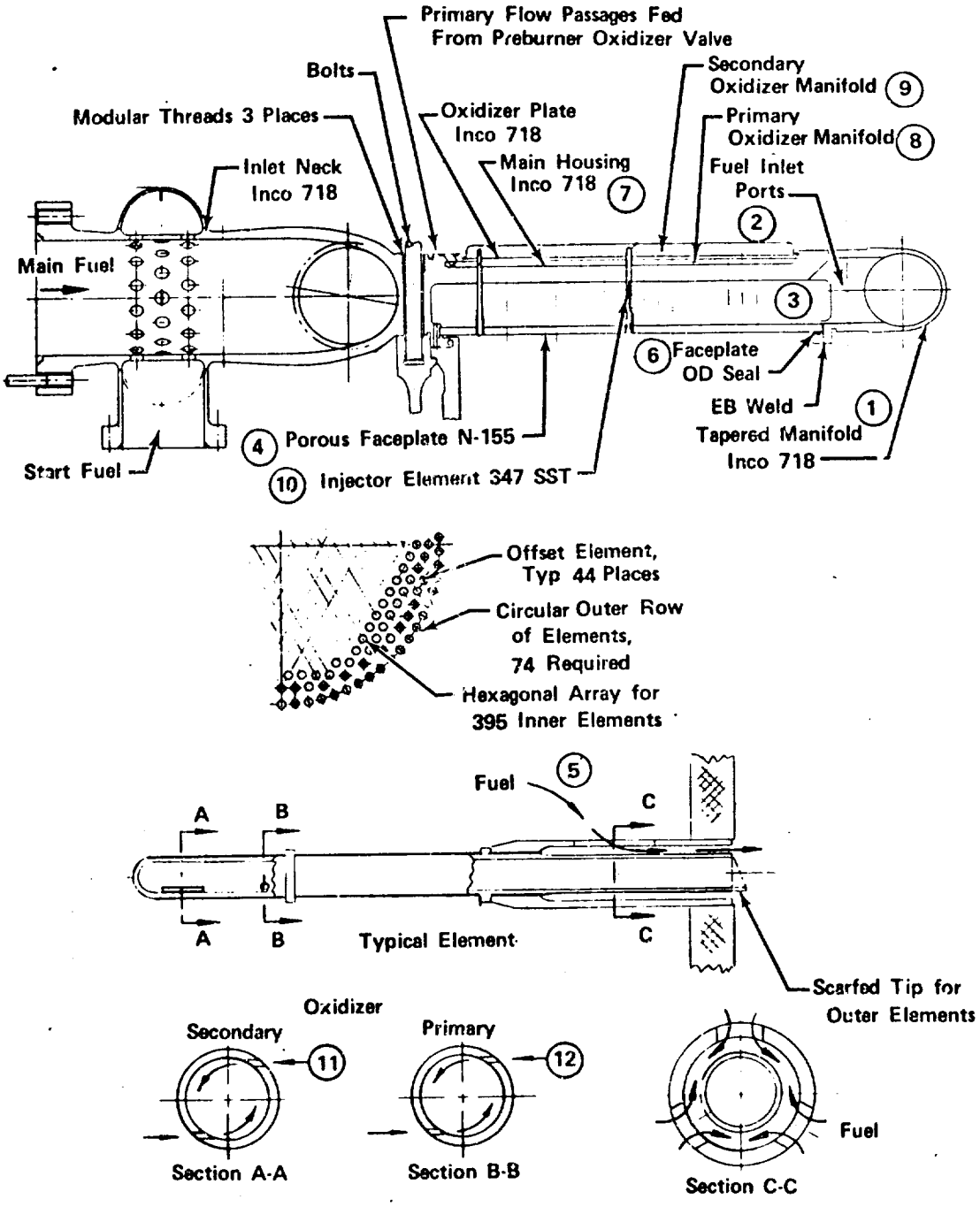

Figure II-2. Slot Swirler Elements Provide Self-Atomization of Liquid Oxygen Over Engine Operating Range

FD 46206

The oxidizer elements which are mechanically simple and durable are fabricated from drawn AISI 347 stainless steel (AMS 5571) tubing having an inside diameter of 0.1246 in. with flow entries electrodischarged-machined tangentially to the tube inner diameter. The primary entries are two 0.0158-in. diameter holes and the secondary entries are two rectangular slots 0.1675 in. by 0.0222 in. Counter-clockwise swirl (as viewed from upstream) is induced by the tangential entry slots. Each element has an integral collar that rests against the injector housing oxidizer element support plate for positioning prior to brazing the elements into the housing. The outer injector elements feature tips scarfed at 45 deg, located 0.7 in. from the preburner chamber wall in an enclosing circular array, to give uniform heat patterns adjacent to the preburner wall. The preburner injector incorporates 513 oxidizer elements arranged in a hexagonal pattern as shown in figure II-2.

The injector housing element support plate (7), figure II-2, extends across the injector and serves as the main structural diaphragm separating the fuel and oxidizer in the injector. A second relatively thin oxidizer plate separates the primary oxidizer manifold (8), figure II-2, from the secondary oxidizer manifold. Ten passages 0.415 in. in diameter are provided through the injector housing to provide the primary oxidizer flow from the preburner oxidizer valve to the primary oxidizer manifold area. The primary oxidizer manifold volume is 36.6 in.^{3}. The secondary oxidizer volume formed when the preburner oxidizer valve mates with the injector is 60.3 in.^{3}. These oxidizer manifolds are sized to minimize oxidizer distribution losses into the primary element manifold. The manifold area is 7.95 which results in a distribution velocity of only 6.5 ft/sec and negligible pressure loss. The total distribution losses from the preburner oxidizer valve to the element primary orifices is 1.35% of the available injection differential. This low distribution loss, along with the individual water flow calibration of the elements, ensures uniform injection and good temperature profile.

The oxidizer secondary manifold volume is minimized for low frequency stability consideration while maintaining uniform flow distribution. The maximum radial distribution pressure differential in the manifold is 8.3% of the injection differential pressure.

The injector faceplate causes the fuel to be distributed under the face for concentric injection around each of the liquid oxygen injection elements. The injector faceplate is supported from the oxidizer elements by sleeves located concentrically around each element. These sleeves are positioned by a shoulder on the injector element and are gold-nickel brazed to the element and silver brazed to the faceplate in accordance with PWA Specification No. 84.

Each sleeve has three openings with four times the exit area to allow fuel to be introduced around each oxidizer element, as shown in figure II-2. These openings are located behind the faceplate to allow flow disturbance attenuation in the concentric fuel injection annulus by the time the fuel reaches the faceplate surface. This design eliminates flow-disturbing tube support tangs as used on the XLR129 preburner injector. These openings also provide a stronger oxidizer element-to-faceplate attachment. The injection element-to-fuel sleeve tip concentricity due to operating loads is designed to be held with 0.002 in. The faceplate is also supported by a circumferential ring welded to the housing, which carries the faceplate load and permits the faceplate to grow, thereby accommodating differential thermal shrinkage between the housing and the faceplate. An O-ring seal is provided between the outer circumference

support and the faceplate to prevent end-around faceplate leakage. The seal is fabricated from AMS 7325 material and is silver plated for wear.

- POROUS FACEPLATE PROVIDES POSITIVE COOLING AND LONG LIFE

The porous preburner injector faceplate is fabricated from a woven and sintered wire mesh of N-155 material. The design porosity is 40 scfm/ft^2 (air) at a pressure differential of 2 psi at ambient pressure and temperature. The faceplate, with fuel sleeves, contains the fixed area fuel annuli which provides a fuel injection area of 6.525 in.^{2}. The faceplate and sleeves together create a 385 psi fuel pressure drop at an engine mixture ratio of 6.5 at 100% thrust. The calculated faceplate thermal gradient is 100°R, which allows the faceplate to easily meet the 400-thermal cycle life requirement. This thermal gradient is maintained low by flowing sufficient fuel to float the combustion process off the face of the injector and limit the thermal heat load into the injector face.

- TAPERED LIGHTWEIGHT FUEL MANIFOLD PROVIDES GOOD FLOW DISTRIBUTION

The main fuel supply passes through the fuel shutoff valve and directly enters the 4.6-in. diameter inlet neck. Immediately downstream within the inlet neck, another manifold with a 3.2 in. inlet diameter is provided for a warm gaseous hydrogen engine starting flow.

The inlet flange/neck transition section of Inconel 718 material is contoured for good flow distribution into the toroidal manifold. It is welded to the Inconel 718 manifold and the transition section uses structural design criteria, based upon geometry-test correlations established from FMDL Report 15153 (presented in the Preburner Injector Design Criteria, PWA FR-4456), in conjunction with the SSME Structural Design Criteria PWA FR-4449.

The toroidal manifold features circular cross sections that taper from a 3.840-in. diameter theoretical at the inlet to a 2.590-in. minimum diameter 180 deg around the injector. Tapering the manifold saves weight and by maintaining relatively constant velocity is compatible with attaining good fuel distribution for entry into the fuel plenum behind the faceplate.

XLR129 250K preburner injector testing showed that the fuel manifold system required additional pressure loss in the manifold feed ports to prevent flow channeling, which resulted in maldistribution of fuel behind the faceplate at low thrust (20%). In the SSME design, pressure losses have been reallocated to improve fuel distribution. Ten percent of the injector overall pressure drop has been incorporated into the feed ports connecting the manifold torous to the plenum behind the faceplate. Additionally, the manifold is tapered to maintain a more uniform velocity and therefore an even static pressure circumferentially. The velocities under the injector face in the fuel plenum are very low with only a 1% of fuel injectorΔP difference radially. Because fuel injection sleeves are matched to oxidizer elements by individual water flow tests prior to injector assembly, uniform fuel distribution at the injector face will result in a uniform injected mixture ratio across the injector face. Figure II-3 presents a summation of fuel distribution pressure losses at the design point.

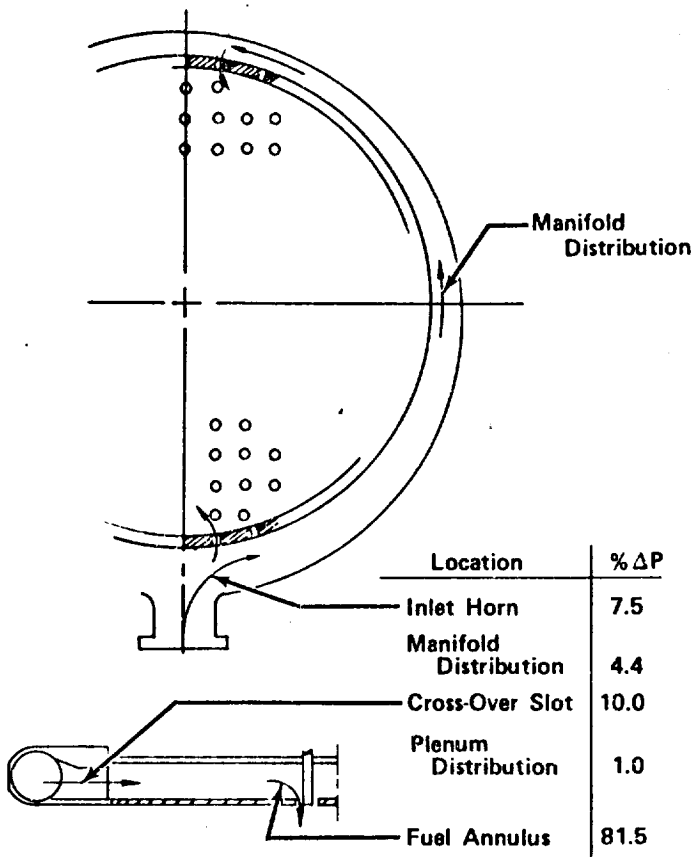

Figure II-3. Preburner Fuel Distribution FD 52665

- FLOW PASSAGES BETWEEN BOLTS PROVIDE LIGHT-WEIGHT DESIGN

The toroidal manifold is welded to the Inconel 718 housing. Fuel from this manifold flows into the plenum through 40 ports spaced between the bolts that are used to retain the injector between the preburner oxidizer valve and the main case. Forty holes 0.100 in. in diameter are located in the housing preburner pilot ring. These holes provide 1.4 lb/sec coolant flow to the preburner combustion duct.

- GOOD ATOMIZATION AND LONG MIXING LENGTH ASSURES GOOD COMBUSTION TEMPERATURE PROFILE

Because of the excellent self-atomization feature of the liquid oxygen injection elements, the fuel injection momentum is less critical than for conventional elements and a good temperature profile can be achieved using a fixed-fuel area. The fuel-to-oxidizer momentum ratio is, however, designed to be above 4 over the engine operating range to enhance mixing and combustion stability. The engine cycle provides fuel to the preburner injector at 70°R to 136°R over the engine's operating range. Engine weight and system pressure drop are saved by not routing the engine main fuel flow through the engine's regeneratively cooled nozzle. Because of the low hydrogen temperature, achieving a good temperature profile in a short combustion chamber length would have been of concern. However, because of the excellent atomization of the liquid oxygen elements and the long preburner combustion and mixing

length of the turbine inlets (in excess of 20 in.), a good combustion temperature profile is ensured at the turbine inlets.

- LOW PREBURNER COMBUSTION CHAMBER VELOCITIES AND GOOD INJECTION MOMENTUM PROVIDES STABLE COMBUSTION

Studies conducted under Contract NAS8-11024, "Investigation of Combustion Instability with Liquid Oxygen and Liquid or Cold Gaseous Hydrogen Propellant" have demonstrated that at high contraction ratios (i.e., low chamber velocities) even with moderate to low-momentum ratios, stable combustion can be achieved with low hydrogen injection temperatures. In the preburner combustor, chamber geometry allows for low chamber velocities, (Mach 0.06). Testing at the 250K size has demonstrated stable combustion to 90°R fuel temperature. During testing of 50K thrust-size preburner, operation at 55°R fuel temperature was always stable.

- GASEOUS HYDROGEN TO PREBURNER INJECTOR DURING STARTING TRANSIENT ASSURES GOOD PROFILE AND STABLE COMBUSTION

Gaseous hydrogen from the primary nozzle is diverted to the injector inlet manifold during the starting transient to provide a higher injector ΔP during the early part of the transient and to eliminate the extremes in the combustion temperature profile, which would have occurred from the subcritical injector fill transient to liquid hydrogen.

- CLOSE-COUPLED LIQUID OXYGEN SHUTOFF VALVE PROVIDES SMOOTH START AND SHUTDOWN

The preburner oxidizer control and shutoff valve is close-coupled to the preburner injector, similar to that shown in figure II-4. The valve is used to control the primary-to-secondary oxidizer flow split and to provide a close-coupled shutoff. By incorporating a shutoff function in this valve, the system up to the valve can be preconditioned prior to engine start and the liquid oxygen manifold volume downstream of the shutoff is minimized. This allows the oxidizer injector to become filled with liquid oxygen almost immediately during the liquid oxygen lead portion of the starting transient and minimizes combustion temperature variations and chamber pressure spiking during injector filling. Small liquid oxygen volumes downstream of the shutoff valve also provide for a clean engine shutdown with negligible temperature spiking.

- PREBURNER INJECTOR DESIGNED FOR LOW FREQUENCY STABILITY MARGIN

Small liquid oxygen secondary cavity volume is also important for good low frequency combustion stability (chugging). A preburner fuel system and combustion process analog representation has been formulated and utilized in the design. A basic conclusion from the study indicates that low frequency combustion instability can result from improper matching of secondary cavity volume and the existing combustion delay time. Figure II-5 is an example of a stability trade used in the design varying secondary volume from the design base. Figure II-6 shoes stability margin with the selected secondary cavity volume. Damping ratio is calculated from the logarithmic decrease of the oscillatory amplitude.

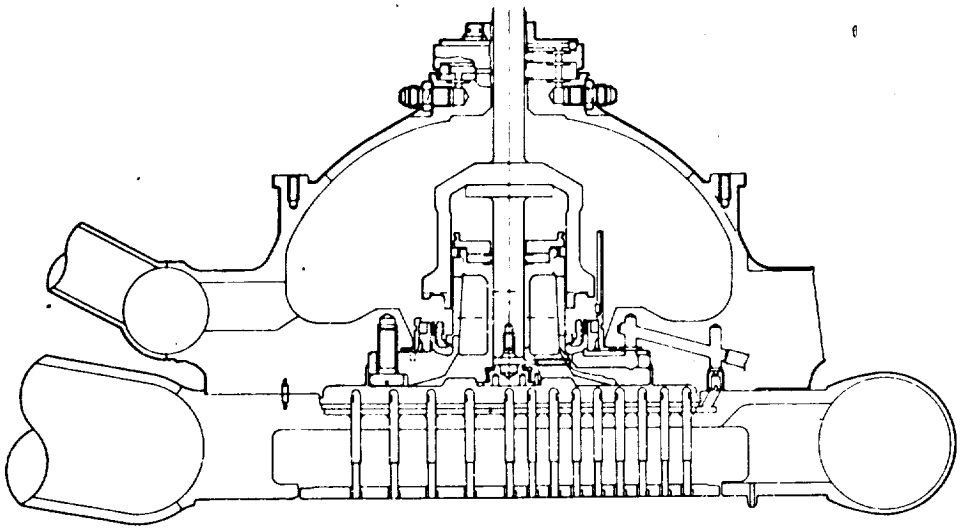

Figure II-4. Close Coupled Preburner Valve Minimizes Oxidizer Volumes for Smooth Start and Shutdown Transients

FD 52666

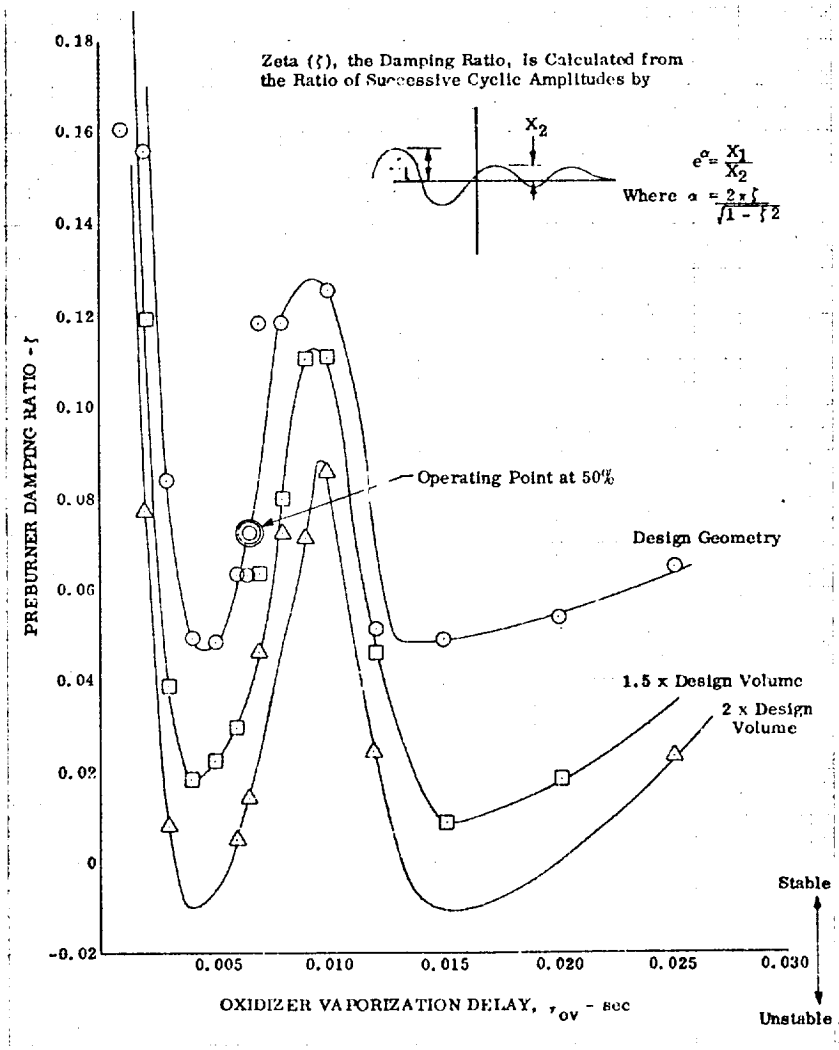

Figure II-5. Secondary Volume Influences Preburners Chugging Stability

DF 85092

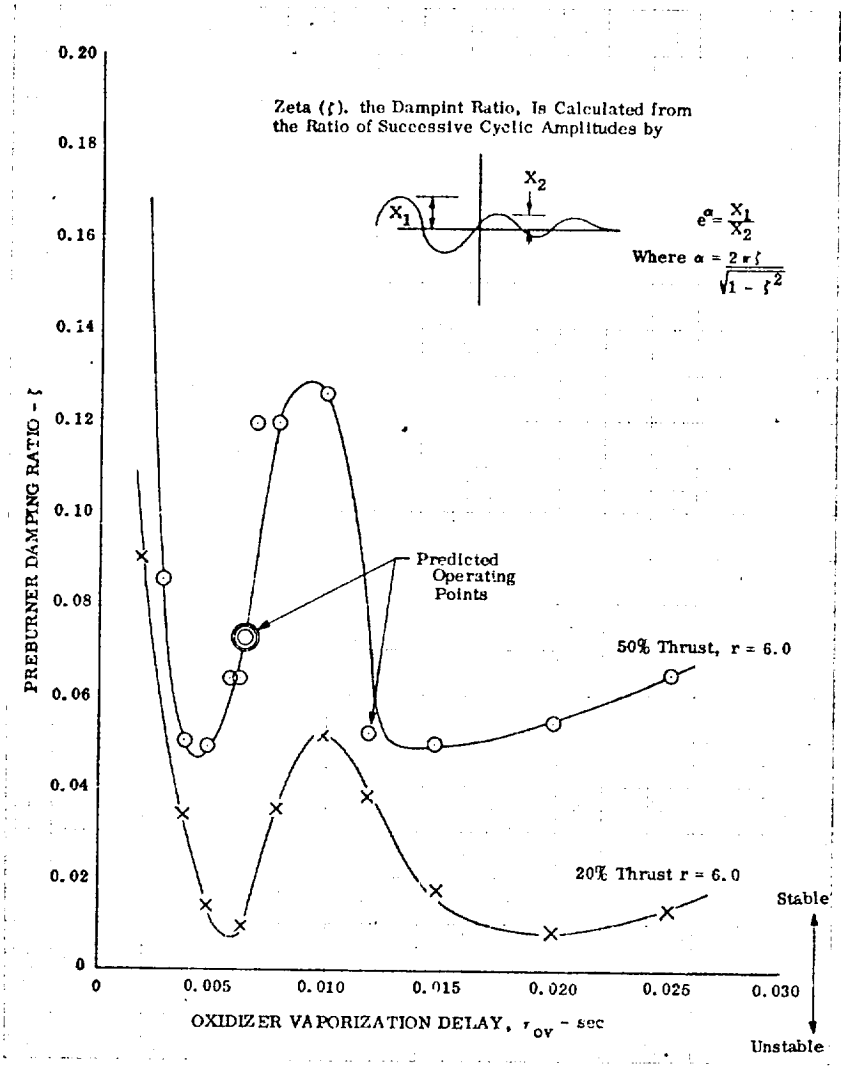

Figure II-6. Preburner Design Has Low Frequency Stability Margins DF 85096

- TOROIDAL SEALS MEET LEAKAGE REQUIREMENTS

External leakage seals are of the toroidal segment type and are fabricated from Inconel X-750 material which has been proven to meet low leakage requirements. All of the injector flanges are designed for 0.002 in. maximum total deflection at their seal points. This considers the maximum possible loading in the assembly which includes blowoff, seal, thermal, fluid momentum, and externally-applied loads. The full details of flange design criteria is specified in the Plumbing Design Criteria, PWA FR-4455.

- FACE TAPS PROVIDED FOR CHAMBER PRESSURE MEASUREMENT

Provisions for measuring preburner chamber pressure are located in the injector as shown in figures II-7 and II-8. Two Kistler-type transducers, each utilizing an infinite tube tap and hydrogen bleed, will be used during nonflight testing to measure high frequency combustion pressure oscillations. During flight, the ports which accommodate these transducers will be capped

with Dynatube-type bulkhead connectors that retain flight plugs. Preburner chamber static pressure flight instrumentation capability is provided by means of an extended flange integral with the housing. This flange accommodates a transducer that senses combustion chamber static pressure at the injector face.

- BRAZED ASSEMBLY ALLOWS DETAILED INSPECTION DURING FABRICATION

The injector manufacturing sequence provides for rigorous step-by-step inspection, quality control, flow calibration, and testing. Procedures required at subassembly levels include:

1. Pressure check of injector elements
2. Flow check of injector elements
3. Flow check of faceplate
4. Proof test of fuel manifold

Cleanliness, handling, and preservation of parts through assembly are accomplished in accordance with MSFC-SPEC-164 and PWA Specification 382. After brazing in accordance with PWA Specification No. 19, followed by the lower temperature braze of PWA-84, the structure will be precipitation hardened in accordance with PWA 11-17.

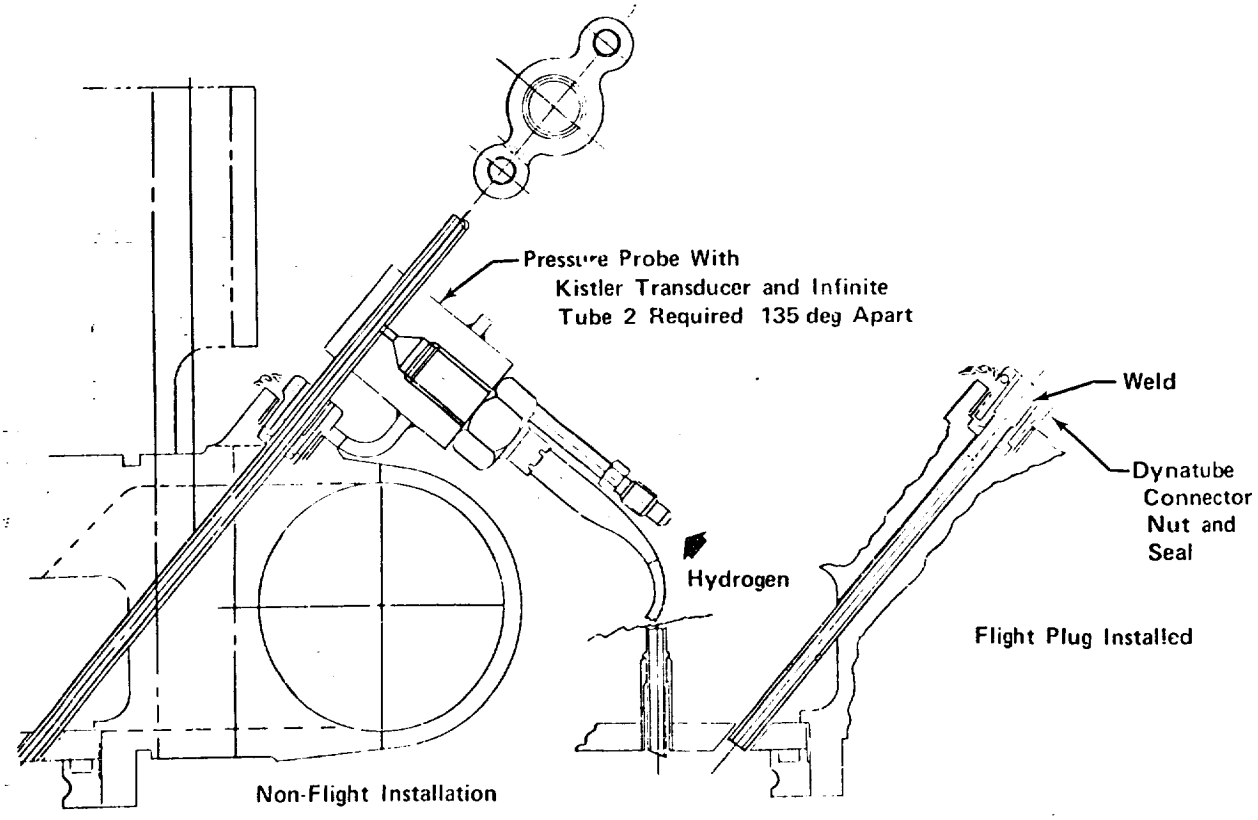

Figure II-7. Preburner Injector Provides for Measuring Preburner Combustion Pressure Oscillations

FD 46207

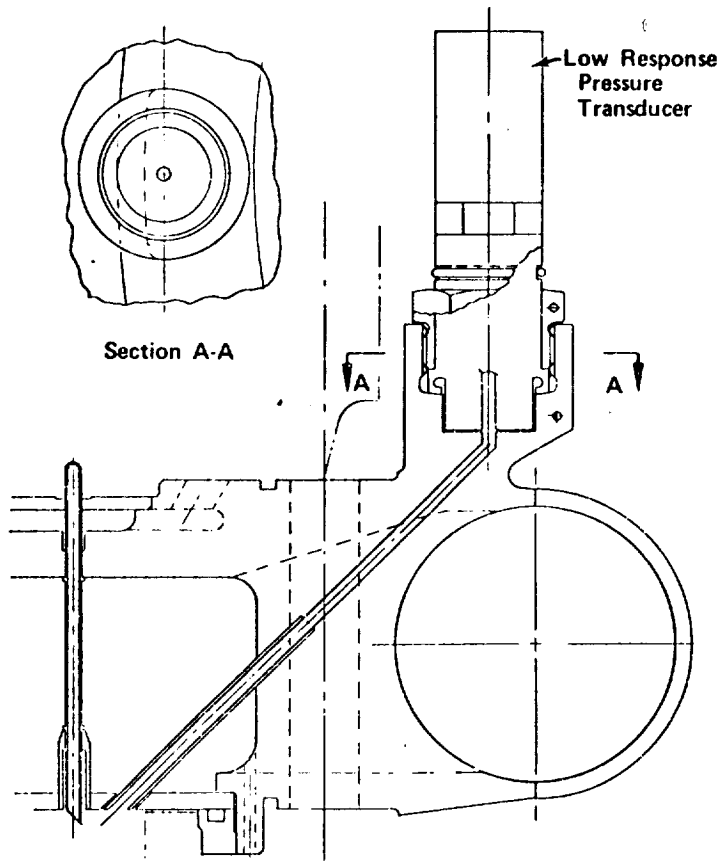

Figure II-8. Preburner Injector Provides for Measuring Combustion Chamber Steady-State Pressure

FD 52574

The preburner injector is designed for first bending natural frequency margin of greater than 75% relative to combustion excitation. The preburner combustion first longitudinal mode is 1210 to 1375 Hz. The injector first bending mode is 672 Hz nominal.

- REQUIRED PREBURNER INJECTOR OPERATING CONDITIONS

The preburner injector operating characteristics are determined by the engine cycle power balance while operating within the turbomachinery maximum allowable temperature. The required engine cycle preburner combustion temperature-versus-thrust is shown in figure II-9 and the cycle fuel temperatures are shown in figure II-10.

Sufficient injector pressure drop is maintained to provide stable combustion. Figures II-11 and II-12 show the injector propellants pressure drop as a percentage of preburner chamber pressure over the engine operating range. The preburner chamber pressure is shown in figure II-13. The oxidizer flow split is varied according to the schedule shown in figure II-14 to control the oxidizer injector pressure drop.

The preburner injector propellant flow rates and resultant momentum ratios are shown in figures II-15, II-16, and II-17. The preburner injector

mixture ratio versus thrust are shown in figure II-18 for all three engine mixture ratios.

C. REQUIREMENTS

The preburner injector has been designed to conform to CEI Specification CP2291.

1. The preburner injector meets the following general Pratt & Whitney Aircraft requirements:

    1. P&WA/SSME Engine Structural Design Criteria, PWA FR-4449.

    2. Design approach to utilize P&WA demonstrated experience and technology applicable to fixed-area preburner injectors.

2. Specific requirements as applicable to engine design cycles are:

    1. Combustion temperature profile: ≤120°R peak-to-average at turbine inlet.

    2. Throttling: orbiter: 2107 to 5492 psia; booster: 2153 to 5601 psia, stable start and shutdown transient.

    3. Injector mixture ratio for booster: 0.89:1 to 1.191:1; for orbiter: 0.84:1 to 1.149:1.

    4. Injector target weight: 175 lb

    5. Durability: 100 starts minimum with factor of 4; 7.5 hours minimum time between overhauls; emergency power level run ability at 109% thrust, mixture ratio 6.

    6. Propellant conditions:

	TEMPERATURE RANGE°R		FLOW RATE RANGE (lb/sec)	
	Orbiter	Booster	Orbiter	Booster
Liquid oxygen:	186-218	186-219	21-186	20-187
Hydrogen:	70-135	70-136	23-157	25-164

Emergency power level liquid oxygen to 6730 psia maximum
Emergency power level hydrogen to 6330 psia maximum
Emergency power level combustion to 5765 psia maximum.

    7. Ignition ability at sea level and altitude

    8. Stable combustion with instrumentation provision for measurement of high and low frequency oscillations.

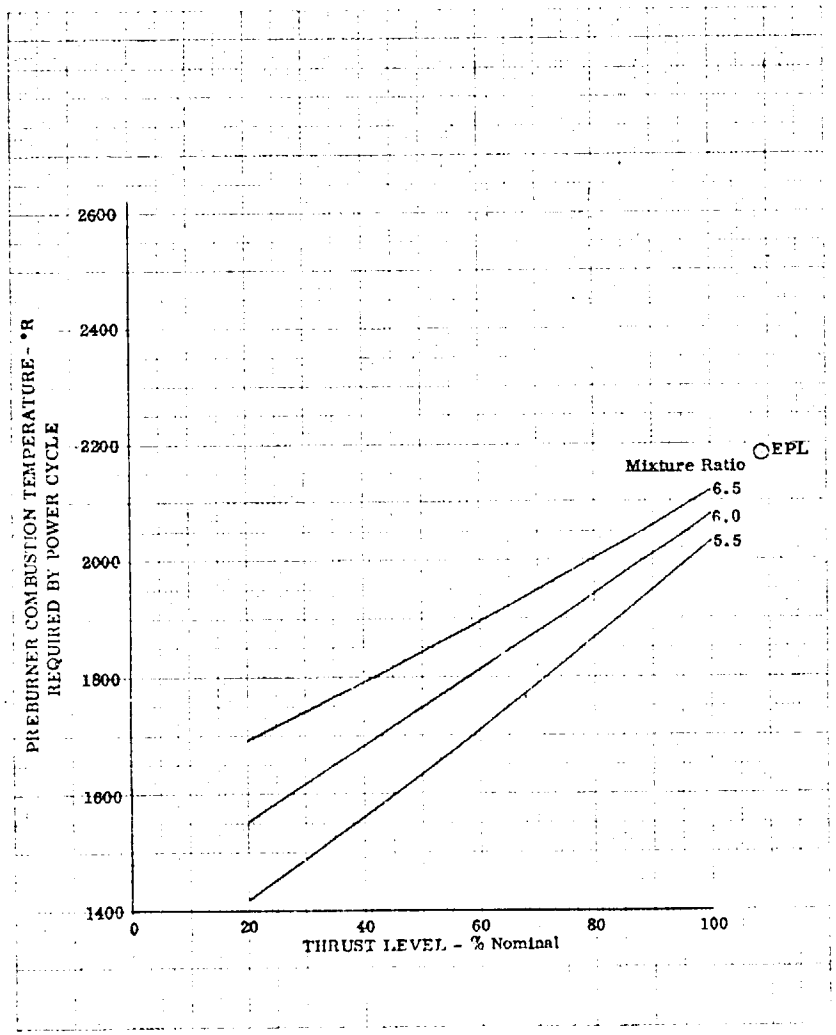

Figure II-9. Required Preburner Combustion Temperature Is Within Demonstrated Technology

DF 85655

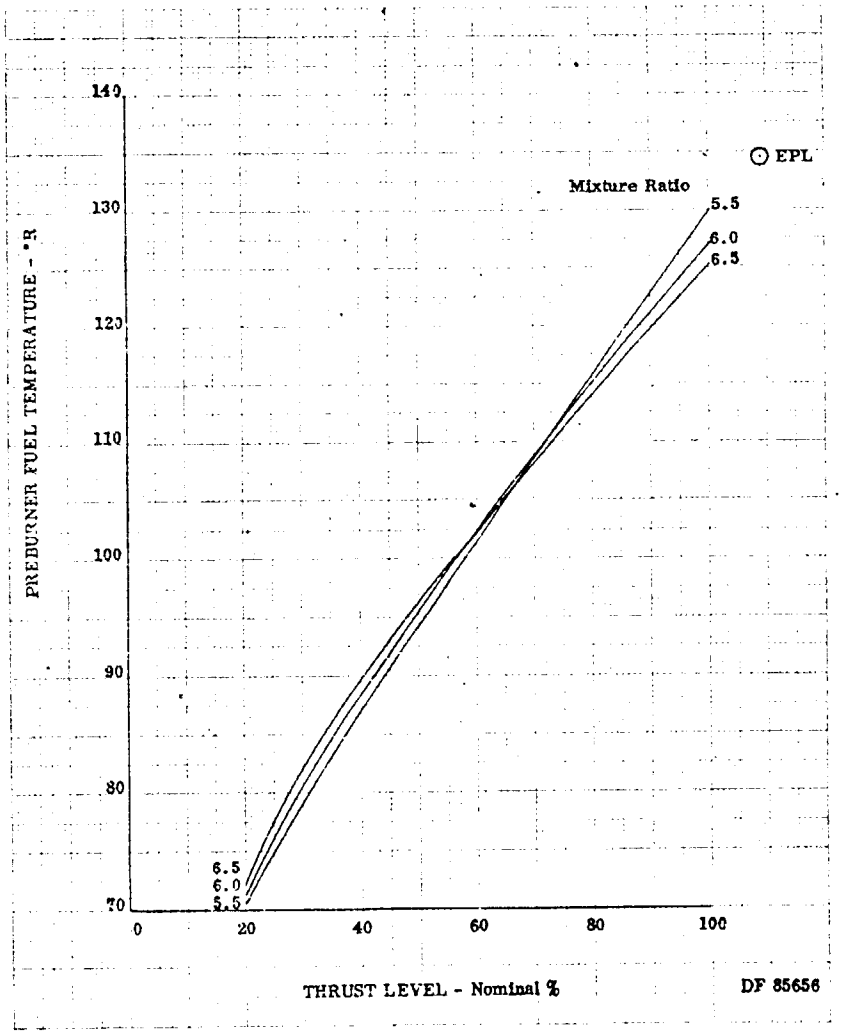

Figure II-10. Preburner Fuel Temperature vs Thrust Level

DF 85656

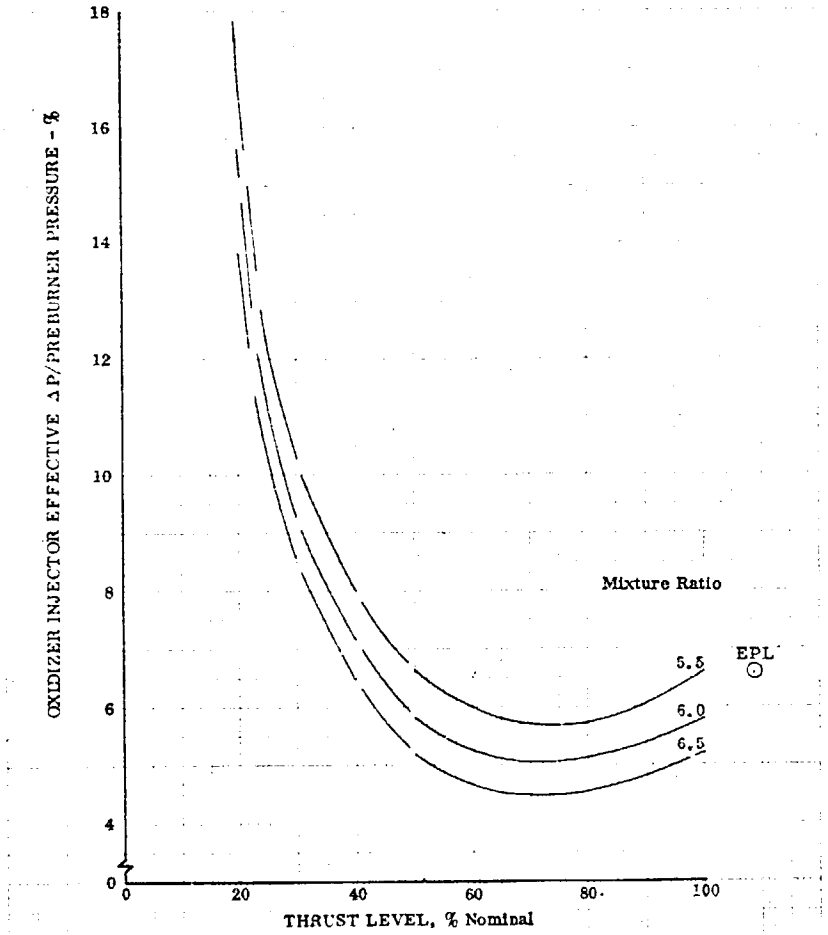

Figure II-11. Effective Pressure Loss Oxidizer Preburner Injector vs Thrust

DF 85535-2

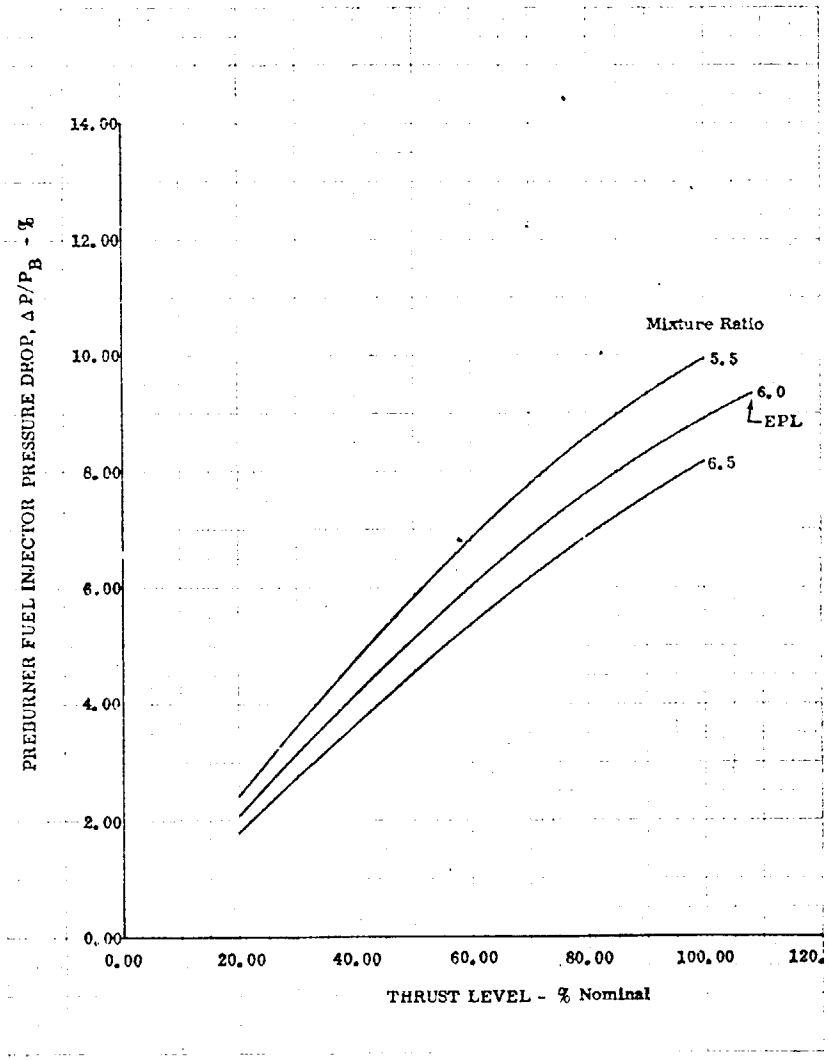

Figure II-12. Fuel Injector ΔP/Over Operating Range Provides Stable Low Frequency Combustion

DF 85535-1

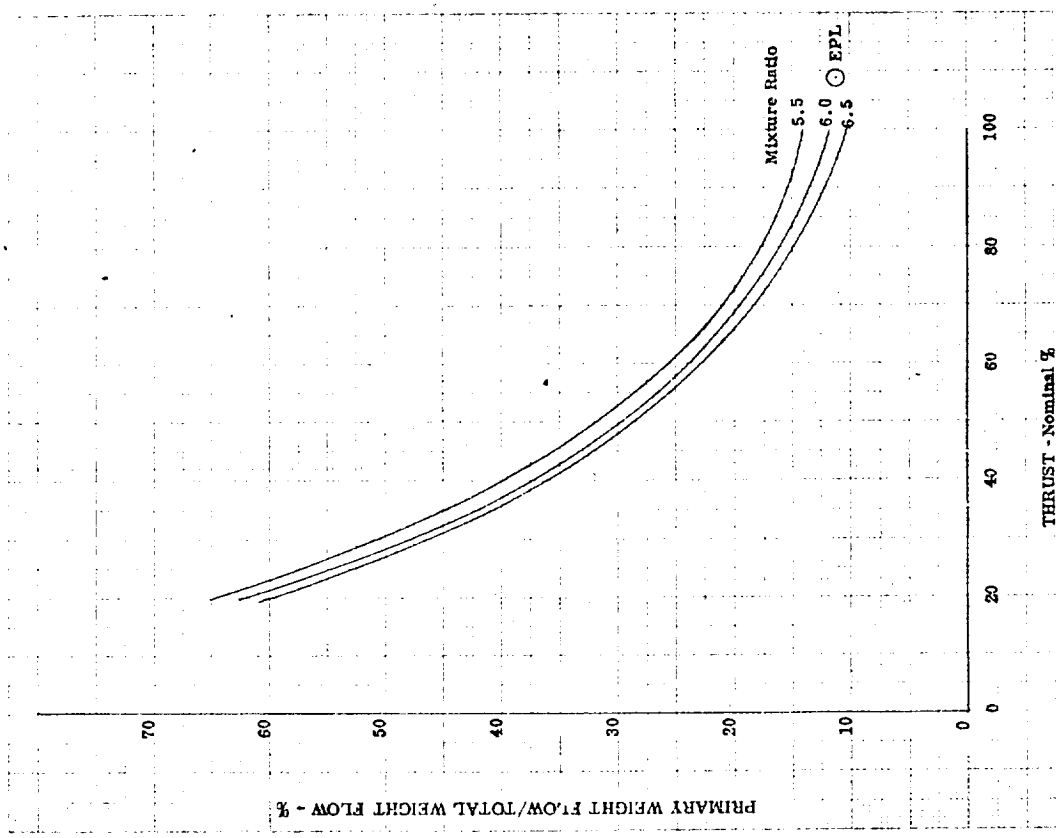

DF 85658

Figure II-14. Oxidizer Dual Orifice Flow Split Is Varied to Maintain High Injection Pressure Drop

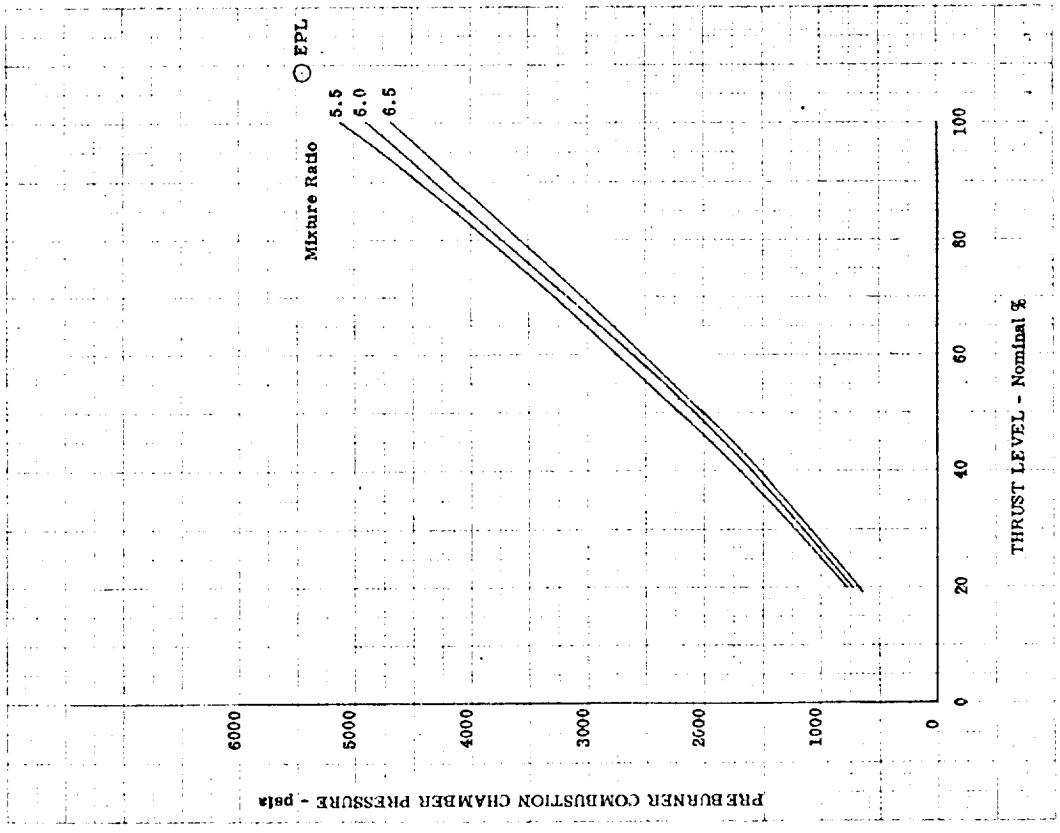

DF 85657

Figure II-13. Preburner Combustion Chamber Pressure vs Thrust Level

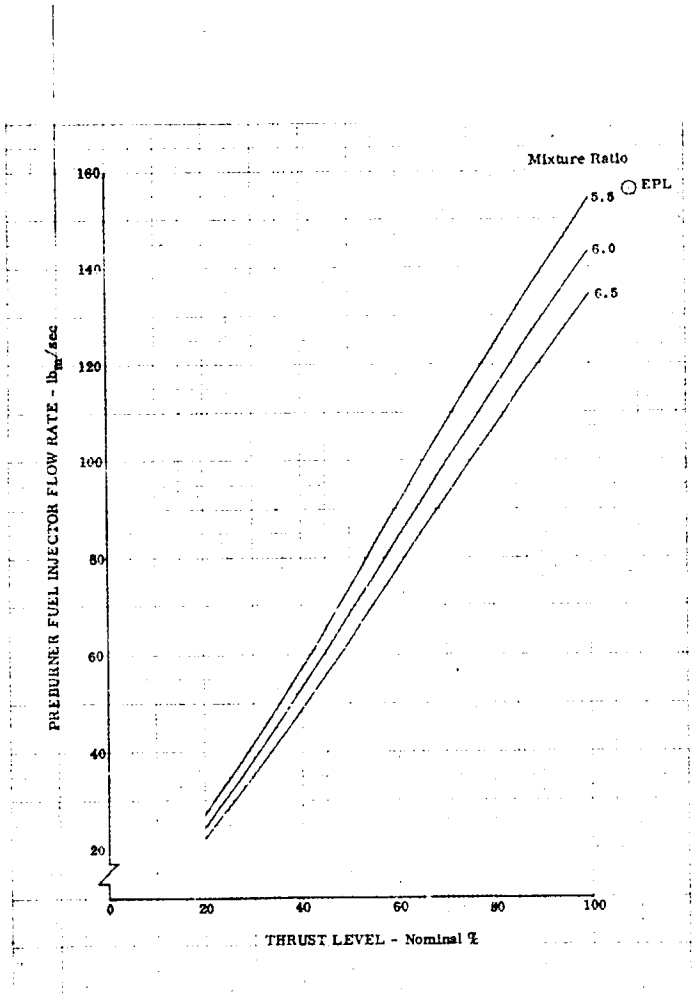

Figure II-15. Preburner Fuel Flow Required in the Engine Power Cycle DF 85659

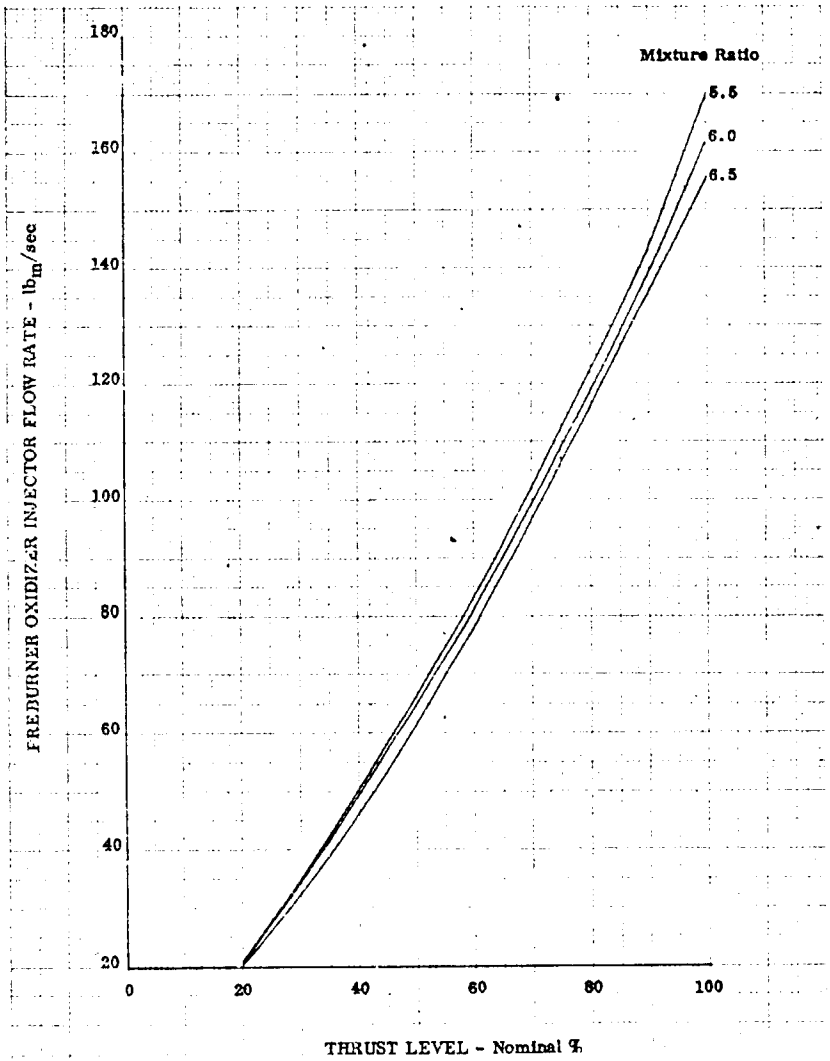

Figure II-16. Preburner Oxidizer Flow Controlled to Provide the Required Combustion Temperature DF 85660

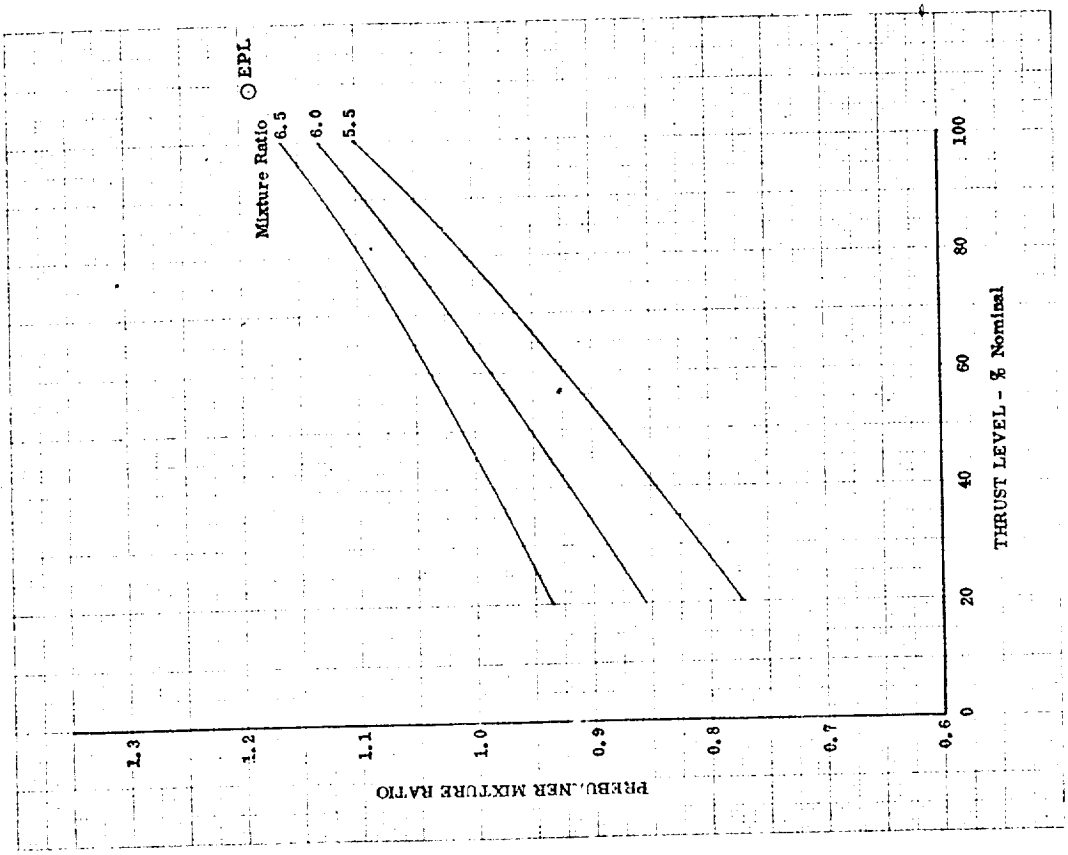

DF 85662

Figure II-18. Preburner Mixture Ratio Controlled to Provide Required Turbopump Power

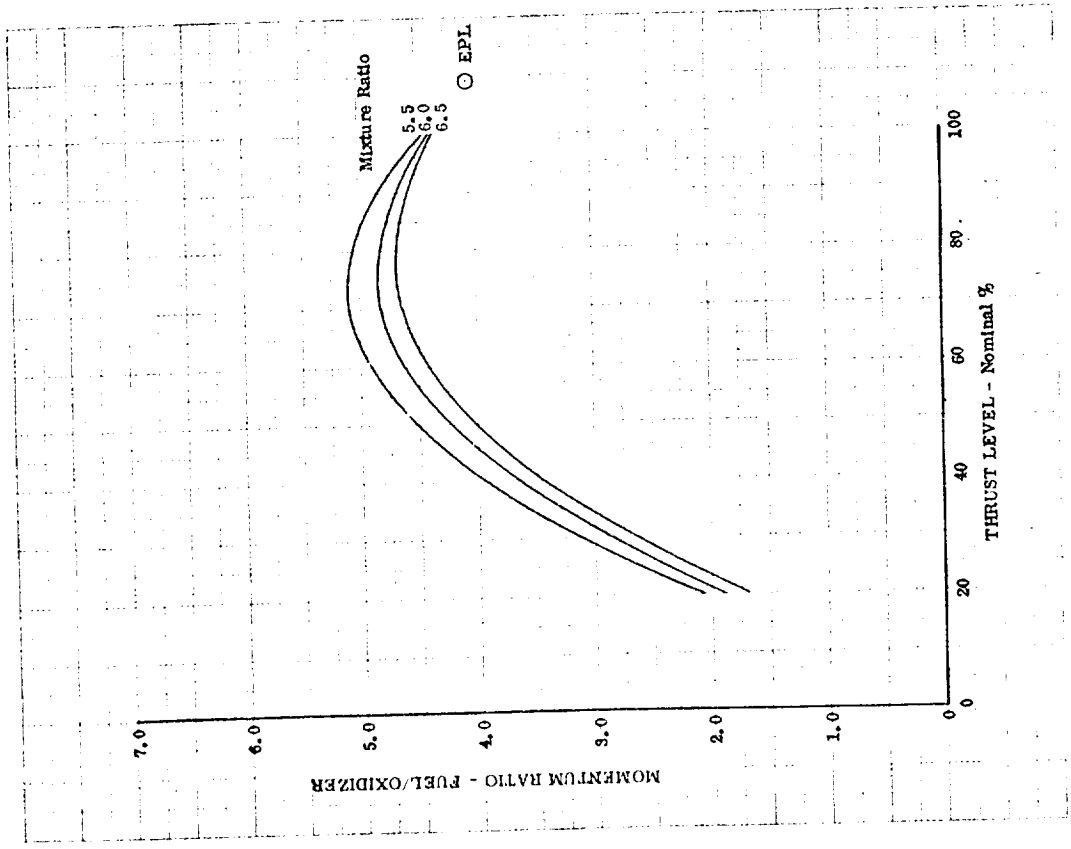

DF 85661

Figure II-17. Momentum Ratio Important Only to Mixing Rather Than Atomization

3. Additional design provisions to accomplish P&WA-imposed requirements for the SSME preburner injector include:

1. Propellant manifolding to minimize flow distribution pressure losses and maintain manifold losses to less than 20% of the injection Δ P.

2. Oxidizer volumes minimize with respect to fill and purge.

3. Dual-oxidizer self-atomizing elements to accommodate start transient and throttle excursions, maintaining injection pressure differentials above 4% of the chamber pressure.

4. Element spacing based on XLR129 250K injector experience consisting of a hexagonal array co-rotating injector element pattern geometry with 0.480 spacing where possible.

5. Fuel-to-oxidizer momentum ratio >2.5.

6. Fuel annuli sleeves to eliminate flow disturbing tangs.

7. Porous transpiration cooled faceplate for durability.

8. Injector manufacturing sequence that provides for in-process inspection, quality control, and handling and cleanliness preservation.

9. Outer injector elements with scarfed tips to be located 0.7 inch from the preburner chamber is an uniformly spaced circular array.

10. A faceplate outer support integral with the main housing.

11. A durable seal that can accommodate the faceplate outer edge thermal deflection.

12. Incorporation of design features which enable the preburner injector and mating oxidizer valve to be handled as a modular unit.

13. Minimize weight by using a tapered toroidal fuel manifold and scalloped fuel ports between bolt holes.

14. Injector element and fuel sleeve discharge eccentricity due to operating loads to be within 0.002 in.

15. Fuel inlet manifold to incorporate an additional 4.0 sq in. effective area ingestion port for gaseous starting fuel.

The requirements of the applicable paragraphs CEI Specification No. CP2291 have been met as follows:

1. The engine shall have long service life, with provisions for ease of access, minimum maintenance, and economic overhaul as stated by paragraphs 1.2K, 3.6.2, and 3.7.7.3.

Compliance - The injector is not life limited. There are no mechanically driven parts eliminating wear as a factor. The face is transpiration-cooled to eliminate low cycle thermal fatigue and high cycle fatigue is avoided by natural frequency margin from combustion driven modes. The plug-in concept allows disassembly by removal of one set of bolts and the inlet flange. Inspection parts have been provided for face and duct inspection without injector disassembly. The injector face can be simply removed by acid etch and a new face rebrazed if required because of an oxidizer system malfunction resulting in face burning. Individual elements can be replaced in the same manner.

2. The engine shall be capable of variable thrust and mixture ratio operation as stated by paragraphs 1.2.C, 3.1.1.1, and 3.1.2.

Compliance - Stable combustion is maintained over a wide range of mixture ratios and thrusts by using dual-orifice oxidizer injector elements that maintain high injection differential pressures and excellent atomization characteristics at all engine power levels and during start transients.

3. The preburner shall have stable combustion over the engine operation range within the limits of paragraph 3.2.9.1.

Compliance - Design features of paragraph 2 also applies here. The proven very small drop size self-atomization of the dual orifice slot swirler liquid oxygen elements created the short ignition delay and burning time required for inherently stable combustion and good performance. The dual-orifice feature of the element allows for high $\Delta P/P$ isolation of the oxidizer supply system to eliminate low frequency hydraulic instability. Low combustion chamber velocity in the preburner provides stable combustion even with cold fuel. Chamber wall absorption has been incorporated to provide damping capability and to ensure high frequency combustion stability.

4. Mechanical connect points shall be configured by size and/or design to preclude inadvertent cross-connections as stated in paragraph 3.5.1, and parts of common part number be interchangeable as stated in paragraph 3.7.8.

Compliance - A faceplate retaining ring is employed in the preburner injector that permits close control of machined surfaces between mating parts. This enables the preburner combustion liner interface seal to mate with a positively fixed surface and enhances interchangeability by eliminating the need for matched components; i.e., the seal does not mate with the faceplate or a surface which is difficult to dimensionally control or position. Dowel pins on the main interfaces are provided to preclude improper assembly orientation.

5. Capability for acquisition of flight data shall be provided for within the engine as stated by paragraph 3.5.3.2.

   Compliance - The preburner injector has an extended flange integral with the housing. This flange accommodates a transducer that senses combustion chamber static pressure at the injector face.

6. Capability for acquisition of nonflight data shall be provided for within the engine as stated by paragraphs 3.2.9.2 and 3.5.3.3.

   Compliance - Two housing bosses with access to the injector face are provided 135 deg apart. During flight, these ports are capped with a Dynatube-type bulkhead connector to retain a flight plug. Adjacent to each port within the same raised boss, two tapped holes are provided to accommodate nonflight instrumentation. Two Kistler-type transducers, utilizing an infinite tube tap hydrogen bleed, will be mounted to the bosses during development testing. These transducers will sense high frequency combustion chamber pressure oscillation levels at the injector face.

7. Materials exposed to gaseous hydrogen that will fail due to hydrogen embrittlement shall not be used in the engine as stated by paragraph 3.7.1.2.

   Compliance - Inconel 718 material used in the preburner injector is exposed only to cryogenic temperature high pressure hydrogen. Extensive material testing confirm the suitability of this material for strength margins in high pressure cryogenic hydrogen applications.

D. SUBSTANTIATION

The following reports prepared over the past several years described in detail the evaluation of P&WA preburner injector design. Substantiation comments will refer to these reports where applicable.

Reference Reports

1. Final Report High Pressure Rocket Engine Feasibility Program PWA FR-1171, December 1964.

2. High Chamber Pressure Staged Combustion Research Program Final Report FR-1676, June 1966, AFRPL-TR-66-70.

3. Advanced Cryogenic Rocket Engine Program Staged-Combustion Concept Final Report, December 1967 - FR-2597, AFRPL-TR-67-298.

4. Seventh Program Review on the Air Force Reusable Rocket Engine Program - August 1970, PWA GP 70-262.

5. Air Force Reusable Rocket Engine Program XLR129-P-1 Demonstrator Engine Design - FR-3337 April 1970, AFRPL-TR-70-6.

The SSME Design evolved from seven years of preburner test programs. The original high chamber pressure preburner injectors were 10K thrust level size and run in 1964, and with staged combustion tests in 1965. They were fixed area designs. Two 10K preburner injectors were designed and fabricated. One injector was a 128-concentric element design with straight-through liquid oxygen injection. The other injector was a 19-element configuration with ribbon swirlers for liquid oxygen injections and concentric hydrogen annuli. A cross section of these injectors is shown in figure II-19.

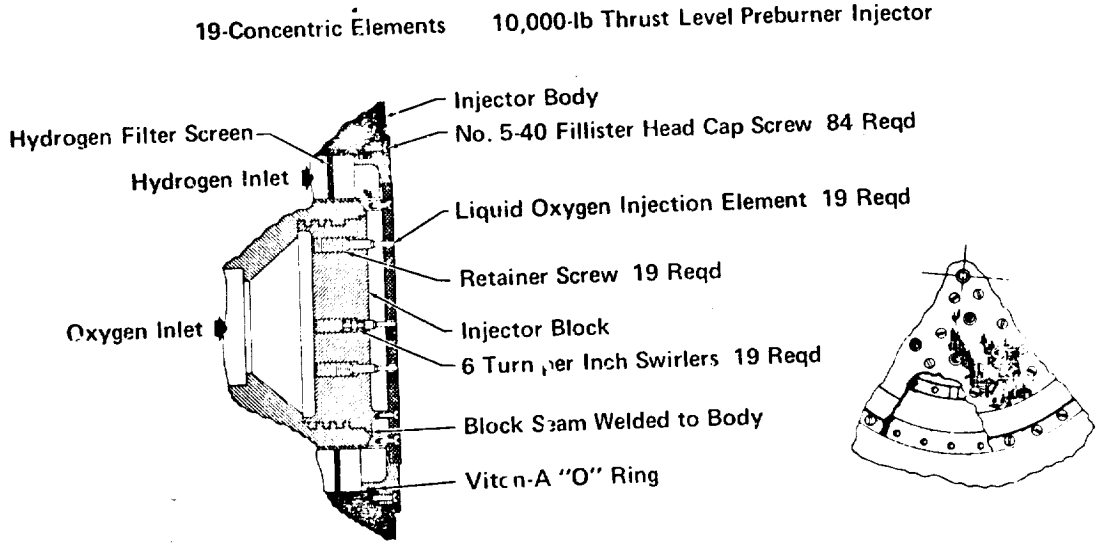

Figure II-19. Early Fixed-Area Preburner Injectors Provided Gas (GH_2) - Liquid (LO_2) Test Experience FD 52304

Tests of these preburner injectors were made with liquid oxygen and gaseous hydrogen propellants. Gaseous hydrogen was used because of

a 1000 psig pressure limitation on the liquid hydrogen run tank on the 10,000-lb thrust level test stand. A total of 35 hot firings were made with these two preburner injectors. A summary of the test data is given in tables II-1 and II-2.

Table II-1. Table Summary of Data for 10,000 lb Thrust Level High Chamber Pressure Preburner Test Series

Test[1] No.	Date	Propellants	Chamber Pressure	Fuel Flow lb/sec	Lox Flow lb/sec	Preburner Mixture Ratio r[2]	Average Chamber Temp, °R	Chamber Temp Variation, Maximum °R
10PB-1	17 Nov 64	LO_2/GH_2	3865	3.06	2.75	0.90	1875	1970-1665
10PB-2	19 Nov 64	LO_2/GH_2	4115	2.64	3.57	1.35	2520	2650-2410
10PB-3	9 Dec 64	LO_2/GH_2	4160	3.71	2.96	0.80	1660	1730-1440
10PB-4	9 Dec 64	LO_2/GH_2	3140	2.46	3.15	1.28	2445	2590-2310
10PB-5	9 Dec 64	LO_2/GH_2	3190	2.58	3.06	1.19	2165	2240-1995
10PB-6	16 Jan 65	LO_2/GH_2	3235	4.43	1.64	0.37	1130	1160-1110
10PB-7	18 Jan 65	LO_2/GH_2	3230	3.88	1.76	0.45	1180	1270-1140

[1] The 128-element injector was used in all tests except 10PB-6 and 10PB-7; in these tests the 19-element (with swirlers) was used.

10K Preburner proved feasiliby with acceptable profile

Table II-2. Summary of Data For Uncooled 10,000 lb Thrust Level Staged Combustion Test Series

Test No.	Date	Preburner Injector Type	Main Burner Injector Type	P/B Chamber Pressure	Main Burner Chamber Pressure	P/B Mixture Ratio	Main Burner Mixture Ratio	Average P/B Combustion Temperature °R	P/B Temp. Variation, max/min °R 950/830
10SC-1	8 Jan 65	128 element	1 rect. slot spraybar	3095	3035	0.17	1.4	860	
10SC-2	22 Jan 65	19 element swirler	1 rect. slot spraybar	3115	2935	0.56	1.5	1430	1550/1250
10SC-3	22 Jan 65	19 element swirler	1 impinging slot spraybar	3200	3025	0.80	1.7	1500	1620/1220
10SC-4	23 Jan 65	19 element swirler	1 impinging slot spraybar	3100	2940	0.495	1.3	1285	1475/1240
10SC-5	25 Jan 65	19 element swirler	4 impinging slot spraybars	3170	2990	0.295	4.5	960	1020/840
10SC-6	10 Feb 65	19 element swirler	101 element	3195	2970	0.395	3.9	1210	1260/1145
10SC-7	13 Feb 65	19 element swirler	101 element	3210	3010	0.53	4.1	1340	1420/1275
10SC-8	13 Feb 65	19 element swirler	101 element	3230	2970	0.745	5.3	1645	1660/1530
10SC-9	14 Feb 65	19 element swirler	101 element	3220	3050	0.80	6.15	1765	1810/1700
10SC-10	16 Feb 65	19 element swirler	101 element	3230	3050	0.84	7.35	1835	1965/1730
10SC-11	22 Feb 65	19 element swirler	56 element swirler	3270	3135	0.66	4.6	1540	1600/1420
10SC-12	23 Feb 65	19 element swirler	56 element swirler	3150	2970	0.80	6.55	1740	1800/1665
10SC-13	22 Mar 65	128 element	56 element swirler	3140	2970	0.61	4.3	1445	1500/1380
10SC-14	23 Mar 65	128 element	56 element swirler	3215	3050	0.64	6.9	1485	1620/1410
10SC-15	23 Mar 65	128 element	56 element swirler	3250	3035	0.82	7.7	1730	2120/1595
10SC-16	25 Mar 65	128 element	4 spraybars with swirlers	3205	3030	0.55	3.7	1330	1395/1290

Table II-2. Summary of Data For Uncooled 10,000 lb Thrust Level Staged Combustion Test Series (Continued)

Test No.	Date	Preburner Injector Type	Main Burner Injector Type	P/B Chamber Pressure	Main Burner Chamber Pressure	P/B Mixture Ratio	Main Burner Mixture Ratio	Average P/B Combustion Temperature °R	P/B Temp. Variation, max/min
10SC-17	1 Apr 65	128 element	4 impinging doublet spraybars	3070	2950	0.48	3.3	1280	1350/1260
10SC-18	1 Apr 65	128 element	4 impinging doublet spraybars	3110	2945	0.63	5.6	1410	1435/1390
10SC-19	2 Apr 65	128 element	4 impinging doublet spraybars	3025	2935	0.60	7.3	1435	1490/1385
10SC-20	2 Apr 65	128 element	4 impinging doublet spraybars	3130	2960	0.70	3.9	1585	1620/1510
10SC-21	2 Apr 65	128 element	4 impinging doublet spraybars	3155	2905	0.94	8.0	1960	2010/1870
10SC-22	9 Apr 65	128 element	4 swirler spraybars	3370	3170	0.50	5.4	1295	1315/1265
10SC-23	9 Apr 65	128 element	4 swirler spraybars	3270	3010	0.82	6.9	1790	1845/1700
10SC-24	10 Apr 65	128 element	4 swirler spraybars	3290	3035	0.56	6.5	1380	1420/1365
10SC-25	10 Apr 65	128 element	4 impinging doublet spraybars	3110	3030	0.60	7.3	1460	1500/1435
10SC-26	10 Apr 65	128 element	4 impinging doublet spraybars	3155	3017	0.60	6.1	1455	1570/1345
10SC-27	13 Apr 65	128 element	4 swirler spraybars	3335	3110	0.78	6.35	1725	1775/1680
10SC-28	13 Apr 65	128 element	4 swirler spraybars	3315	3030	0.90	7.1	1900	

The preburner combustion gas temperature profiles obtained with these injectors were satisfactory during preburner and staged combustion testing and there was no indication of any significant combustion instability. With these injector configurations, no injector face burning problems at high pressures were encountered.

Subsequent to the 10K testing and based on satisfactory testing of the fixed-area 10K preburner injectors, two 50K preburner injectors were designed and fabricated. One injector has 54 concentric elements with ribbon swirlers in the liquid oxidizer element. The other injector design was a 320-multiple concentric element pattern. The oxidizer element utilized straight-through (nonswirl) liquid oxygen injection. A cross section of these injectors is shown in figures II-20 and II-21.

A total of 25 hot firings was made with these two 50K preburner injectors in both a preburner rig and a staged combustion rig. The propellants were liquid hydrogen and liquid oxygen. A summary of the test data is given in tables II-3 and II-4. There was no indication of any significant combustion instability during any of this testing.

In 1966 during Phase I of the Advanced Cryogenic Rocket Engine Program Staged Combustion, a 250K variable fuel area preburner injector was fabricated and tested to provide high fuel injection velocities over a 10:1 throttling range. This 250K variable fuel preburner injector consisted of 84 dual orifice injector elements arranged in 7 circles of 12 elements each as shown in figure II-22.

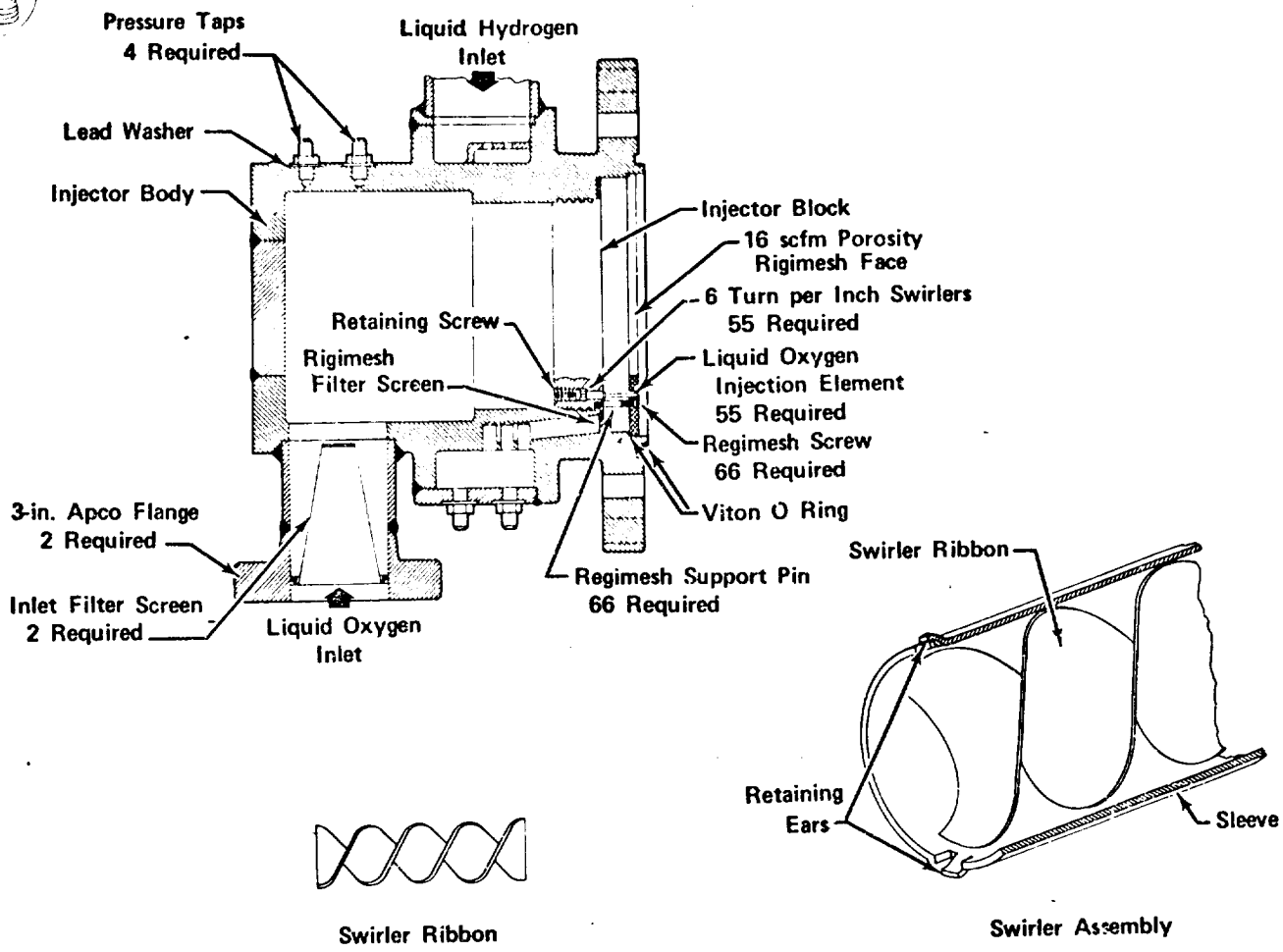

Figure II-20. Ribbon Swirlers Used in 54 Element 50K Injector FD 52660

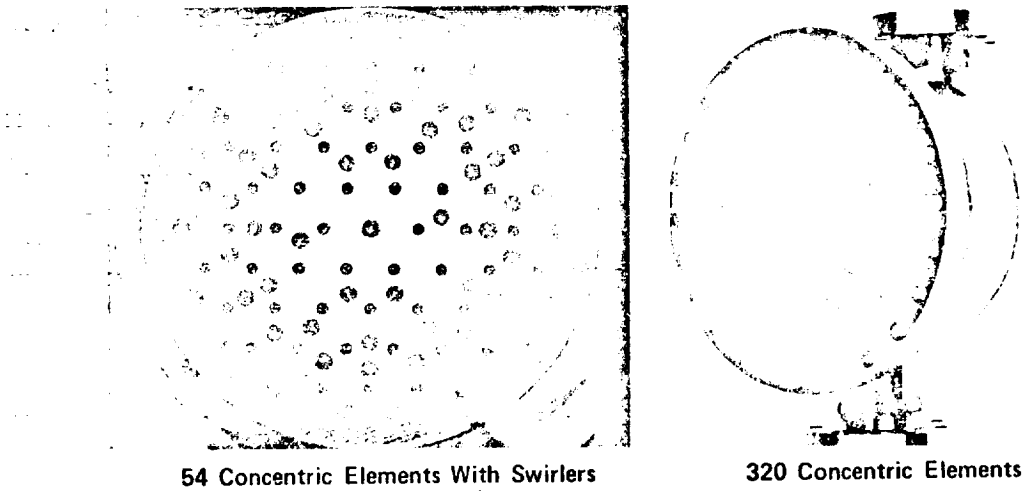

Figure II-21. Early 50K Fixed-Area Preburner Injectors Provided Liquid Hydrogen - Liquid Oxygen Test Experience With Hydrogen Injection Temperature of 50°R FD 52305

Table II-3. Test Data for 50,000-lb Thrust Level High Chamber Pressure Preburner Test Series Using the 320-Multiple-Concentric-Element Preburner Injector

Injector Type	Test No.	Chamber Pressure, psia	Fuel Flow, lb/sec	Oxidizer Flow, lb/sec	Preburner Mixture Ratio	Avg Chamber Temperature, °R	Chamber Temp Variation, Max/Min °R
54 Element	50PB-1	3540	15.9	11.8	0.75	1405	1375-1470
54 Element	50PB-2	3940	16.0	13.9	0.87	1705	1575-1830
54 Element	50PB-3	3940	14.5	14.4	0.99	1840	1650-1950
320 Element	50PB-4	3525	12.5	12.4	1.00	1735	1615-1945
320 Element	50PB-5	3130	12.6	10.7	0.85	1510	1025-1730
320 Element	50PB-6	3480	12.4	12.5	1.00	1725	1205-2190
320 Element	50PB-7	3795	15.2	13.3	0.87	1415	870-1925

Table II-4. Acceptable Temperature Profiles and Stable Combustion Attained in Staged 50K Combustion with Liquid Fuel

Test No.	Date	P/B Injector Type	MB Injector Type	P/B Chamber Pressure psia	Main Burner Chamber Pressure psia	Preburner Mixture Ratio	Main Burner Mixture Ratio	Average P/B Combustion Temperature	P/B Temp Variation, °R Max	P/B Temp Variation, °R Min	Fuel Temp °R	Oxidizer Temp °R
50SC-1	28 June 65	54 element swirler	192 element	3015	2765	0.92	4.95	1525	1790	1365	54.3	163.8
50SC-2	29 June 65	54 element swirler	192 element	3165	2690	0.75	3.4	1385	1560	1175	53.5	160.5
50SC-3	16 July 65	320 element	192 element	3175	2933	0.98	5.7	1765	1945	1585	53.4	156.7
50SC-4	24 July 65	320 element	20 spraybar	2690	2515	(1)	(1)	1310	1435	1205	54.0	157.8
50SC-5	16 Aug 65	320 element	192 element	3000	2805	1.18	7.65	1950	2240	1820	54.4	164.5
50SC-6	17 Aug 65	320 element	192 element	3210	2980	1.11	7.15	1890	2130	1730	53.5	161.0
50SC-7	24 Aug 65	320 element	192 element	3070	2830	1.24	7.65	1915	2085	1665	54.0	167.8
50SC-8	27 Aug 65	320 element	20 spraybar	3260	2980	1.06	6.9	1780	1955	1560	53.5	169.7
50SC-9	2 Sep 65	320 element	20 spraybar	3135	2870	1.18	7.25	1980	2230	1830	53.7	165.1
50SC-10	3 Sep 65	320 element	20 spraybar	3500	3120	0.85	4.1	1490	1625	1390	53.4	170.3
50SC-11	10 Sep 65	320 element	20 spraybar	3300	3080	0.84	5.1	1460	1580	1395	53.5	167.0
50SC-12	18 Sep 65	320 element	192 element	3265	2990	1.15	5.2	1775	2060	1655	56.9	161.3
50SC-1C	24 Sep 65	320 element	20 spraybar	3175	2765	0.85	3.3	1450	1520	1390	53.2	165.7
50SC-2C	28 Sep 65	320 element	192 element	3100	2740	0.84	3.2	1460	1600	1400	53.9	167.3
50SC-3C	28 Sep 65	320 element	192 element	2955	2700	0.69	3.3	1205	1285	1150	53.6	172.3
50SC-4C	30 Sep 65	320 element	192 element	2785	2620	0.71	4.25	1220	1290	1150	53.4	167.6
50SC-5C	30 Sep 65	320 element	192 element	2765	2580	1.06	5.6	1795	2005	1650	55.5	163.0
50SC-6C	30 Sep 65	320 element	192 element	3020	2755	0.845	4.05	1360	1760	1090	53.6	168.1

(1) Nozzle throat insert failed during start transients. Steady-state conditions not achieved.

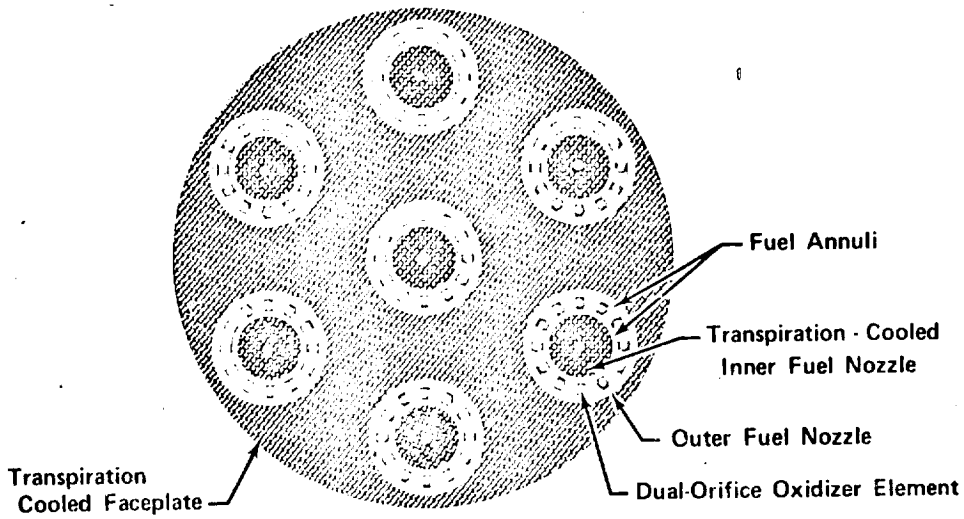

Figure II-22. 250K Variable Area Injector Pattern Has Small Number of Elements Because of Gear Drive Mechanism FD 52663

The fuel entered through an annulus surrounding the circular rows of oxidizer elements. The fuel area was variable, being driven by a gear arrangement as shown in figure II-23.

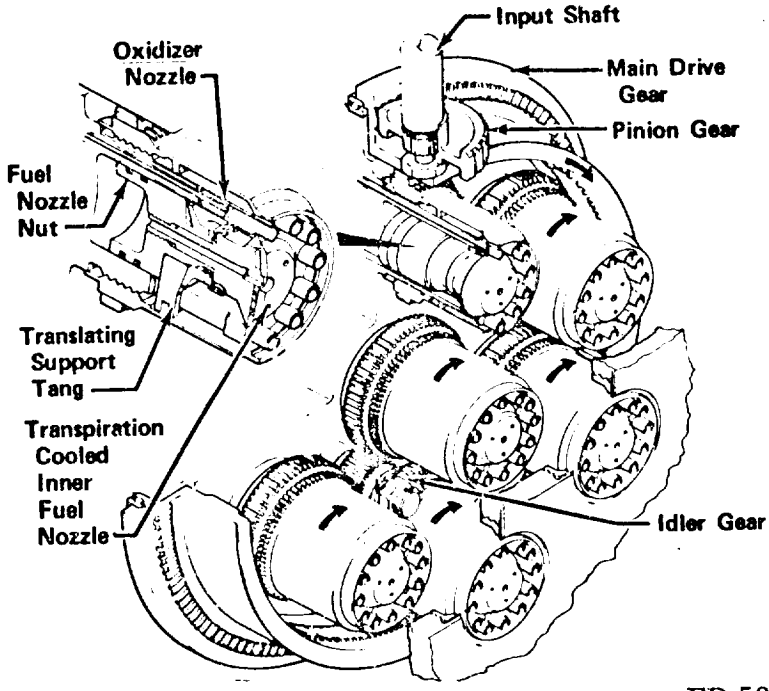

Figure II-23. Gear Drive Mechanism Necessary to Attain 10:1 Throttling Range FD 52662

A total of 104 preburner hot firings were accumulated in both the preburner rig and staged combustion rig. Many of the tests were made to develop starting techniques. Tables II-5 and II-6 summarize the test data. The 250K variable area injector did not provide a good temperature profile.

During the initial design phase of the XLR129 Reusable Rocket Engine Program, a 250K fixed-area preburner injector with dual-orifice self-atomizing liquid oxygen injection elements was fabricated and tested. This injector provided a uniform temperature profile and stable combustion over a wide range of thrust and tank lead starting conditions.

Table II-5. Variable Area Injector Exhibits Poor Temperature Profile

Test No.	Test Date	Rig No. - Build No.	Total Fuel Flow Rate, lb_m/sec	Oxidizer Flow Rate, lb_m/sec	Total Liner Flow Rate, lb_m/sec	Overall Mixture Ratio	Injector Mixture Ratio[1]	Ideal[2] Temperature R	Avera. Combustion Temperature, R[3]	ΔT[4] Profile R	Chamber[5] Stagnation Pressure	$\eta^*_{c_1}$ (corr)	η_{c_2}[7]	Fuel Injection Velocity, ft/sec	Oxidizer Injection Velocity, ft/sec	Fuel-Oxidizer Momentum Ratio	Remarks
	11 Mar 1967	F-33447-1	-	-	-	-	-		1529	260	32	-	-	-	-	-	Ignition Check, Flow Meters Out of Range
	28 Mar 1967	F-33447-1	5.4	4.1	0.28	0.77	0.81	1724	1688	296	323	88.4[10]	99.0	1788	126.3	13.5	
	30 Mar 1967	F-33447-1	5.1	3.8	0.28	0.74	0.78	1679	1680	235	315	92.4[10]	100.0	1797	121.3	16.3	
	31 Mar 1967	F-33447-1	8.1	3.9	0.31	0.63	0.66	1467	1445	257	335	90.6[10]	99.3	1847	127.8	14.8	
	2nd Apr 1967	F-33463-2A	26.0	16.1	1.09	0.62	0.64	1421	1513	302	1351	100.0[6]	103.2	1462	53.0	39.1	
250PB1	2 May 1967	F-33463-2A	13.4	9.7	0.57	0.65	0.68	1490	1490	181	725	100.7[6]	100.0	1455	34.8	55.5	
			12.7	9.3	0.53	0.74	0.77	1655	1665	193	740	100.4[6]	100.3	1410	35.2	46.8	
			12.2	9.6	0.51	0.79	0.82	1745	1750	185	740	100.0[6]	100.1	1365	36.3	41.5	
			14.8	8.4	0.61	0.57	0.59	1335	1335	153	740	100.5[6]	99.3	1545	33.6	70.0	
250PB2	3 May 1967	F-33463-2A	14.2	8.1	0.48	0.57	0.59	1320	1265	221	710	100.9[6]	97.9	1235	32.5	59.2	5 T/C Out
			13.9	8.7	0.47	0.63	0.65	1425	1350	226	725	100.1[6]	97.3	1210	33.1	52.2	5 T/C Out
			13.2	9.0	0.44	0.68	0.71	1530	1455	231	730	99.6[6]	97.5	1150	34.4	43.8	5 T/C Out
			15.1	8.2	0.50	0.54	0.56	1270	1175	198	725	100.0[6]	96.2	1270	31.7	66.6	5 T/C Out
250PB3	5 May 1967	F-33463-2A	37.8	25.5	1.46	0.67	0.70	1410	1465	192	2000	100.7[6]	101.9	1090	81.0	17.5	5 T/C Out
	28 Jun 1967	F-33447-3	54.3	50.2	1.80	0.93	0.96	1893	2011	929	3491	98.8[6]	103.4	1045	149.3	6.7	
	16 Jul 1967	F-33447-4	34.1	28.3	1.26	0.83	0.86	1727	1506	408	1975	94.6[6]	96.4	1124	90.6	13.2	
250PB4	22 Jul 1967	F-33447-5	34.6	27.0	1.12	0.78	0.81	1648	1618	473	1518	99.9[8]	99.1	1233	87.2	17.0	1 T/C Out
250PB5	23 Jul 1967	F-33447-5	65.6	66.8	2.01	1.02	1.05	2058	1962	490	3390	98.1[8]	97.6	1329	197.5	6.2	1 T/C Out
250PB6	24 Jul 1967	F-33447-5	67.2	68.2	2.05	1.01	1.05	2050	2028	279	3464	98.2[8]	99.5	1329	203.5	6.0	3 T/C Out
250PB7	25 Jul 1967	F-33447-5	78.7	70.0	2.35	0.89	0.92	1748	1717	350	3414	97.1[8]	98.0	1241	209.7	6.2	3 T/C Out
250PB8	26 Jul 1967	F-33447-5	68.2	66.5	2.34	0.98	1.01	1853	1809	734	3217	95.8[8]	98.6	907	196.9	4.4	3 T/C Out
250PB9	26 Jul 1967	F-33447-5	12.4	8.7	0.34	0.71	0.74	1418	1470	626	475	97.0[8]	101.9	751	37.2	26.2	3 T/C Out
250PB10	26 Jul 1967	F-33447-5	56.6	70.0	1.75	1.24	1.28	2364	(9)	(9)	3293	97.1[8]	(9)	1117	207.6	4.0	5 T/C Overscaled
	1 Aug 1967	F-33447-5B	13.4	8.4	0.40	0.48	0.50	1145	1092	158	300	(11)	97.7	1686	53.4	61.5	
	1 Aug 1967	F-33447-5B	12.8	8.5	0.39	0.51	0.53	1176	1148	121	286	(11)	98.7	1656	51.5	59.5	

(1) Injector fuel flow rate = total fuel flow rate - total liner coolant flow rate
(2) Based on injector mixture ratio
(3) Based on area-weighted thermocouple data 11.2 inches downstream of injector
(4) ΔT = maximum temperature - average temperature
(5) Stagnation pressure equals static pressure within data roundoff
(6) Corrected for C_d = 0.954 (geometric throat area = 6.78 in^2)
(7) η_{c_2} (average temperature - ideal temperature / ideal temperature) x 100.
(8) Using C_D = 0.956 (throat area = 9.0732 in^2)
(9) Calculations could not be made because 5 T/C were overscaled
(10) Corrected for C_d = 0.954 (geometric throat area = 5.94 in^2)
(11) Not calculated. Throat $A(C_d)$ not available for this configuration.

Table II-6. Poor Profile Limits Maximum Average Preburner Temperature

Test No.	Date	Staged Combustion/Preburner	Total Fuel Flow Rate, lb_m/sec	Oxidizer Flow Rate, lb_m/sec	Total Liner Flow Rate, lb_m/sec	Overall Mixture Ratio	Injector[1] Mixture Ratio	Ideal[2] Temperature, °R	Average[3] Temperature, °R	T[4] Profile, °R	Chamber Static Pressure	η_{c^*}[5]	Fuel Injection Velocity, ft/sec	Oxidizer Injection Velocity, ft/sec	Fuel Oxidizer Momentum Ratio
250SC1C	18 Aug 1967	F-35108-1/F-33463-5	13.3	6.4	0.68	0.48	0.50	1166	1188	57	589	100.9	1979	42.9	87.2
250SC2C	30 Aug 1967	F-35108 1/F-34463-5	13.8	8.3	0.47	0.60	0.62	1397	1406	281	604	100.3	1546	38.1	63.0
			35.9	23.3	1.21	0.65	0.67	1459	1484	327	1596	100.8	1520	78.3	28.0
250SC3C	31 Aug 1967	F-35108-1/F-33463-5	13.6	8.0	0.46	0.59	0.61	1379	1442	339	606	102.3	1519	36.7	66.1
			35.4	23.2	1.21	0.65	0.68	1474	1472	359	1600	100.0	1504	77.5	27.7
			68.1	40.8	2.28	0.60	0.62	1341	1314	235	3021	99.0	1550	125.9	19.3
250SC4C	1 Sept 1967	F-35108-1/F-34463-5	13.7	8.3	0.50	0.60	0.62	1396	1433	264	618	101.3	1666	38.5	67.0
			35.6	23.2	1.29	0.65	0.67	1460	1500	196	1599	101.4	1628	78.6	29.7
			68.1	39.8	2.40	0.58	0.60	1306	1382	226	3095	102.9	1587	122.8	20.7
250SC5C	8 Sept 1967	F-35108-1/F-34463-5	14.2	8.1	0.23	0.57	0.58	1308	1354	164	644	101.7	1630	39.0	69.9
			36.3	23.0	0.58	0.63	0.64	1405	1428	198	1600	100.8	1670	78.9	31.9
			70.9	39.2	1.10	0.55	0.56	1233	1261	216	3088	101.1	1677	121.8	23.7
250SC8C	9 Sept 1967	F-3510601/F-34463-5	13.8	8.2	0.23	0.59	0.60	1337	1359	235	615	100.8	1574	38.9	65.3
			35.5	23.0	0.57	0.64	0.66	1424	1459	275	1567	101.2	1572	78.6	29.4
			62.1	45.7	0.95	0.73	0.74	1557	1571	367	3065	100.4	1492	138.9	13.9
250SC7C	14 Sept 1967	F-35108-1/F-34463-5	14.2	8.1	0.25	0.57	0.58	1320	1326	174	633	100.2	1644	38.6	70.6
			36.4	22.9	0.60	0.63	0.64	1404	1448	265	1595	101.6	1687	78.6	32.5
			74.3	52.0	1.17	0.70	0.71	1472	1563	399	3264	103.0	1587	157.8	13.7
250SC8C	15 Sept 1967	F-35108-1/F-34463-5	11.7	7.0	0.19	0.60	0.61	1367	1432	264	575	102.3	1515	36.4	66.0
			44.8	29.1	0.71	0.65	0.66	1433	1447	241	2180	100.5	1570	96.0	24.0
			65.3	44.2	1.01	0.67	0.68	1461	1488	274	3133	100.9	1494	136.1	16.5
250SC9C	15 Sept 1967	F-35108-1/F-34463-5	11.5	7.4	0.21	0.64	0.66	1453	1471	161	567	100.6	1493	35.8	61.3
			44.6	29.2	0.75	0.65	0.66	1448	1485	202	2183	101.3	1549	95.9	23.4
			63.6	43.9	1.05	0.69	0.70	1495	1510	273	3089	100.5	1592	135.6	16.2
			63.6	43.5	1.06	0.68	0.69	1486	1466	217	2956	99.3	1650	133.8	17.2
250SC10	18 Sept 1967	F-35108-1/F-34463-5	17.3	10.7	0.23	0.62	0.63	1399	1513	438	689	104.0	1602	45.4	54.5
250SC11C	18 Sept 1967	F-35108-1/F-34463-5	17.1	9.0	0.25	0.52	0.53	1231	1254	222	655	101.0	1638	43.0	69.3
			59.2	35.2	0.82	0.59	0.60	1268	1370	380	2319	103.9	1380	113.0	19.7
			85.5	53.7	1.20	0.63	0.63	1315	1356	232	2887	101.6	1579	167.0	14.4
250CP1C	28 Sept 1967	F-35111-1/F-33463-6	14.0	8.1	0.25	0.55	0.56	1280	1345	168	642	102.5	1534	38.6	68.3
250CP2C	29 Sept 1967	F-35111-1/F-33463-6	14.0	8.0	0.22	0.57	0.58	1261	1407	285	643	105.6	1427	37.9	63.3
			69.7	36.7	0.95	0.53	0.53	1121	1220	166	3160	104.3	1365	112.5	22.1
250CP3C	29 Sept 1967	F-35111-1/F-33463-6	13.2	8.2	0.19	0.63	0.63	1383	1574	210	630	106.7	1361	36.7	56.7
			52.5	35.0	0.74	0.67	0.68	1421	1491	249	2781	102.4	1286	107.4	17.2

(1) Injector fuel flow rate = total fuel flow rate - total liner coolant flow rate
(2) Based on injector mixture ratio
(3) Based on area weighted thermocouple data 11.2 inches downstream of injector
(4) ΔT = maximum temperature - average temperature
(5) η_{c^*} = (average temperature/ideal temperature) $^{0.5} \times 100\%$

A comprehensive cold flow test matrix, summarized in table II-7, which tested 36 tangential slot swirler element configurations was run to cover the design parameters of the self-atomizing preburner injector elements. Individual units were water and nitrogen flow tested to determine effective flow area, cone angle, and stability characteristics (ref. 5). The influential parameter on hydraulic stability was found to be slot-to-tube area ratio (A_S/A_O) as shown in figure II-24. The 0.124-in. inner diameter element with an area ratio (A_{slot}/A_{tube}) of 0.54 was the element selected for the fixed-area preburner injector because it was stable and fit the engine cycle requirments. The element selected from this cold flow program has been used in all 250K fixed area preburner injectors as well as selected for the SSME design.

Table II-7. Cold Flow Test Matrix Determines Stable Injector Elements

Tube Length

Slot Area	Nominal ID (in.)		Short Length Configuration					Long Length Configuration				
			0.075	0.085	0.095	0.110	0.124	0.075	0.085	0.095	0.110	0.124
Constant Area Ratio A_s/A_o = 1.5 Nominal	Constant W/D, Slot Width to Tube Diameter of 0.245	Element Letter	P	H	B	L	D	P	H	B	L	D
		Spray Cone	Unstable	Unstable	Unstable	Unstable	Unstable	Unstable	Unstable	Unstable	Unstable	Unstable
		Gas Core						Unstable	Unstable	Unstable	Unstable	Stable
		Secondary Gage Fluctuation	±5 psi max	±5 psi max	%2 psi max	±5 psi max	±2 psi max	±4 psi max	±2 psi max	%2 psi max	±3.5 psi max	±2.5 psi max
		Oscilloscope Secondary ΔP Frequency and Amplitude	6 psi max 600 cps max	8 psi max Frequency not Recorded	Not Recorded	1.0 psi max at 50 cps	Not Recorded	6 psi max 300 cps max	8 psi max Frequency not Recorded	Not Recorded	1.6 psi max 100 cps max	Not Recorded
		Spray Cone Angle and Drop Size	45 to 60 deg Fine to Medium	35 to 45 deg Medium to Fine	20 to 30 deg Fine Drop Size	55 to 65 deg Fine at All Times	12 to 25 deg Fine Drop Size	20 to 40 deg Heavy to Medium	15 to 60 deg Very Heavy to Fine	20 to 50 deg Medium to Fine	45 to 65 deg Medium to Fine	24 to 50 deg Heavy to Medium
	Slot Width of 0.010 in. min Nominal	Element Letter	O	G	A	K	C	O	G	A	K	C
		Spray Cone	Unstable	Unstable	Unstable	Unstable	Unstable	Unstable	Unstable	Unstable	Unstable	Unstable
		Gas Core						Unstable	Unstable	Unstable	Unstable	Unstable
		Secondary Gage Fluctuation	±3 psi max	±3 psi max	±3 psi max	±1.0 psi max	±0.5 psi max	±6 psi max	±4 psi max	±2 psi max	±2.0 psi max	±2 psi max
		Oscilloscope Secondary ΔP Frequency and Amplitude	2 psi max Frequency not Recorded	3.6 psi max Frequency not Recorded	Not Recorded	5 psi max Frequency not Recorded	psi max Frequency not Recorded	2 psi max Frequency not Recorded	3 psi max Frequency not Recorded	Not Recorded	3 psi max Frequency not Recorded	3 psi max Frequency not Recorded
		Spray Cone Angle and Drop Size	25 to 45 deg Heavy to Fine	45 to 55 deg Heavy to Fine	15 to 30 deg Medium to Fine	25 to 45 deg Heavy to Fine	40 to 65 deg Medium to Fine	20 to 30 deg Heavy to Fine	30 to 50 deg Heavy to Fine	24 to 50 deg Heavy to Fine	15 to 45 deg Very Heavy to Medium	35 to 45 deg Heavy to Fine
Constant Equivalent Cycle A_{eq}	Constant W/D, Slot Width to Tube Diameter of 0.245	Element Letter		J	B	N	P		J	B	N	F
		Spray Cone		Unstable		Unstable	Stable		Unstable		Unstable	Stable
		Gas Core							Unstable		Unstable	Stable
		Secondary Gage Fluctuation		±8 psi max	Same As Element "B" Above	±6 psi max	±5 psi max		±8 psi max	Same As Element "B" Above	±5 psi max	±4 psi max
		Oscilloscope Secondary ΔP Frequency and Amplitude		9.5 psi max at 100 cps		1 psi max Frequency not Recorded	6 psi max Frequency not Recorded		9 psi max at 200 cps		1 psi max Frequency not Recorded	5 psi max Frequency not Recorded
		Spray Cone Angle and Drop Size		50 to 65 deg Medium to Fine		30 to 45 deg Heavy to Fine	55 to 70 deg Heavy to Fine		25 to 35 deg Heavy to Medium		15 to 50 deg Heavy to Fine	35 to 45 deg Heavy to Fine
	Slot Width of 0.010 in. min Nominal	Element Letter		I	A	M	E		I	A	M	E
		Spray Cone		Unstable		Stable	Stable		Unstable		Stable	Stable
		Gas Core							Unstable		Stable	Stable
		Secondary Gage Fluctuation		±1 psi max	Same As Element "A" Above	±1.5 psi max	±2 psi max		±2 psi max	Same As Element "A" Above	±1 psi max	±4 psi max
		Oscilloscope Secondary ΔP Frequency and Amplitude		4.2 psi max at 200 cps		1 psi max at 100 cps	1 psi max Frequency not Recorded		3 psi max at 200 cps		0.2 psi max at 100 cps	5 psi max Frequency not Recorded
		Spray Cone Angle and Drop Size		60 to 65 deg Medium to Fine		55 to 65 deg Fine Drops at All Times	35 to 65 deg Medium to Fine		30 to 60 deg Heavy to Fine		40 to 55 deg Medium to Fine	25 to 50 deg Medium to Fine

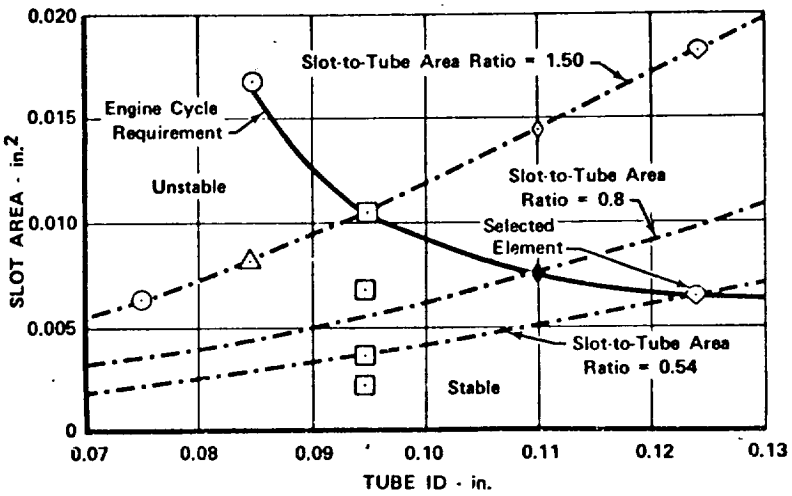

Figure II-24. Injector Element Selected for Stability FD 46424

- SELECTED ELEMENT CONFIGURATION VERIFIED IN HOT FIRING

During the XLR129 Program, a fixed-area injector was designed and two injectors of this type were fabricated. Fourteen preburner combustion tests were conducted. The supporting data and analysis (SDA) 250K fixed-area injector is shown in figure II-25. The SDA injector consisted of 252 dual-orifice tangential slot swirler oxidizer elements. The element configuration used was that selected from the cold flow. Fuel is injected concentrically around the oxidizer element. The basic injector pattern was a uniformly-spaced hexagonal pattern with an element-to-element centerline distance of 0.480 in. Using two injectors with fuel annuli designed for 200 and 400 psi pressure drops yielded typical data as shown in figure II-26. The temperature profile was greatly improved over the variable area preburner profile.

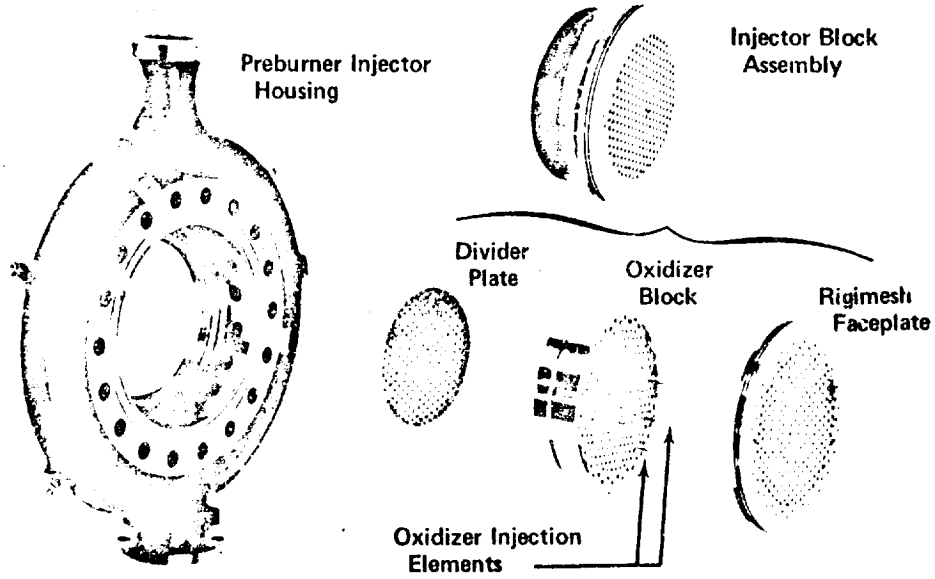

Figure II-25. Preburner Injector Uses Self-Atomizing Oxidizer Element in 252 Uniformity Spaced Places FD 52306

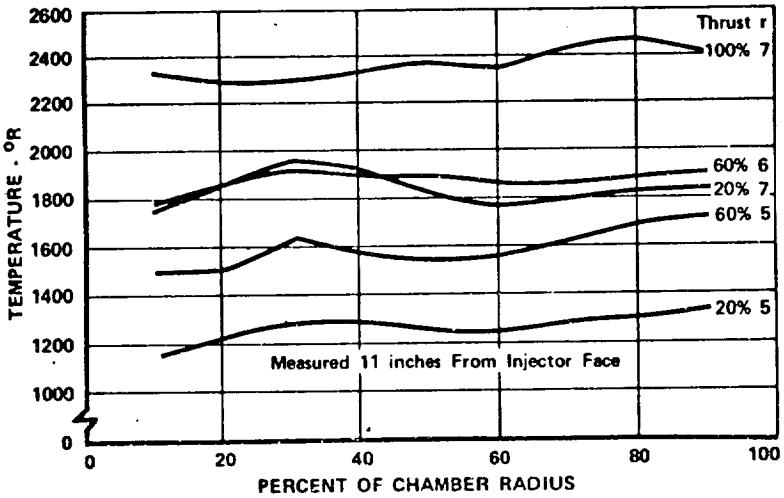

Figure II-26. Demonstrated Preburner Temperature Profile FD 46282

SECONDARY VOLUME DECREASE ELIMINATES COMBUSTION OSCILLATIONS

During the combustion testing of the SDA preburner injector, low frequency, limited amplitude, combustion instability was encountered at thrust levels below 25% and several tests were programmed to obtain data on influential parameters. An analog model of the preburner injector, combustion chamber, and a portion of the test stand was constructed to determine the influence of various parameters on low frequency stability. The analog model, which essentially duplicated the test results of frequency and amplitude, indicated that the large oxidizer secondary volume contributed significantly to the instability and that reducing the liquid oxygen secondary manifold volume would detune this cavity and eliminate the instability, figure II-27. The SDA injector had a secondary volume of 54.4 cubic in. The XLR129 injector was subsequently designed to change the secondary volume from 54.4 cubic in. used in the SDA injector to 27.2 cubic in. No chugging was experienced with this injector during XLR129 preburner testing.

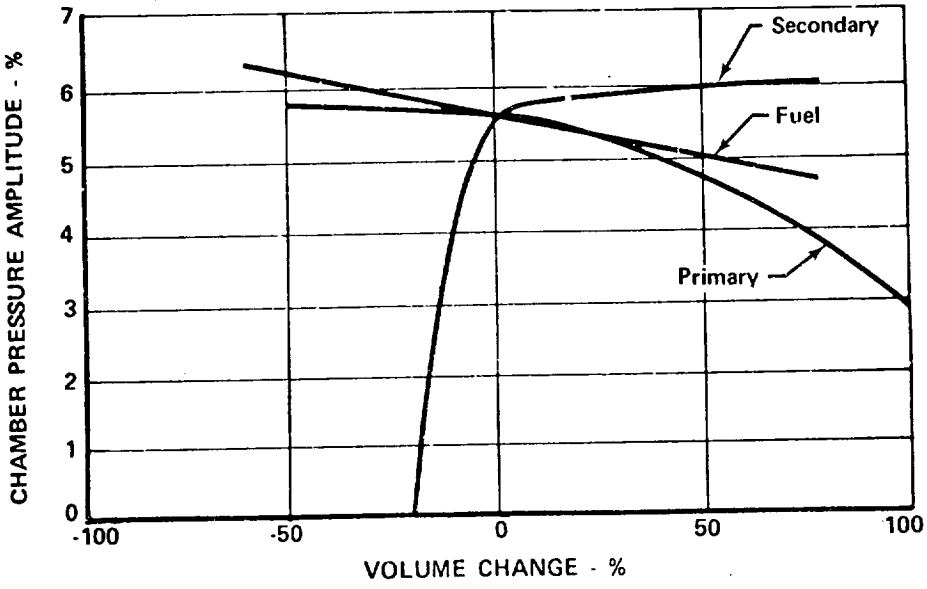

Figure II-27. Predicted Volume Influence on P/B Stability FD 52303

- XLR129 FLIGHT WEIGHT INJECTORS ACCUMULATE 34 HOT FIRINGS IN THREE RIG CONFIGURATIONS

Preburner testing was conducted during the XLR129 program in the following three test categories: (1) preburner rig tests, (2) hot gas system tests, and (3) hot turbine tests.

Two preburner injectors, shown in figure II-28, were designed and fabricated during the demonstrator phase of the XLR129 Program with 14 rig firings conducted with the first preburner injector. Twenty firings were made with the second injector. This second injector was used eight times in preburner rig tests, six times in hot gas system tests, and six times in hot turbine tests. These two injectors were fired a combined total of 34 times through 13 August 1970. (Refer to SSME Related Data, PWA FR-4460, for detailed information on these test.)

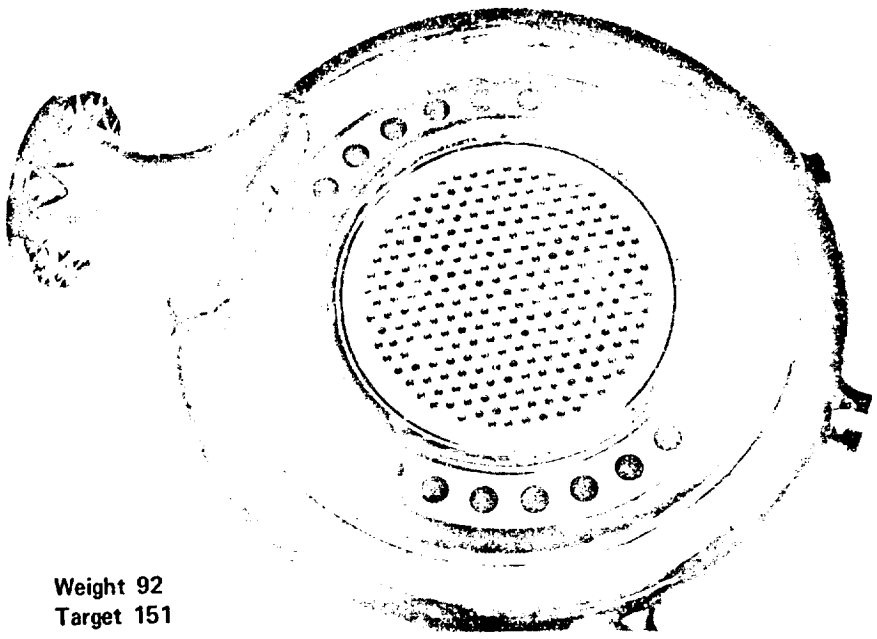

Figure II-28. XLR129 Flight Weight Injector Based on SDA Injector Design FD 31502B

These flightweight injectors were based on the SDA injector design. The XLR129 injectors used 253 dual-orifice tangential slow swirler oxidizer elements, concentric fuel injection, and uniform 0.480-in. spaced hexagonal pattern.

- PREBURNER RIG TESTS VERIFY INJECTOR SUITABLE FOR HOT GAS SYSTEM AND HOT TURBINE TESTS

Twenty-two hot fire tests were made on five builds of preburner rigs 35131 and 36133 between 13 August 1969 and 14 February 1970. The initial six rig tests displayed unacceptable temperature profiles as a result of fuel maldistribution caused by facility fuel plumbing and the uncooled combustion chamber liners were damaged. The subsequent 16 perburner rig tests demonstrated acceptable temperature profiles and only minor erosion and heat discoloration of the combustion chamber liners was evident. A test summary is shown in table II-8.

Table II-8. Acceptable Temperature Profile Attained at 15 Inch Plane After Run 6.01

Build	Run	Preburner Chamber Pressure (psia)	Percent Thrust (%)	Engine Mixture Ratio	Average Combustion Temperature (°R)	Maximum Temperature Minus Average (°R)	Comments
Rig 35131 Using No. 1 Injector							
1	1.01	669	20	5	1306	72	Burned through uncooled scrub liner
		672	20	6	1722	98	
		673	20	7	2115	114	
		1247	35	5	1263	121	
2	2.01	693	20	5	1302	215	Uncooled scrub liner blued in same area as build 1
		691	20	6	1639	190	
2	3.01	691	20	5	1303	159	Uncooled liner blued area burned through
		700	20	6	1702	234	
		704	20	7	2090	263	
3	4.01						LO_2 Flowmeter error caused advance at +1.4 sec
3	5.01						Liner thermocouple error caused advance at +6.7 sec
3	6.01	726	20	5	1430	539	Added transpiration-cooled liner and two new temperature rakes in burned area. Burned through transpiration-cooled liner in same area as builds 1 and 2.
		741	20	6	1827	621	
		739	20	7	2297	611	
4	7.01	701	20	5	1349	216	Full duration run of 52.9 sec
		2020	50	5	1402	190	
4	8.02						Advanced at +1.4 sec due to high outer combustion liner temperature
4	9.01						Advanced at +1.4 sec due to high outer combustion liner temperature
4	10.02	694	20	5	1349	186	Fuel injector ΔP error caused advance at +29.1 sec
4	11.01	2032	50	5	1415	119	Full duration run of 35.0 sec
		1985	50	6	1769	155	
		1964	50	7	2106	173	
4	12.01						Outer liner temperature error caused advance at +16.4 sec
4	13.01	3283	75	5	1692	150	Outer liner temperature error caused advance a +25.0 sec
		2982	75	7	2268	244	
4	14.01	2967	75	7	2260	312	Overboard fuel leak caused advance at 30.5 sec
		4276	100	6	2054	259	
	1.01	724.4	20	5	1344	280	Full duration run of 28.36 sec. Liners are in good condition.
		2071	50	5	1427	155	
	2.01						False low file purge pressure advance at 17.53 sec which is prior to reaching 20%/5, due to sequencer patching error.
	3.01						False high scrub liner temperature advance at 6.8 sec. which is prior to reaching 20%/5 due to incorrect voltage level setting on the comparator circuit.
	4.01						Low igniter combustion temperature at 0.1 sec prior to SSV up caused by foreign material in igniter gaseous O_2 metering orifice
	5.01	707.2	20	5	1368	207	Full duration run of 44 sec. Liners in good condition. Small dime sized eroded area in zone one of the transpiration liner.
		708.4	20	6	1765	258	
		708.4	20	7	2145	275	
		2042	50	5	1429	203	
		1998	50	6	1797	217	
		1964	50	7	2138	269	

Build	Run	Preburner Chamber Pressure (psia)	Percent Thrust (%)	Engine Mixture Ratio	Average Combustion Temperature (°R)	Maximum Temperature Minus Average (°R)	Comments
Rig 35133 Using No. 2 Injector							
	6.01						False high combustion temperature advance at 23.72 sec. which is prior to reaching the first data point caused by bad patch pin connect in the controls board. Liner still in good condition.
	7.01	2957	75	7	2190	252	False low combustion temperature advance at 26.4 sec. which is near the end of the 75%/7 data point caused by burned instrumentation cable. Liners still in good condition.
	8.01	2964	75	7	2203	258	Manual advance at 28.2 sec. which is just prior to reaching 100%/6 data point, because of stand fire.

Rig build 35131-4, run 11.01 exemplifies 50% thrust level performance and figures II-29 and II-30 show the fixed area preburner injector temperature profile for various thermocouple positions at 50% thrust. The shape of the temperature profile shown at 50% is typical of the shape at all thrust levels. Predicted versus actual performance parameters are shown in table II-5.

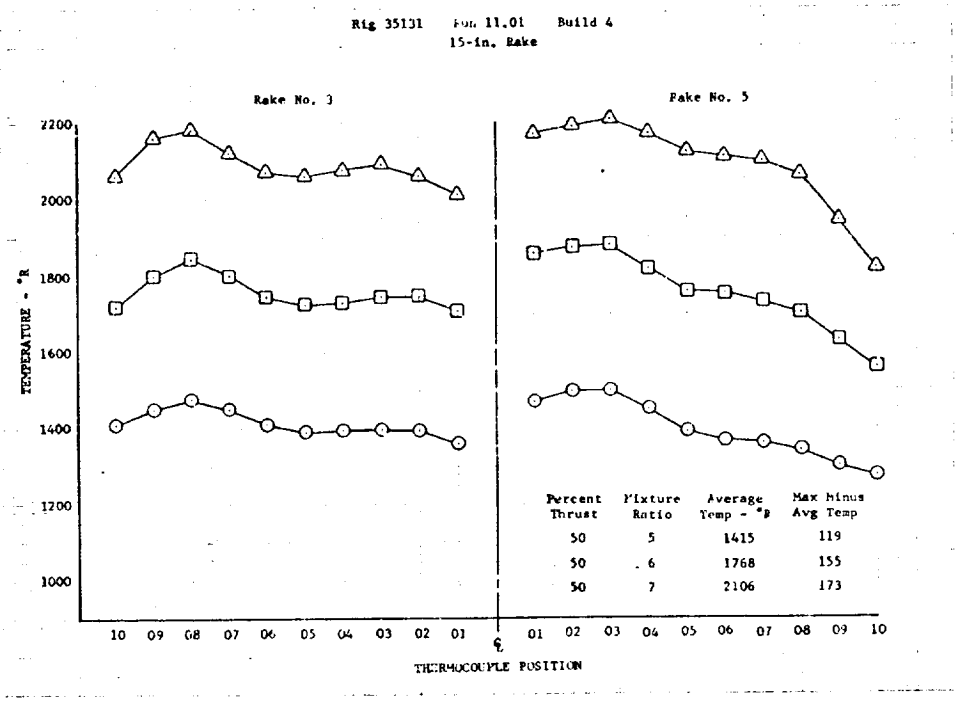

Figure II-29. Fixed Area Preburner Temperature Profile DF 79865

- PULSING OF PREBURNER RIG DEMONSTRATED INJECTOR STABILITY

Figure II-31 shows XLR129 preburner chamber pulsing tests at the 20% thrust level. An overpressure spike of 8.9% $\Delta P/P$ at 15 in. axially from the injector and of 12.8% at 2.7 in. was produced. The pulse resulted in a frequency response of approximately 3000 Hz which damped in three milliseconds. This short damp time is well within the SSME CEI specification limit of $1600/\mu f$ milliseconds.

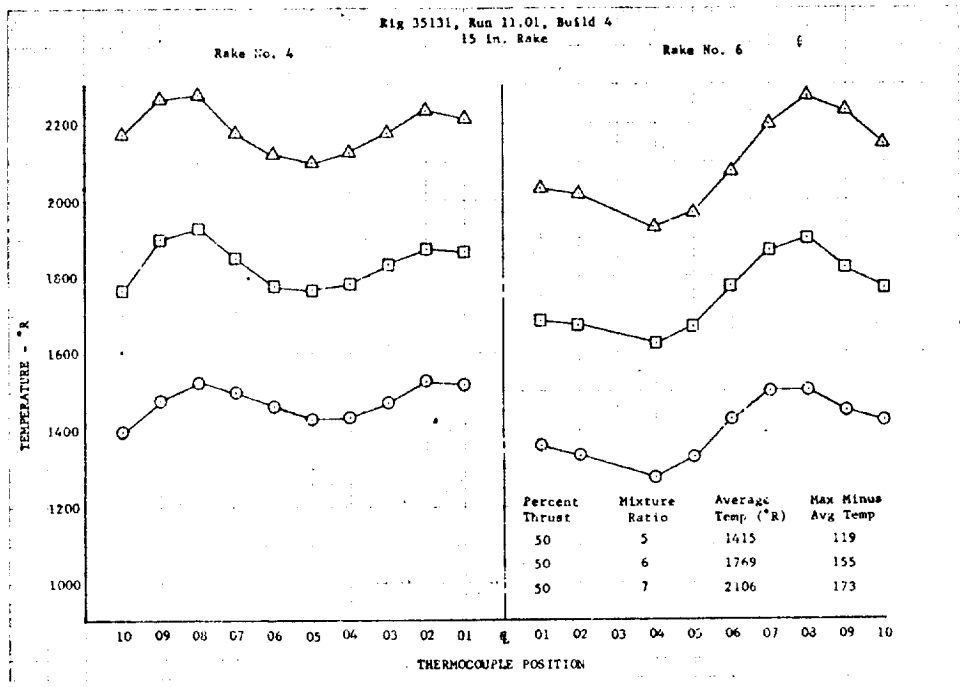

Figure II-30. Fixed Area Preburner Temperature Profile DF 79866

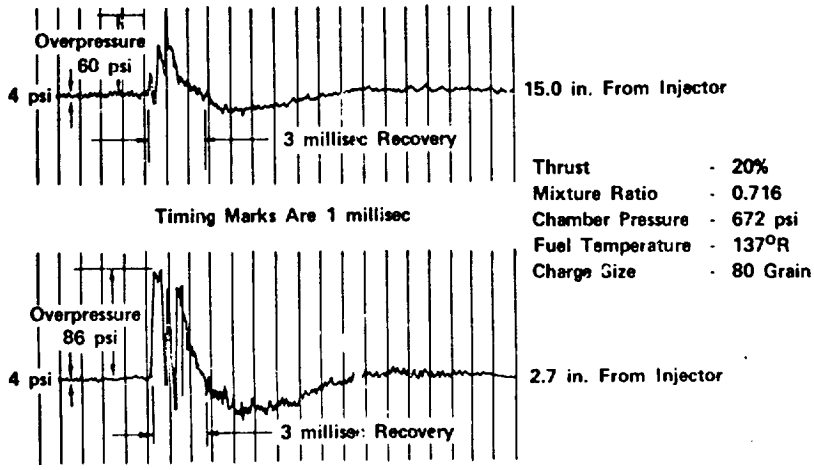

Figure II-31. Pulsed Preburner Rig Exhibits Rapid Recovery To Stable Combustion FD 31515B

- TRANSPIRATION-COOLED PREBURNER LINER NECESSARY EVEN WITH GOOD TEMPERATURE PROFILE

The general conclusions that can be made from the preburner rig test are:

1. The temperature profile is acceptable for driving the fuel turbopump.

2. A transpiration cooled liner is necessary in the high-energy release zone of the preburner chamber.

- PREBURNER INJECTOR OPERATES SATISFACTORY WHEN FIRED INTO HOT GAS SYSTEM DUCTS

The hot gas system tests combined the preburner oxidizer valve, preburner injector, transition case assembly, and rig hardware fuel and oxidizer turbopump simulators. The hot gas system rig permitted testing of the integrated components under engine conditions and allowed the preburner injector to be check fired in the hot gas ducts before use of actual fuel turbopump hardware.

The No. 2 demonstrator preburner injector and No. 1 trasition case were fired six times at the E-8 test stand. This series of tests demonstrated that the preburner injector ran satisfactorily when integrated with the hot gas system hardware. The turbine inlet temperature profile on the fuel pump simulator of 103°R maximum to average at an average temperature of 1452°R was acceptable for operation of the fuel turbopump.

Table II-9 shows a summary of test data for the hot gas system firings. Table II-10 and II-11 show test results versus predicted for rig No. 35139-1 at an engine mixture ratio of five and thrust levels of 20% and 50% of nominal.

It was concluded that the hot gas system had performed properly and was sufficiently checked out to allow its use to drive the turbine of a fuel turbopump assembly.

Table II-9. Six Hot Firings Confirm Hot Gas System Satisfactory for Driving Fuel Pump

Run	Preburner Chamber Pressure psia	Pump Simulator Discharge Pressure psia	Percent Thrust %	Engine Mixture Ratio	Average Combustion Temperature °R	Maximum Minus Average Temperature °R	Comments
1.01							False high transition case differential pressure advance at 8.9 sec.
2.01							High combustion temperature advance at 0.5 sec due to slow fuel delivery.
3.01	2071	1555	50	5	1452	122	Full duration run of 13.7 sec. P/B liner locally discolored.
4.01							False high transition case differential pressure at 6.7 sec. Centerball liner and P/B heatshield buckled during hard ignition caused by facility valve dragging.
5.01							False low combustion temperature at 2.8 sec.
6.01	679	501	20	5	1330	221	Full duration run of 10.1 sec.

Table II-10. Hot Gas System Operated As Predicted, Engine Thrust Level 50% Mixture Ratio 5

Preburner	Predicted Engine Cycle 6 *(Cycle 8)	Test Results
Oxidizer Primary Flow - lb/sec	7.856**	6.63
Oxidizer Secondary Flow - lb/sec	20.30**	21.8
Oxidizer Primary/Total Flow Split	0.2782**	0.233
Injector Face Fuel Flow - lb/sec	36.9*	37.48
Rigimesh Liner Flow - lb/sec	NAV	0.104
Coolant Liner Flow - lb/sec	0.2286*	0.064
Injector Mixture Ratio	0.763**	0.756

**Predicted rig conditions.

Table II-10. Hot Gas System Operated As Predicted, Engine Thrust Level 50% Mixture Ratio 5 (Continued)

Preburner	Predicted Engine Cycle 5 *(Cycle 8)	Test Results
Chamber Discharge Mixture Ratio	0.760*	0.754
Chamber Pressure - psia	2010.0	2071.0
Oxidizer Injector Temperature - °R	208.2**	193.0
Fuel Injector Temperature - °R	142.0**	143.0
Primary Effective Area - in^2	0.063**	0.0491
Secondary Effective Area - in^2	0.5897**	0.667
Fuel Injector Plate Effective Area - in^2	3.7	3.33
Oxidizer Turbine Simulator		
Turbine Inlet Temperature - °R	1465.0	1406.0
Fuel Turbine Simulator		
Turbine Inlet Temperature - °R	1465.0	1471.0
Oxidizer Primary Flow - lb/sec	5.782**	6.34
Oxidizer Secondary Flow - lb/sec	3.809**	2.78
Primary/Total Oxidizer Flow Split	0.6029**	0.696
Injector Face Plate Fuel Flow - lb/sec	13.33**	13.52
Rigimesh Liner Flow - lb/sec	NAV	0.71
Coolant Liner Flow - lb/sec	0.833*	0.0486
Injector Mixture Ratio	0.716	0.672
Chamber Discharge Mixture Ratio	0.713*	0.669
Chamber Pressure - psia	732.4	679.0
Oxidizer Temperature - °R	200.0**	185.7
Fuel Temperature - °R	125.4	128.7
Primary Effective Area - in^2	0.063**	0.0733
Secondary Effective Area - in^2	0.2526**	0.179
Fuel Injector Plate Effective Area - in^2	3.7	3.3
Oxidizer Turbine Simulator		
Turbine Inlet Temperature - °R	1367.0	1235.0
Fuel Turbine Simulator		
Turbine Inlet Temperature - °R	1367.0	1372.0

**Predicted rig conditions.

- PREBURNER INJECTOR SUCCESSFULLY DRIVES FUEL TURBOPUMP IN HOT TURBINE TESTS

Six hot firing tests from 15 July 1970 to 13 August 1970 accumulated 95.8 seconds of hot turbine testing using the No. 2 demonstrator preburner injector. This series of test demonstrated the capability of the integrated fuel turbopump, main case, preburner injector and preburner oxidizer valve to operate at conditions equivalent to 50%, 75%, and 100% engine thrust conditions with mixture ratios of 5, 6, and 7.

Table II-11. Preburner-Transition Case Test Results Rig No. 35139-1, Run No. 6.01, Engine Thrust Level 20%, Mixture Ratio 5

Preburner	Predicted Engine Cycle 6	Test Results
Oxidizer Primary Flow - lb/sec	5.782**	6.34
Oxidizer Secondary Flow - lb/sec	3.808**	2.76
Primary/Total Oxidizer Flow Split	0.6029**	0.696
Injector Faceplate Fuel Flow - lb/sec	13.33**	13.52
Rigimesh Liner Flow - lb/sec	NAV	0.71
Coolant Liner Flow - lb/sec	0.833*	0.0486
Injector Mixture Ratio	0.716	0.672
Chamber Discharge Mixture Ratio	0.713*	0.669
Chamber Pressure - psia	732.4	679.
Oxidizer Temperature - °R	200.**	185.7
Fuel Temperature - °R	125.4	128.7
Primary Effective Area - in^2	0.063**	0.0733
Secondary Effective Area - in^2	0.2526**	0.179
Fuel Injector Plate Effective Area - in^2	3.7	3.3

Table II-11. Preburner-Transition Case Test Results Rig No. 35139-1, Run No. 6.01, Engine Thrust Level 20%, Mixture Ratio 5 (Continued)

Preburner	Predicted Engine Cycle 6	Test Results
Oxidizer Turbine Simulator		
Turbine Inlet Flow - lb/sec	6.76	6.89
Turbine Coolant Flow - lb/sec	0.43*	0.078
Outer Case Coolant Flow - lb/sec	0.16	0.158
Turbine Discharge Static Pressure - psia	566.3	509.0
Turbine Inlet Total Pressure - psia	NAV	685.3
First Stator Discharge Total Pressure - psia	727.4	654.4
Turbine Discharge Total Pressure - psia	582.8	501.6
Diffuser Inlet Total Pressure - psia	NAV	NAV
Diffuser Discharge Total Pressure - psia	NAV	507.3
Turbine Inlet Temperature - °R	1367.	1235.
Fuel Turbine Simulator		
Turbine Inlet Flow - lb/sec	16.52	15.87
Turbine Coolant Flow - lb/sec	0.27*	0.0802
Outer Case Coolant Flow - lb/sec	0.16	0.417
Turbine Discharge Static Pressure - psia	577.1	505.3
First Stator Discharge Total Pressure - psia	725.6	644.3
Turbine Discharge Total Pressure - psia	595.6	485.6
Diffuser Inlet Total Pressure - psia	NAV	483.8
Diffuser Discharge Total Pressure - psia	NAV	540.3
Turbine Inlet Temperature - °R	1367.	1372.
Overall Performance		
Total Oxidizer Flow - lb/sec	9.59**	9.12
Main Run Line Fuel Flow - lb/sec	14.16	13.78
Total Fuel Flow - lb/sec	14.48	14.56
Overall Mixture Ratio	0.622	0.627
Temperature Profile - °R	0*	221
Average Combustion Temperature - °R	1394.**	1330.
Transition Case Plenum Pressure - psia	557.7	500.6
C* Efficiency (Based on Pressure and Flow) - %	100	97.2

*Cycle 8
**Predicted rig conditions

Table II-12 shows a summary of test data for the hot turbine test rig. Tables II-13 and II-15 show test results versus predicted for rig numbers 35155-1 and -2 at various engine mixture ratios and thrust levels.

Figure II-32 shows the major components of the hot turbine test after the last firing. The injector used in these tests was in good condition.

- SSME PREBURNER INJECTOR HAS SAME FEATURES AS XLR129 INJECTOR

Figure II-33 shows the relative size of the SSME preburner injector versus the XLR129 injector. The new injector is essentially a scaled-up version of the XLR129 injector and features the same basic design approach.

Table II-12. Preburner Successfully Drives Fuel Turbopump During Six Hot Firings

Run	Thrust Level Percent	Engine Mixture Ratio	Average Combustion Temperature Based on Average Mixture Ratio (°R)	Preburner Chamber Pressure (psia)	Pump Discharge Pressure (psia)	Pump Speed (rpm)	Pump Inlet Flow (gpm)	Comments
1.02	50	5	1,450	1,868	2,340	29,360	7,400	Full duration test of 13.7 seconds. Rig in good condition.
2.01								False high main case liner differential pressure advance at 6.4 seconds.
3.01	75	5	1,605	2,970	3,610	35,630	7,530	False high main case skin temperature advance at 14.5 seconds.
4.01	75 75	5 6	1,615 1,985	2,965 2,682	3,560 3,368	35,360 34,610	7,460 7,310	False high main case skin temperature advance at 17.2 seconds.
5.02	75 100 100	5 6 7	1,610 2,070 2,395	3,045 4,086 3,889	3,737 4,981 4,623	36,500 40,800 39,500	7,540 7,651 7,422	Full duration test of 22 seconds. Rig in good condition.

Table II-12. Preburner Successfully Drives Fuel Turbopump During Six Hot Firings (Continued)

Run	Thrust Level Percent	Engine Mixture Ratio	Average Combustion Temperature Based on Average Mixture Ratio (°R)	Preburner Chamber Pressure (psia)	Pump Discharge Pressure (psia)	Pump Speed (rpm)	Pump Inlet Flow (gpm)	Comments
6.01	50	7	2,115	1,612	2,423	30,000	7,076	False loss of pump speed advance at 20 seconds. Rig in good condition.
	100	5	1,912	4,200	5,554	44,500	9,956	

Table II-13. Summary of Hot Turbine Test Data Shows Preburner Operates as Predicted, Engine Thrust Level 75%

Preburner	Mixture Ratio 5.0 Predicted Engine Cycle 6	Mixture Ratio 5.0 Test Results	Mixture Ratio 6.0 Predicted Engine Cycle 6	Mixture Ratio 6.0 Test Results
Total Fuel flow - lb_m/sec	61.14	60.784	51.88	49.6
Total Oxidizer Flow - lb_m/sec	50.20	47.630	48.52	50.432
Oxidizer Primary - lb_m/sec	9.82	10.127	8.075	9.528
Oxidizer Secondary - lb_m/sec	40.38	37.503	40.44	40.904
Primary/Total Flow Split	0.1956	0.213	0.1665	0.189
Injector Fuel Flow - lb_m/sec	56.36	55.924	47.53	47.234
Rigimesh Coolant Flow - lb_m/sec	NAV	0.844	NAV	0.672
Coolant Liner Flow - lb_m/sec	0.351*	0.253	0.293*	0.202
Injector Mixture Ratio	0.891	0.839	1.021	1.053
Chamber Pressure - psia	3281	2965.8	3097.	2882.4
Average Combustion Temperature - °R	1713.	1625**	1934	1980**
Oxidizer Temperature - °R	221.	179.0	213.	177.
Fuel Temperature - °R	160.	162.1	173.	172.
Oxidizer Turbine Simulators				
Turbine Inlet Temperature (Average) - °R	1687.	1502.	1904.	1854.
Turbine Discharge Temperature - °R	1572	NAV	1789.	NAV
Temperature Profile (Maximum-Average) - °R	0	28.0	0	56.
Fuel Turbine				
Turbine Inlet Temperature - °R	1687	1519.4 (***)	1904.	1868. (***)
Turbine Discharge Temperature - °R	1566.	1420.1	1780	1765.
Injector Effective Areas				
Oxidizer				
Primary A_{cd} - $in.^2$	0.063	0.0721	0.063	0.0754
Secondary A_{cd} - $in.^2$	0.658	0.676	0.677	0.677
Fuel				
Overall - $in.^2$	3.48	3.04	3.48	3.18
Plate - $in.^2$	3.70	3.46	3.70	3.44

*Cycle 8
**Based on Average Mixture Ratio
***Based on Single Temperature Probe

Table II-14. Summary of Hot Turbine Test Data Shows Preburner Operates as Predicted

Preburner	75% Thrust Mixture Ratio 5 Predicted Engine Cycle 6	75% Thrust Mixture Ratio 5 Test Results	100% Thrust Mixture Ratio 6 Predicted Engine Cycle 6	100% Thrust Mixture Ratio 6 Test Results	100% Thrust Mixture Ratio 7 Predicted Engine Cycle 6	100% Thrust Mixture Ratio 7 Test Results
Oxidizer Turbine Simulator						
Turbine Inlet Temperature (Average) - °R	1687.	1658.	2055.	2085.	2292.	2398.
Turbine Discharge Temperature - °R	1572.	NAV	1911.	NAV	2144.	NAV
Temperature Profile (max - avg) - °R	0.0	45.0	0.0	94.0	0.0	126.0
Fuel Turbine						
Turbine Inlet Temperature - °R	1687	NAV	2055.	NAV	2292	NAV
Turbine Discharge Temperature - °R	1566.	1404.	1901	1786.	2132	2086.

Table II-14. Summary of Hot Turbine Test Data Shows Preburner Operates as Predicted (Continued)

Preburner	75% Thrust Mixture Ratio 5 Predicted Engine Cycle 6	Test Results	100% Thrust Mixture Ratio 6 Predicted Engine Cycle 6	Test Results	100% Thrust Mixture Ratio 7 Predicted Engine Cycle 6	Test Results
Injector Effective Areas						
Oxidizer						
Primary A_{cd} - $in.^2$	0.063	0.067	0.063	0.065	0.063	0.059
Secondary A_{cd} - $in.^2$	0.658	0.679	0.710	0.724	0.723	0.734
Fuel						
Overall - $in.^2$	3.48	2.79	3.48	2.82	3.48	2.97
Plate - $in.^2$	3.70	3.27	3.70	3.19	3.70	3.29
Total Fuel Flow - lb_m/sec***	56.71	56.83	64.63	64.12	55.86	55.25
Total Oxidizer Flow - lb_m/sec	50 20	47.73	71.45	70.71	70.02	71.54
Oxidizer Primary - lb_m/sec	9.82	9.70	8.15	8.45	6.08	6.24
Oxidizer Secondary - lb_m/sec	40.38	38.03	63.31	62.26	63.94	65.31
Primary/Total Flow Split - lb_m/sec	0.196	0.203	0.114	0.120	0.086	0.087
Injector Fuel Flow - lb_m/sec	56.36	55.67	64.23	62.85	55.52	54.20
Rigimesh Coolant Flow - lb_m/sec	NAV	0.868	NAV	0.976	NAV	0.806
Coolant Liner Flow - lb_m/sec	0.351*	0.267	0.398*	0.293	0.338*	0.242
Injector Mixture Ratio	0.891	0.844	1.112	1.108	1.261	1.301
Chamber Pressure - psia	3281	3045.	4367.	4086.	4175.	3889.
Average Combustion Temperature - °R	1713.	1634.**	2086.	2080.**	.2326	2405.**
Oxidizer Temperature - °R	221.	178.	220.	177.	215.	178.
Fuel Temperature - °R	160.	159.	183.	178.	197.	199.

*Cycle 6 Values

** Based Upon Average Mixture Ratio

***For Rig 35155-2 This is Injector Total Fuel Flow (Includes P/B Coolant and Rigimesh Flows)

Table II-15. Summary of Hot Turbine Test Data Shows Preburner Operates as Predicted, Engine Thrust Level 50% and 100%, Mixture Ratio 7.0 and 5.0

Preburner	50% Thrust Mixture Ratio 7.0 Predicted Engine Cycle 6	Test Results	100% Thrust Mixture Ratio 5.0 Predicted Engine Cycle 6	Test Results
Total Fuel Flow - lb_m/sec	26.56	27.25	75.70	75.74
Total Oxidizer Flow - lb_m/sec	30.59	30.74	79.99	76.43
Oxidizer Primary - lb_m/sec	8.16	8.50	13.43	7.81
Oxidizer Secondary - lb_m/sec	22.44	22.24	66.56	68.62
Primary/Total Flow Split	0.267	0.276	0.168	0.102
Injector Fuel Flow - lb_m/sec	26.40	26.65	75.23	74.18
Rigimesh Coolant Flow - lb_m/sec	NAV	0.427	NAV	1.202
Coolant Liner Flow - lb_m/sec	0.163*	0.128	0.465*	0.361
Injector Mixture Ratio	1.159	1.134	1.063	1.031
Chamber Pressure - psia	1915.	1620.	4817.	4212.
AVG Combustion Temp. - °R	2157.	2125.**	2009.	1920**
Oxidizer Temp. - °R	207.	176.	234.	177.
Fuel Temp. - °R	183.	183.	183.	171.
Oxidizer Turbine Simulator				
Turbine Inlet Temp (AVG) - °R	2122.	2137.	1986.	1872.
Turbine Discharge Temp - °R	2019.	NAV	1823.	NAV
Temp Profile (max-avg) - °R	0.0	65.0	0.0	65.0
Fuel Turbine				
Turbine Inlet Temp. - °R	2122.	NAV	1986.	NAV
Turbine Discharge Temp - °R	2008.	1783.	1813.	1582.
Injector Effective Areas				
Oxidizer				
Primary A_{cd} - $in.^2$	0.063	0.068	0.063	0.061
Secondary A_{cd} - $in.^2$	0.620	0.617	0.690	0.731

Table II-15. Summary of Hot Turbine Test Data Shows Preburner Operates as Predicted, Engine Thrust Level 50% and 100% Mixture Ratio 7.0 and 5.0 (Continued)

Preburner	50% Thrust Mixture Ratio 7.0 Predicted Engine Cycle 6	50% Thrust Mixture Ratio 7.0 Test Results	100% Thrust Mixture Ratio 5.0 Predicted Engine Cycle 6	100% Thrust Mixture Ratio 5.0 Test Results
Fuel				
Overall - in.^{2}	3.48	2.85	3.48	2.86
Plate - in.^{2}	3.70	3.29	3.70	2.37

*Cycle 8 values
**Based on average mixture ratio

Figure II-26 shows combustion gas temperature profile data for the XLR129 preburner injector over a range of engine thrust and mixture ratio conditions.

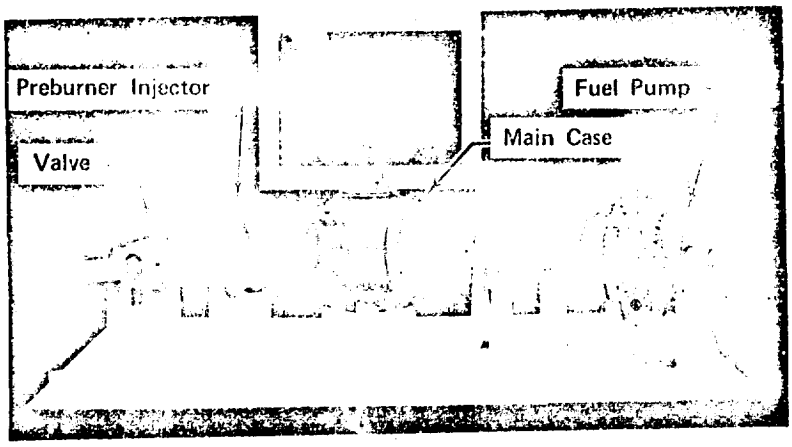

Figure II-32. Hot Turbine Test Rig Major Components, In Good Condition After Six Hot Firings

FD 52474

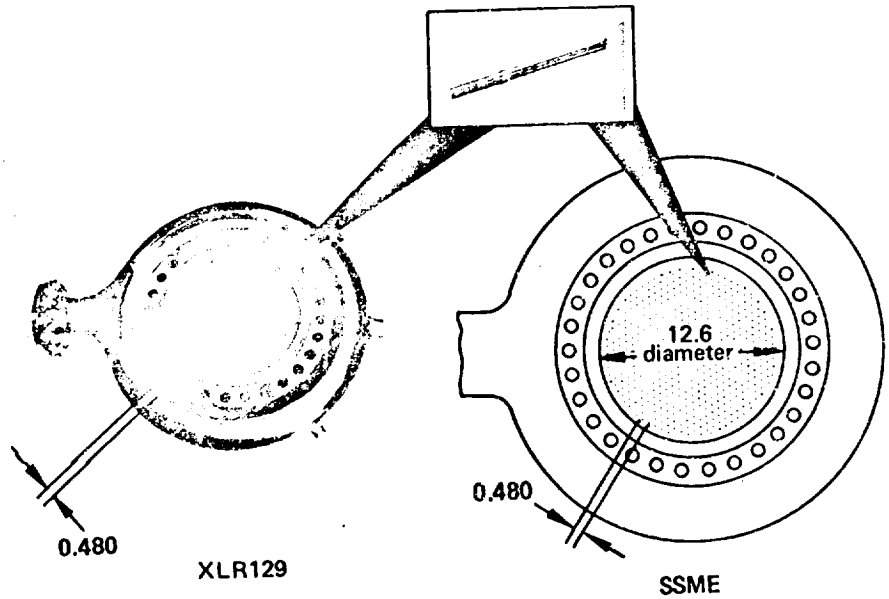

Figure II-33. SSME Preburner Injector Based on Demonstrated Technology

FD 42229C

SECTION III
ENGINE MAIN CASE ASSEMBLY

A. MAIN CASE

1. Introduction

A spherical pressure vessel main case was selected for the SSME. It utilizes a design concept that has been proven during the XLR129 Reusable Rocket Engine Program.

As shown in figure III-1, the engine main case assembly serves as the mounting structure for four major engine components; the preburner injector, high pressure oxidizer turbopump and fuel turbopump, and main chamber injector. Three of these components interface at three flanged spherical segments that intersect the main spherical vessel in the same plane. The fourth component, the main chamber injector, interfaces a fourth spherical case segment flange that is perpendicular to the plane of the other three segments.

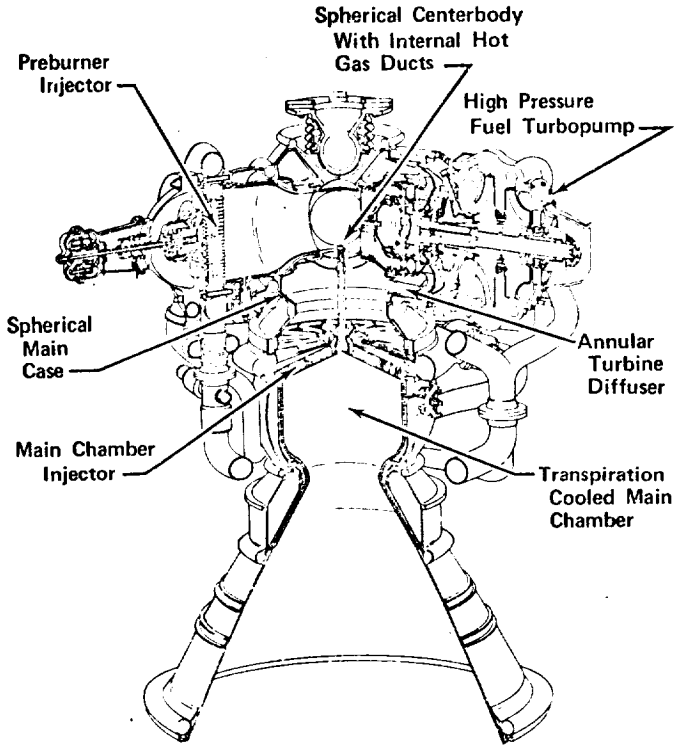

Figure III-1. A Compact Powerhead is Provided By the Spherical Main Case FD 50306A

Modular plug-in of these components into the engine main case assembly provides exceptional maintainability because any one of these components can be removed without disturbing the others.

The spherical powerhead concept eliminates an independent thrust structure by incorporating the thrust gimbal socket and gimbal retainer into the engine main case assembly. Internal case pressure is utilized to balance full engine thrust that is transmitted through the main case powerhead to the gimbal.

Internally, the main case contains ducting that routes preburner gases through the fuel and oxidizer pump turbines to the main chamber injector as shown in figure III-2. This internal ducting includes a single long preburner chamber that ensures complete combustion before burning the combustion gases; this provides a more uniform temperature profile to the turbine inlets. The turbine discharges are turned and diffuse into the main case, in a plenum-mixing chamber that surrounds the internal ducting. Between this mixing chamber and the main chamber injector, a local constriction causes a small pressure loss that results in further mixing of the gases. This flattens the mass profile of the gases before they go to the main chamber injector.

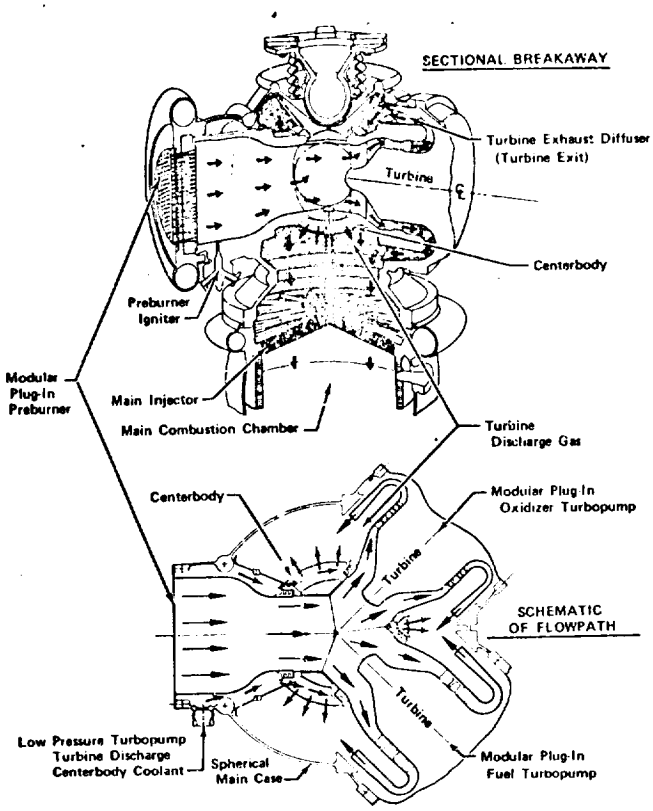

Figure III-2. Low Risk is Provided With Main Case Internal Ducting FD 52583

The turbine discharge pressure in the main case mixing plenum also provides external pressure to the hot gas ducting. This reduces the ΔP on the normally hot, high pressure ducting by over 60%. As a result, preburner combustion ducting contained by the main case can be designed for a differential pressure of only 2100 psi instead of 5500 psi, equivalent external ducting.

2. Description - SPHERES BEST SOLUTION FOR PRESSURE CONTAINMENT

When the powerhead concept was first conceived, four intersecting cylinders were studied for the configuration. The primary structure was essentially a nonsymmetric pressure vessel consisting of three large diameter cylinders, the centerlines of which intersected the centerline of a

fourth, and larger diameter cylinder, at right angles. The centerline of the larger cylinder coincided with the engine thrust axis. This cylinder served as a collecting manifold for the turbine exhaust gases.

This original intersecting cylinder concept was rejected because of excessive weight, and complex fabrication considerations, particularly because of stiffening problems at intersections.

A complete analysis of the various alternatives for the main case configuration was conducted. The design analysis of the main case was substantiated by subscale model tests that assisted in the evaluation of the selected design.

- INTERSECTING SPHERES MAIN ENGINE CASE CONCEPT

A design concept of intersecting segmented spheres was proposed for the main case configuration. Because a sphere is inherently a more efficient pressure vessel than a cylinder or cone, this concept provides the following advantages:

1. Lighter construction because a thinner shell is required to resist pressure; the material is loaded in tension, no bending.

2. Easier construction because intersecting spheres provide circular intersections, where stiffening is required, instead of elliptical intersections for cylinders and cones, where even more stiffening would be required.

3. A decreased bending stress at the flanges and other boundaries because of the radial load component.

- ALTERNATE ENGINE MAIN CASE ARRANGEMENTS STUDIED

Five intersecting sphere configurations were initially studied; three co-planar component designs and two canted component designs. Calculations and computer programs were conducted on each of these designs to determine whether they could perform under the predicted pressures and stresses. Two of these designs, one canted version and one co-planar version, were selected for further study and model testing. These are shown in figure III-3.

The canted components entered the main case at an angle, and the co-planar components entered perpendicular, all in the same plane. Engine models were made to study the engine packaging aspects of these two main case configurations. Figures III-4 and III-5 show two of the various engine models made with the canted and co-planar main cases. These engine models showed that, as far as plumbing was concerned, the engine packaging envelope was improved with the canted version. From this study, a model testing program evolved that included a co-planar sphere model and a canted model.

Comparision of the co-planar and canted versions showed that either was a prime candidate for selection. For example, the canted version main case was attractive because of weight, approximately 8% less than the co-planar design. The co-planar configuration was attractive because of the ease of fabrication and the elimination of a high internal duct thrust load inherent in the canted component design.

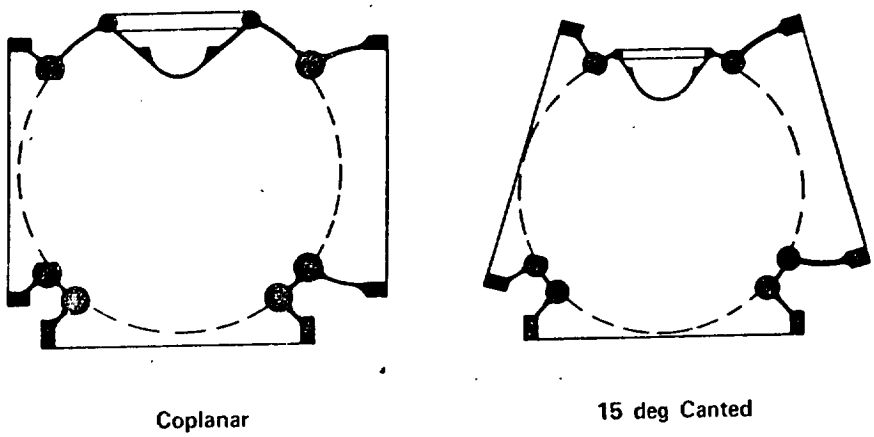

Figure III-3. Candidate Main Case Configurations FD 46394

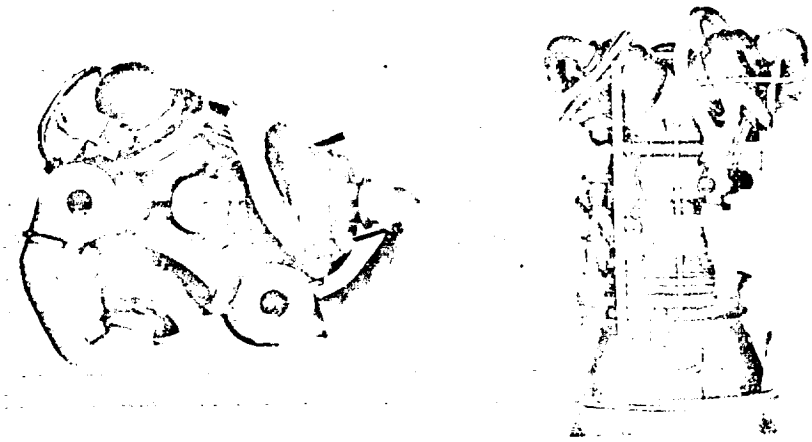

Figure III-4. Component Arrangement Study With Canted Main Case FD 52591

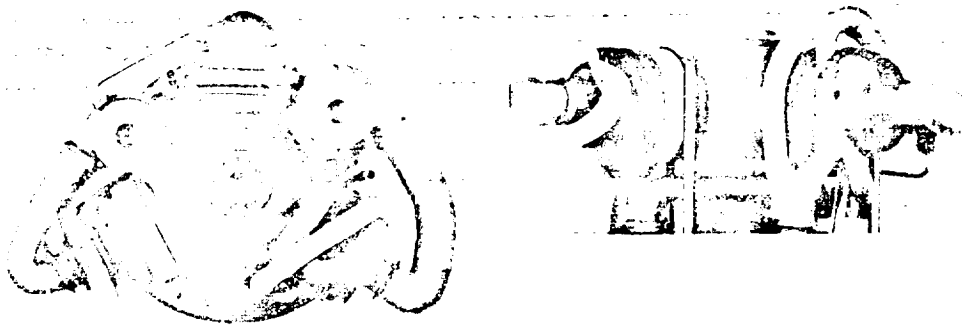

Figure III-5. Component Arrangement Study With Coplanar Main Case FD 52592

Further design studies were conducted with a focus on the internal ducting of the main case, particularly with respect to the effects that the canted and co-planar concepts would have upon the internal ducts.

A problem encountered with the canted internal ducting was that large axial loads were induced on the lower center duct towards the main chamber injector. These axial loads were caused by the differences in areas between the upper and lower portions of the ducts; the lower portions have more area and therefore, greater pressure loads. This large axial load was the major disadvantage of the canted main case configuration.

It was concluded that the co-planar main case offered the best solutions for the overall design regarding inner duct design, thrust load handling, assembly, and manufacturing.

This spherical co-planar components main case concept has been proven by sub-scale intersecting sphere models, by proof pressure/thrust testing, using the test fixture shown in figure III-6, by engine lightweight hardware tests on the XLR129 Program, and by staged combustion rig tests conducted during Phase B of the SSME Program.

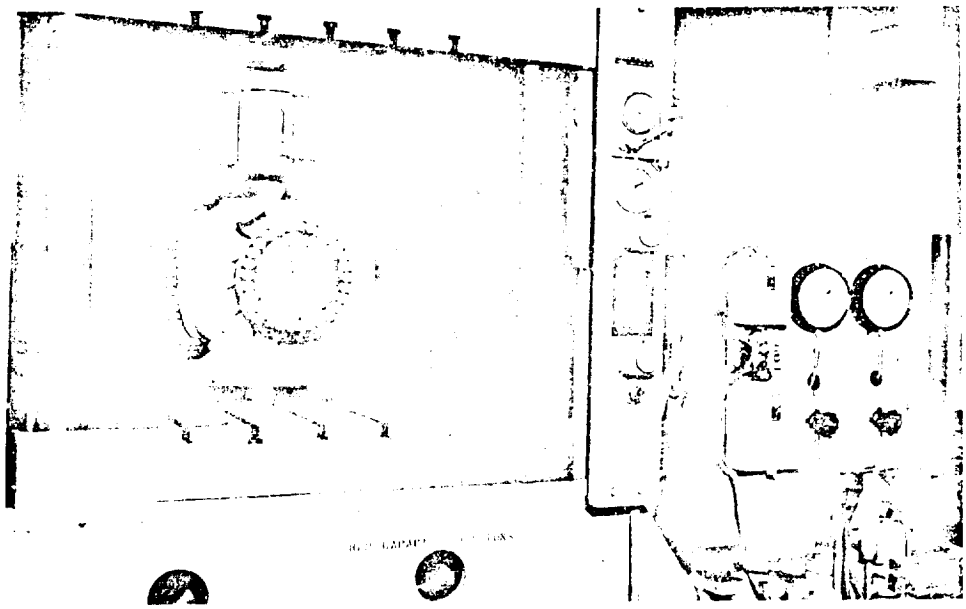

Figure III-6. Spherical Main Case Concept Proved By Proof Pressure/Thrust Testing FD 52593

- SSME MAIN CASE CO-PLANAR INTERSECTING SPHERES DESIGN

Pratt & Whitney Aircraft's powerhead main case consists of four intersecting spheres and a thrust gimbal support cone intersecting a central sphere as shown in figure III-7, FR-4289.

The main case is fabricated from two hydroformed hemispheres, ring-rolled forgings, and one pancake segment from a cylindrical forging as shown in figure III-8. The hemispheres are welded together to form the central sphere. The ring rolled forgings form the component flanges and stiffening rings and the

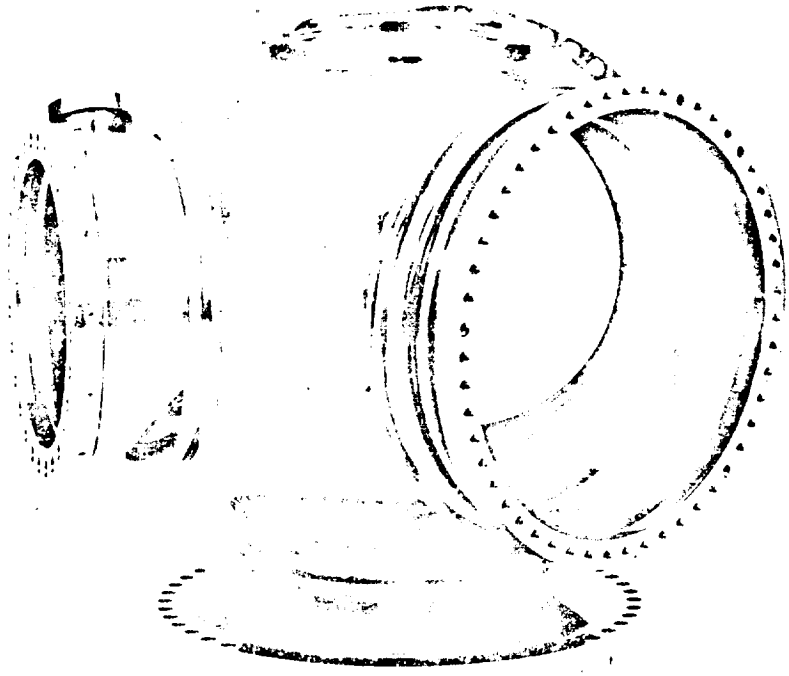

Figure III-7. Main Case Outer Structure FD 42897

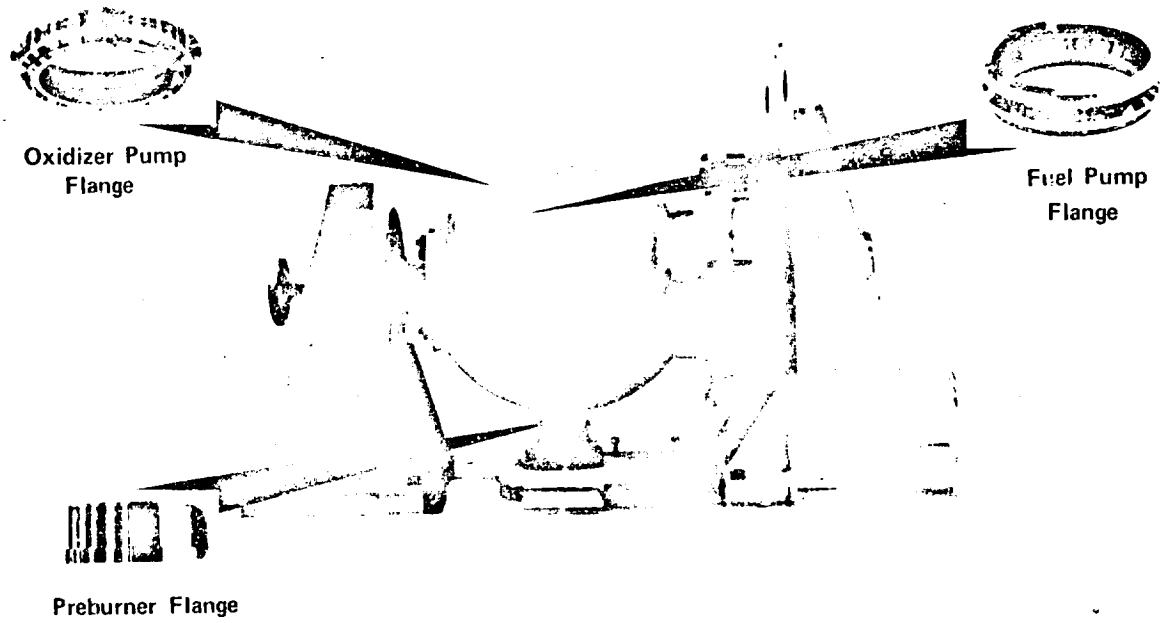

Figure III-8. Intersecting Spheres Provide Simpler Construction FD 52594

The ring rolled forgings form the component flanges and stiffening rings the pancake forging forms the gimbal support cone. A small preburner igniter boss and cooling inlet boss on the preburner sphere are machined from bar forgings. After welding and heat treatment, the forgings are finished machined, the results of which are shown in figure III-9.

The gimbal support cone intersects the central sphere at a circle diameter that provides a pressure area term that balances engine thrust. Thrust is transmitted efficiently through the main case with only an increase in hoop load as a result. A spherical seat is incorporated into the gimbal cone to accept the gimbal thrust ball joint for gimbaling at full engine thrust as shown in figure III-10. An easily replaceable liner made of Teflon impregnated glass cloth is bonded to the thrust ball to reduce friction. The average bearing stress is limited to 20,000 psi maximum.

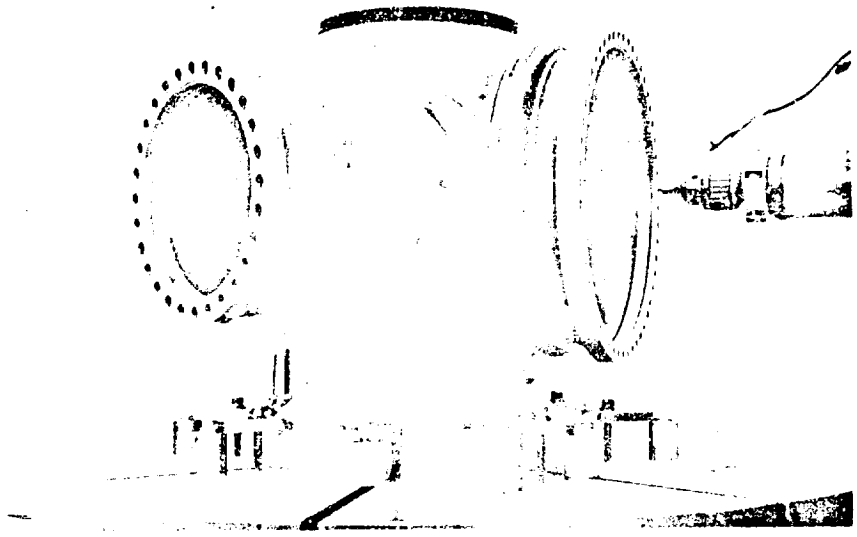

Figure III-9. Drilling of Bolt Holes Completes Fabrication of the Initial Spherical Main Case FD 52595

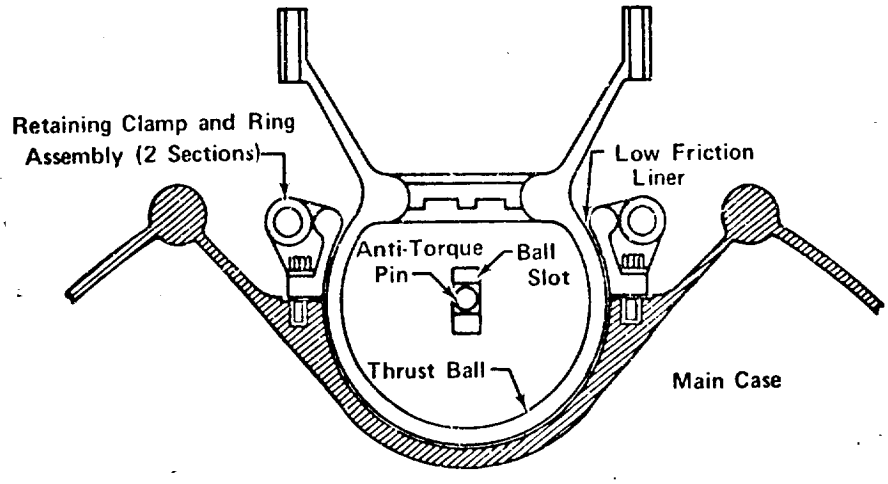

Figure III-10. Integral Main Case Socket Design Eliminates a Separate Thrust Structure FD 52596

- MAIN CASE FABRICATED FROM HYDROGEN COMPATIBLE HIGH STRENGTH PWA 1053

The main case is fabricated from PWA 1053 material. (Refer to Combustion Devices Trade Studies, PWA FR-4440.) Where required, welding is accomplished by electron beam welding techniques.

"A Basis" minimum material properties at room temperature are:

0.2%	150,000	- parent material
	128,000	- in weld
Ultimate	170,000	- parent material
	160,000	- in weld

Inconel 718 was selected as a backup material for the main case design. A hydrogen barrier inner surface liner that is vented to ambient was used for the backup design. The protective liner is made from 0.015-in. thick AISI 347 stainless steel sheet and 0.016-in. thick AISI 304 wire mesh backing liner. These are formed to the inner surface contour of the structural shell as shown in figure III-11. The wire mesh, sandwiched between the structural shell, and the thin 347 sheet provides a foundation for pressure transmission through the AISI 347 liner. It also forms a plenum that is vented to a hydrogen sensor to detect any leaks that may occur in the hydrogen barrier.

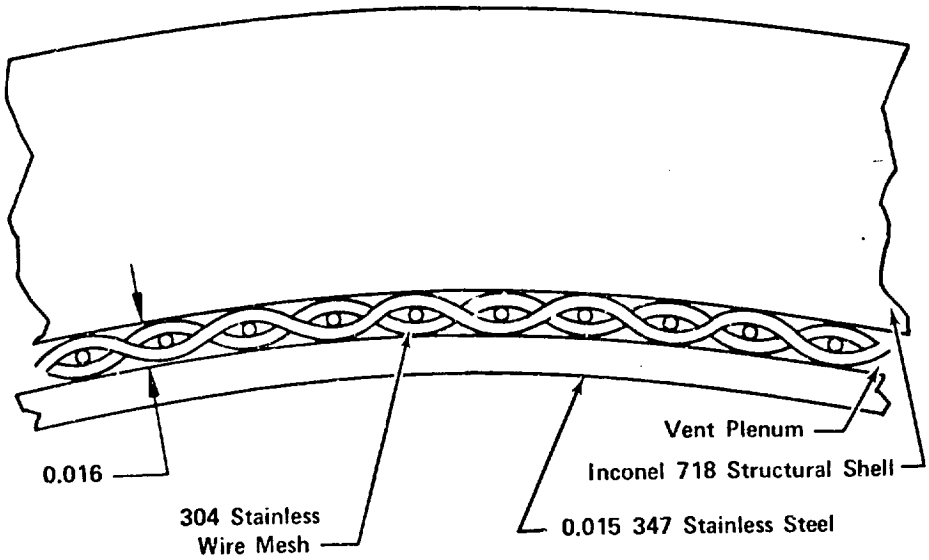

Figure III-11. Protective Liner Provides Hydrogen Barrier for Main Case FD 46294

- LINE-OF-ACTION FLANGE REDUCES WEIGHT BY MINIMIZING FLANGE TWIST

Flange twist and lift-off normally encountered with L-flanges are minimized or eliminated by line-of-action main case flange designs so that shell or case loads pass through or near the flange cross-sectional centroid

to eliminate flange twists as shown in figure III-12. The shell or case load is designed through or near the centroid to balance the flange statically, considering pressure area, shear, and moment induced by the shell and mating flange pilot load.

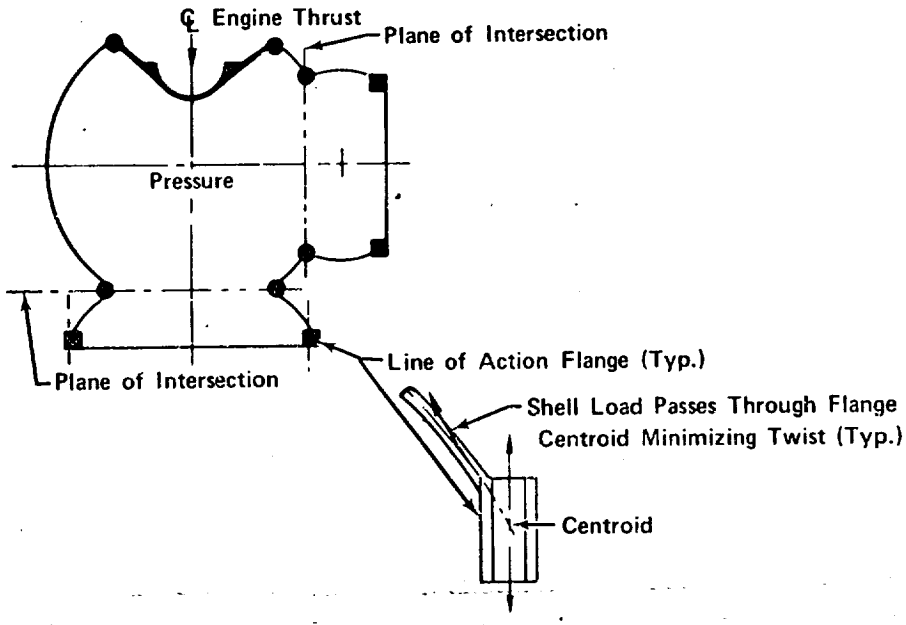

Figure III-12. Line of Action Flange Reduces Weight FD 46293

- POROUS MAIN CASE COOLING LINER PROVIDES LOW OPERATING WALL TEMPERATURES

A cooling liner is incorporated into the main case to shield the case structural shell from high temperature turbine exhaust gases as they flow from the turbines to the main case. The liner is hydrogen transpiration-cooled and maintains the main case temperature at 600 °R. This precludes adverse radiation effects on surrounding external engine components and minimizes component interface problems due to thermal growth. The cooling liner is fabricated from an AISI 347 porous liner. AISI 347 is used because it meets structural requirements and it is not degradated in hydrogen.

External pressure imposed on the liner requires that it be designed to preclude buckling. Because of this, the volume between the cooling liner and inner surface of the main case is held to a minimum to prevent excessive pressure loads across the liner at shutdown. However, the pressure differential is large relative to the distribution losses behind the liner and relative to the pressure gradient associated with the mainstream flow past the liner downstream face. This assures that there is no severe maldistribution of coolant due to the number or location of coolant supply joints.

The liner takes the shape of the outer case and is assembled into the outer case by welding together preformed spherical segments fabricated from sintered wire mesh as shown in figure III-13. This creates a porous metal barrier between the outer case and turbine exhaust products. Hydrogen passes through the liner forming an insulating boundary.

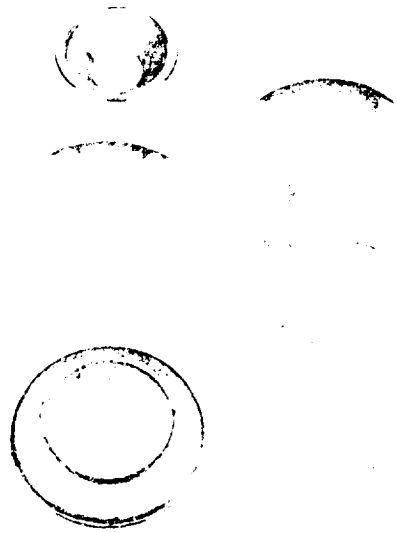

Figure III-13. Pre-Formed Cooling Liner Segments Allow Simple Installation FD 52597

Because porous liner flow rates have proven to be unpredictable, particularly after forming the liners, the flow porosity will be tailored by flame spray to the liner locally on its back side. Previous experiences shows the bonding to be permanent under severe conditions.

The liner provides support for the centerbody and is itself supported at each of the stiffening rings by corrugated spacers that are welded to the liner. The corrugated spacers assure a constant flow annulus between the ring inner surface and cooling liner. Except for minor differences, the cooling liner for the SSME main case is identical to the cooling liner for the XLR129 case shown in figure III-14. The XLR129 liner was successfully tested during the XLR129 Program and is now being tested in Phase B of the SSME Program.

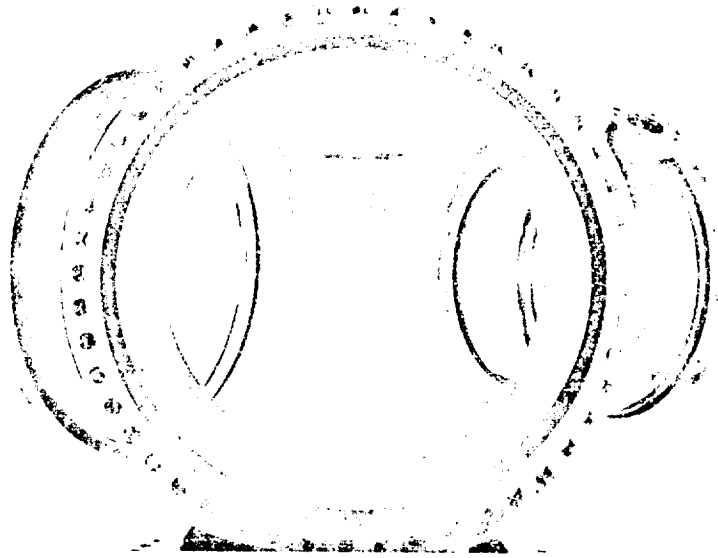

Figure III-14. Installation of Cooling Liner Completes Main Case Assembly FD 52598

Positive cooling is provided to the liner from the primary nozzle heat exchanger at a temperature of 350°R.

- INTEGRAL THRUST GIMBAL MEETS REQUIREMENTS WHILE REDUCING WEIGHT

The gimbal thrust ball, an assembly external to the main case, provides for engine attachment to the vehicle while permitting engine gimbaling. The gimbal ball uses a uniball joint to distribute thrust and side loads into the main case. This eliminates the need for a standard cross pin universal joint and provides a simpler, lighter, and more stable joint.

3. Requirements

The main case satisfies the imposed requirements of CEI Specification CP2291 and the ICD. The CEI specification paragraphs having a major effect on the design are as follows:

3.4.4.4 Acceleration Load Factors

Maincase designed to table 2, figure 4. (10g longitudinal - 1 g lateral).

3.4.5.1 Vibration/Shock/Acoustic/Aerodynamic Loads

3.7.1.2 Hydrogen Embrittlement

The material selected for the main case experiences no degradation in hydrogen and has exceptional strength. A high nickel content iron base material, designated as PWA 1052 and 1053, is used.

3.7.7.1 Structural Criteria

Main case (see 3.7.7.1.2, Special Structural Criteria). Bolts have been designed to a minimum yield factor of safety 1.10 minimum ultimate factor of safety of 1.40 using limit pressure. Limit pressure is emergency power level (EPL) pressure plus 2.5% pressure overshoot.

3.7.7.1.1 Material Properties and Design Allowance

MIL-HDBK-5 ("A" Basis) minimum material properties used in main case design to ensure low risk design.

3.7.7.1.2 Special Structural Verification Criteria

The main case has been designed for the following minimum verification pressures.

Limit pressure = maximum pressure at EPL + 2.5% overshoot

Limit thrust = maximum thrust at EPL + 2.3% overshoot

Proof pressure = 1.2 x Limit Pressure

Burst pressure = 1.5 x Limit Pressure

Proof thrust = 1.2 x Limit Thrust or Fracture Mechanics factor, whichever is highest

Burst thrust = 1.5 x Limit Thrust

3.7.7.1.3 Fatigue Criteria

The main case has been designed to:

400 engine cycles (LCF)

1000 engine cycles (HCF)

3.7.1.3.1 Flange Joint Design

The main case flanges have been designed using the following criteria:

1. Bolt circle diameter kept to minimum
2. High strength studs used for weight savings
3. Through-holes where possible. Blind tapped holes incorporate non-locking inserts.
4. Flange twisting couples are eliminated using the action line design shown in figure III-12.

In addition to the above mentioned requirements, the main case temperature is designed to 600°R maximum to ensure materials strength, avoid radiation to other components, and to minimize thermal interface problems. The main case cooling liner has been designed to withstand an engine shutdown pressure of 200 psi. A 1.3 margin for buckling is used for a safety factor.

4. Substantiation

The spherical powerhead main case for the SSME evolved from XLR129 trade studies. The co-planar components spherical powerhead has been substantiated by subscale spherical model tests in the XLR129 Program, by static pressure and thrust tests under levels exceeding normal test expectation, and by preburner and staged combustion rig hot firings, several of which were at 100% engine conditions. Further substantiation is now being accomplished in Phase B staged combustion rig testing of the SSME Program. All of the main case hardware tested to date is low-weight flight-type hardware.

5. Capability

The main case plug-in powerhead is a low-risk design that meets all CEI specification requirements. It is designed to the engine cycle condition at at 109% r = 6.0.

Limit pressure = 109% + 2.5% overshoot

Limit thrust = 109% + 2.3% overshoot

Strain on the case is limited to 1.0% for 400 cycles engine life, based on fracture mechanics criteria or low cycle fatigue criteria, whichever is the most critical at limit pressures.

A 1.2 safety factor is employed for proof pressure at 0.2% yield stress and a 1.5 safety factor for burst pressure at ultimate stress.

A 1.1 and 1.4 safety factor is used for 0.2% yield and ultimate stress respectively for flight when maneuver loads and limit pressures combine to load the main case.

The main case design exceeds CEI specification life requirements by a factor of 1.5. Life predictions were made using low cycle fatigue data from the P&WA Materials Development Laboratory (MDL) and considering that EPL conditions existed for 100% of the engine life instead of using a time-weighted analysis.

The main case can withstand 1200°F with only a 10% loss of material properties. Yield safety factors provide a margin of 10% at limit pressures.

Main case studs are designed with a safety margin of 1.1 for proof and 1.4 for burst at limit pressure. Bolt preload has a 10% tolerance to ensure minimum bolt loads. High preload prevents flange separation and minimizes cyclic strain to ensure life requirements. At limit loads, there is no plastic strain in these bolts. Nuts and studs are stress matched and tapped holes have 1.5 times the thread engagement of a comparable nut and have helicoil inserts.

Main case gas temperatures may be increased to gain added performance during the development program.

The life of the main case exceeds CEI specification requirements as designed. It provides a light weight, low risk concept and has been substantiated by many tests of a mechanically and functionally similar main case at the 100% power level.

B. MAIN CASE CENTERBODY DUCT

1. Introduction

The centerbody provides the shortest possible plumbing for the intersection of the fuel, oxidizer, and preburner hot gas ducts, and provides the sealing surfaces for the piston rings that are installed as part of the individual duct assemblies. A porous liner encloses the structural sphere and protects the structure of the centerbody from the hot turbine exhaust gases.

Two sets of internal liners complete the centerbody assembly. The innermost liner, the only portion of the centerbody that directly contacts the hot preburner combustion gas, is used to divide and divert the preburner gas flow between the two turbopumps and to prevent the hot preburner gases from

scrubbing the structural wall of the centerbody. An intermediate liner, installed between the structural wall and innermost liner, is incorporated as a radiation heatshield to protect the cooler surfaces of the centerbody from the hot gases.

The centerbody as shown in figure III-15, is located immediately downstream of the preburner combustion chamber and just upstream of the turbine inlets. It adds length to the preburner combustion chamber and provides more time for the mixing of the combustion gases so that a more uniform temperature profile is delivered to the two main pump turbine inlets.

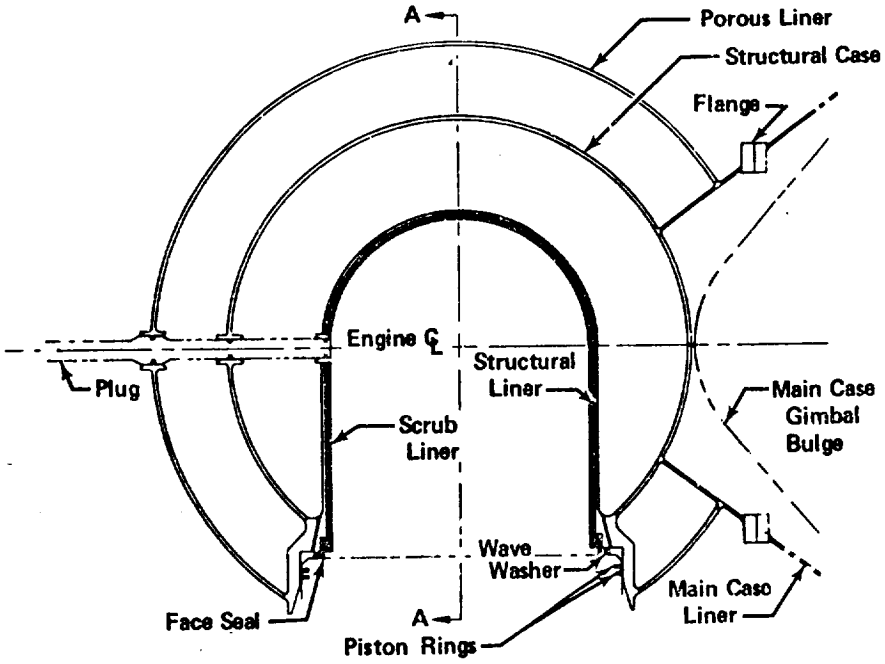

Figure III-15. Liners Provide Protection for the Centerbody Structural Case FD 46128

2. Description - DESIGN AND FABRICATION IS BASED ON THE XLR129 CENTERBODY

The SSME centerbody plug-in hot gas duct system is based on the successful XLR129 centerbody design shown in figures III-16 and III-17. The XLR129 centerbody has been tested many times on the preburner and staged combustion rigs, including several runs at 100% design points. One problem, not detrimental to testing, was encountered during this period. Centerbody seal land deflections occurred as a result of nonuniform loads on the centerbody which caused the piston rings to locally disengage out of their grooves. The centerbody was subsequently stiffened and the problem has not reoccurred.

During the conceptual stage of the XLR129 design, consideration was given to intersecting the preburner and turbopump ducts at the center of the main case with mitred intersections and butt seals. Studies were conducted of several possible seal designs for the joint made by the intersection of the three ducts. Requirements included a provision for positive sealing of the ducts at their intersection, and at the same time allow for axial thermal

growth of the ducts. Provisions for misalignment due to normal manufacturing tolerances were also required. Additionally, maintainability considerations required that individual assembly or disassembly of the preburner, oxidizer and fuel pump ducts could be accomplished without special techniques or tools.

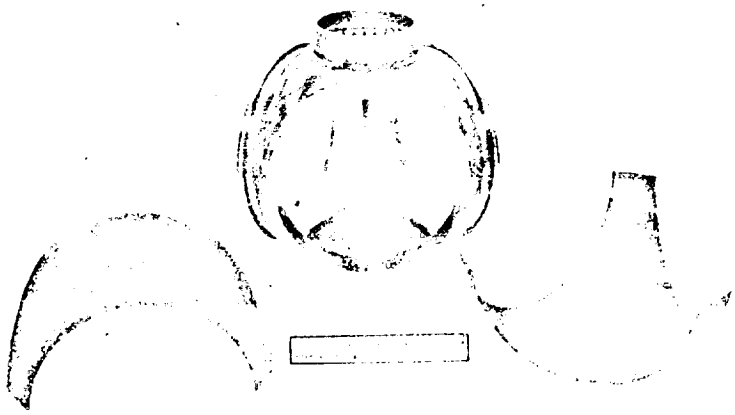

Figure III-16. Formed Outer Cooling Liner Completes Centerbody Assembly FD 52601

Figure III-17. Centerbody is Supported in Main Case Assembly FD 52600

The major problem concerning all of the inner duct seal designs considered, was that the tolerance stackup caused duct centerline mismatch. Any duct flange that was off by 0°8' caused 0.030 deflection at the duct intersection. Because of this, it was concluded that manufacturing tolerances alone would cause problems in obtaining adequate sealing of the ducts at their intersection lines when using mitred intersections.

Design studies were started to provide a centerbody that would provide the sealing requirements of the intersecting ducts and allow for thermal growth, mismatch, and normal manufacturing tolerances. The centerbody must also allow individual assembly and disassembly of the individual intersecting duct, the plug-in concept.

- CENTERBODY STRUCTURAL SPHERE LIFE IS ENHANCED BY USE OF PROTECTIVE LINERS

The centerbody figure III-18, is functionally divided into two sections. In addition to the structural sphere, an internal hot flow section is used for protection of the structural wall and for directly dividing and diverting preburner combustion gases to the turbine inlets.

The hot flow section includes a Y-shaped scrub liner, the only centerbody part which actually contacts the exhaust flow. In addition to diverting the preburner exhaust flow to the high pressure turbopump turbines, it prevents hot gas contact with the structural case, thereby eliminating a possible low cycle fatigue problem.

A radiation liner surrounds the scrub liner and shields the structural case from radiation. The radiation liner consists of three identical segments. The segments are not joined to each other at their intersections at the center of the centerbody. Rather, a 0.020-inch gap is left as shown in figure III-18 to avoid the thermal expansion problems of a redundant liner system.

- RADIATION LINER DOUBLES AS STRUCTURAL MEMBER

These liners are welded to the cylindrical rings that intersect the three holes in the structural case. This is to aid the rings in resisting discontinuity loads in the structural case caused by the three holes in the case. The cylindrical rings tend to ovalize because of the nonuniform loads around the circumference of each rings.

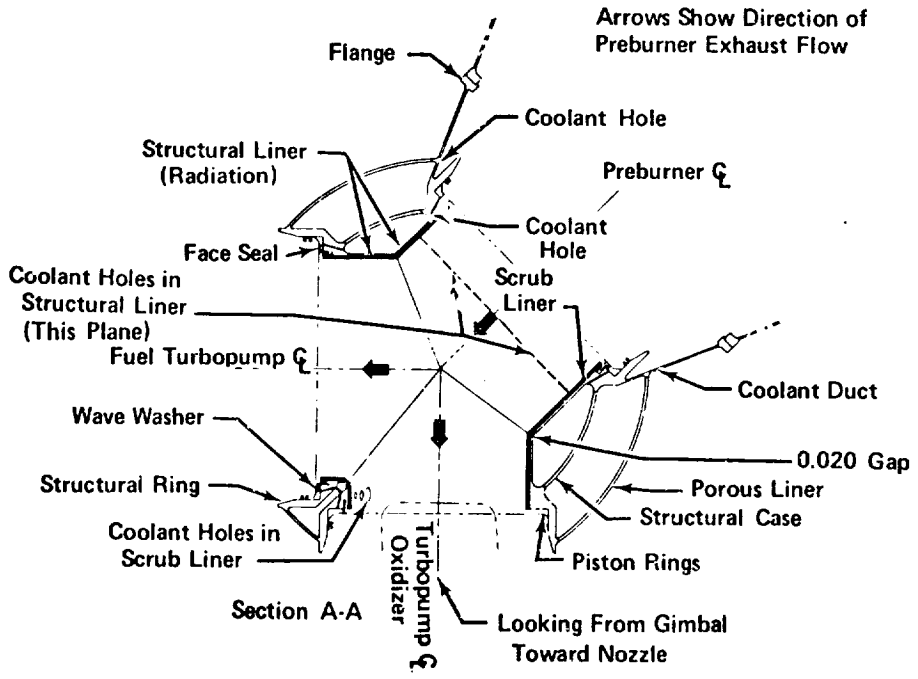

Figure III-18. Preburner Exhaust Case Section Perpendicular to Engine Centerline FD 46129

- OUTER COOLING LINER PROTECTS STRUCTURAL CASE FROM TURBINE DISCHARGE GASES

An outer porous cooling liner surrounds the structural case. This is a wire mesh (1000 scfm) sphere that protects the structural case from the turbopump turbine exhaust. It does this by guiding coolant, taken from the low pressure turbopump turbine exhaust, over the exterior of the structural case. The coolant then exhausts into the main case plenum by way of the outer porous liner, readily mixing with turbine discharge gases in the main case plenum.

Three face seals and wave washers are designed in conjunction with the centerbody. A face seal rides in a groove in each structural liner segment. A wave washer holds each face seal against the end of a preburner or turbopump duct. Preburner duct coolant flows into the space bordered by the end of the preburner duct, the cylindrical ring, the face seal, and the end of the structural liner. (See figure III-18.) The cooling flow then enters the interior of the structural case through several small holes spaced circumferentially around the end of the structural liner section. The coolant flows around the interior of the structural case and into the space between the structural and scrub liner by way of the 10 holes in the structural liner section nearest the preburner. The coolant flow then discharges into the exhaust stream through six holes in the scrub liner.

A mounting case and flange are welded to the structural case. The flange bolts to another flange that is attached to the main case liner. This is the main support for the centerbody.

A wiremesh duct is welded to the cylindrical ring nearest the preburner. The duct surrounds that portion of the preburner inside the main case and the duct flange bolts to a flange attached to the main case liner. This duct provides a path for the low pressure turbopump turbine exhaust in the space between the duct wall and the preburner. The duct is wiremesh (300 scfm) and allows transpiration coolant to prevent damage to the duct from the high pressure turbopump turbine exhaust.

- HOT DUCT SECTION INSPECTION POSSIBLE WITH EXISTING BORESCOPE PROVISIONS

A provision for borescope inspection of the SSME hot gas section is included. A plug extends from the center of the main chamber injector through the centerbody porous liner, the structural case, and radiation and scrub liners. Piston ring seals prevent significant leakage at the porous liner, structural liner, and scrub liner. When inspection is desired, the plug is removed and the borescope is inserted. Preburner combustion instability can be initiated by inserting a specially designed pulse bomb in place of the borescope plug and detonating the pulse bomb on command.

3. Design Requirements

The pertinent paragraphs of CEI Specification CP 2291 and methods of compliance are as follows:

1. Shall shut down safely from any power level, paragraph 1.2.e.
   Compliance - All orifices sized to allow pressure bleed-down.

2. Shall be capable of EPL runs of 460 sec maximum per run, paragraph 3.7.1.2.
Compliance - Designed to EPL conditions

3. Materials shall not be sensitive to hydrogen, paragraph 3.7.1.2.
Compliance - Hydrogen-sensitive materials not used.

4. Pressure vessels shall be designed for proof pressure 1.2 times the limit pressure; burst pressure 1.5 times the limit pressure, paragraph 3.7.7.1.2.
Compliance - Pressure vessels designed to requirements.

5. Fatigue factors shall be 4 for low cycle and 10 for high cycle (both based on cycles), paragraph 3.7.7.1.3.
Compliance - Scrub liner prevents exhaust gases from touching structural parts.

6. Internal engine leaks shall not be harmful to engine function, paragraph 3.7.12.2.
Compliance - All internal leaks are from cold to hot.

4. Capability

Centerbody design requirements are met or exceeded by the SSME design. The scrub liner that contacts the 2181°R preburner exhaust gases is fabricated of Haynes 188, a high-temperature alloy. This liner has a temperature margin of 200°R before its strength margin begins to drop. Because material thickness is the limiting factor, the structural margin of safety is greater than twice that required at nominal operating temperatures.

To ensure a lightweight design, the structural case material is PWA 1053, a high nickel content, iron base alloy. The structural liner and the deflection-sized cylindrical rings are also PWA 1053. Excess temperature margin is 500°R while the structural margin of safety is 1.7 for the structural case. The PWA 1053 face seal has a temperature margin of 500°R. Because the material thickness is the limiting factor, the structural margin of safety is twice that required. The wave washer is also PWA 1053 which has a temperature margin of 500°R.

5. Substantiation

During the early phases of the design of the XLR129 centerbody and other flow duct system hardware, a method was required to express the three-dimensional flow characteristics of these components as a function of the properties of the flowing fluid and the geometry of the flowpath. This would allow parametric studies which would describe the changes in the flow characteristic associated with engine cycle and hardware changes. An analytical method was derived which provided the relationships. However, since several empirically derived loss coefficients were used in this method, testing of their applicability was required. This was accomplished by a three-dimensional transparent test rig.

A full-scale, transparent model was constructed and flow tested in a closed-loop water tunnel. Flow characteristics were recorded photographically as shown in figure III-19 to determine the areas where instrumentation would be installed.

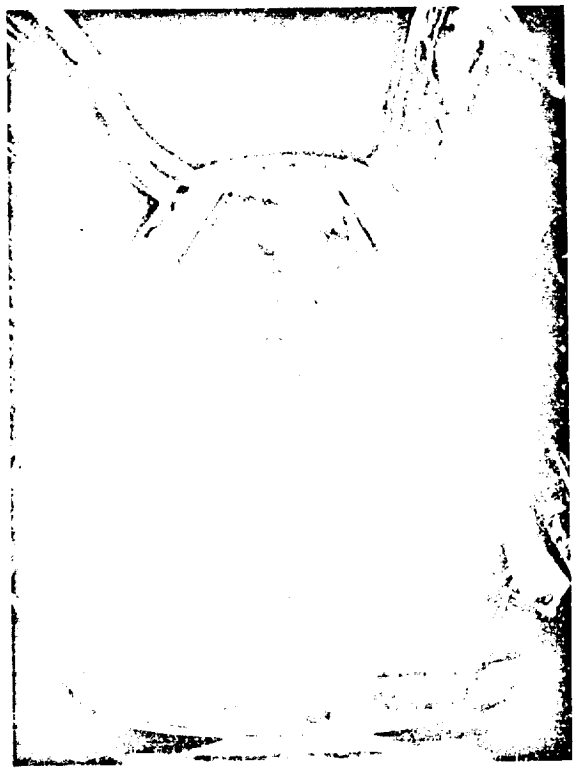

Figure III-19. Photograph of Plastic Model Flow Ducts Reveals Flow Characteristics FD 52593

The results provided by this instrumentation were analyzed to determine the three-dimensional flow characteristics. Coefficients included losses in turning, expansion, contraction, and wall friction. It was concluded that the analytical method used was valid and that the design would meet the total pressure losses allowed. (Refer to XLR129 Main Case Flow Characteristics, PWA DR-4448.)

A series of tests with varied thrusts and mixture ratios including two 100% thrust runs were made in a test series that ended in the summer of 1970. Six of the tests used turbopump simulators and six used an XLR129 fuel turbopump. All utilized an XLR129 centerbody. Test data for the fuel pump hot turbine tests are shown in table III-1.

Additional testing is being conducted on the XLR129 staged combustion rig. Successful tests have been conducted in this series and include several at 100% thrust levels.

This second series of tests was conducted during February, March, and April 1971. These tests were conducted using pump simulators, a reinforced centerbody, and a piston ring clearance reduced to 0.033 to 0.040 inch from 0.058 to 0.062 inch. This centerbody is functionally identical and mechanically similar to the SSME centerbody. The pump simulators incorporated low turbine differential pressure orifice plates so that rig run duration could be increased. These tests accumulated 251 seconds and 14 starts. Further substantiation will be accumulated with continued testing of the "Test Plan B" program.

Table III-1. Hot Turbine Test Summary

Test No.	% Thrust/r	Test Duration, sec	Preburner Combustion Temperature, °R	Preburner Combustion Pressure, psia	Main Case Pressure, psia	Net Centerbody, Pressure, psi
1.02	50/5	13.7	1450	1868		
2.01		6.4				
3.01	75/5	14.5	1605	2970		
4.01	75/5	17.2	1615	2965	2022	943
	75/6		1985	2882	2010	872
5.02	75/5	22.0	1610	3045	2062	983
	100/6		2070	4086	2817	1269
	100/7		2395	3889	2738	1151
6.01	50/7	20.0	2118	1612	1014	598
	100/5		1900	4200	2543	1657

C. PREBURNER COMBUSTION CHAMBER

1. Introduction

The preburner combustion chamber is that portion of the engine hot gas duct system adjacent to the preburner injector that provides a low-velocity volume for combustion to take place. The combustion propellant mixture ratio in the preburner is nominally one. The preburner chamber ducts the hot gases to the centerbody, which divides and diverts the flow to the two main pump turbine inlets.

2. Description

Figure III-20 shows the preburner chamber as mounted in the plug-in main case. The lower portion of the figure shows a combustion flowpath schematic. The plug-in preburner chamber duct is lighter than an external duct because it carries only the pressure differential between the preburner chamber (turbine inlet) and turbine discharge. The plug-in concept has reduced the differential pressure the structural wall must carry by a factor of 2.5 from an externally ducted system. All hot line external leaks have been eliminated. Internal leakage of cold hydrogen at the front O-ring and leakage of less than 2 ft^3/min of 800°R gas at the piston ring seals are tolerable.

The entire preburner combustion assembly is modularly designed to enable placement into the main case with a loose fit so as to provide maximum ease of service and maintainability. The uncooled liner is loosely assembled at the bayonet joint and held from rotating by the two tight fits (0.012-0.016T diametral) on the cooled liner. These tight fits on the cooled liner form the seals for the cooled liner coolant manifold in a very small radial space. This design reduces weight and provides a compact envelope by pulling the preburner injector, oxidizer valve, and main case bolt circle into the smallest possible radius.

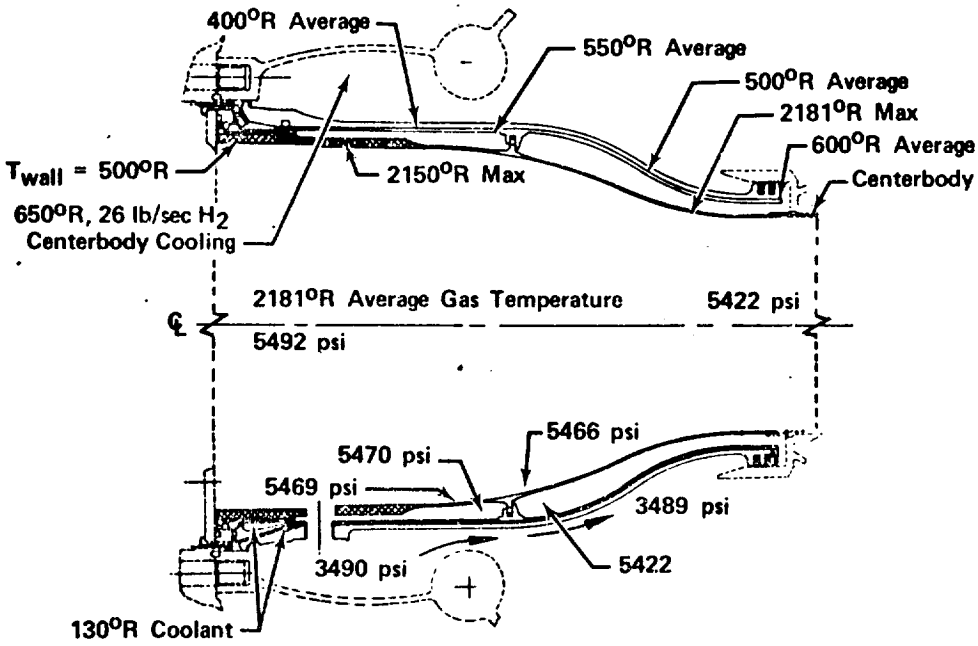

Figure III-20. Structural Margin and Life Provided by Temperatures and Pressures - 109% Thrust, r = 6.0, Orbiter FD 52227

The end of the duct that interfaces with the centerbody has two sets of piston rings to seal high pressure gases from leaking out of the main flowpath. These piston rings allow for chamber plug-in at assembly and thermal and pressure growth.

A long combustion chamber is a benefit that results from using the single preburner plug-in main case concept. Because long length provides more time for the mixing of the gases after the combustion process, a more uniform temperature profile is obtained at the turbine inlets. The same benefit resulted during the XLR129 design, which produced temperature profiles with a maximum peak-to-average temperature profile of 122°R at an average temperature of 2325°R at the turbine inlet. This low profile permits a lightweight, uncooled turbine.

A regeneratively cooled structural duct was selected for use because it was determined to be the lightest and the safest. The inner diameter of the duct is protected against high heat flux by liners that extend along the entire length of the duct. The duct is cylindrical in shape with a necked down section where the liner discharges the gases into the centerbody. This design, which is similar to the XLR129 in that it has long length, was selected by studying the sperical combustion chamber. (Refer to Combustion Devices Trade Studies, PWA FR-4440.) A spherical chamber has geometrical advantages over the cylindrical chamber, but the severe problems of fabrication, assembly, and maintenance, as compared to the cylindrical chamber, demanded that the spherical chamber be discarded. The first two inches of the inner liner are porous and transpiration-cooled, the next three and one-half inches are porous but uncooled, and the balance of the liner is sheet metal and uncooled.

The SSME chamber diameter is determined by allowing 0.7 inch from the centerline of the outer spud to the chamber wall. During earlier XLR129 tests

using smaller distances, the liners experienced wall erosion, discoloration, and local burning, whereas the 0.7-inch distance with a cooled liner proved successful during both rig and powerhead testing. Five and one-half inches of constant chamber diameter downstream of the injector ensures complete burning of the gases at low Mach numbers prior to being accelerated in the contraction area of the duct. This straight diameter section also provides a low static pressure variation along the chamber which improves stability. The exhaust diameter of the preburner is sized to limit the Mach number of the gases to approximately 0.15. The contraction ratio of 1.5 promotes stability even at low fuel inlet temperatures.

Acoustical damping and protection in the high energy release region are provided by a porous, cooled liner. Because of longer reflection distances, lower acoustical modes are the result of a longer chamber length. To ensure further stability, the porous chamber liners incorporated into the first 5.5 inches of combustion length have absorption capabilities two to three times that required. The front cooled liner has a coefficient of absorption of 70 percent and the front of the rear liner has a coefficient of 40 percent. Combustion chambers with absorption coefficients in excess of 20 percent, that have at least half the chamber length, are always stable with hydrogen oxygen propellants. Low mixture ratio combustion with low chamber velocities have been proved by testing to be inherently stable even with cooled hydrogen. A transpiration-cooled liner provides active cooling on the first two inches of the chamber walls in the high energy release region of the combustion process. An uncooled porous liner is used downstream of the cooled liner.

Both the cooled and the uncooled liners protect the duct assembly from erosion and hot spots. They eliminate a potential low cycle fatigue problem by preventing hot combustion gases from scrubbing directly onto the duct liner wall. A large thermal gradient in the wall and high thermal stresses would result because of high heat fluxes. The liners are parts of the chamber assembly that may be easily replaced if damaged.

- COOLANT TO THE CENTERBODY PROVIDES SAFETY MARGIN FOR PREBURNER COMBUSTION DUCT

The duct exterior is surrounded by 650°R low pressure turbopump turbine exhaust gases. This hydrogen, which is ducted coaxially around the chamber and into the main case centerbody, is used for centerbody cooling and is reinjected into the turbine discharge flow upstream of the main chamber injector. This flow stabilizes the outer duct pressure vessel temperature.

The primary operating limits governing the design of the preburner combustion chamber are temperatures and pressures. The limit conditions are shown in table III-2.

Continously variable engine thrusts up to 109% and variations in engine mixture ratio of 5.5 and 6.5 were considered in establishing clearances in the plug-in chamber joint to the centerbody and at the rear of the uncooled liner. The cavities between the preburner chamber and the uncooled liner are vented at the front and rear to prevent damage to hardware during the shutdown transients.

Table III-2. Temperature and Pressure Limits

Design Point	Temperature, °R	Pressure, psia	ΔP
Booster 109% r=6.0	2118	5601	2066
Orbiter 109% r=6.0	2181	5492	2021
Orbiter 100% r=6.0	2082	4908	1728
Booster 50% r=5.5	1558	2253	805

An igniter is located nominally 2.75 inches from the injector face because this location is sufficiently proximate to the injector to prevent accumulation of gases prior to ignition and is at a short enough distance to prevent the formation of a detonation wave strike-back to the injector face during ignition.

Location of the pulse gun in the same plane is an ideal location for pulsing the chamber to test for combustion instabilities because it is in the area of high energy release and constant static pressure.

The chamber cooling flow requirements are minimal (0.3 lb/sec). The coolant is used to protect or purge the inside of the centerbody from hot gases and is then routed into the hot exhaust flowpath with no measurable performance degradation in the preburner. Significant temperatures and pressures in the preburner combustion chamber assembly are shown in figure III-21.

- DESIGN AND FABRICATION IS BASED ON THE XLR129 PREBURNER COMBUSTION CHAMBER

The preburner duct assembly is fabricated from two single-piece PWA 1052 forgings. The iron base material is selected for its high strength, good low cycle fatigue properties, and its compatibility with hydrogen. Eighty-eight duct coolant grooves are machined on the outside of the inner duct and this duct is then tightly fitted (0.005 diametral) into the outer duct. Electron-beam welds are used to seal each end of the duct assembly to prevent this tight fit from becoming loose during engine operation. The outer duct is the main structural member of the preburner combustion chamber assembly because it carries the 2066 psi operating differential pressure. This entire design concept is the same as was used during the XLR129 Program except that it uses less expensive and more easily machineable materials and it eliminates the requirement for brazing and associated inspection problems. Use of similar materials for both ducts significantly increases the predictability of stress levels, thereby increasing design confidence and reducing risk.

The duct cooling system is designed with excess cooling capability because holes less than 0.030 inch in diameter are not desired in the system due to the possibility of contamination plugging. The maximum contaminant size allowable is 0.010 inch in accordance with CEI Specification No. CP 2291.

The excess coolant has no measurable effect on overall preburner performance, but does provide a low risk design with temperature margin and growth capability. The cooling system is shown in figure III-21.

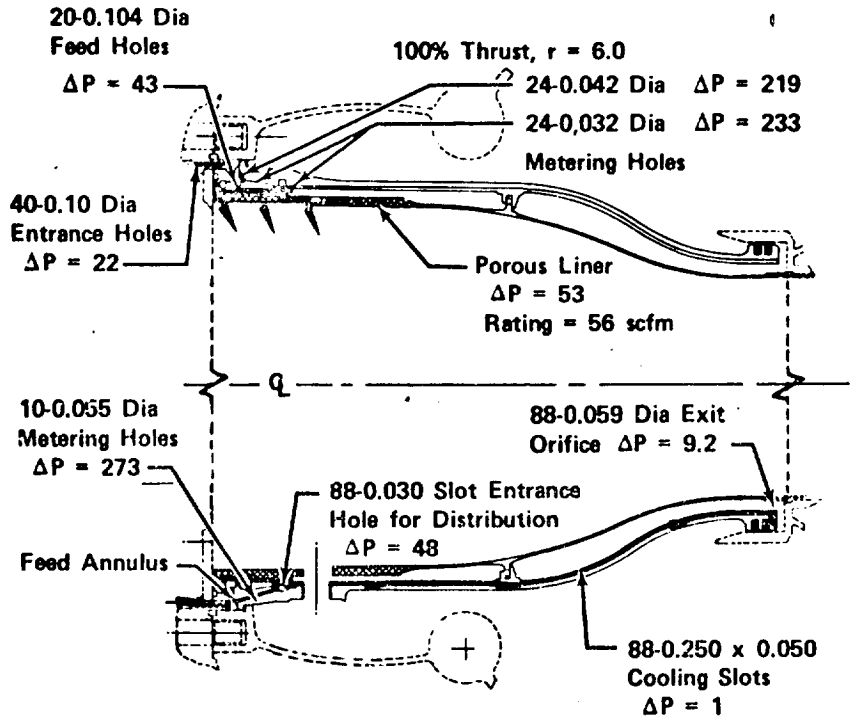

Figure III-21. Coolant Ensures a Low Risk Preburner FD Chamber

In the cooling system, the control orifices are drilled holes which regulate total flow rate to the feed annulus and isolate the cooling system from variations due to fuel inlet pressure. The 0.030 inch distribution holes prevent variations in groove flow rates due to variations of heat input into the grooves from the inner wall. This promotes heat exchanger stability. The 0.250 x 0.050 inch grooves are designed to provide pressure losses required to cool the wall. The pressure drop of 9.2 psi in the individual groove exit holes are used to isolate individual slot flow rates from circumferential variations in exit plenum pressures. The cooled duct passages are paired for redundancy of supply in the event of hole plugging.

The outer duct has bosses for the igniter and the pulse gun. These bosses are sized with sufficient area to have cold fuel pressure between the thread and an O-ring seal to prevent hot combustion gases from leaking through the duct wall and causing a hot spot. These holes can be used for borescoping during preburner inspection. Figure III-22 shows the pulse gun boss.

The front flange of the duct assembly locates the duct assembly axially and transmits an axial blowoff load due to duct differential pressures of approximately 180,000 pounds into the main case flange, through the sealing and load gasket. The Teflon-coated O-ring on the front of the duct assembly has a 0.002 springback which will accommodate the 0.0005-inch thermal shrinkage at the seal groove. The interface at the front of the duct assembly is designed to occupy a minimum radial space to provide the lightest possible hardware. This is summarized in FR-4447, Design Substantiation for 415K Preburner Combustion Chamber, Appendix G.

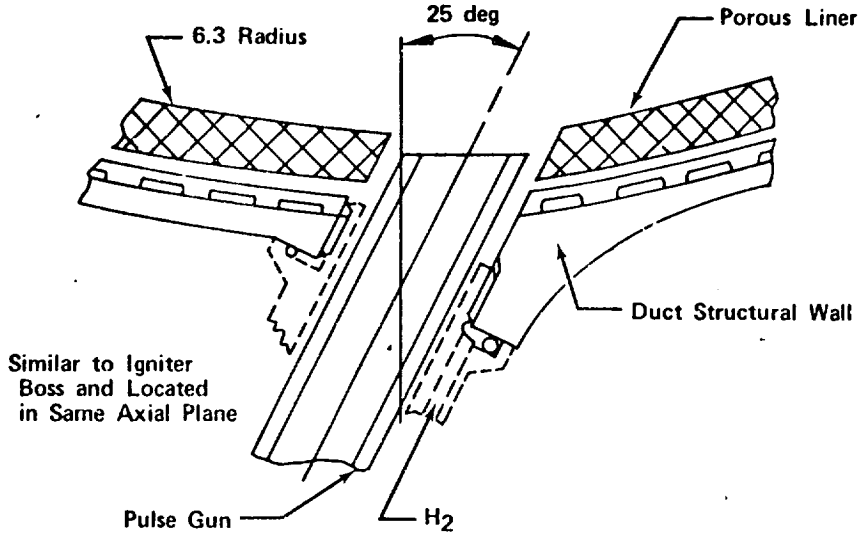

Figure III-22. Pulse Gun Boss Provides for Positive Hydrogen Dam Seal FD 46189

When the cooling system is in use, the duct wall temperatures and gradients are low as shown in figure III-20. This provides safety margins and reduces risk in an area where exact temperature solutions are difficult.

On the inside wall of the inner duct, a joint for accepting the bayonet joint of the uncooled liner also provides an anti-aspiration sealing surface. The differential pressure on the uncooled liner holds the liner against this sealing surface on the duct to provide the seal which prevents flow behind the liner. With this type of liner mounting, the liner may easily be replaced at overhaul.

The low risk nature of the duct design is exemplified by the fact that the duct can rupture and the failure will be contained by the main case. The result will be a failsafe engine shutdown. In addition, because the duct is excessively cooled, it can tolerate low cycle fatigue cracking on the inner duct in the event hot combustion gases scrub along this area. The duct wall structural member temperatures are stabilized by the 26 lb/sec flow on the outside which provides additional safety to the design.

The regeneratively cooled preburner combustion chamber design with liners is based upon proved hardware testing. This design provides low risk, is maintainable and enables maximum stable combustion with a resulting low temperature profile.

- PISTON RING SEALS PROVIDE LEAKAGE CONTROL AND ALLOW THERMAL DEFLECTION FOR THE PLUG-IN CONCEPT

The spherical plug-in concept utilizes piston ring seals at the centerbody to allow deflection freedom for thermal and pressure growths. The seals also provide an assembly radial clearance for taking up tolerance stackups. These seals operate at an approximate 2066 psi maximum pressure differential.

Study of a mitered butt seal to be used with intersecting cylinders indicated that the problems associated with high delta pressure, tolerances, growths, and assembly were severe. Of the schemes considered, piston rings were selected because they provide the lowest risk approach. Two ring sets at each of the three ports in the centerbody provide redundant sealing. The seal design is shown in figure III-23.

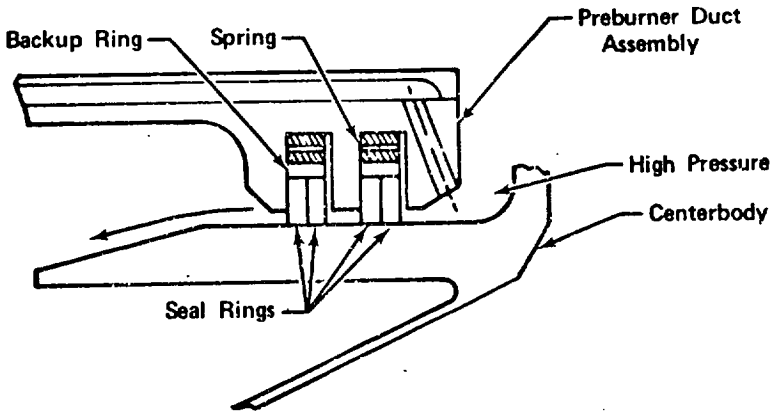

Figure III-23. Piston Ring Seals Allow Freedom of Movement FD 46159

Selection of piston rings required three seal lands and a body to carry the lands. Because of the high pressure involved, the centerbody selected is spherical to obtain minimum weight. The piston rings permit plug-in of the major components into the main case and is the basis for exceptional maintainability.

Improper assembly of the piston rings can be tolerated. The only potential risk of leaking any significant quantity of hot gases would be the result of the square-end gaps in the two sets of rings all lining up. The results of this leakage would be to leak away some of the centerbody internal coolant at approximately 500°R to 1000°R. The centerbody would continue to operate satisfactorily.

Early XLR129 powerhead testing resulted in some piston ring deformations or extrusions because of excessive centerbody seal land deflections or ovalizations, primarily due to nonuniform centerbody loads and excessive ring carrier/land assembly gaps. These problems have not recurred during recent (February and March 1971) powerhead hot firings because the excessive deflection and gap problems have been corrected. A detailed discussion is contained in Design Substatiation for 415K Preburner Combustion Chamber, page 21, 22 and Appendix D, PWA FD-4447. All XLR129 experience has been considered and utilized for the SSME design where it was applicable. Reduction of the carrier/land clearance to 0.025 inch will be one factor that will provide satisfactory seal operation.

- HOT SPOTS METAL EROSION, AND LOCAL BURNING IS PREVENTED AND ACOUSTICAL DAMPING IS PROVIDED BY A TRANSPIRATION-COOLED PREBURNER CHAMBER LINER

The transpiration-cooled liner protects preburner hardware in the region of the highest energy release within the preburner chamber. The 0.25-inch thick porous material contributes a major portion of the acoustical damping capability for combustion instabilities. The cooled liner is shown in figure III-24.

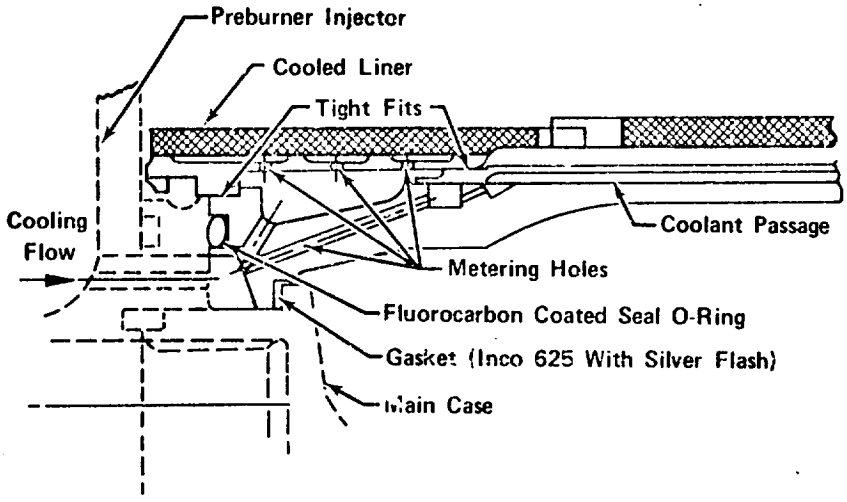

Figure III-24. Compact Cooled Liner Ensures Protection in the High Energy Release Area and Provides Acoustical Dampening FD 46160

The transpiration-cooled liner is fabricated from 0.25-inch thick L-605 coolant distribution housing. L-605 cobalt base material is used because of its superior oxidation resistance and cryogenic strength. The assembly is tightly fitted at two snaps (0.005T diametral) into the duct assembly. These fits enable the coolant manifold end seals to be constrained within a minimum radial space. The rear end of the porous sheet of this tight fitted liner assembly has fingers that interlock with the uncooled liner, providing an anti-rotation constraint for itself and 12 axial slots. The 12 axial slots relieve thermal stresses that would result from the axial thermal gradient.

Uniform flow to sections of the porous liner is guaranteed because the coolant distribution manifold has 72 separately fed compartments. Effects of unequal cooling flow distribution are reduced by this compartmentized design. Local flow variations over a compartment (0.4 x 1.65) will be minor because the porosity variation over the area is small.

Fifty-six scfm-rated porous material was selected based on analytical and test experience. Local metal erosion experienced during the early phases of the XLR129 program resulted in the change from a lower flow rate liner to the 56 scfm liner. This liner proved successful on subsequent tests. The liner can be easily replaced using the puller grooves provided on the front outer diameter of the liner housing.

The end of the liner is in the same plane as the igniter and pulse gun to eliminate aspiration flow behind the uncooled liner. The liners are vented in this plane and allow access for the igniter and pulse gun. Holes in another plane to accommodate the igniter and pulse gun would permit aspiration flow behind the uncooled liner because of a driving pressure caused by the static pressure drop along the chamber. The preburner/main case/cooled liner interface is the result of many requirements and study sketches and is the result of the study in Design Substantiation for 415K Preburner Combustion Chamber, Appendix G, PWA FR-4447.

- DOWNSTREAM UNCOOLED LINER PROVIDES ADDITIONAL THERMAL PROTECTION AND ACOUSTICAL DAMPING

The uncooled liner protects the duct assembly from hot spots and local burning downstream of the cooled liner. This liner further provides low cycle fatigue life on the inner wall of the duct assembly by preventing hot gases from scrubbing on the duct wall. This would result in large thermal gradients across the structural duct that would reduce life. The porous section of the liner, in conjunction with the cooled liner, also provides acoustical damping to prevent combustion instabilities.

The uncooled liner is a four-piece weldment fabricated from H-188 (PWA 1042) cobalt alloy. The front porous section, 0.25-inch thick, is fabricated from L-605 which is also a cobalt alloy. These materials are used because they have excellent oxidation resistance, high temperature creep strength, and are compatible with the combustion gases.

The liner assembly is mounted by a simple bayonet joint that fits into the grooved joint provided on the inner duct. This joint is shown in figure III-25. This type of mounting was selected because it is simple, lightweight, and allows for radial thermal movement. A sealing surface is provided on the liner that axially restrains the uncooled liner assembly. The liner is loaded against a sealing surface on the inner duct by a 2000-pound axial load, the result of the static pressure drop causing differential pressures on the liner. The seal prevents aspiration flow of hot gases behind the liner. The front section of the liner, a combination of the porous section and a length of 0.050 sheet, is in creep buckling with a very low inward acting pressure differential (0 to an estimated 1 psi). The required creep buckling margin of 30 percent is exceeded by more than a factor of 40. The rear portion of this liner is in hoop creep tension with a maximum differential pressure of approximately 44 psi. Because the material was selected to be 0.022 to 0.027-inch thick to provide resistance to hot spots and erosion, the resulting creep stress is well below the allowable.

Mechanical liner vibrations are damped because of contact with the cooled liner tangs at the front, contact with the centerbody heatshield at the rear, and a 0.002 to 0.006L fit at the bayonet joint. This prevents bayonet joint lug fatigue (Design Substantiation for 415K Preburner Combustion Chamber, page 23, PWA FR-4447 gives a complete story of XLR powerhead rig joint rig failure versus XLR129 success).

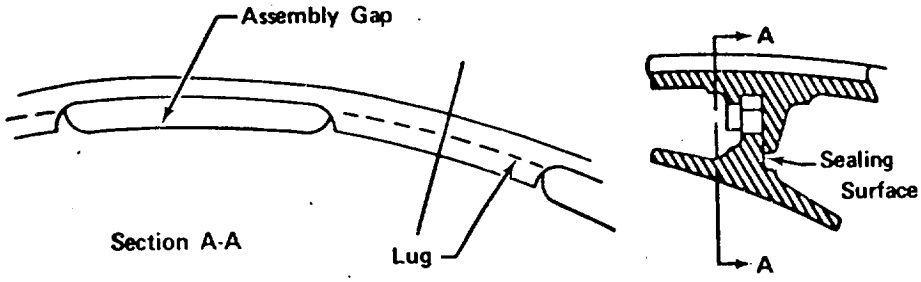

Figure III-25. Uncooled Liner Bayonet Joint Provides Seal Surface and Allows Radial Thermal Growth FD 46161

Two and one-half years of design and testing experience obtained during the XLR129 rig and flight design has been applied to the SSME design.

The SSME is similar to the XLR129 except for the following primary features:

1. External heatshield is not required because coolant in route to the centerbody first cools the preburner chamber outer diameter

2. Uses 0.25-inch thick porous material on the cooled liner for greater acoustical damping capability

3. Uses 0.25-inch thick porous material on the front of the uncooled liner for additional acoustical damping capability

4. Duct assembly is tightly fitted instead of brazed to form the assembly of the two ducts, thereby reducing cost.

The design substantiation effort for the original (415K engine size, which is applicable to the 550K engine size, may be referred to in Design Substantiation for 415K Preburner Combustion Chamber, PWA FR-4447.

3. Requirements

The applicable paragraphs of CEI Specification No. CP2291 and the method of compliance are as follows:

1. The engine shall shut down safely from any power level as stated in paragraph 1.2e.

   Compliance - The cavities behind the uncooled liner have vent holes to prevent collapsing of liners.

2. The engine shall have long service life and require minimum maintenance as started in paragraph 1.2K.

   Compliance - The entire preburner combustion chamber assembly can be replaced in the main case as a module, the inner liners are replaceable, and the duct is not life limited.

3. Chamber pressure disturbances shall not be outside the limits stated in paragraph 3.2.9.1.

   Compliance - Liners of 0.25-inch thick porous material provide required acoustical damping.

4. The engine shall have a provision for artificial pulsing as stated by paragraph 3.2.9.3.

   Compliance - A pulse gun port is provided at a location in the igniter plane (2.75 inches from the injector face).

5. The engine shall be designed for 7.5 hr and 100 starts without requiring overhaul as stated by paragraph 3.6.1

   Compliance - Uncooled liners provided prevent excessive thermal gradient in the inner shell of the duct assembly and permit an excess of 400 starts. The uncooled liner is designed for more than 7.5 hr creep and creep buckling.

6. Combustion instabilities shall be damped within the prescribed time limits stated by paragraph 3.6.4.1.

   Compliance - Liners of 0.25-inch thick porous material provide required acoustical damping.

In addition to the requirement of CEI Specification CP2291, Pratt & Whitney Aircraft imposed requirements are:

1. The engine design shall utilize experience.

   Compliance - The engine design is functionally and mechanically similar to XLR129 demonstrated hardware.

2. The engine shall be designed to the SSME structural design criteria. (Refer to SSME Structural Design Criteria, PWA FR-4449.)

   Compliance - The engine design complies with the above.

3. The minimum hole size shall be 0.020 inch in diameter.

   Compliance - Eighty-eight distribution holes in the duct assembly cooling system are 0.030-inch in diameter.

4. The preburner shall be removable independently of pumps.

   Compliance - A piston ring slip joint is used.

4. Capability - DESIGN FALLOUTS RESULT IN INSURANCE AND GROWTH POTENTIAL WITHOUT A WEIGHT PENALTY

The preburner combustion chamber assembly possesses capabilities in excess of many of the other areas of the design. This is due to most sections of the design being designed to meet requirements other than stress. The stress summary defines all excessive SSME natural or inbuilt capabilities, the primary features of which are the provisions of growth and/or low risk capabilities. (Refer to Design Substantiation for 415K Preburner Combustion Chamber, PWA FR-4447.)

The long preburner design resulting from using the spherical plug-in concept provides a maximum peak-to-average temperature profile at the inlet to the turbine of 100°R. This low temperature profile allows the uncooled turbine design to have the capability of accepting an additional temperature spike of up to 120°R with no life reductions. A spike on a cooled turbine design magnifies the thermal gradient in the blades and reduces the low cycle fatigue capability of the blades.

The duct pressure vessel is burst limited using a 1.5 burst safety factor. Calculations did not consider the additional strength contributed by the inner duct at the 0.033 inch to 0.050 inch walls. This duct strength will provide a 5% to 10% margin, provided that the material protected by the liner is relatively cool.

As the duct is excessively cooled, higher short duration or long duration temperatures of the combustion gases can be tolerated by the duct assembly. This is because the flat stress/temperature curve of PWA 1052 will show little stress degradation in the event the duct structural wall experiences a minimal temperature increase. The duct can also tolerate a local hot spot because of the same reason. The duct can operate with less margin even with some or all of the passage plugged and not flowing coolant.

The inner duct has an excessive low cycle fatigue capability by a factor of 3 on strain, except at the bayonet joint. Low cycle fatigue cracking, if experienced on the inner duct, would be tolerable. This is because the leakage established through a crack would be small compared to the total flow in a passage and the duct can operate if there is no flow in one, two, three, or all passages. Potential cracking at the bayonet joint seal would allow small and tolerable amounts of aspiration flow behind the liner.

The cooled porous liner temperature gradient of 300°R to 400°R permits a greater number of life cycles than the required 400 cycles. The design differential pressure of 286 psi on the cooled liner assembly places the housing and liner in hoop compression to less than 1/10 of the allowable yield strength and to less than 1/5 of the critical buckling pressure. This pressure differential actually relieves and replaces some of the 20,000 maximum psi compressive stress due to the assembly tight fits of 0.012 to 0.016T. The allowable compressive stress at the assembly is 24,000 psi.

The front porous section of the uncooled liner has a creep buckling margin of more than 40% over the 30% required. The rear section of the uncooled liner has a margin greater than 1.5, based upon 0.5% creep strength. This section is just to the rear of the bayonet joint and the margin increases as the liner differential pressure decreases to zero, going rearward.

The piston rings can tolerate excessive pressure differentials because their resistance to rolling or extrusion is not a function of pressure, because of the carrier/land gap-to-ring wall thickness ratio. An SSME ratio (0.050/0.180) of approximately 0.28 versus an estimate of 0.4 allowable, provides a substaintial margin to prevent ring extrusion. The SSME gap of 0.025 means that should 0.050 inches of centerbody ovalization occur, the seal carrier and centerbody land come into contact. The seal carrier stiffness then contributes to stiffening the seal land.

The XLR129 preburner combustion chamber was subjected to 12 tests in the powerhead configuration. The excellent performance exhibited by the preburner combustion chamber during these tests is the substantiation for the SSME preburner combustion chamber design approach.

A series of 12 test totaling more than 100 seconds of hot firing were completed by the end of the XLR129 program (summer 1970). Specific test conditions were:

Two tests at 100% thrust:

One test at an oxidizer/fuel ratio of five to six (equivalent engine oxidizer/fuel ratio).

One test at an oxidizer/fuel ratio of seven (equivalent engine oxidizer/fuel ratio).

Six tests included a fuel main pump in the powerhead.

Six tests used pump simulations with orifice plates to simulate the turbine pressure drop. The results are summarized in table III-3.

The results of these tests showed the preburner combustion chamber design to be satisfactory for the purpose intended. The only problem was the previously mentioned piston ring distortion and extrusion that was due to excessive ring carrier/seal land assembly gaps and ovalization of the seal lands on the centerbody. No engine damage resulted from this distortion. The uncooled liner operated as intended. Minor cracking was seen at the fillets of the 12 slots of the front end. These fillets have been enlarged for the SSME configuration to 0.078 to 0.109R. The cooled liner, developed during XLR129 preburner rig testing, operated above expectations and showed no deterioration due to hot spots. No high frequency acoustical vibration problems were seen. The XLR129 testing of the duct "brazement" substantiated the operational validity of the cooled duct design concept.

A second series of tests was conducted during February, March, and April 1971. These tests were conducted using pump simulators, a reinforced centerbody, and a piston ring clearance reduced to 0.033 to 0.040 from 0.058 to 0.062. The pump simulators incorporated low turbine differential pressure orifice plates so that rig run duration could be increased. These test are summarized in table III-4. Further substantiation will be accumulated with continued testing of the "Test Plan B" program.

Preburner combustion system flow characteristics were experimentally determined on a full scale transparent model of the XLR129 powerhead. The

results determined the validity of the analytical method used to predict the main case three-dimensional flow characteristic. This information is contained in XLR129 Main Case Flow Characteristics, PWA FR-4448.

Table III-3. Hot Turbine Test Summary

Test No.	Thrust/ Mixture Ratio	Combustion Temperature, °R	Combustion Pressure, psia	Pump Speed rpm	Pump Discharge Pressure, psia	Duration
1.02	50/5	1450	1868	29,360	2340	13.7
201	Instrumentation Advance					6.4
3.01	75/5	1605	2970	35,630	3610	14.5
4.01	75/5	1615	2965	35,360	3560	17.2
	75/6	1985	2882	34,610	3367	
5.02	75/5	1610	3045	36,085	3737	22.0
	100/6	2070	4086	40,782	4981	
	100/7	2395	3889	39,498	4623	
6.01	50/7	2118	1612	30,000	2420	20.0
	100/5	1900	4200	44,592	5512	

Table III-4. XLR Powerhead Test Summary Using Pump Simulators Staged Combustion

Run No.	Date	Duration	% Thrust/of	Preburner Comb. Temp.	PB Comb. Press.	Main Case	Turbine Disch. Temp.
5.01		22.50	50/5.5 & 6.0 & 92%	1926°R	2795 psi	2692 psi	
6.01	3/1	26.03	50/5.5 & 6.0/100/6	1860	1860	2881	1638
7.01		24.21	100/6 & 6.5	1851	3076	2873	1590
8.01	3/2	23.15	100/6	1799	3057	2829	1641
9.01	3/15	22.54	100/6	2203	2827	2696	1838
10.01	3/15	21.63	100/6	2145	2857	2657	1929
11.01	3/18	16.79	100/6	1502	2774	2605	1457
12.01	3/22	22.71	100/6	1703	3135	2963	1606
13.01	3/22	22.71	100/6	1678	3124	2942	1635
14.01	3/22	17.58	100/6	1638	3033	2866	1546

SECTION IV
MAIN CHAMBER INJECTOR

A. INTRODUCTION

Several main chamber injection concepts were evaluated to confirm the selection of the best configuration. This evaluation included performance, stability, durability, cost, weight, ease of manufacture, and test experience. The spraybar configuration main chamber injector configuration was selected for the SSME design. The SSME main chamber injector is a scaled-up configuration of the demonstrated XLR129 design using the same self-atomizing tangential slot swirler liquid oxygen injection elements and spacing. A comparison of the SSME and XLR129 main chamber injectors is shown in figure IV-1.

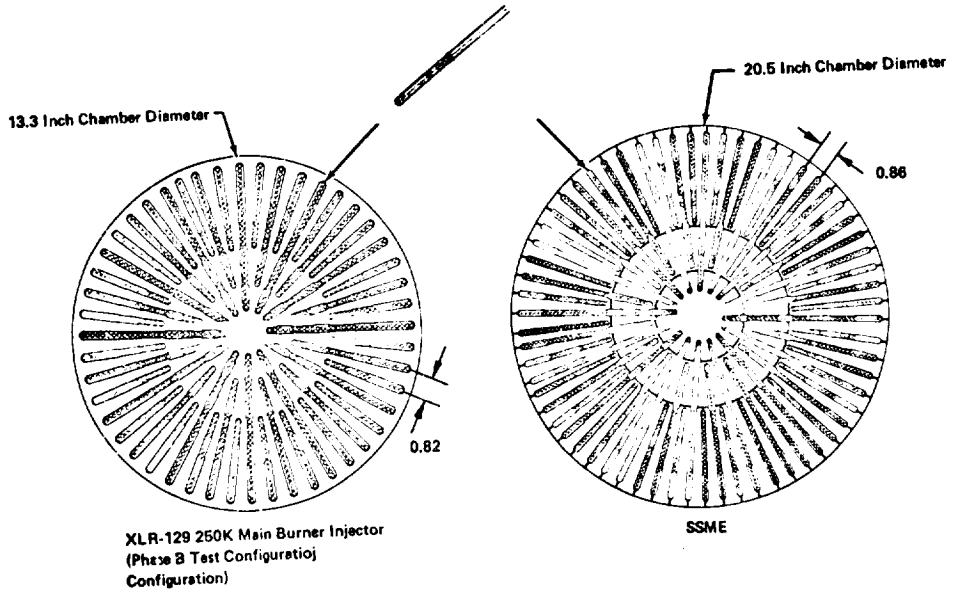

Figure IV-1. SSME Main Injector Scale Factor 1.5 FD 47147A

A radial spraybar configuration yields better combustion efficiencies than a uniformly-spaced pattern because of the greater number of injection elements inherent to the design. The SSME spraybar injector pattern provides over 2400 injection points compared to only 600 injection points for a 0.625 inch uniform-spaced pattern (RL10 spacing) for the same injector face diameter. This significantly increased element density provides for better liquid oxygen atomization and distribution. The radial spraybar injector concept permits a separate fuel faceplate structure. The hot gaseous fuel flows through the injector in a completely uniform manner and fuel manifolding is not required. The radial pattern of the injector allows for free thermal differential growths between the hot faceplate and colder liquid oxidizer elements.

Development and improvements of this injector concept have progressed over the past 5 years to the point where the fabrication process has been highly developed. The injector has demonstrated performance and good durability

over a wide range of operating conditions. Early Phase B 250K staged combustion testing shows that the spraybar main chamber injector performance shown in figure IV-2 will exceed the SSME performance requirements.

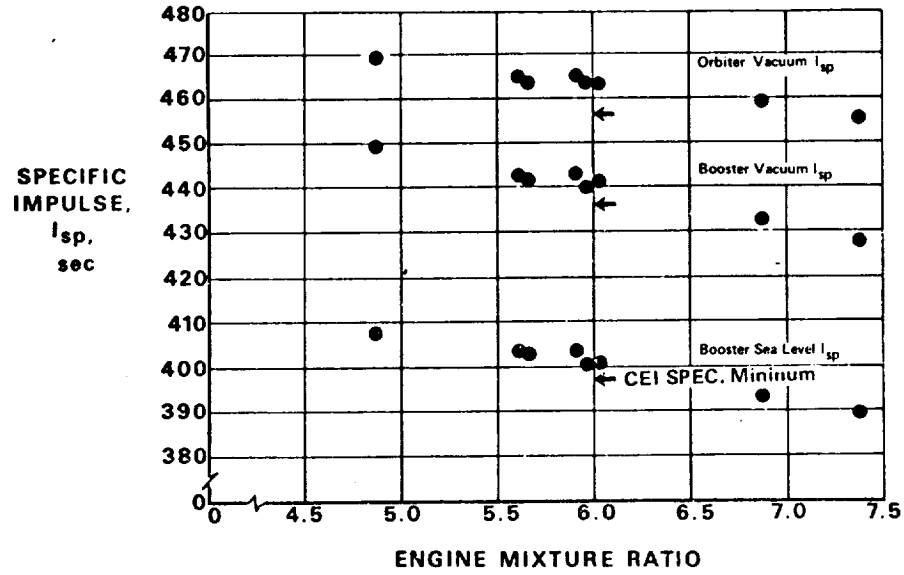

Figure IV-2. Early Phase B Test Data Exceeds 550K SSME Performance Goals FD 52445

B. MECHANICAL DESCRIPTION

1. Function

The main chamber injector introduces, atomizes, and mixes liquid oxidizer (205.8°R at a flow rate of 1009.87 lb/sec, and a pressure of 4977.6 psia for 100% r = 6 orbiter) with the hot, fuel-rich turbine discharge (preburner combustion products) (1616.2°R at a flow rate of 346.15 lb/sec, and a pressure of 3156.3 psia). This must be done in such a manner that efficient and stable combustion is achieved. The injector functions over an engine operating range of 50% to 109% thrust at mixture ratios of 5.5 to 6.5. An integral oxidizer heat exchanger for vehicle oxidizer tank pressurization gas, (2.55 lb/sec of gaseous oxygen at 800°R ±50°) is incorporated into the injector.

2. Configuration

The main chamber injector is a radial spraybar configuration concept shown in figure IV-3 which allows differential thermal expansion between a hot fuel metering faceplate and the colder liquid oxygen spraybars, with a minimum effect on the injection pattern. An injector faceplate is used to distribute the fuel (hot turbine discharge gas) around the liquid oxygen injection elements. The high injection element density provides a finely atomized and uniformly distributed oxidizer to uniformly mix and burn with the hot turbine discharge gases.

The external liquid oxygen enters the main chamber injector through a single inlet. It then flows into the oxidizer inlet manifold which is wrapped

around the circumference of the injector, maintaining essentially equal distribution to all of the spraybars.

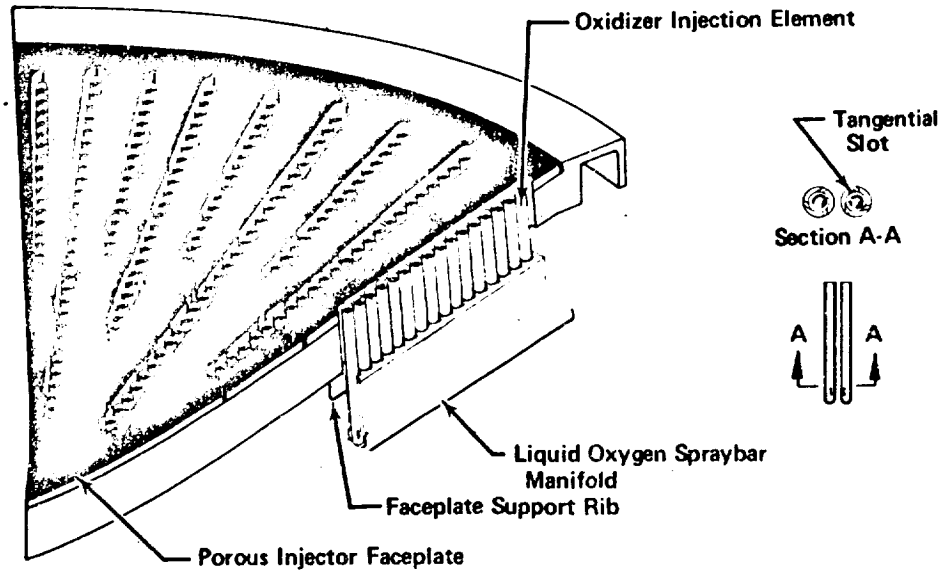

Figure IV-3. Main Chamber Injector FD 46271 A

A small portion of the oxidizer flow is diverted from the wraparound manifold through drilled passages connected to struts protruding into the hot gas stream. The hot gases from the main case flow around these struts providing heat to this oxidizer flow. This flow is returned by the struts to an auxiliary wraparound manifold, where it is collected and exited from the injector for use as vehicle oxidizer tank pressurization gas.

The major portion of the liquid oxygen that flows from the wraparound manifold flows through crossover passages to the radial spraybars that serve as internal manifolds for the oxidizer injector elements. A single tapered hole down the length of each spraybar allows sufficient area to maintain the overall injector pressure drop essential constant to each of the injection elements.

There are 2466 self-atomizing injection elements spaced along the 72 radial spraybars to obtain a high density of liquid oxygen injection elements and a resultant fine oxidizer atomization and distribution. These elements have flow entries machined tangentially to the tube inside diameter which causes the flow to leave the elements and enter the main combustion chamber in a hollow swirl cone made up of very small droplets. Alternate injection elements are counter-swirled for uniformity of injection pattern. To prevent the spray cone from impinging on the chamber wall, the outer element discharge tips are cut at an angle.

The turbine discharge gases flow around injector spraybars and elements to the injector faceplate, which is constructed of a porous faceplate welded to a webbed support structure. The major portion of this gas passes through the faceplate through slots surrounding the oxygen elements where it is mixed

with the oxidizer flow. To prevent the main burner combustion products from recirculating and burning the faceplate, a portion of the fuel-rich gas flows through the porous faceplate creating a protective barrier.

The main chamber injector consists of five major components as shown in figure IV-4: the oxidizer manifold and housing, the heat exchanger struts, the spraybar-type internal manifolds, the oxidizer injection elements, and the fuel faceplate assembly. The major components will be assembled by brazing and welding techniques that simplify the manufacturing requirements of the individual components. This configuration represents, in a minimum overall length and weight, a design that satisfies the performance and durability cycle requirements, while still simplifying manufacturing. The SSME injector is identical in concept to the lightweight injector shown in figure IV-5 currently being tested for design confidence and substantiation. Each of the major components is discussed separately in the following paragraphs.

a. Main Chamber Injector Housing

The main injector housing, fabricated from Inconel 718 material, consists of the oxidizer inlet, the main oxidizer manifold, heat exchanger collector manifold and exit, and the cross-over passages to the spraybars. The injector housing has clearance holes uniformly spaced around the main chamber bolting diameter for the chamber bolts which pass through the injector housing. A single oxidizer inlet is welded to a transition piece which forms part of the wraparound manifold that is welded to the main housing. Flow cross-over passages between bolt holes connect the external manifold to the spraybar-type injector element manifolds. Oxidizer cross-over passages also connect the external manifold to the heat exchanger struts, and return passages connecting the heat exchanger struts to an auxiliary wraparound manifold. This auxiliary manifold in turn is welded to the main housing. A single tank pressurization exit is welded to a transition piece which forms part of the auxiliary manifold.

The oxygen heat exchanger for tank pressurization flow consists of 36 individually machined struts fabricated from AISI 347 material. The struts are brazed into the main housing. The struts are placed directly in front of the short spraybars to minimize hot gas pressure loss.

b. Injection Elements - OXIDIZER INJECTION ELEMENTS ARE SELF-ATOMIZING

The tangential slot entry into the element uses the static injector pressure drop to form a high velocity film of oxidizer as it passes through the slot. Once inside the element, the thin film is maintained by the centrifugal motion of the oxidizer which creates a vortex with a gas filled core. The gas core fills most of the inside volume of the element leaving only a thin film of oxidizer adjacent to the wall. As the thin sheet of oxidizer leaves the element, the sheet continues to expand due to the centrifugal force of the liquid. The hollow cone of oxidizer thus formed continues to thin out as the end point of the cone increases in diameter, until the sheet breaks apart into droplets. The atomization drop size distribution for this element is shown in figure IV-6. The element does not require high fuel ΔP to atomize the oxygen. The dependency on fuel for atomization could be a problem for chamber life in some injector designs during start and shutdown.

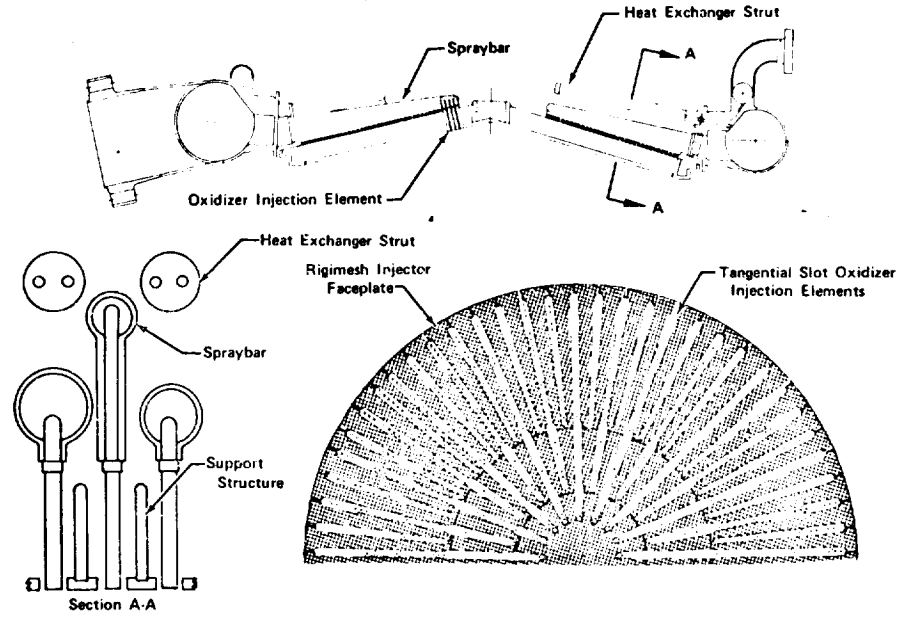

Figure IV-4. Main Injector Configuration FD 46270

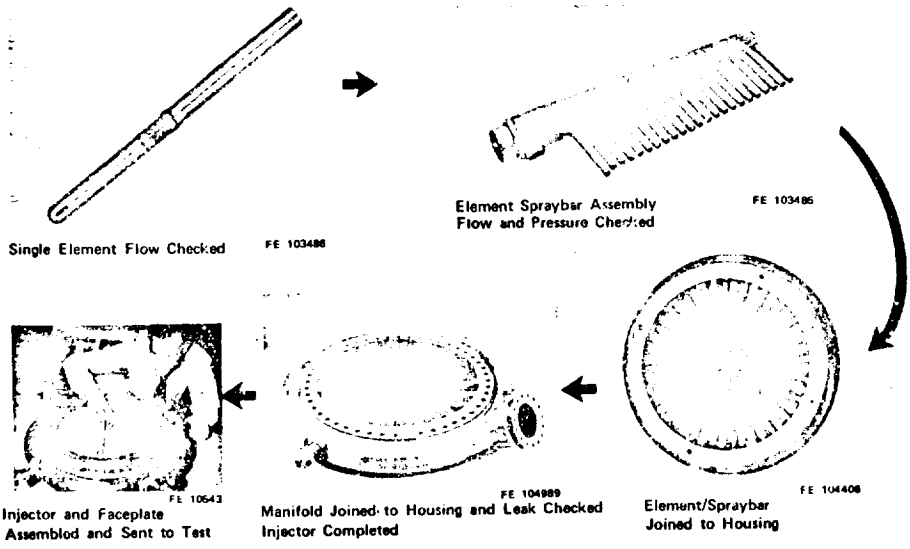

Figure IV-5. Spraybar Concept Mechanical Attractive FD 52231

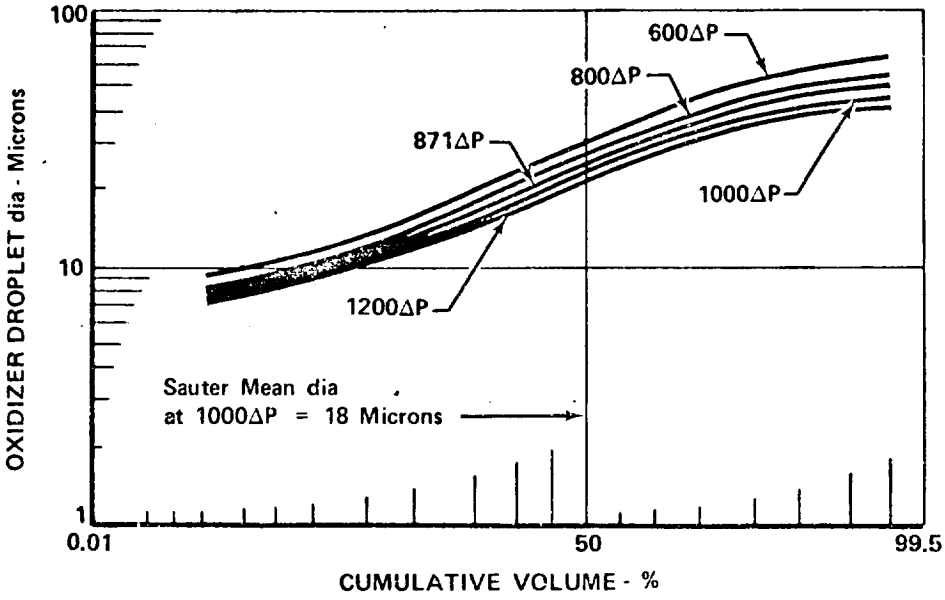

Figure IV-6. LO_2 Droplet Size Distribution Main Chamber Injector Element ΔP FD 52677

The element is formed from a small diameter tube with one end rolled closed. A narrow slot is cut through the tube wall tangent to the tube inside diameter. The elements are mechanically simple, durable, provide excellent atomization, and can be easily manufactured from drawn tubing. The tangential entry slot can be accurately electric-discharge machined into the tube. The slot swirler element can be individually flow calibrated to qualify the item for an injector assembly.

- THE INJECTION ELEMENT IS NOT PRESSURE LIMITED

The wall thickness of the element is sized to ensure tangential directivity to the oxidizer and therefore is not pressure limited. The stress induced in the elements results from internal hoop pressure and the bending stress due to the pressure drop at the tangential entry slots. AISI 347 material was selected based on ease of fabrication, cost, and weight comparison with the TD nickel element used on previous designs.

Factors	AISI 347	TD Nickel
Machineability Ratio	1	2.5
Cost Ratio	1	30
Density	0.286 lb/in.^{3}	0.322 lb/in.^{3}

A thermal analysis trade study was conducted on the elements to ensure the temperature distribution on the element tip was within an acceptable range for AISI 347, as compared to TD nickel. The temperature map, shown in figure IV-7, was generated utilizing a nodal breakup heat transfer program, IBM digital computer program 5550. The deck uses a finite difference technique in computing local heat flux and temperature to compare AISI 347

and TD nickel. This program indicates that the selection of the material for the elements is thermally acceptable.

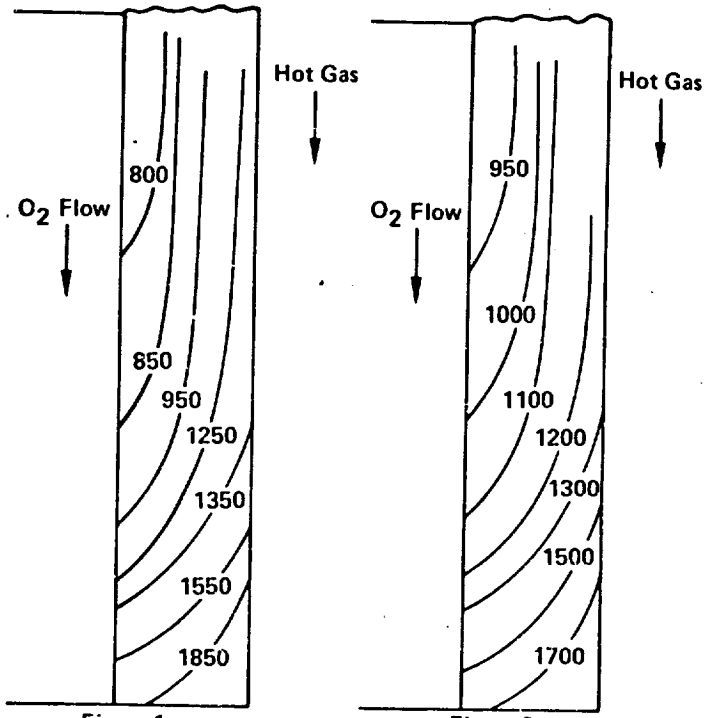

Figure 1. AISI 347 Element Wall Section Temperatures - °R

Figure 2. TD Nickel Element Wall Section Temperatures - °R

Reference: 109% and 6.0

Figure IV-7. Oxidizer Element Tip Temperature Distribution FD 46194

- ELEMENTS ARE CLASSED TO IMPROVE MASS DISTRIBUTION

The previously tested main chamber injector had nonuniform injected mass distribution across the injector face due to the radial configuration of the injector. It is postulated that because of this uneven injected mass distribution, a mixture ratio profile is generated during the initial combustion process due to the greater mobility of the hydrogen and hot initial combustion products compared to the yet unreacted liquid oxygen drops. The areas of the chamber of higher injected mass per unit chamber volume become oxygen rich as the more mobile combustion constituents move to areas of lesser mass density to equalize static pressures in the chamber.

An improved mass and propellant mixture ratio profile has demonstrated improved performance during Phase B 250K staged combustion testing with the new XLR129 main chamber injector. The new XLR129 injector incorporates three flow classes of oxidizer elements with matching fuel slots which flattens the injected mass profile over that of the main burner injector used during Phase I testing. Figure IV-8 shows a comparison of the mass profile of the Phase I and Phase B 250K main injectors. The SSME main injector is designed

with three flow classes of liquid oxygen injection elements to provide a more uniform injected mass distribution. The mass profile classing for the 550K SSME is shown in Main Chamber Injector Design Calculations, PWA FR-4411, page II-21. The flow classes are placed along the oxidizer spraybars to create a mass injection per unit area that is within ±10% of nominal. The injection elements are individually flow calibrated and are copper brazed into the spraybars. The faceplate fuel slot widths are shaped to supply an amount of fuel at a given location that matches the classed oxidizer flow to create a uniform injected propellant mixture ratio.

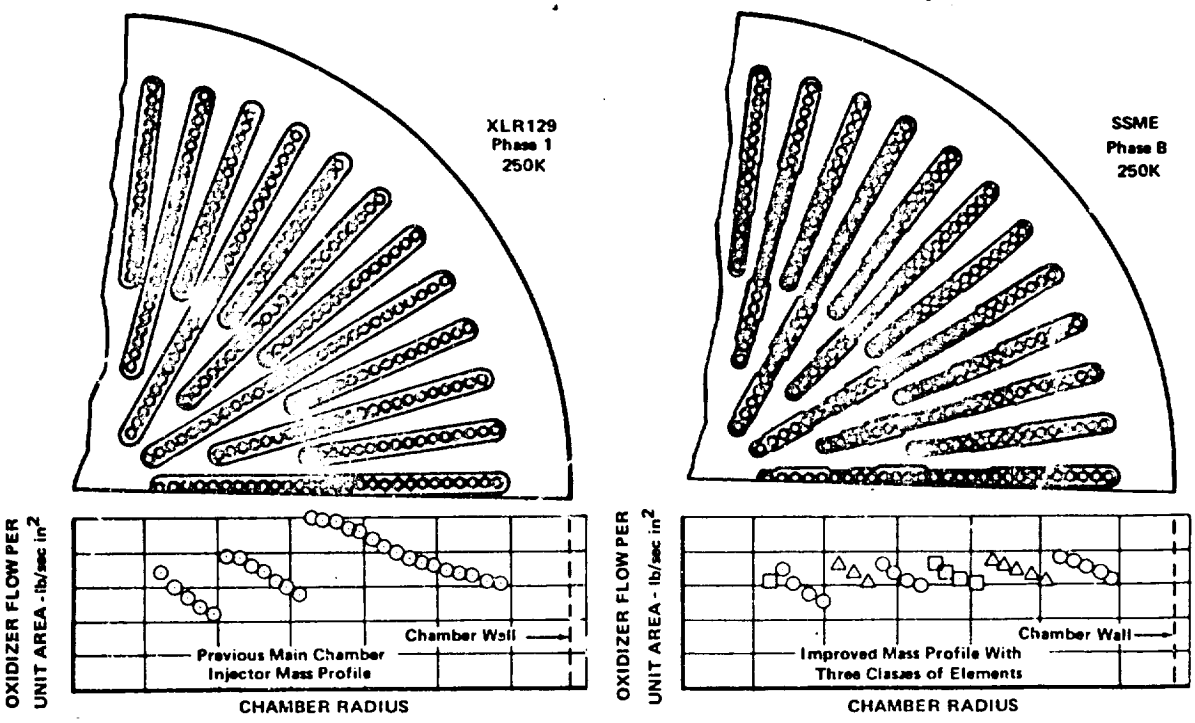

Figure IV-8. Main Chamber Injector Mass Distribution FD 46275

- ELEMENT CLASSING USES SAME ELEMENT BLANK

The liquid oxygen injection element A_{cd}'s have to be designed for three values to fit the required three-flow class. Element A_{cd} is a function of the slot area-to-tube area ratio (A_S/A_O). The Element A_{cd} can be varied by holding A_S/A_O constant and varying the element diameter, or maintain the tube diameter constant and vary A_S/A_O. A constant element inside diameter with varying A_S/A_O was used for this design. This decision was based upon mechanical and handling considerations. It allows for one size tubing raw material and one element blank to fit all classes.

The design element spacing along the spray bars is based on a computerized injection mixing program and the following criteria:

1. Tube wall thickness sized to ensure tangential directivity

2. Distance between adjacent tubes of no less than 0.037 in. to allow additional braze rings around the element.

3. A_s/A_o equal to 0.615 maximum to ensure stable flow.

c. Spraybars - SPRAYBARS ARE MECHANICALLY ATTRACTIVE OXIDIZER MANIFOLDS

The injector has 72 individually machined AISI 347 spraybars brazed into the main housing. The spraybars are supported at the outside diameter only, thereby permitting free thermal growth. The spraybars can be fabricated and flow checked individually before the injector assembly is made. This approach simplified manufacturing and provides a lightweight design.

The 72 radial spraybars are divided into three types. There are: 18 long spraybars, equally spaced around the circumference; 18 medium spraybars, equally spaced between the long spraybars; and 26 short spraybars, equally spaced between the medium and long spraybars. This arrangement yields good oxidizer element density and uniform radial flow distribution. The spraybars are offset axially to minimize the hot gas pressure loss in the flowpath between spraybars. Each spraybar is tapered with the largest end being at the injector housing where oxidizer flow enters the spraybar. The spraybar then tapers to a minimum dimension at the tip. This allows lightweight bars as well as minimum hot gas flow area blockage.

An investigation was made of the material choice for the SSME main chamber injector oxidizer (spraybars). AISI 347 was selected as a lighter weight, lower cost material which is more easily machined than the Inconel 625 previously used.

Factors	AISI 347	INCO 625
Machineability Ratio	1	2.5
Cost Ratio	1	5
Density lb/in.^{3}	0.286	0.305

The 250K Phase B main chamber injector oxidizer spraybars are machined from wrought Inconel 625. To reduce cost and machining effort, AISI 347 was chosen for the design of the SSME main oxidizer spraybars, which is structurally adequate for the application. The oxidizer spraybars are subject to hoop stress from internal pressure and bending stress due to main stream gas loading. Additionally, web stress results from the hoop stress being taken through the material between adjacent oxidizer elements. This web stress establishes the thickness of the oxidizer spraybars.

Low cycle fatigue predictions for the XLR129 oxidizer spraybars indicate that their cycle life is limited by thermal strain. AISI 347 provides better cycle life within a hydrogen environment than Inconel 625 at the existing strain level.

The main chamber injector spraybar is subjected to hot preburner combustion gas at 1700°R on its outside surface and cold liquid oxygen at 200°R on its inside surface. The resulting thermal gradient across the spray nozzle wall produces thermal strains which limit its life. Figure IV-9 shows the

maximum thermal strain in the spraybar as slightly less than 0.5%. This corresponds to a spraybar cycle life of 1100 cycles.

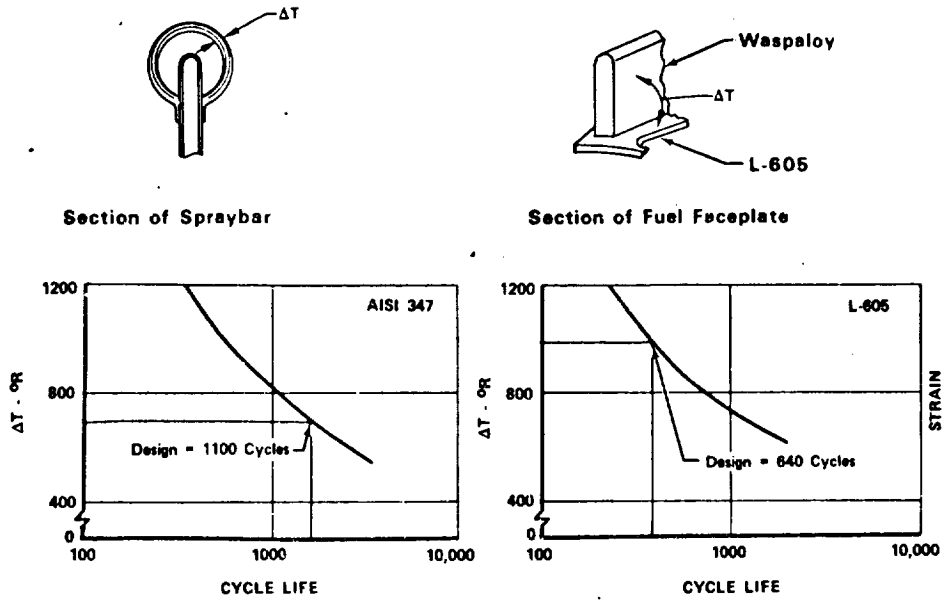

Figure IV-9. Design Meets Cycle Life Requirements FD 47140

The SSME oxidizer spraybars will be brazed into the Inconel 718 main chamber injector housing. On the XLR129 and Phase B 250K testing designs, the thermal coefficients of expansion of the materials put the attachment braze joint in tension which is not preferred practice. However, the use of AISI 347 will put the braze in compression.

As a result of this investigation, wrought AISI 347 was selected for the SSME main chamber injector oxidizer spraybars rather than Inconel 625. It is of lighter weight, lower cost, easier to machine, has longer cycle life, and puts the attachment braze joint in compression.

- ELEMENTS AND ELEMENT SPRAYBAR ASSEMBLIES FLOW CALIBRATED BEFORE INJECTOR ASSEMBLY

The injection elements are first individually flow checked before being brazed into the spraybar. Each spraybar, with elements in place, is flow checked individually because they are not part of the housing. This approach simplifies manufacturing and reduces cost because unacceptable assemblies can be identified before incorporation into the main housing. A typical spraybar assembly with the oxidizer elements in place is shown in figure IV-10.

Braze joint geometry has undergone a development program to substantiate it as a reliable, strong, leak-free joint. The oxidizer injection elements are brazed to the spraybars, and then these subassemblies are brazed into the main chamber injector housing. The first braze cycle

incorporates a high-temperature (2460°F) copper braze. The second braze cycle incorporates a pure silver braze.

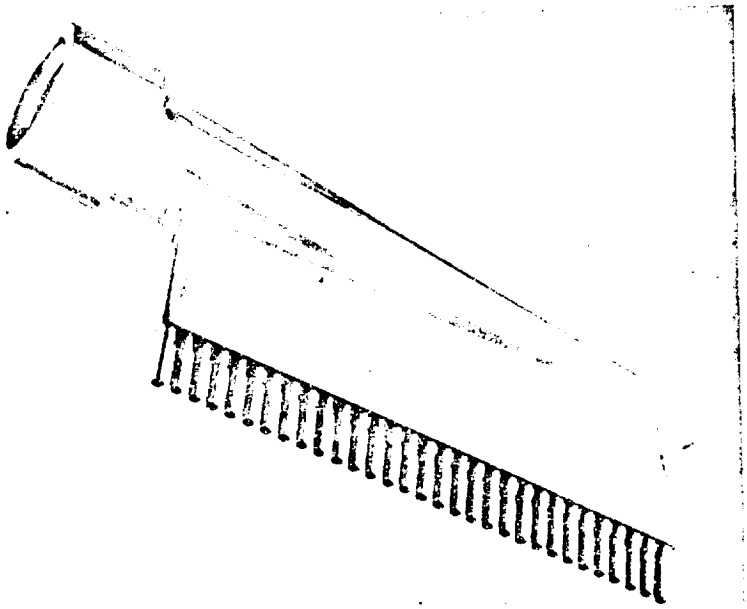

Figure IV-10. Flow Checking Spraybar Assembly Prior to Braze Simplifies Manufacturing and Reduces Cost FD 52669

Because the copper material of the first braze cycle is applied by plating, a controlled location of the braze joint is ensured. Penetration to a given depth in the braze joint is achieved by plating the copper material onto the injection elements to a given dimension. The plating is prevented from flowing into the tangential feed slots on the element by the use of a nickel-plate dam just below the copper. For other braze alloys which cannot be plated, the braze material must be melted and then flowed into the braze joint. This could cause the braze material to run completely through the joint and onto the tangential feed slots, which would be detrimental to the injection spray pattern. In addition, the high temperature of the copper braze material permits a wide variety of braze considerations for the spraybar second braze cycle.

This braze joint was first successfully used during Contract AF04(611)-11401. Subsequent testing has demonstrated that copper braze is qualified as an acceptable method of jointing the injection elements to the spraybars and provides a reliable, strong, and leak-free joint.

The second braze cycle is a silver braze. The lower temperature of the silver braze will prevent a remelt of the element braze. In addition, silver braze, like copper, has the advantage of being plated directly to either or both of the parts to be joined. This advantage ensures braze coverage to any desirable depth by plating braze material to the desired dimensions. The joint between the injector housing and the spraybar requires absolute sealing, in addition to reliable strength. To substantiate this joint, testing of simulated joints has been completed. The results of this testing, as shown by X-ray and microscopic examination, revealed no voids and the braze coverage was rated at 100%. All fillets were completely filled and continuous. The braze

samples underwent gaseous helium and hydrostatic pressure tests designed to simulate the operating conditions in the injector. These tests were at 1500 psig (65% greater than operating differential pressure) and were held for five minutes. No signs of leakage or failure were noted. Both of these braze joints were used on the main chamber injector which was tested during Phase B.

d. Fuel Faceplate - FACEPLATE DISTRIBUTES FUEL-RICH TURBINE DISCHARGE GASES

The prime function of the main chamber injector faceplate is to distribute the fuel-rich preburner combustion flow around the liquid oxygen injection elements. This is accomplished by incorporating radial slots in the faceplate, in line with the radial oxidizer injection element spraybars. The fuel flow exits the faceplate through these slots, which surround the oxidizer injection elements, and is mixed with the oxidizer flow creating a uniform injected mixture ratio.

To prevent the faceplate from burning due to recirculation of main combustion products, the faceplate is made porous, thereby allowing a portion of the preburner combustion gases to flow through the faceplate and creating a protective barrier and floating the main chamber combustion products off the face. The fuel faceplate distributes approximately 97.6% of the fuel-rich hot preburner combustion gases through slots surrounding the oxygen injection elements. The slot width is shaped to supply an amount of fuel at a given location that matches the classed oxidizer flow to create a uniform mixture ratio. The radial slots in the faceplate are sufficiently long to permit differential radial thermal growth between the hot faceplate and cooler spraybars. The radial layout of both the spraybar and fuel slot is in line with radial thermal growth thereby minimizing the effects of thermal growth on injection pattern.

The fuel faceplate assembly is pressure loaded against the main chamber flange. Providions are incorporated onto the injector housing to provide for centering of the faceplate and radial and axial stops are provided on the faceplate.

- INJECTOR FACEPLATE PRODUCES FUEL INJECTION VELOCITY FOR GOOD MIXING IN COMBUSTION CHAMBER

The faceplate employs a pressure drop across the face to create proper mixing for the combustion process. The plate is designed as a structural member capable of withstanding this injection pressure drop. In addition, the faceplate structure must be deflection limited. This is due to either of the following conditions. If the oxidizer elements extend beyond the face to such a degree that their exits would be in danger of burning off due to combustion recirculation, or were so far recessed as to cause combustion adjacent to the face resulting in the danger of local face burning, performance and durability would be affected.

The Phase I, Contract AF04(611)-11401, fuel faceplate configuration shown in figure IV-11 was considered for the present design. This concept incorporated a porous faceplate, N-155 (AMS 5794), which is electron-beam welded to an N-155 (AMS 5794) spoked support cage. Waspaloy (AMS 5706) was substituted for N-155 on the supporting cage of the initial configuration to compensate for the increased stress level because of elimination of the midspan support

bolts, and L-605 (AMS 5796) was substituted for the N-155 faceplate. This was accomplished to more closely match the coefficient of thermal expansion of the Waspaloy supporting structure.

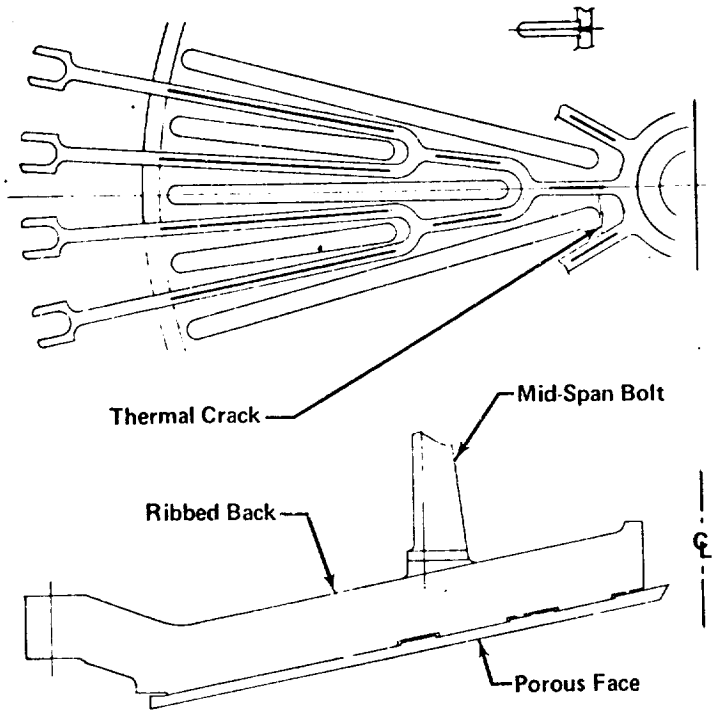

Figure IV-11. 250K Phase I Main Injector Fuel Faceplate FD 46192

Structural analysis employing the finite element structures program was used in establishing the maximum working stress in the supporting sturcture. The program inputs were the radial and axial loads resulting from the maximum pressure drop acting across the structure and includes a thermal breakup of the structure. The resultant deflection induced a maximum stress level, which is below the 10-hour stress rupture or yield strength of Waspaloy, and therefore produces a design approach that is structurally adequate.

The main chamber injector fuel faceplate is exposed to the hot pressure combustion gas flow and therefore assumes a 1700°R temperature throughout. Upon engine shutdown, the porous faceplate temperature response rate leads the support structure rate. This produces a temperature differential of 1000°R, which is based upon revised XLR129 data. The resulting 0.8% thermal strain preestablishes the faceplate structure cycle life as 640 cycles. This life is predicted as 10% of Manson's theoretical calculated life and is shown in figure IV-9.

- THERMAL RELIEF SLOT INCORPORATED INTO FACEPLATE TO ELIMINATE STRAIN

During the 250K Phase I staged combustion test demonstrator program, distress on the porous faceplate was evident as shown in figure IV-12. This distress was in the form of fatigue cracks in the area of the inner fuel slots adjacent to the weld joint on the web. These cracks were repair welded and the demonstrator program was completed. The cause of the cracks was determined to be due to different coefficients of thermal expansion between the porous face and the solid back web.

The cracks produced in the 250K Phase I face resulted from thermal transients experienced during start and shutdown sequences. Subsequent analysis and review of this structure resulted in the incorporation of thermal relief slots in the radial fuel slots to avoid the type of distress experienced on the original 250K staged combustion tests. Testing to establish design confidence and substantiation of this solution proved the relief slots eliminated the problem shown in figure IV-12.

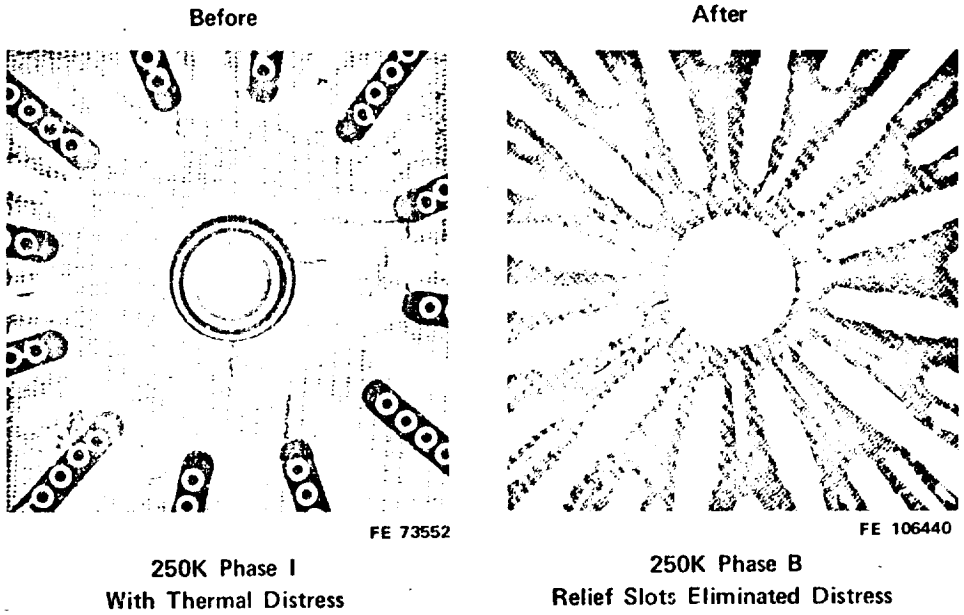

Figure IV-12. Relief Slots Eliminate Fatigue Cracks Caused by Thermal Transients FD 52230

A faceplate design for the main chamber injector, consisting of a porous face incorporating both radial and circumferential thermal relief slots joined to a solid webbed backplate of minimum thickness will meet the structural and durability requirements of the SSME with a minimum of development risk and cost.

e. Main Chamber Injector Operating Conditions

A high liquid oxygen injection ΔP is provided for good self-automization energy and to provide a stiff propellant feed system for low frequency combustion stability. The fuel injection ΔP is kept to a minimum consistent with good mixing and high combustion performance as the hot gas system pressure loss represents a significant penalty to the engine power cycle and required inlet temperature. The main chamber injector operating parameters as defined by the SSME Design Cycle Balance are shown in figure IV-13.

f. Borescope and Bombing Provisions

Borescope provisions have been incorporated into the center of the main chamber injector faceplate to allow inspection upstream of the main chamber injector without disassembling the engine. The plug for this borescope port

attaches to the main chamber injector faceplate and extends into the preburner exhaust case.

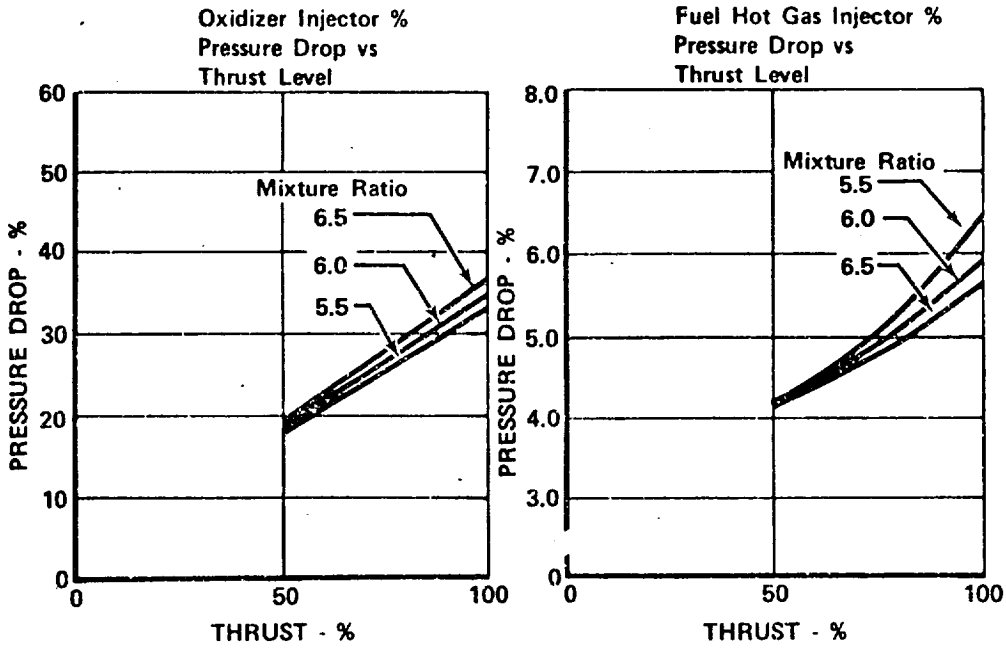

Figure IV-13. Main Chamber Injector ΔP/P FD 52670

To provide combustion stability testing capabilities, the borescope plug may be replaced with a pulse bomb adapter. This adapter supports and shields the high energy explosive bomb in the 500°R gas stream which normally cools the borescope plug. The pulse bomb may be projected into the main chamber and detonated at any desired thrust level. Detonation may be accomplished at any desired distance from the faceplate by incorporating stops in the actuator portion of the adapter. The borescope plug may be replaced with the pulse bomb adapter by the same procedure used to remove and replace the borescope plug. Additional pulse bomb and pulse gun provisions have been incorporated into the main chamber case.

C. DESIGN REQUIREMENTS

The applicable paragraphs of CP2291 and the method of compliance are:

1. The injector shall be capable of operating and varying thrust and mixture ratio described in paragraphs 3.1.1, 3.1.1.1, and 3.1.2.

   Compliance - When applied in the proposed engine system, the injector is capable of delivering the required pressures and flow rates required by table 1 of CEI Specification No. CP2291. A computer cycle analysis, which simulates the characteristics and interaction of components in the engine system, has been run at the required thrust levels and mixture ratio ranges to verify that the injector can meet these requirements. The injector is a fixed-area injector free of moving parts. Injection elements have excellent atomization characteristics over a

wide throttle and mixture range. Sufficient oxidizer ΔP/chamber pressure is maintained at all engine power levels including 20%.

2. The engine shall be capable of providing tank pressurization gases as stated in paragraphs 3.5.1 and 3.5.2.3.1.

   Compliance - The main chamber injector includes 36 heat exchanger struts exposed to turbine discharge temperature to provide gaseous oxygen for use in tank pressurization as indicated in figure 7 of CEI Specification No. CP2291.

3. The injector shall not generate low frequency thrust oscillations as specified in paragraph 3.2.8.

   Compliance - The fuel and oxidizer injection $\Delta P/P_c$ is maintained at 4% or greater to provide propellant feed system stiffness sufficient to prevent low frequency combustion instability.

4. The injector shall not generate combustion instability as stated in paragraph 3.2.9.

   Compliance - The radial spraybar concept allows the use of a large number of injection elements without high fuel manifold losses, or undesirable propellant distribution. The reduced fuel manifold pressure loss associated with this design allows higher injection momentum ratios for a given cycle pressure budget. P&WA experimental studies (PWA FR-1374, Contract NAS 8-11024) show that increasing injection momentum ratio provides increased combustion stability.

   Large numbers of injection elements result in an even propellant distribution which aids combustion stability. Small droplet size and the hot fuel which is characteristic of the staged combustion cycle, combine to provide an extremely fast burning time. Rapid burning is stabilizing when the burn time is much less than the wave time, as is the case with this design. (Influence Of Combustion Process On Stability, NASA TN D-2957, 1965)

5. The engine shall have artifical pulsing provisions as stated in paragraph 3.2.9.3.

   Compliance - The main chamber injector provides for accepting bomb mounting provisions capable of accepting the bomb holder. This is accomplished by replacing the borescope adapter mounted in the center of the injector with an interchangeable pulse bomb holder.

6. The engine shall satisfy the engine system weight as stated in paragraph 3.3.2.

Compliance - Engine weight goals allocated to the injector will be met or exceeded. Continuing weight reduction studies provide assurance that these goals will be met.

7. The engine shall not be capable of misassembly as stated in paragraph 3.5.1.

Compliance - Dowel pins on the main interfaces are provided to preclude improper assembly orientation.

8. The engine shall satisfy structural criteria of paragraphs 3.7, 3.7.1, and 3.7.7.

Compliance - The injector is designed under the PWA FTDM-373, "Design Criteria Memo," using only high grade, non-corrosive materials, Materials selected are compatible with the environment in which the part operates and is exposed.

9. Materials selected must be compatible as stated in paragraphs 3.7.7.1.5 and 3.7.7.1.6.

Compliance - Materials will be proved to be compatible by the use of specialized laboratory tests and PWA Specs 80, 81, and 82. These PWA Specifications are being negotiated with the NASA as a compatible substitution for the MSFC-Specification 106.

10. The engine shall be designed for ease of servicing as stated in paragraph 3.7.7.3.

Compliance - The injector provides access at its center for borescope inspection while installed in the engine.

11. The engine must be physically and functionally interchangeable as stated in paragraphs 3.7.8 and 3.7.9.

Compliance - All main injectors having the same P&WA part number and change designation are functionally and physically interchangeable.

12. Welding processes must be proven satisfactory in accordance with paragraph 3.7.10.

Compliance - Demonstrated suitability of the welds for the application intended will be furnished in data reports on special tests of weld samples for critical applications.

13. Subsystem design features shall be in accordance with paragraph 3.7.13.

Compliance - The injector has the capability of meeting the required life and start requirements, with each part designed for steady-state operation at its worst operational condition.

14. System Design Analysis shall be accomplished in accordance with paragraph 3.7.18.

Compliance - The main injector includes a failure mode, effect, and criticality analysis.

High oxidizer injection element density is incorporated to provide uniform distribution.

Highly atomized oxidizer injection is incorporated to provide good atomization. There is no oxidizer impingement on combustion chamber walls in order to provide increased durability.

Effect of temperature on fuel injection areas is minimized to provide even mixing.

Fuel and oxidizer distribution is controlled for uniform mass and mixture ratio profile.

Stagnation areas exposed to the main burner chamber combustion zone are minimized for stability.

Mechanical allowance for differential thermal expansion.

D. CAPABILITIES

- MAIN CHAMBER INJECTORS CAPABILITY EXCEEDS REQUIREMENTS ALLOWING UPRATING WITHOUT REDESIGN

A computer cycle analysis, which simulates the characteristics and interaction of components in the engine system, has been run at the required thrust levels and mixture ratio ranges to verify that the injector can meet the SSME requirements.

The calculated combustion efficiency of the SSME main chamber injector exceeds the cycle requirements by 0.275%, allowing increased performance of 1.28 seconds of specific impulse.

Throttling capability is provided by maintaining a sufficiently high pressure drop across the injector elements to produce good atomization throughout the entire throttling range. The injector is capable of being throttled to 20% thrust without any change of geometry. Mixture ratio control is provided by valve scheduling, since the SSME main chamber injector contains no moving parts.

Combustion stability is assured by the very fine liquid oxygen atomization and the very hot fuel, because the fuel and oxidizer injection momentum ratios are at 47% above chamber pressure throughout the engines operating range to provide propellant feed system stiffness for good low frequency combustion stability. The combustion zone characteristics are the same as those previously demonstrated which did not have chamber pressure oscillations and/or disturbances greater than 0.27% of the mean steady-state chamber pressure. The small oxidizer droplet size and large number of injection points with an even propellant distribution, which is characteristic of the SSME main combustion injector, gives an extremely fast burning time which is stabilizing.

The heat exchanger turnaround manifolds are the life-limiting components on the SSME main chamber injector. Their 450-cycle limit allow a 12.5% increase in the number of engine starts.

The oxidizer spraybar establishes the limits of the oxidizer pressure vessel components. The minimum wall thickness established for this spraybar allows a 6.5% increase in oxidizer pressure, which will still satisfy the 1.2 proof pressure criteria of pressure vessels on the SSME. Fuel supply pressure may be increased 10% on the present support structure of the fuel face plate. Allowable local nondetrimental yielding will occur using the 1.1 load factor criteria of the SSME.

E. DESIGN SUBSTANTIATION

All of the concepts and design features were evaluated to determine whether the choices were valid and ensured low potential development risk. This evaluation included performance, stability, durability, cost, weight, ease of manufacture, related test experience, etc.

1. Oxidizer Injection Elements - DROPLET SIZE DETERMINES COMBUSTION EFFICIENCY

P&WA selected a tangential swirl injection element which produces smaller droplet sizes than ribbon swirl or simple orifice elements for a fixed number of elements, flow, and density. The droplet diameters are 25, 150, and 250 microns respectively. Figure IV-14 shows these droplet diameters superimposed on JANNAF's. "Interim Performance Calculation Methodology for use in the SSME Proposal Response", (Addendum No. 1 to CPIA Publication No. 178). As can be seen, droplet size controls efficiency. Efficient combustion is obtained by good atomization. The faster and more complete the reaction of the propellants, the higher the efficiency within a given combustor volume.

Analytical work developed by P. Wieber, NASA-Lewis, for convective heating at supercritical pressures determines transient droplet temperatures. Small droplets produce extremely short droplet lifetime in the liquid state. Larger droplets require much longer heating delay times, reducing the time available for efficient mixing and total combustion.

The Rosmer modification of Spalding's supercritical burning rate solution evaluates the time required for complete combustion once the droplet achieves its critical temperature. A small droplet size results in a short burning time and high combustion efficiency. Larger droplet sizes require much longer durations for complete combustion, thus reducing combustion efficiency and delivered specific impulse. Therefore, as shown in figure IV-15, heating and burning times of the oxidizer are very sensitive to droplet diameter.

In an effort to accurately evaluate SSME performance losses caused by maldistribution of injected propellants, P&WA has undertaken development of an analytical spray distribution and mixing model. This model describes the droplet injection, supercritical heating and vaporization, and turbulent gas phase mixing for the SSME gas-liquid main chamber injector. The model is discussed in detail in, "SSME Performance Using JANNAF Methodology", PWA FR-4451. The P&WA "Injector Striation Evaluation Model" is used to describe the injection and mixing process in the injector. Specifically, the model is capable of accurate

characterization of droplet information and behavior. Evaluation of the combustion efficiency for very small droplets produce efficiencies of 100%.

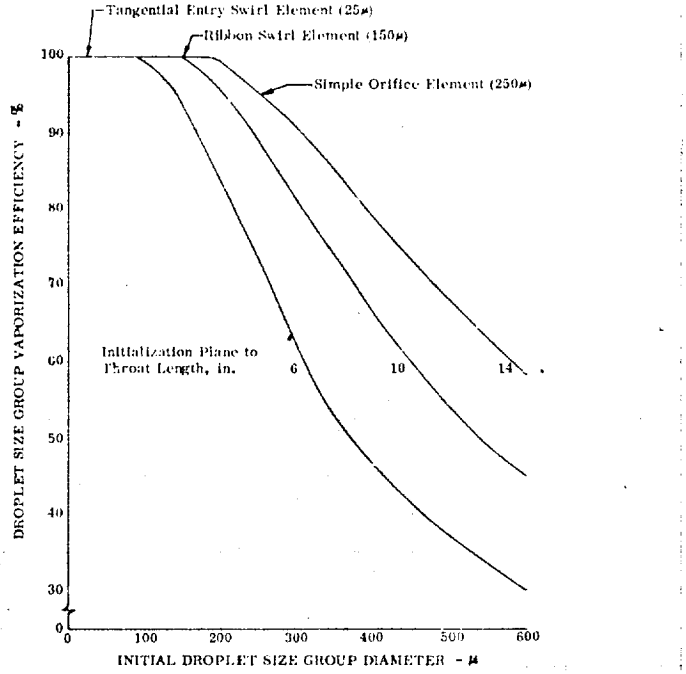

Figure IV-14. Droplet Size Group Vaporization Efficiency, 3.0 Contraction Ratio, 3000 psia Chamber Pressure DF 84770

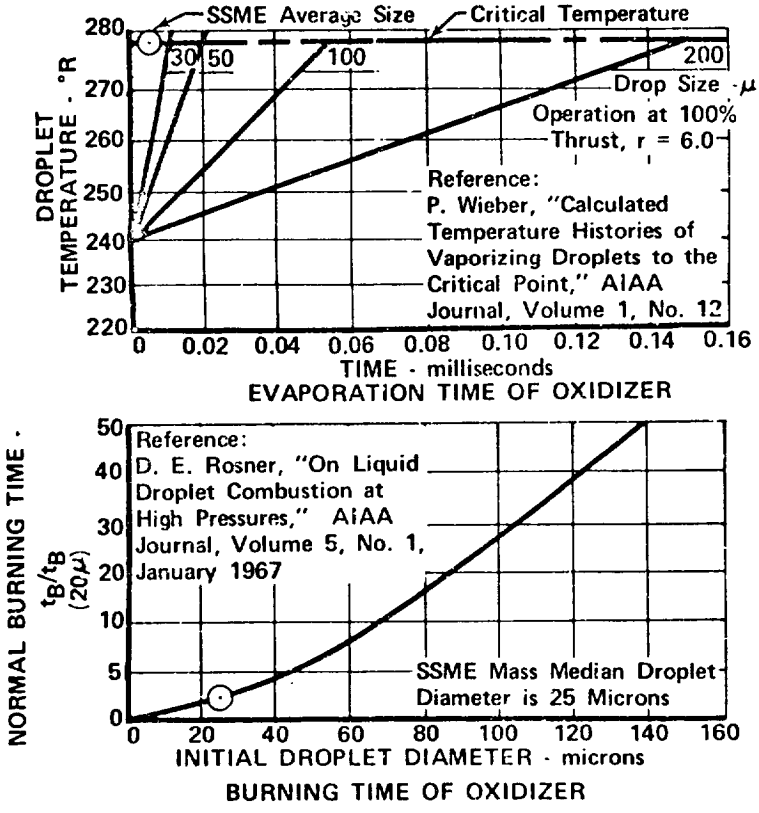

Figure IV-15. Droplet Size Controls Efficiency FD 46274

P&WA uses the direct droplet collection method to determine droplet size. Actual water droplet distribution as caught from a flowing spraybar assembly and collected in Delavan Manufacturing Company's immiscible fluid bath are shown in figure IV-16 at a magnification of 50. Mean droplet size and distribution are determined using photographic and a light scanning technique. All of the liquid mass leaving the element is used in determining the mean drop size and distribution. Surface tension, viscosity, and density correction factors are employed to convert water droplets to liquid oxygen droplets. The frozen wax technique was eliminated for determining droplet size because it was felt conversion factor correlation between wax fragments and liquid oxygen droplets were not valid. The liquid oxygen droplet distribution for the self atomizing tangential slot swirler injection elements is shown in figure IV-17. The very fine atomization is evidenced in figure IV-18 showing a single element flow at 300 psi.

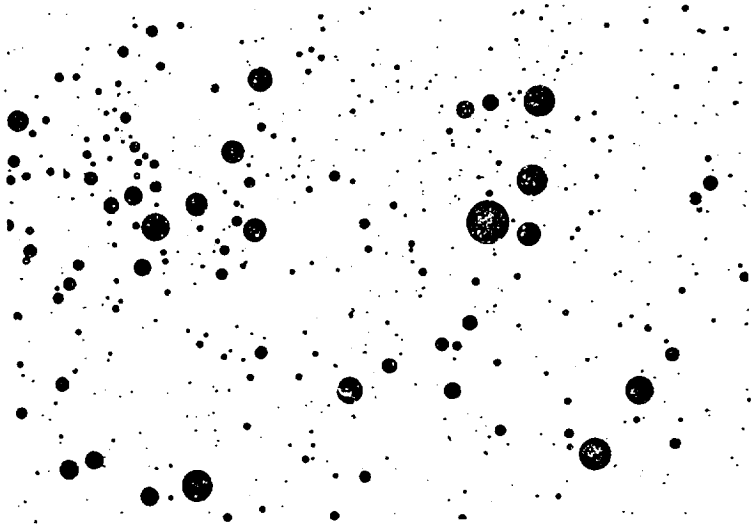

250K Injector Drop Size; 50K Magnification;
300 psid Actual Photograph

Figure IV-16. Direct Droplet Collection Method Used to Determine Droplet Size and Distribution FD 46273

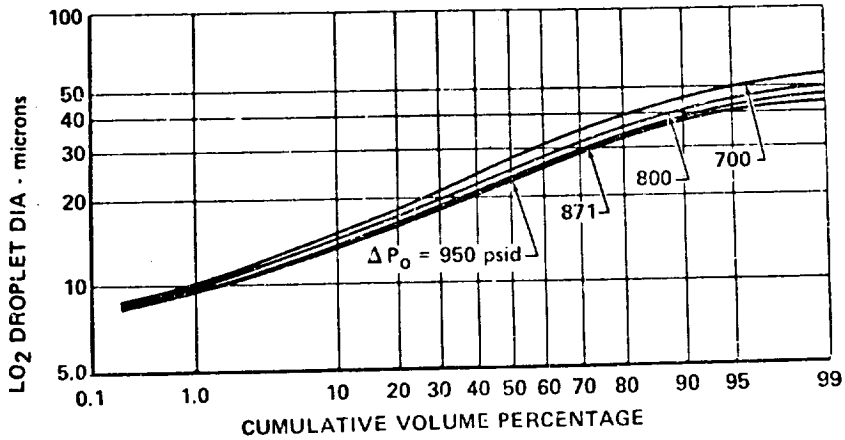

Figure IV-17. Very Small Droplets Provided by Main Injectors Self Atomizing Liquid Oxygen Injection Elements FD 27388C

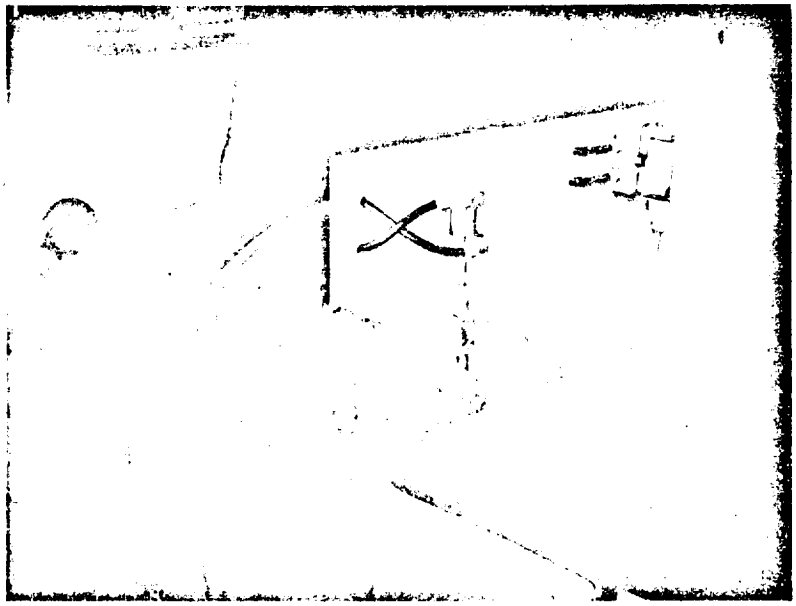

Figure IV-18. Slot Swirler Element Provides Very Fine Atomization FD 46273

2. Injector Pattern

Trade studies of various injector patterns were performed to establish relative efficiencies. (Refer to Combustion Devices Trade Studies, PWA FR-4440.) Radial injection schemes with variations in the numbers of slots and concentric uniform pattern injection patterns were investigated. The study concluded that the radial injection pattern yielded higher combustion efficiencies than either of the uniform patterns. This is a result of the greater number of liquid oxygen elements inherent in the design with finer oxidizer distribution.

All three candidate schemes used tangential entry swirl elements. This was done to take advantage of the higher efficiency due to the smaller droplet size already discussed. The exception to this is the 0.625-inch spacing that incorporated a simple orifice similar to the RL10. As shown in figure IV-19, this element change significantly affects C* efficiency.

3. Spraybar Concept

Alternative configurations were developed in support of the previously mentioned trade studies, one of which, the annular plenum design, is shown in figure IV-20. This configuration is similar in concept to the RL10 developed in 1958. The oxidizer and fuel orifices are supplied from two separate chambers that are formed by the assembly of three mutually supported conical plates. Liquid oxidizer is supplied to the forward chamber through a central manifold.

Tubes projecting from the center plate form the oxidizer orifices. The tubes extend through holes in the rear plate, forming annular fuel orifices. The rear plate is formed of porous welded steel mesh to provide transpiration cooling of the injector face. It illustrates quite dramatically the various advantages of the spraybar injector concept.

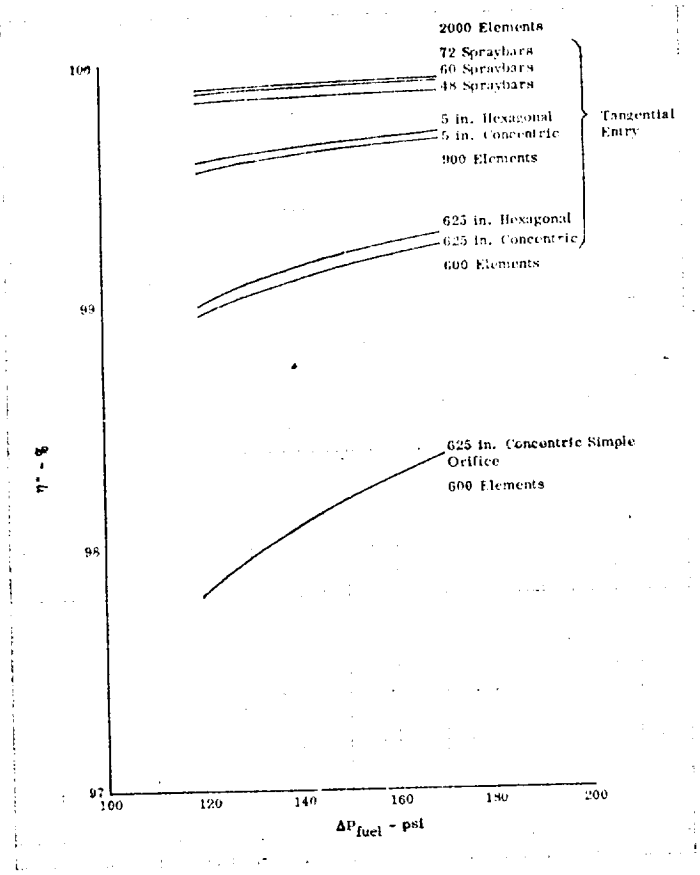

Figure IV-19. SSME Main Injector Combustion Efficiency vs Fuel Pressure Drop

DF 84771

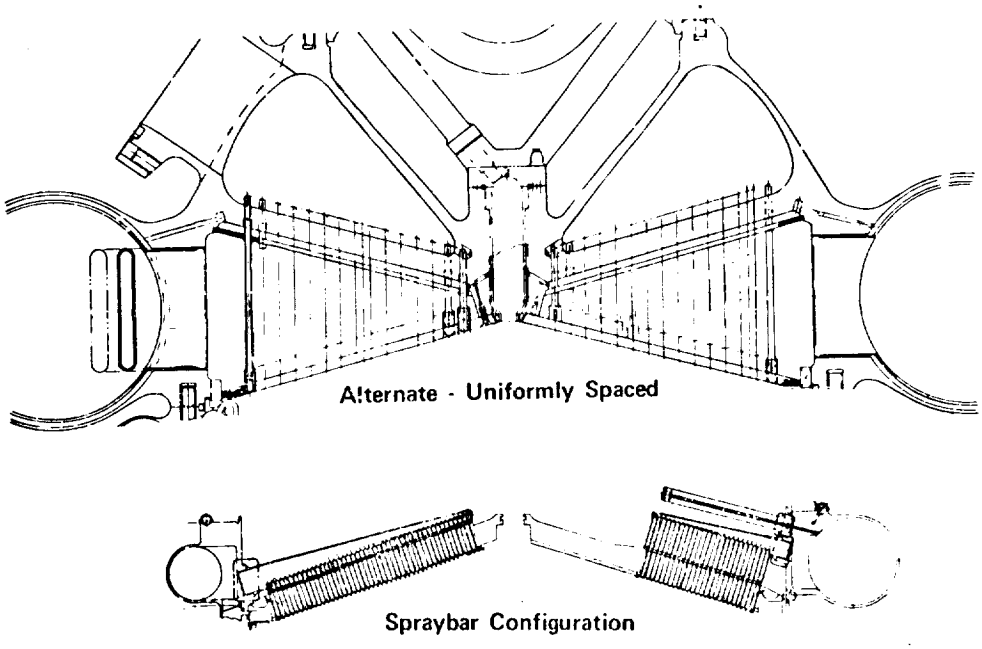

Figure IV-20. Superior Mechanism Configuration With Spraybar Injector

FD 51899

The spraybar injector allows for a larger number of oxidizer injection points and provides a more complete and even distribution of propellants across its face than is possible with the alternate configuration. Its lightweight configuration, attractive mechanical features, avoidance of potential development problems, and high combustion performance make the radial spraybar injector the P&WA choice for the main chamber injector.

Fuel distribution in the annular plenum configuration enters the injector at two discreet locations. Therefore, this flow should be matched for flow around all the oxidizer injection elements; this could result in uneven pressure and flow distribution, causing varying r = 6 profiles across the injector face. The spraybar concept provides uniform distribution of premixed combustion products to the face and completely avoids this problem.

The fuel entering the annular plenum injector is hot and therefore may require the pressure vessel manifold to be heatshielded to ensure structural integrity within a reasonable weight envelope. The spraybar concept does not require a hot fuel manifold in the injector and completely avoids this problem. The hot fuel in the annular plenum configuration also surrounds varying-length oxidizer injection elements and may cause carying oxidizer densities resulting in uneven r = 6 profiles across the injector face. The spraybar concept exposes the same length of element to the fuel throughout the injector and completely avoids this problem.

In the annular configuration, each row of oxidizer elements requires a different length tube which could cause manufacturing and handling problems.

The annular plenum configuration requires long elements to allow for differential expansion between the hot face and cold element. The radial pattern of the spraybar injector provides for free differential expansion between the hot fuel distribution faceplate and the colder oxygen-carrying members with a minimum effect on injection pattern, and completely avoids this problem.

4. Fuel Faceplate

The injector faceplate must be protected from burning due to recirculation of main combustion products. A trade study was conducted to determine the best type of faceplate to satisfy this requirement. (Refer to Combustion Devices Trade Studies, PWA FR-4440.)

A faceplate structure similar to the one demonstrated during the 250K Phase I stage combustion tests, which incorporated thermal relief slots on the porous faceplate, meets the SSME requirements. This type of faceplate structure has been incorporated in the Phase B 250K main injector which is presently being tested and has shown excellent durability. The part shown in figure IV-5 has undergone 14 start and shutdown transients with a total hot firing time of 251 seconds, 33 seconds of which have been at 100% thrust, of which 5 seconds was at 100% and an injector mixture ratio of 8.3 with the fuel inlet temperature over 2000°R. No injector face distress has been evident except at one excessively wide electron beam weld. This weld width can be reduced for the SSME design. The fuel faceplate consists of a two-piece assembly. The assembly consists of an L-605 sintered wire matrix which forms the porous face. This face is electron-beam welded to a Waspaloy radial beam support structure.

An alternate design approach was investigated which offered the desired porosity of the face and the structural capability of the radial beam design. The assembly consisted of an inner ring connected to an outer ring by hollow radial beams. By using thin-walled hollow beams and techniques developed from beam flexure theory, it was anticipated that a composite structure could be developed that would satisfy structural criteria and have a sufficiently rapid thermal response rate to ensure adequate cycle life.

Analysis has shown, however, that the thermal response rates of the box structure is approximately the same as a web structure that has a thickness equal to the sum of the thicknesses of the two legs of the box structure. Investigation with Manufacturing indicated that a web or wall section of a box structure would be manufacturing-limited to approximately 0.100 inch. This limitation is based upon positioning tolerances of the work piece and the fixture required for tracking the weld. Therefore, the support structure cannot be produced and assembled sufficiently thin to substantially reduce the thermal gradient over the existing design.

The possibility of utilizing regenerative heat exchanger discharge coolant in a box section was investigated. This would produce a steady-state thermal gradient of 700°, which is sufficiently high to cause plastic strain. A noncooled porous faceplate having no steady-state thermal gradient is selected for this configuration.

5. Conical Face for Combustion Stability

The conical face of the injector produces an energy release profile which is optimum for combustion stability. At the pressure sensitive axial location, the energy release profile is a mirror image of the face. A concave face produces a convex energy profile because the propellants near the engine centerline have been permitted more time to react. Therefore, they have released more energy than the propellants near the chamber wall.

The main chamber injector currently being tested incorporates all major features of SSME injector design, the SSME main chamber injector is a scaled-up version of the lightweight XLR129 main chamber injector. The 250K main chamber injector currently being tested by P&WA contains all of the design concepts and features of the proposed SSME main chamber injector design. The same tangential slot self-atomizing liquid oxygen injection elements are used. The number of spraybar and elements have been increased in the SSME design to maintain the thrust-per-element at about 200 per element and same relative spraybar spacing. Fourteen runs for a total hot running time of 25 seconds were performed using this injector, which included 35 seconds at 100% thrust and injector propellant mixture ratios from 5.3 to 8.4 with fuel inlet temperature over 2000°R. The injector is in excellent condition confirming the durability of the configuration and has demonstrated performance in excess of that required to meet the SSME requirements, figure IV-2..

Main chamber injector background from the High Chamber Pressure Staged Combustion Research Program, Contract AF04 (611)-10372 conducted in 1965 and 1966, included testing of the following types of main chamber injectors at the 10K thrust level.

1. Spraybars with rectangular slot injector elements

2. Spraybars with impinging slot injection elements

3. Spraybars with impinging double injection elements

4. Spraybars with ribbon swirler injection elements

5. Large number of concentric oxidizer injection elements (100% thrust/element)

6. Lesser number of concentric elements with swirler (200-lb thrust/element).

A performance summary curve is shown in figure IV-21. The spraybar injection with swirlers demonstrated unsurpassed performance over a wide range of propellant mixture ratios. In the spraybar-type injectors, the hot fuel from the preburner entered the main chamber through slots surrounding the liquid oxygen injection elements. The oxidizer injector port or element protruded through the fuel slot. In the concentric element designs, the fuel entered through an annulus that was concentric around tubular oxidizer injection elements. In all cases, the fuel faceplate was made from Rigimesh (a porous sintered wire structure), which is the same injector faceplate material presently being used.

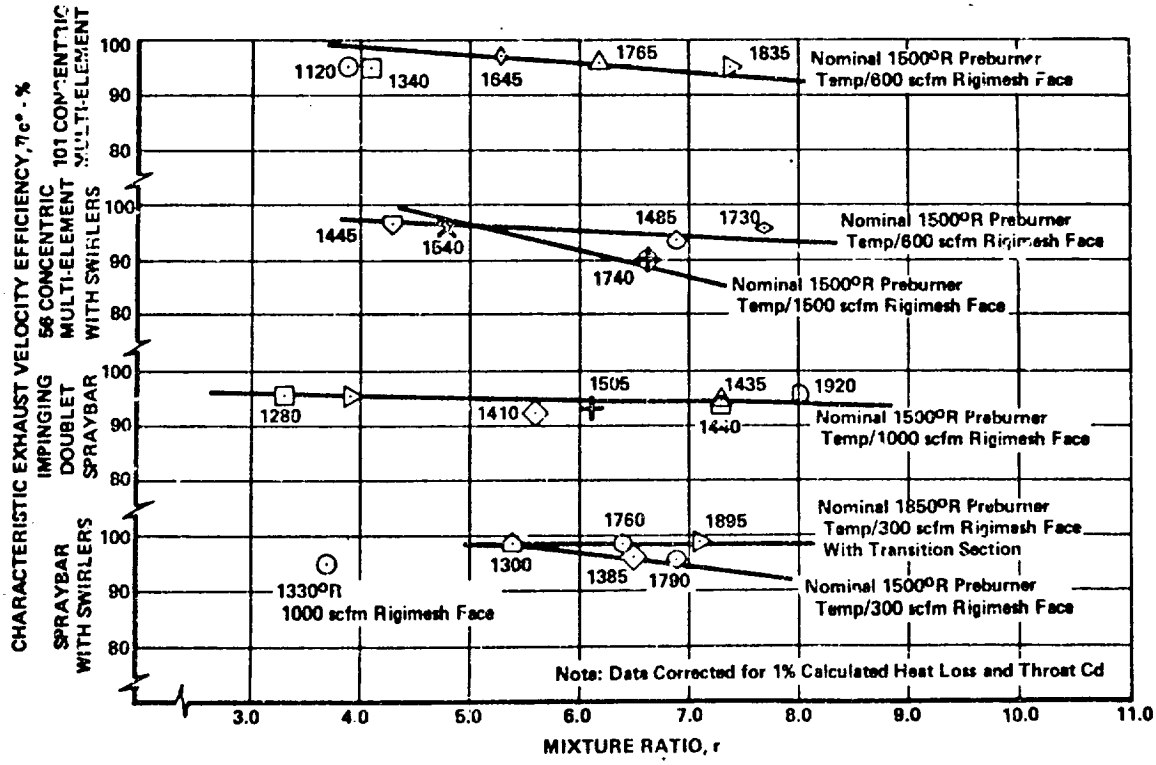

Figure IV-21. Combustion Performance vs Mixture Ratio for Various Main Chamber Injector Configurations FD 52672

The results of the 10,000-pound thrust test are summarized below:

1. Spraybars with impinging doublets and ribbon swirlers were the better performing of the four types of spraybar injectors tested

2. A multiple concentric injector performs well

3. Rigimesh exhibits good durability as a faceplate material

4. Concentric element injectors cannot be held concentric at all operating conditions without special mechanical features

5. Radial spraybar injectors allow for thermal differential growths between the hot faceplate and colder liquid oxidizer elements while keeping the fuel flow symmetrical about the oxidizer injection elements. Superior, simpler mechanical configuration

6. High oxidizer injection ΔP's for self-atomization is desirable

7. It is not desirable to attach the fuel faceplate directly to the injector housing due to thermal differential growth. Should be attached to allow for thermal growth.

Staged combustion testing at the 50K level was also conducted under Air Force Contract AF04(611)-10372. Based upon the 10K test results, two types of 50K main burner injectors were fabricated and tested; spraybar with ribbon swirler oxidizer injection elements and a 192 concentric-element injector with ribbon swirler injection elements.

The results of this 50K testing showed that high combustion efficiency can be attained with either the spraybar or the concentric element injector, figure IV-22.

Under the cooling investigation portion of the follow-on contract AF04(611)-11401, a new spraybar 50K main chamber injector was fabricated (1966) using slot swirler, tabular elements which had been shown to have superior atomization characteristic. This 50K injector, which has 24 spraybars as shown in figure IV-23 for closer spacing and an increased number of elements, demonstrated good performance and durability.

Fifteen tests were run during the cooling investigation portion of the contract. Tests were made with the 24-spraybar slot swirler injector as well as the 20 spraybar ribbon swirler injector from Contract AF04(611)-10372. The impulse efficiency vs injector mixture ratio is shown in figure IV-24 for these 50K transpiration cooled chamber tests.

The conclusions drawn from the fabrication and testing of the tangential slot swirler spraybar injector are as follows:

1. The atomization of the tangential slot swirler injection element is superior to the ribbon swirler

2. The fuel faceplate can be supported by a ribbed support structure

3. Very high combustion efficiency can be obtained from the slot swirler spraybar injector as shown in figure IV-24.

High performance was attained with the 24-spraybar injector and a 13-inch chamber with a contraction ratio of 3. The use of this chamber geometry and injector for the 250K performance demonstration tests was verified.

The 250K main injector shown in figure IV-25 had 48 spraybar and 984 tangential slot swirler liquid oxygen injection elements.

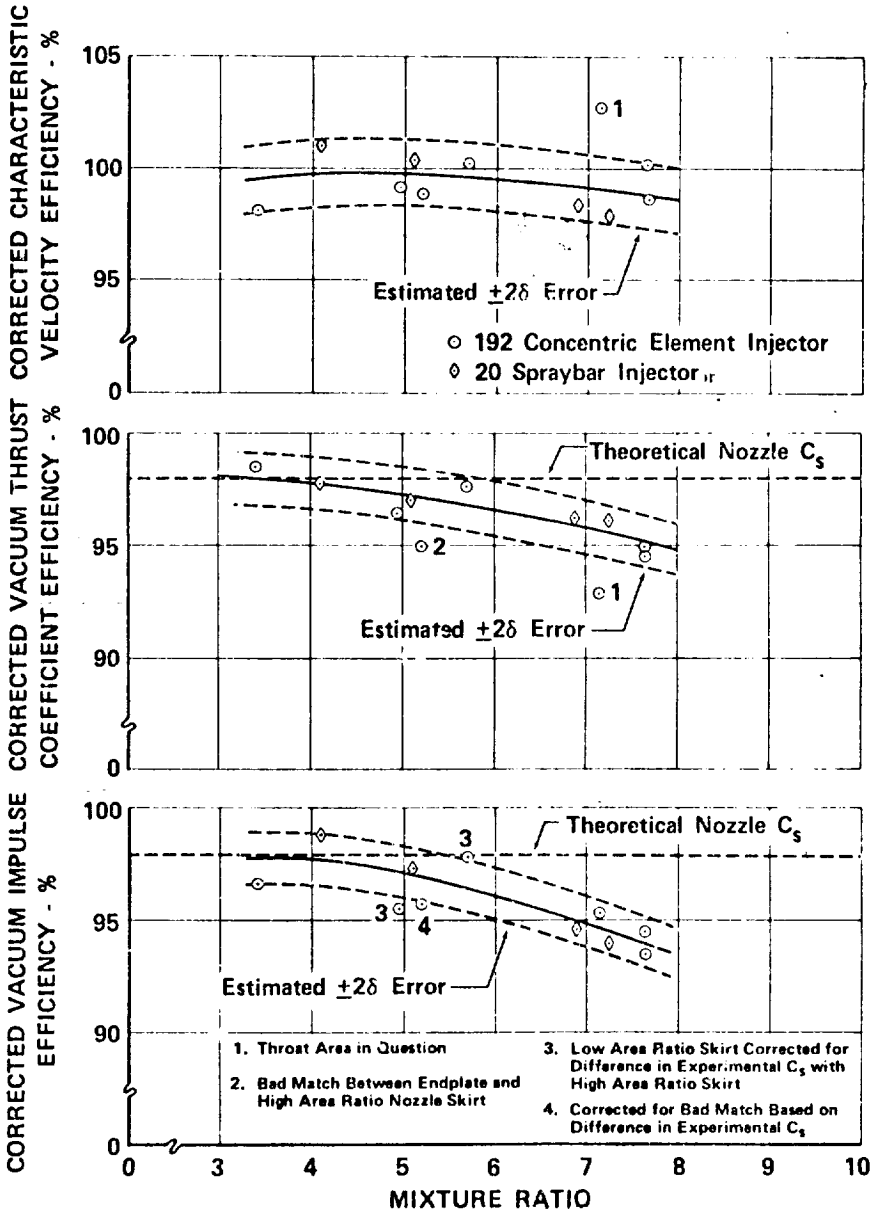

Figure IV-22. 192 Concentric Element and 20 Spraybar Performance Data FD 17263

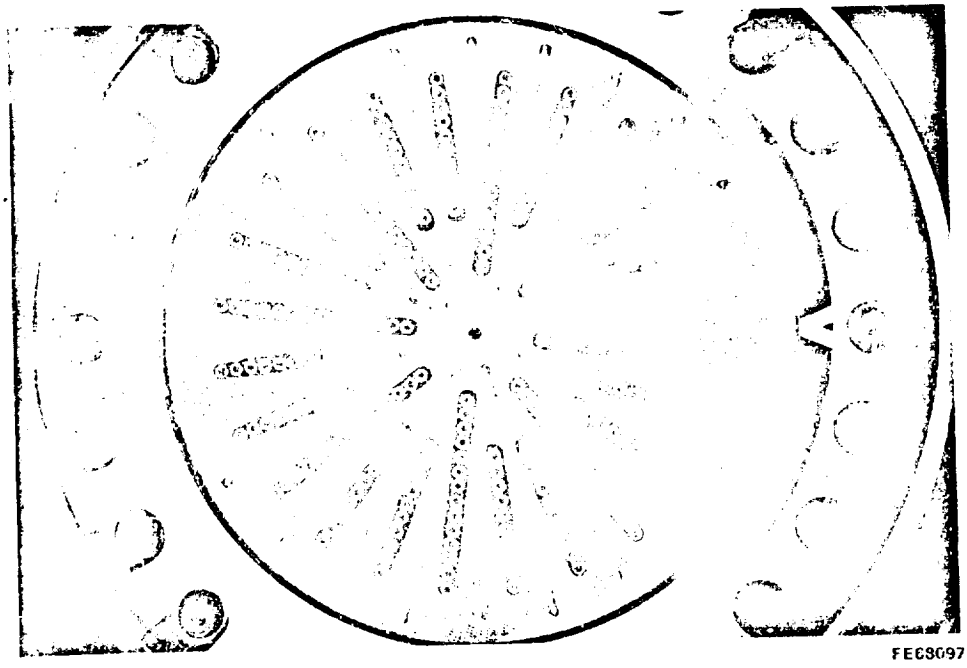

Figure IV-23. Post-test 50K 24- Spraybar Injector FD 52073

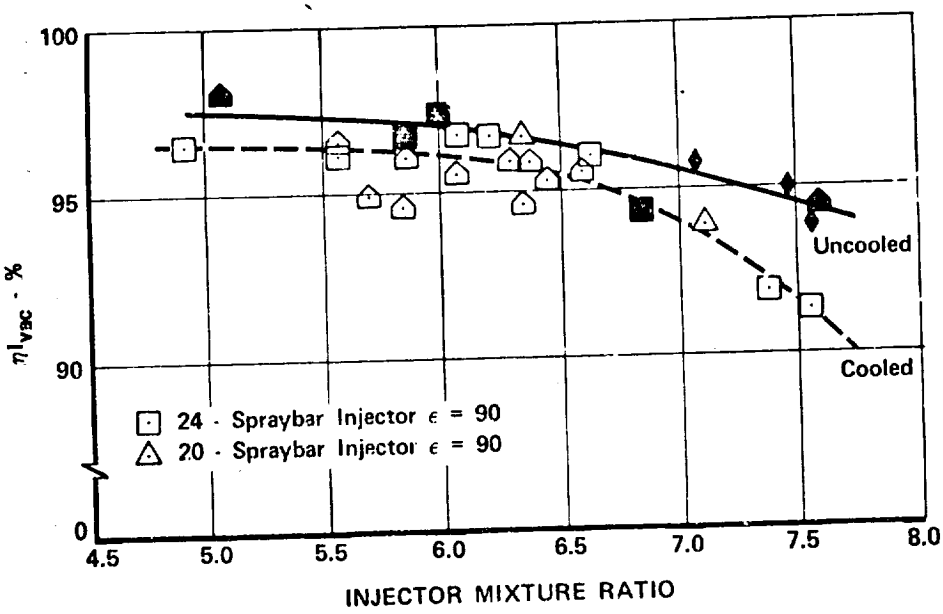

Figure IV-24. 50K 24 and 20 Spraybar Main Injector Test Results FD 51902

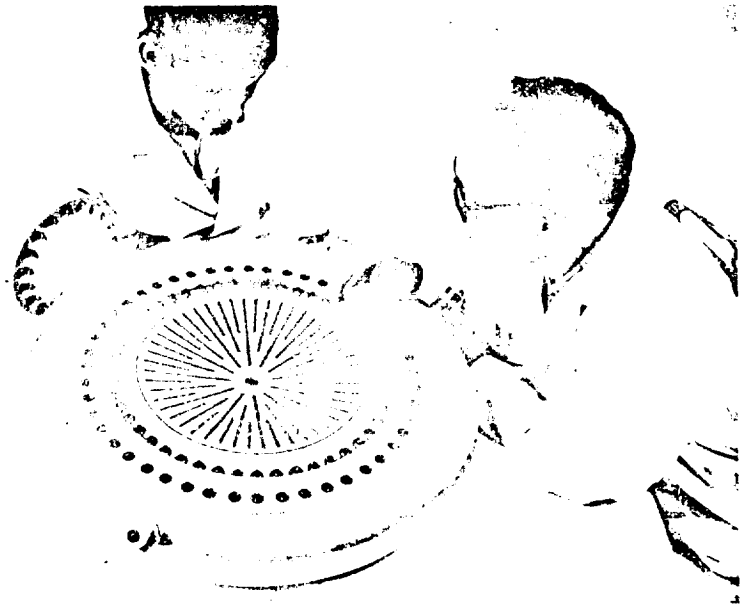

Figure IV-25. ADP (XLR129 Phase I) Main Chamber Injector FD 44392

Ten completely successful cooled thrust chamber tests were conducted over a range of mixture ratio of 3.9 to 7.1, and over a throttling range of 20% to 100% thrust. The results of these tests at 100% thrust are shown in figure IV-26. These test results are reported in detail in the Phase I of the XLR129 Final Report for Contract AF04611-10372 dated December 1967.

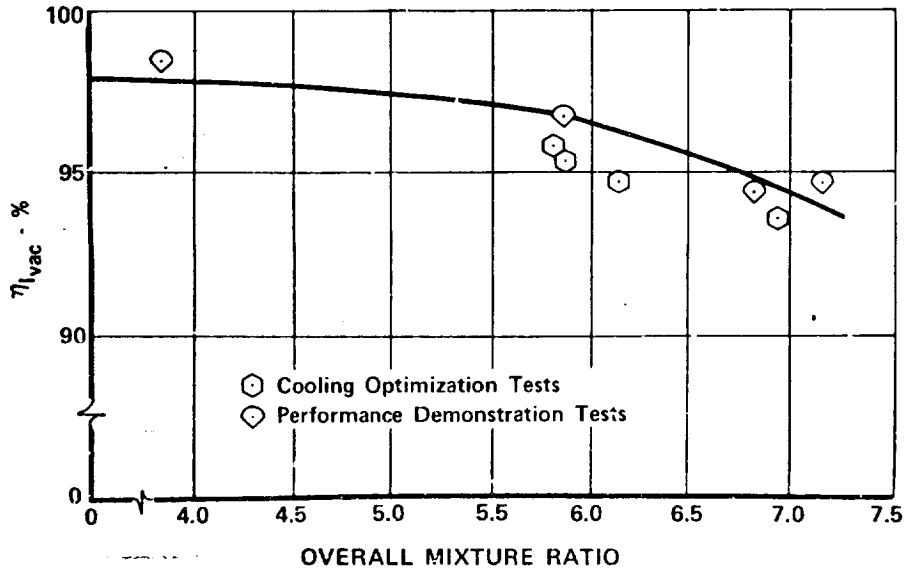

Figure IV-26. High Impulse Performance Demostrated at 250K With Spraybar Main Injector. FD 37044

The XLR129 main chamber injector, shown in figure IV-27 is also a 48 spraybar injector with tangential slot swirler element. However, the elements have been classed to improve the injected mass profile. This in-

jector is currently being tested during Phase B with an engine configuration hot gas system, figure IV-28, using the XLR-129 Preburner and Main Case. The impulse performance demonstrated to date when corrected to the SSME configuration meets the CEI impulse requirements with margin, figure IV-2.

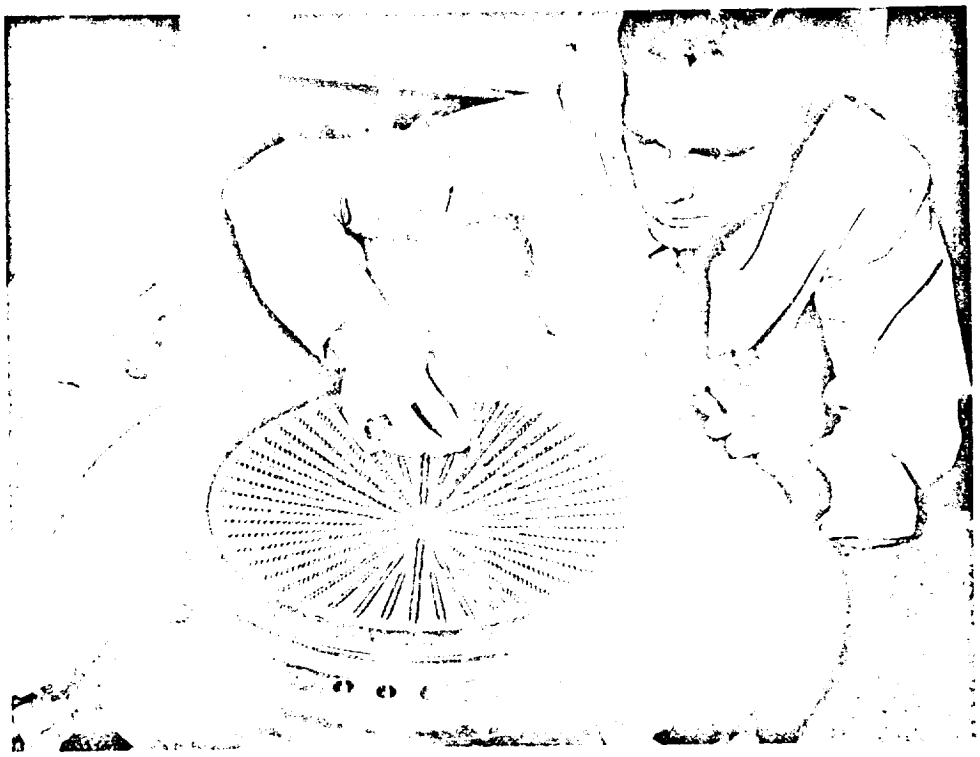

Figure IV-27. XLR129 Main Chamber Injector FE10543

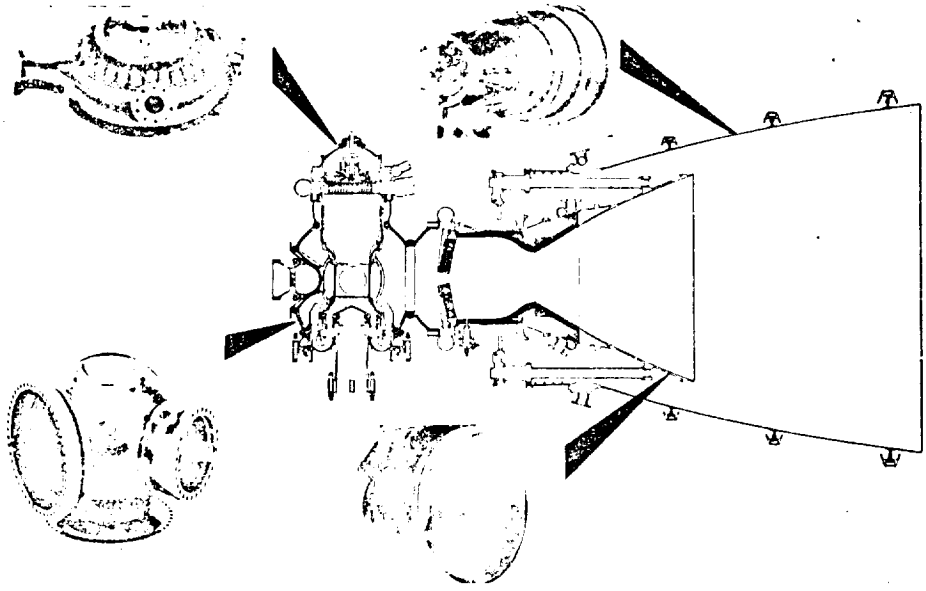

Figure IV-28. Phase B Staged Combustion Test Configuration FD 41073B

SECTION V
MAIN CHAMBER

A. INTRODUCTION

A transpiration-cooled main chamber was selected for the SSME design because of its safety and long life while meeting specification performance requirements. This provides a minimum risk approach to meeting SSME impulse performance, while still allowing for growth during the development program.

Impulse comparison testing is presently being conducted comparing both regenerative and transpiration-cooled chambers. As a result of this testing, a sound decision will be made for the trade of performance-versus-durability and forgiveness of a transpiration cooled chamber. The P&WA SSME engine cycle has bypassed sufficient hydrogen from the preburner power cycle to regeneratively cool the main chamber if this should be shown to be a desirable trade.

B. DESCRIPTION

The function of the main chamber is to contain the high temperature gases resulting from combustion, serve as a structural member for support of both the primary and extendible nozzles, transmit thrust, and react to induced gimbal actuator loads. The brazed copper chamber liner is transpiration-cooled. The welded outer case is spherical and fabricated from PWA 1052 and PWA 1053 material. Two gimbal actuator brackets are welded to the main chamber outer case.

1. Transpiration Cooled Liner

The primary problem in selecting the design of the SSME main chamber is meeting specification performance requirements without adversely affecting durability. The SSME performance requirements result in chamber pressures in excess of 3000 psi and heat fluxes five to ten times higher than found on the RL10 or J-2 engines. This greater chamber pressure and higher heat flux requires different chamber cooling concepts than previously used. The full-flow regenerative cooling concept used on the RL10 and J-2 engines would require thick walled, large diameter tubes to pass the full hydrogen flow through the reduced surface area of the SSME main chamber throat. Because of the multiple-cycle requirements of the SSME, the regeneratively-cooled chamber liner requires a thin wall (approximately 0.030 in.) with its correspondingly lower thermal gradient to approach the 400-cycle low cycle fatigue life. Partial-flow regeneratively cooled chambers or transpiration-cooled chambers made from highly conductive materials are the two contemporary combustion configurations which should be considered for the SSME main chamber.

- TRANSPIRATION COOLED MAIN CHAMBER MEETS PERFORMANCE AND LIFE REQUIREMENTS WITH MARGIN

The difference between the transpiration and regeneratively cooled main chamber concepts, is the manner in which the chamber wall is

protected. (Refer to Combustion Devices Trade Studies, PWA FR-4440.) Transpiration cooling is accomplished by flowing hydrogen through wire mesh wafers that form the liner. Coolant flows radially inward through the porous material of the 0.300-in. thick heat exchanger region, increases in temperature, and exits into the combustion chamber cavity where it forms an insulating boundary layer along the chamber wall. The coolant thus absorbs heat as it passes through the wall and also reduces the heat flux to the wall because of the mass injection within the boundary layer.

Regenerative cooling is accomplished by flowing high pressure hydrogen through channels in the chamber liner. The heat from the chamber wall is transferred to the hydrogen coolant, which exits from the chamber passages and is injected upstream of the main chamber injector. Heat must be transferred through thin (0.030-in.) highly stressed walls and absorbed by a high-velocity coolant. Because there is no injected film into the boundary layer, a purely regeneratively cooled chamber has much higher heat fluxes into the chamber walls than the transpiration-cooled chamber. These high fluxes cause increased thermal gradients which limit life and require thin highly stressed copper walls to prevent chamber inside diameter surface melting.

A transpiration-cooled copper wire mesh wafer main chamber design was selected which will meet the CEI specification impulse performance and life requirements with ample margin.

a. Chamber Liner Construction - CHAMBER LINER FABRICATED WITH POROUS WAFERS

The main chamber transpiration-cooled liners consist of a brazed stackup of 0.250-in. thick oxygen-free high conductivity copper wire mesh wafers. The copper wire mesh was selected to minimize the coolant flow rate by improving the heat exchanger efficiency and the coolant injection method over that previously demonstrated by the less porous photoengraved copper wafers. The high conductivity of copper lowers the thermal gradient, thereby improving the low cycle fatigue life and also disseminates heat from any hot spots which may occur at the chamber wall. As shown in figure V-1, each 0.250-in. thick wafer of the transpiration-cooled liner is made of sintered laminations of 60 by 60 twill weave 0.009 to 0.011-in. diameter oxygen-free high-conductivity copper wire cloth. This copper wire cloth is stacked to form a porous sheet such that layers are progressively oriented 22.5 deg from adjacent layers to provide uniform mechanical properties and flow distribution. The manufacturing sequence is shown in figure V-2.

A 0.007 to 0.010-in. thick copper sheet is bonded to each face of the wafer. These nonporous face sheets provide sealed surfaces which can be brazed to the adjacent wafer and provide positive coolant separation from wafer to wafer. After the sandwiched structure is sintered and rolled to the correct thickness and permeability, the permeability is verified by flow calibration.

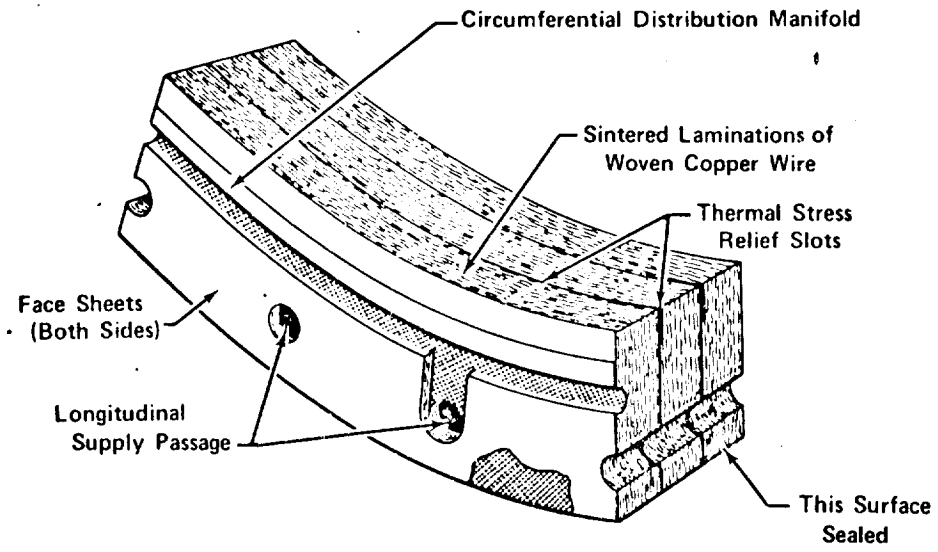

Figure V-1. Copper Wire Mesh Wafers Reduce Transpiration Coolant Flowrate 50% FD 46347

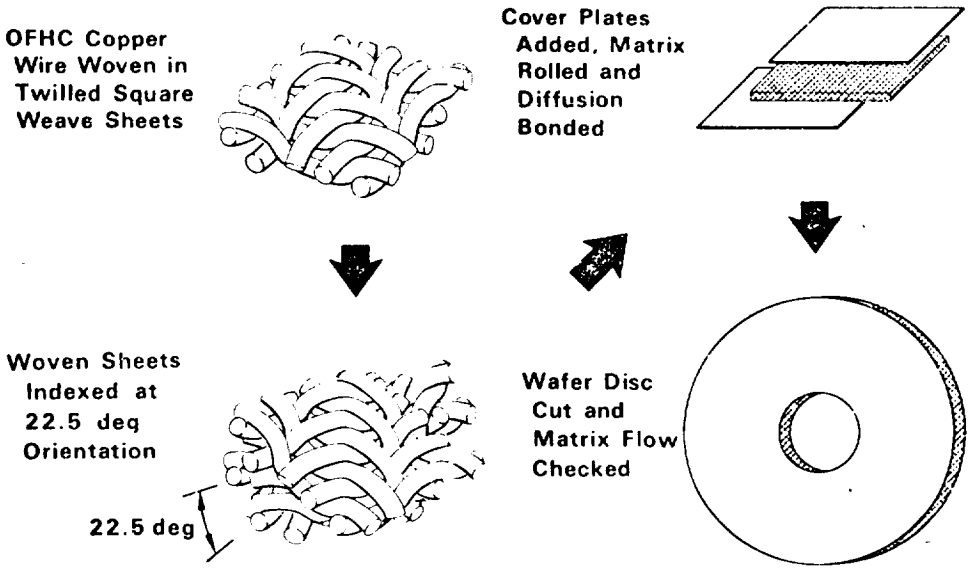

Figure V-2. Copper Wire Matrix Porous Material Production FD 44840

Circumferential coolant distribution manifolds and longitudinal coolant feed holes are machined into each wafer, as shown in figure V-3. The porosity is sealed or restored as required and the wafers are then assembled for brazing. After brazing, internal and external contours are machined, porosity restored on the inner diameter wall, and the outer diameter surfaces sealed. Methods were developed during the Phase B 250K test program for sealing holes and the outer diameter surfaces of the liner to a pressure differential greater than 7000 psia. The transpiration liner assemblies are then flow calibrated and metering orifices installed before uniting the liner assemblies to the outer case in accordance with figure V-4.

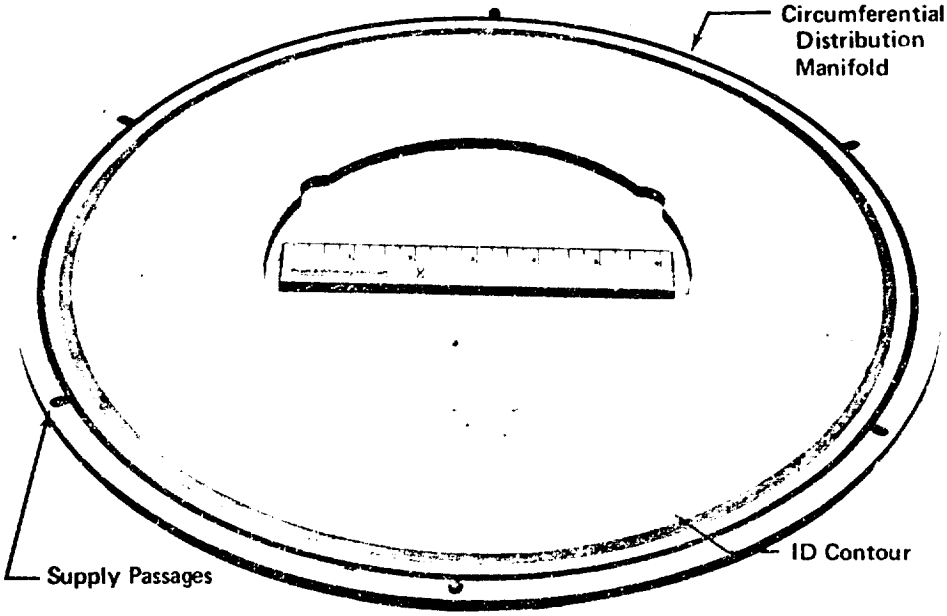

Figure V-3. Phase B-250K Size Copper Wire Mesh Wafer FD 46329

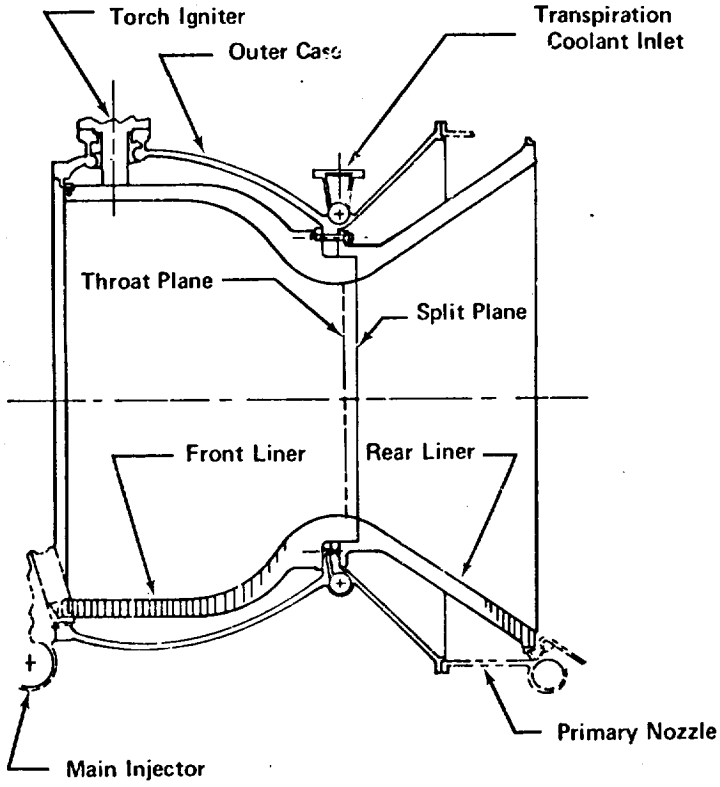

Figure V-4. Minimum Risk Approach to SSME Main Chamber FD 46340

b. Durability - THERMAL RELIEF SLOTS PROVIDE INCREASED LIFE

The high heat fluxes associated with high pressure, high performance rocket engines produce high radial temperature gradients, shown in figure V-5 through the hot inner wall of the chamber liner that are severe enough to cause plastic deformation. This thermal yielding is common to both the transpiration and the regeneratively cooled chambers. At engine shutdown, when the hot wall returns to ambient temperature, the compressively yielded material is subjected to tensile stress as shown in figure V-6. This thermal cycling could cause wearout failure modes which adversely effect the durability of the reusable SSME.

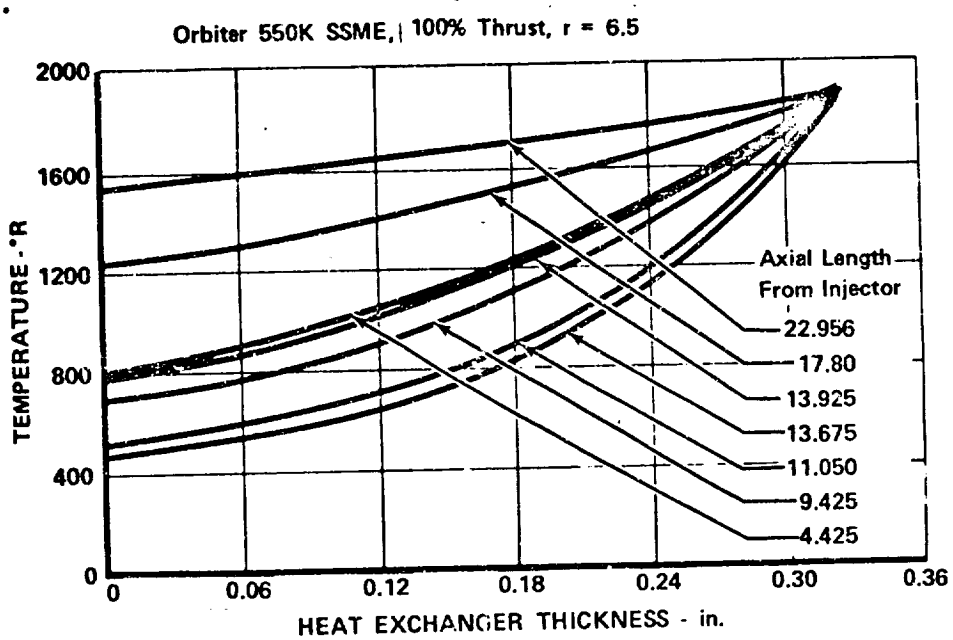

Figure V-5. Radial Temperature Gradient for Transpiration-Cooled Wall FD 52331

If the chamber were a one-piece regeneratively cooled liner of solid material, cycles of high thermal straining could propagate a crack through the thin (0.030 in.) heat exchanger region. This crack could cause excessive coolant to escape and cause coolant starvation in adjacent areas which would lead to an overtemperature condition and probable failure of the chamber liner. In order to prevent this type of failure and to improve the low cycle fatigue life of the chamber liner, design features unique to transpiration cooling are incorporated into the SSME main chamber liner.

The first feature is the use of axial relief slots between wafers to reduce the thermal strain near the hot wall. Thermal stress relief slots are provided in the area of maximum thermal gradient of the wafer heat exchanger region. These slots are formed by removing a portion of the face sheet on one side of the wafer to the required radial depth. The purpose of these slots is to allow the porous material to expand in the axial direction, thereby reducing the thermal stress and increasing the liner's low cycle fatigue life. The idea of thermal relief slots has been demonstrated in past rocket programs. A 50K thrust engine with etched solid copper wafers which were transpiration cooled, was fired at the P&WA Florida Research and Development Center, without relief slots. After seven firings, inspection

showed a contraction of 2.3% in the throat area and separation between wafers on the hot wall in the throat area.

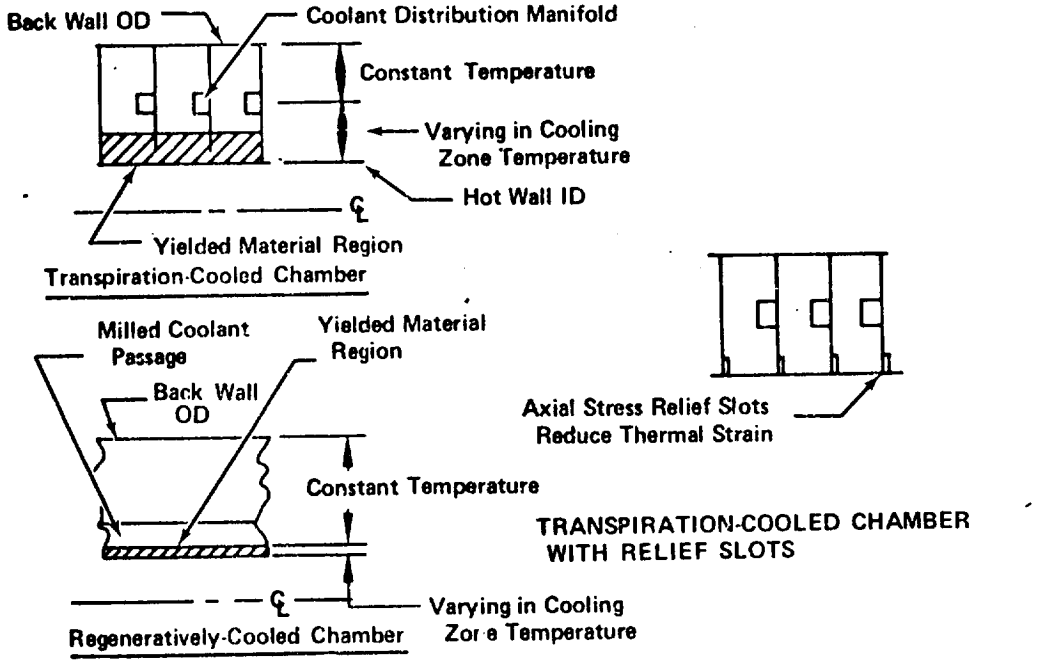

Figure V-6. Design Features, Unique to Transpiration Cooling, Improved Low Cycle Fatigue Life FD 46338

The combustion liner for the Phase I 250K thrust engine was also of etched solid copper wafers, but axial thermal relief slots, 0.001-in. wide and approximately 0.100-in. deep, were provided along the inner diameter edge of each wafer. In addition, radial relief slots in the throat area circumferential plane were used. After 26 firings, no separation was observed in the throat area. The throat area was stable with only 0.26% reduction from the "as fabricated" area.

The second major feature incorporated into the design of the SSME main combustion chamber liner is a wafer composed of sintered wire mesh material. The structural design analysis of the copper wire matrix wafer chamber liner does not require the 0.300-in. heat exchanger region to provide hoop strength; therefore, separation of wires does not alter the structural capability of the liner as shown in figure V-7. If some wire junctions should separate near the chamber inside diameter where the thermal strains are high, on subsequent thermal cycles they can no longer transmit tension and in a sense, provide thermal relief at the locations where needed. Each wire junction is an entity in itself with inter-junction areas providing automatic stress concentration stops. Because the wire mesh material is not in tension in the heat exchanger area, the self-imposed stress relief presents no structural problem.

The transpiration heat exchanger has a 0.300-in. radial thickness compared to the 0.030-in. for the regeneratively cooled chamber. If any local surface melting should occur, the lower stressed, thick transpiration cooled heat exchanger wall provides substantial margin and the flow rate

to that area will increase due to a local decrease in the heat exchanger flow resistance, without adversely affecting the adjacent region of the liner.

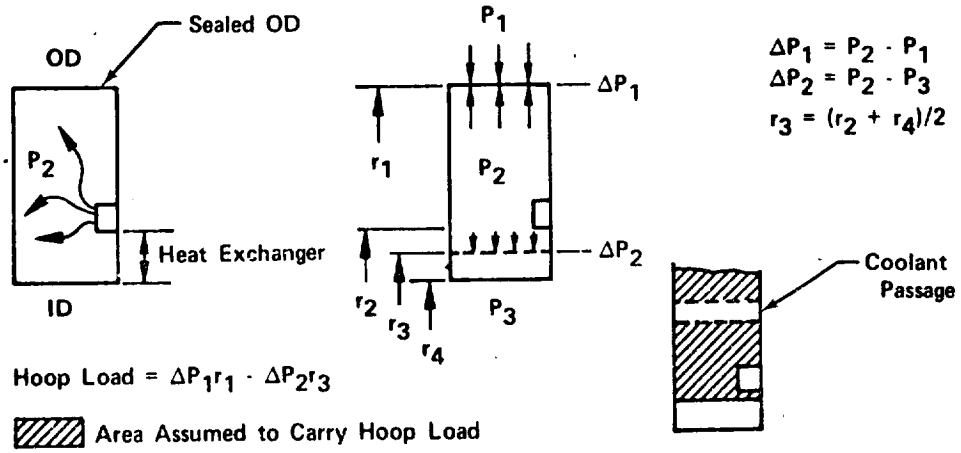

Figure V-7. Pressure Load in Wire Mesh Wafer FD 52375

c. Chamber Contour - CHAMBER GEOMETRY PROVIDES REQUIRED COMBUSTION VOLUME WITH MINIMUM WEIGHT AND TRANSPIRATION COOLING FLOW

The chamber contour is shown in figure V-8. Since the combustion process is super critical, a constant area during the burning process is preferred to minimize momentum pressure losses; a short convergence to the throat, designed to provide a 98.2 throat discharge coefficient, is used to provide the maximum chamber volume for a given length of chamber.

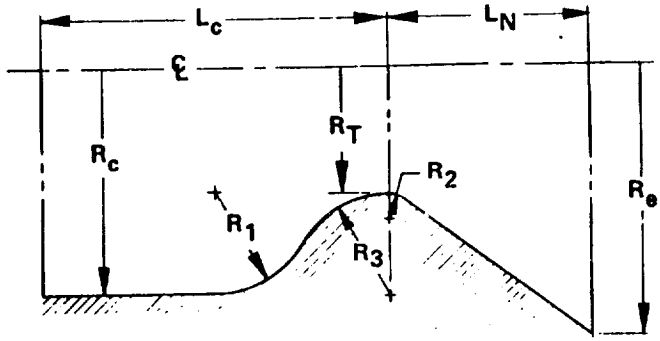

	Booster	Orbiter
Chamber Radius (R_c)	10.240	10.240
Converg. Radius (R_1)	4.600	4.600
Converg. Radius (R_3)	4.540	4.540
Diverg. Radius (R_2)	0.661	0.661
Throat Radius (R_T)	5.902	5.902
Exit Radius (R_e)	12.278	12.278
Chamber Length (L_c)	13.830	13.830
Nozzle Length (L_N)	12.109	9.656

Figure V-8. Chamber Contour Selected to Achieve Maximum Performance FD 46348

The SSME main chamber is 13.8-in. from the injector to the throat, providing the same chamber L* and length as used for the 250K main chambers. This approach also provides a chamber of minimum weight and minimum cooling requirements.

In determining the optimum chamber contour, two trade studies were conducted and may be referred to in Combustion Devices Trade Studies, PWA FR-4440. The first of these studies established a contraction ratio of 3:0 which resulted from an optimization of burning volume and minimum chamber length to ensure complete combustion. The rate of convergence from the cylindrical portion of the chamber to the throat resulted from a trade study to determine the minimum length, while maintaining acceptable pressure drop limits.

d. Nozzle Contour - TRANSPIRATION COOLING ALLOWS MATCHING BOOSTER/ORBITER NOZZLE CONTOURS WITH COMMON POWERHEAD WITHOUT LOSS IN PERFORMANCE

The contour of the supersonic nozzle portion of the main chamber, which differs for the booster and orbiter engines, was selected to provide optimum aerodynamic performance characteristics for the booster/orbiter nozzles.

Each divergent nozzle liner contour (booster/orbiter engine) is matched to the respective nozzle contour and can be easily interchanged after unbolting the forward flange of the primary nozzle. The decision to have two different rear liners for the main chamber was based upon a trade study that indicated one or two seconds of specific impulse were gained by matching booster/orbiter divergent nozzle sections from the throat, as shown in figure V-9. (Refer to Combustion Devices Trade Studies, PWA FR-4440.)

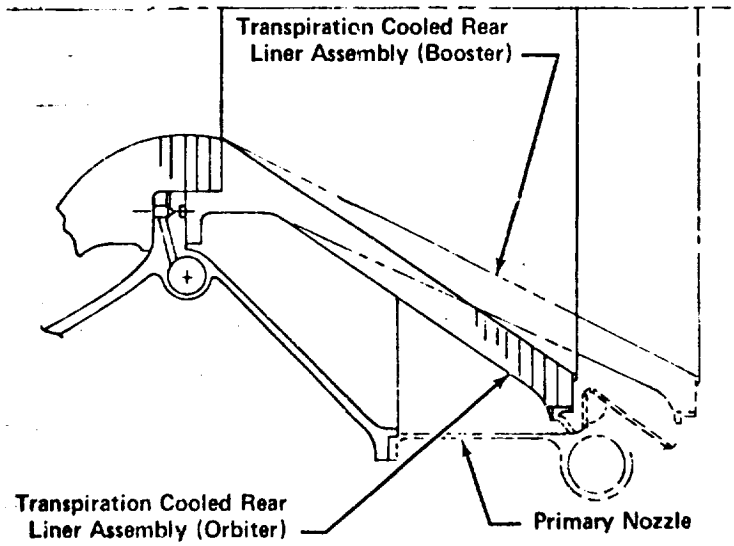

Figure V-9. Transpiration Cooling Allows Matching the Booster/Orbiter Nozzle Contour to Powerhead Without Loss in Performance FD 46335

To enable the engine powerhead and combustion chamber to be compatible for orbiter and booster engines, the breakpoint in the contour is located 0.5 in. downstream of the geometric throat. This precludes

any problems which could occur due to a contour mismatch if the breakpoint was located exactly at the throat.

In order to assemble the chamber liner to the coolant distribution ring, the chamber liner is fabricated in two sections. The forward section, shown in figure V-10, forms the combustion chamber, nozzle throat, and a small portion of the supersonic divergent nozzle. The rear section completes the remaining transpiration cooled part of the supersonic nozzle shown in figures V-11 and V-12. The chamber liners are attached to the outer case at the distribution ring by 48 0.250-in. diameter bolts. Twenty-four 0.190-in. diameter bolts, recessed into the liner flange, are used to retain the front liner when the rear liner is removed.

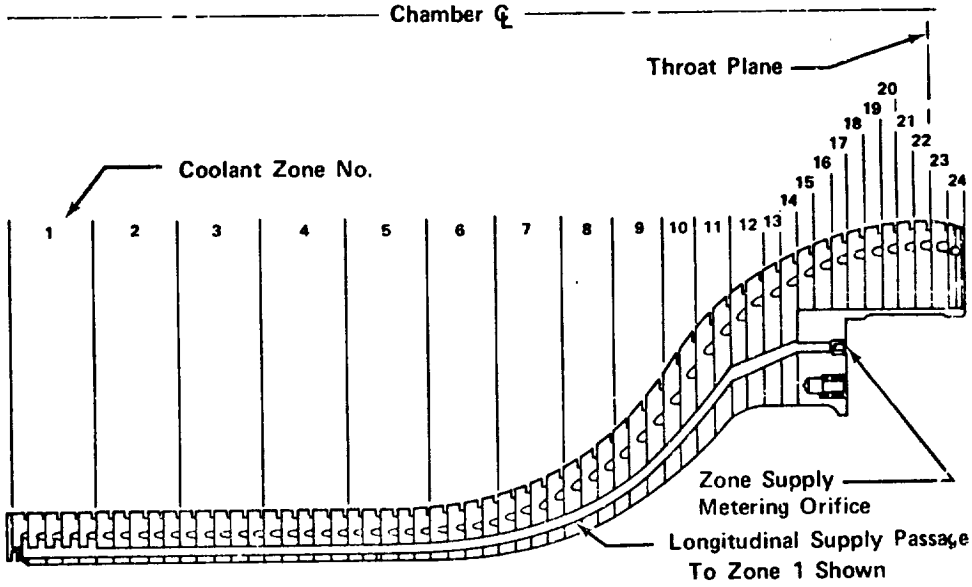

Figure V-10. Transpiration Cooled Front Liner Assembly FD 46332

e. Coolant Distribution - AXIAL COOLANT DISTRIBUTION ZONES ALLOW MATCHING COOLING TO HEAT LOAD REQUIREMENTS

The main chamber liners are divided into 48 axial zones. A zone is a collection of wafers fed by six axial supply passages. Coolant is metered to each coolant zone supply passage through orifices from the main chamber coolant inlet manifold. Zone cooling allows adjusting the cooling to every location within the chamber and thereby minimizes the total coolant flow rate required.

Each wafer in a coolant zone has a circumferential manifold, figure V-13, which distributes the coolant circumferentially in the wafer from the coolant zone axial supply passages. Slots connected to the coolant manifolds intersect the passages to form the flowpath for the coolant. The forward transpiration cooled chamber liner section, figure V-10, contains 24 zones fed by 144 passages. The divergent nozzle liner sections, figures V-11 and V-12, have 24 zones fed by 144 passages.

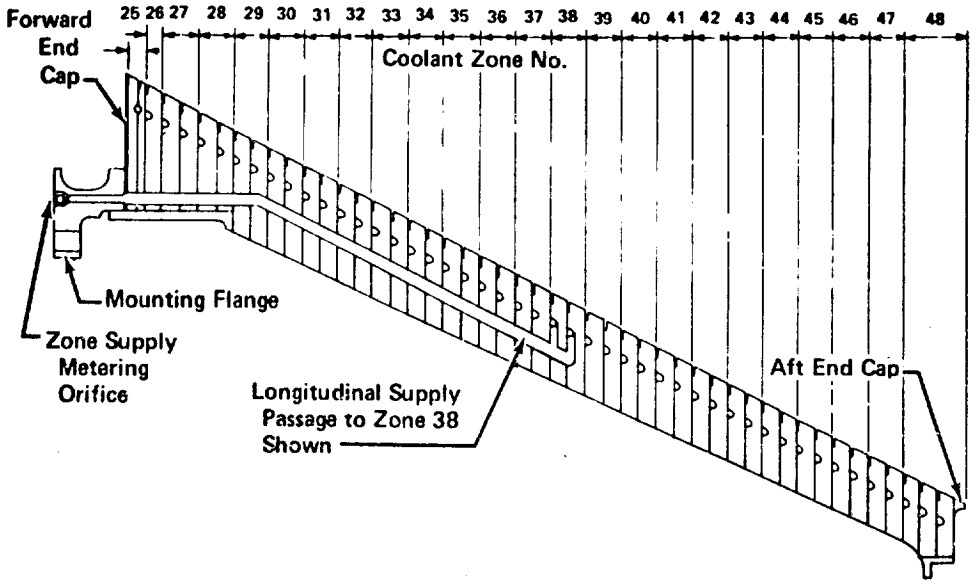

Figure V-11. Transpiration Cooled Rear Liner Assembly (Booster) FD 46333

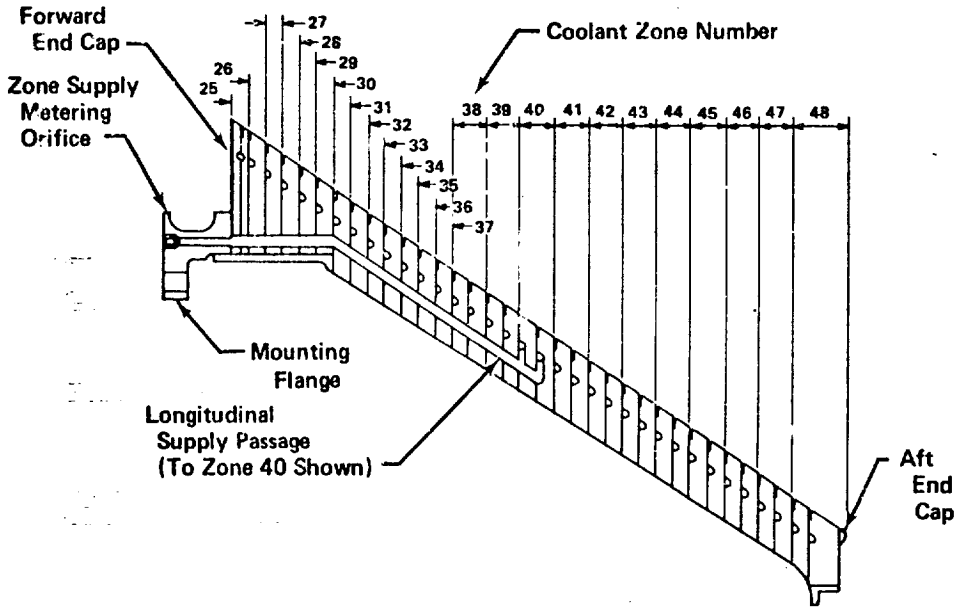

Figure V-12. Transpiration Cooled Rear Liner Assembly (Orbiter) FD 46334

The flow supplied to each coolant zone can be adjusted by the proper selection of the metering orifice plug located at the beginning of each passage as shown in figure V-14. The selection or sizing of these metering orifices is accomplished by flow calibration of the chamber assembly prior to the combustion tests. In addition, local values of coolant flow rate may be readily adjusted by changing orifice plugs to regulate the liner surface temperature as required.

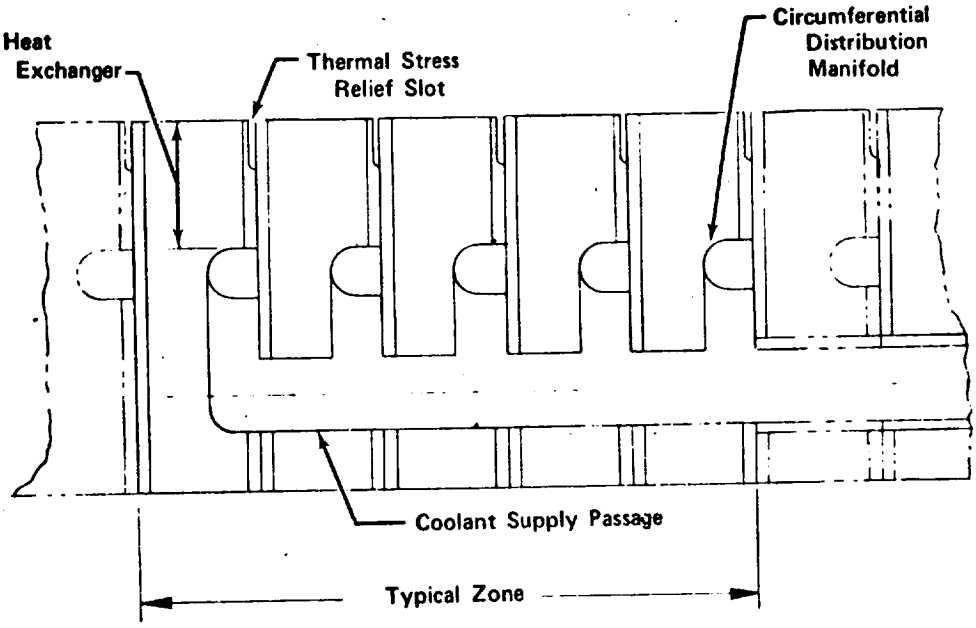

Figure V-13. Zone Distributes Coolant to Match Heat Flux FD 46341

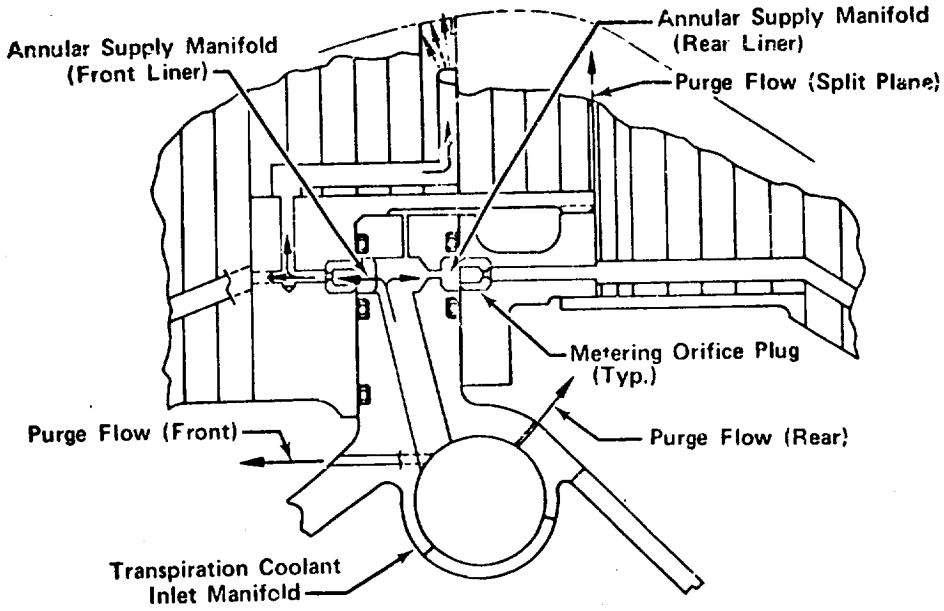

Figure V-14. Coolant Distribution System FD 46336

f. Torch Igniter - TRANSPIRATION COOLED LINER ALLOWS WALL MOUNTED IGNITER

The main chamber torch igniter is installed, as shown in figure V-15. The main chamber radially through the outer case and front section of the cooling liner. When the transpiration cooled chamber inner diameter surface is interrupted by the torch igniter port, overcooling is required to prevent the loss of the insulating boundary layer from causing local hot spots. To minimize the coolant required, the torch igniter region is hydraulically isolated from the rest of the coolant zone so that only a small

area receives the overcooling. As shown in figure V-16, this is accomplished by providing narrow radial dams across the circumferential manifolds and special feed passages to form an independent 15 deg sector.

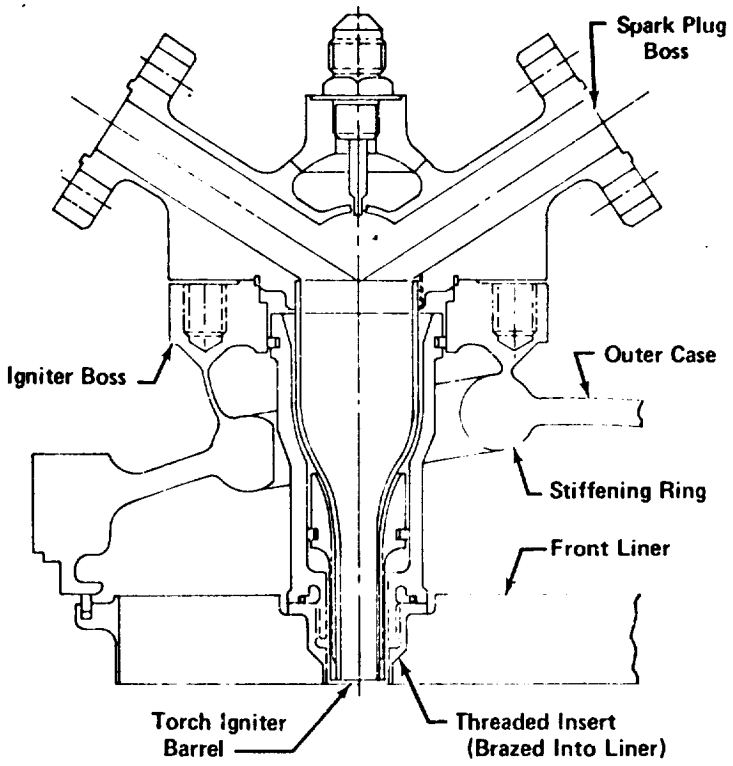

Figure V-15. Interchangeable Torch Igniter FD 46339

An investigation of the location for the main chamber igniter showed that alternative routes through the main case or main chamber injector would present problems. (Refer to Combustion Devices Trade Studies, PWA FR-4440.) An additional penetration in the main case in an area of high stress is undesirable and the long distance to the center of the injector presented a heat shielding problem for the high tension spark plug lead. Also, by locating the igniter in the main chamber wall, the igniter is identical with the preburner torch igniter, can have a close coupled spark igniter, and is easily accessible for maintenance. This side port in the main chamber could serve as a chamber pulsing location if required.

g. Instrumentation - DESIGN PROVIDES FOR HIGH AND LOW FREQUENCY CHAMBER PRESSURE MEASUREMENTS

Provisions for pressure instrumentation for the main chamber consist of two capped ports capable of accepting "infinite tube" mounted Kistler probes and one Statham static pressure transducer. The dynamic pressure probe ports penetrate the outer case forward flange at two locations spaced 135 deg apart. Slots are provided in the main chamber injector to receive the pressure sensing tubes as shown in figures V-17 and V-18 show the dynamic pressure port capped and the probe installed, respectively. The static pressure probe mounted in the spherical portion of the case with a sensing tube connected to a port in the forward flange is shown in figure V-19.

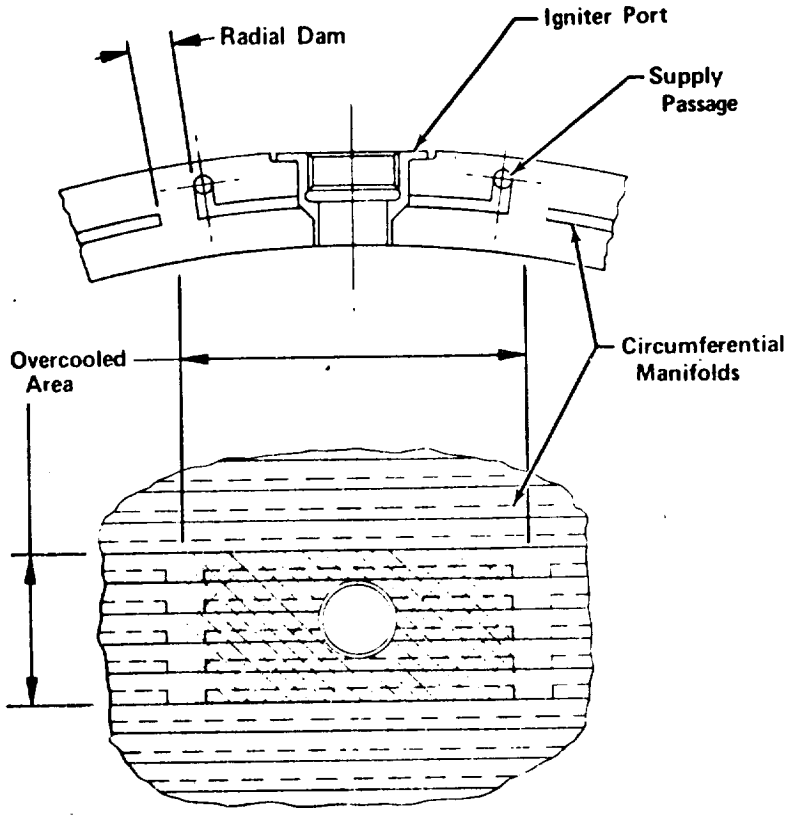

Figure V-16. Overcooling Minimized in Torch Igniter Port Region FD 46349

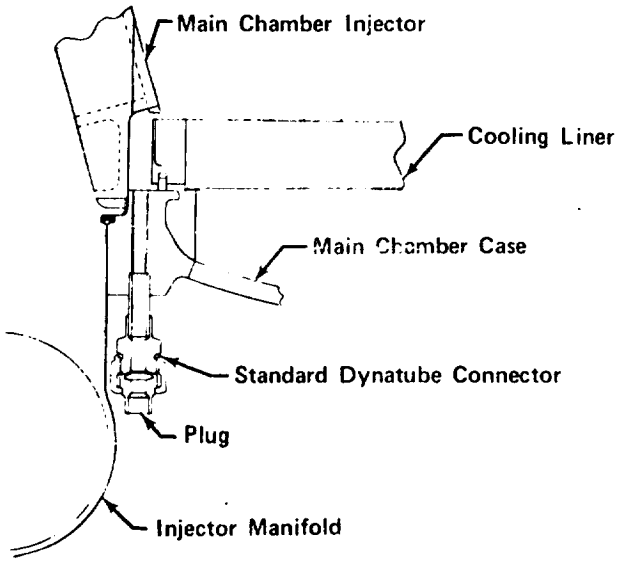

Figure V-17. Capped Dynamic Pressure Probe Port FD 46344

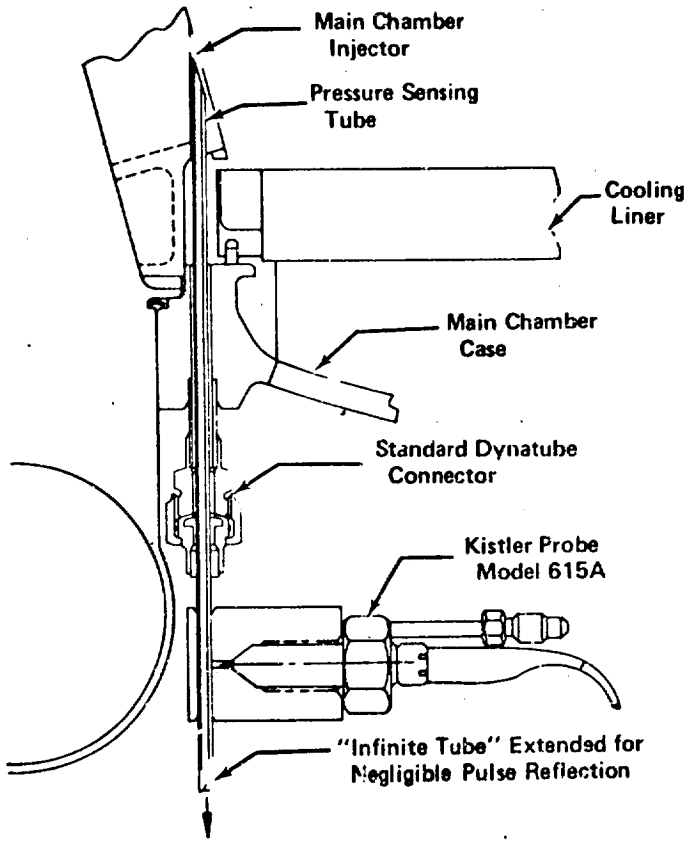

Figure V-18. Typical Dynamic Probe Installation FD 46342

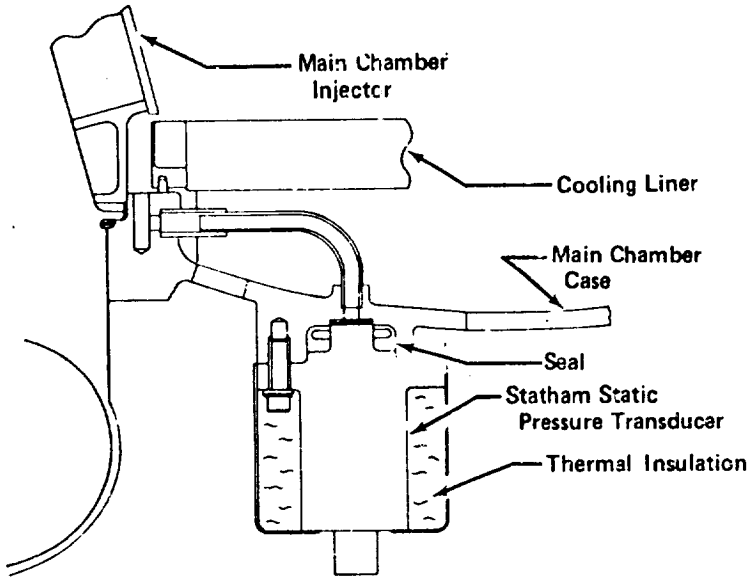

Figure V-19. Static Pressure Transducer Installation FD 46346

"Infinite tube"-type mounting provisions have been selected for the dynamic pressure probes to provide high frequency response without requiring close mounting of the pressure sensing element. This approach allows the requirements of paragraph 3.2.9.2 of CEI Specification CP2291 to be met without instrumentation penetrating the chamber liner and without subjecting the instrumentation to the severe environment of the main chamber.

The static pressure probe is connected to the acoustic resonator cavity by a sensing tube routed through the forward purge cavity in order to avoid penetrating the chamber liner. This design isolates the transducer from the severe environment of the main chamber without jeopardizing reliability with high pressure external tubing.

h. Acoustic Damping Devices - POROUS TRANSPIRATION-COOLED LINER DESIGN PROVIDES ACOUSTIC ABSORPTION

The SSME main chamber design concept has demonstrated stable and efficient combustion during the 50K and 250K staged combustion testing. The porous wire mesh chamber liner provides suppression of high frequency combustion instability by inherent absorption by the porous chamber walls which can be enhanced by proper design. This damping is the result of acoustic resistance, analogous to friction in a mechanical system, which directly opposes the acoustic wave motion in the liner. Energy from the wave is therefore dissipated by the liner due to viscous losses as shown in figure V-20.

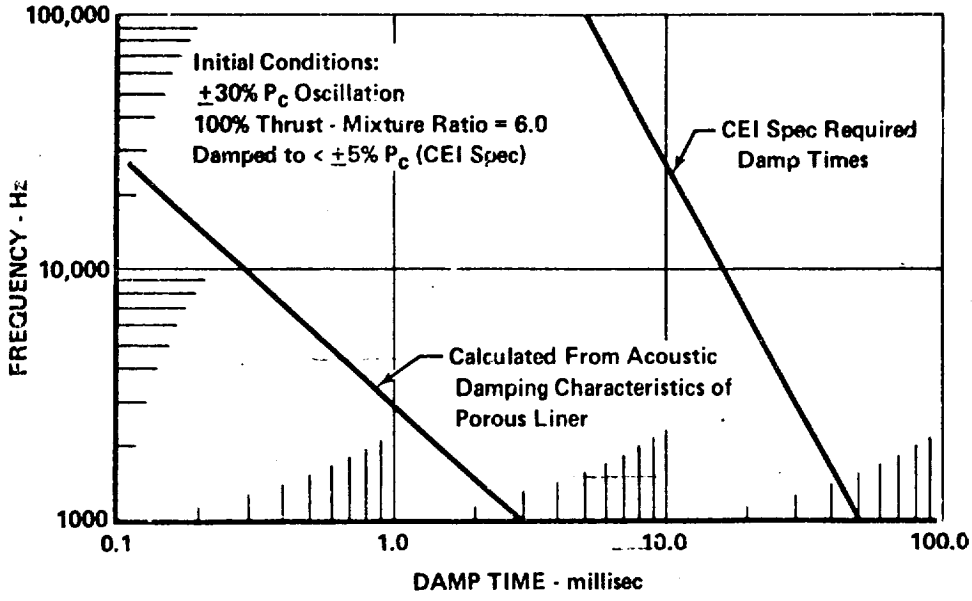

Figure V-20. Porous Chamber Liner FD 52328

Another acoustic damping device incorporated into the main chamber, and shown in figure V-21 utilizes the Helmholtz resonator theory. The design is based upon the Blackman theory, which has been investigated at P&WA FRDC under NASA/MSFC Contracts NAS8-21310 and NAS8-11038. The acoustic absorber consists of a mass of gas in the resonator aperture and a volume of gas in the resonator cavity which form an oscillatory system analogous to a spring-mass system. This system has a frequency response typical of a damped oscillator. Stability analysis indicates that should the combustion chamber become spontaneously unstable, the most probable mode is the 10th tangential, which ranges from 11,827 Hz at 100% thrust at a mixture ratio of 5.5 to 11,114 Hz at 20% thrust at a mixture ratio of 6.5. The Helmholtz cavity is sized to damp 11,573 Hz at 100% thrust at a mixture ratio of 6.0.

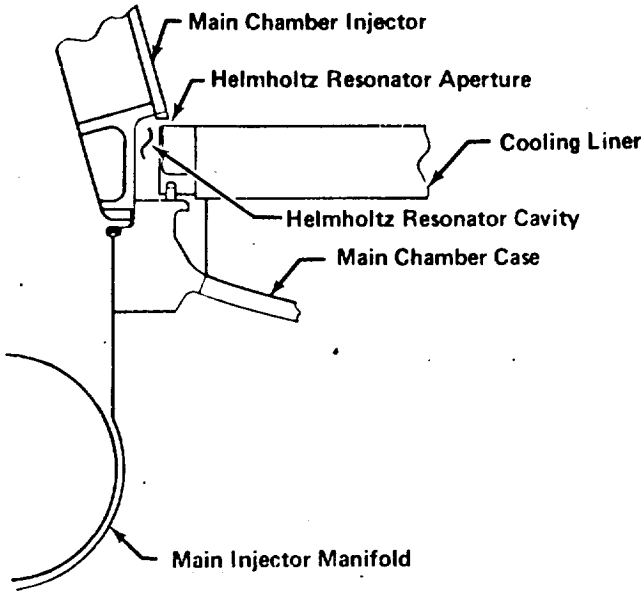

Figure V-21. Combustion Instability Damping Provisions FD 52679

The main chamber can be equipped with an artificial pulsing device as shown in figure V-22 to provide self-induced chamber pressure oscillations. A bomb mounting adapter is also provided through the center of the main chamber injector faceplate.

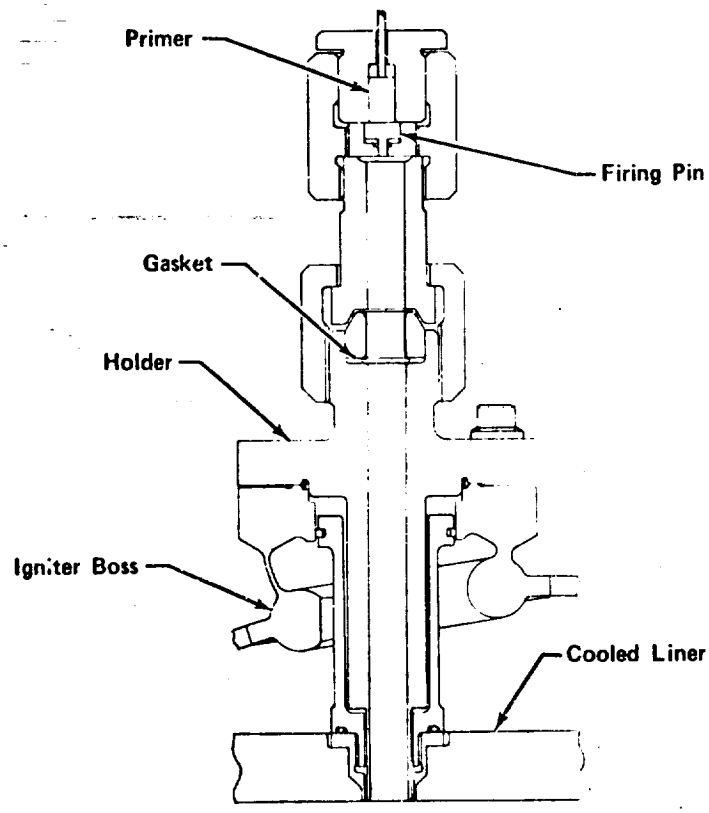

Figure V-22. Pulse Gun Installation in the Igniter Boss FD 46343

Additional information on the main chamber combustion stability is available in Section IX.

2. Outer Case

a. Design Approach - FLOATING LINER CONFIGURATION ALLOWS LIGHTWEIGHT SPHERICAL OUTER CASE

The transpiration cooled chamber liner is attached to the outer case only at the mounting ring as shown in figure V-4 . This configuration allows the remaining part of the chamber liner to float free of the outer pressure case.

The advantages of floating the chamber liner free of the outer pressure shell are: (1) the higher thermal growth of the copper chamber is not restrained by the colder supporting structure; (2) the chamber liner is lighter because it is neither the main pressure vessel nor the thrust carrying structure, it is a cooling chamber liner; (3) the high pressure area of the outer case can assume the more efficient spherical contour for a pressure vessel; and (4) the pressure vessel can be fabricated of high strength material.

The front section of the outer case contains high pressure hydrogen purge gas at a maximum pressure of 3411 psi. This section of the outer case has the structurally efficient pressure vessel shape of a sphere as shown in figure V-23.

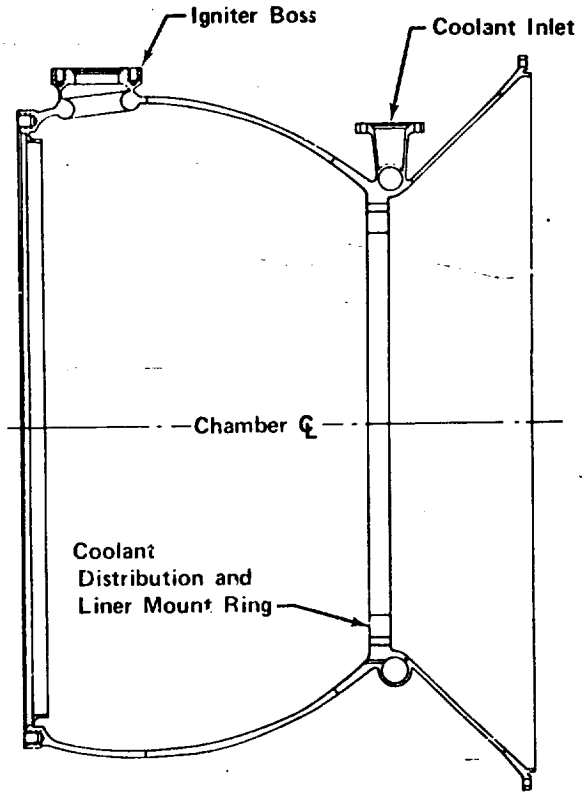

Figure V-23. Main Combustion Chamber Outer Case FD 46331

The design approach for the spherical section of the outer case is to take the major loads in shell tension (i.e., without bending) and to minimize discontinuity stresses by means of deflection matched stiffening rings. The relationship of the spherical shell to the forward flange and the distribution ring is such that the shell load paths pass through or near the centroids of the rings to minimize twist; this design method ensures better sealing capability and reduces the weight of the flange. The intersection of the spherical section of the outer case and the torch igniter flange is stiffened with a simple hoop ring which takes the discontinuity loads as pure tension. Cylinders and cones have elliptically warped plane intersections and make stiffening difficult; the spherical concept is more predictable and therefore, more reliable and lighter in weight. The conical rear section of the case is subjected to loads which produces a buckling condition and was sized considering this criteria.

b. Material Selection - HYDROGEN COMPATIBLE HIGH STRENGTH PWA 1053 SELECTED FOR OUTER CASE

The material selection for the outer case is PWA 1052 and PWA 1053. PWA 1052 and PWA 1053 have the high strength of Inconel 718 (150,000 psi yield strength), but are unaffected by the room temperature, high pressure hydrogen environment which degrades the allowable operating strength of Inconel 718.

The use of MP35N material, with 235,000 psi yield strength with 35% ductility, for the bolts and studs in the main chamber, saved 33 lb per engine over fasteners made from Inconel 718 material.

c. Fasteners and Flanges - LINE OF ACTION DESIGN REDUCES FLANGE WEIGHT

The main chamber outer case is attached to the main case and main chamber injecter by 72 0.4375-in. diameter studs. The trade study of through studs versus bolts showed that studs provide a weight savings, primarily because the use of through studs permits incorporation of a line-of-action flange. As shown in figure V-24, the flange concept reduces flange twisting by passing the shell load approximately through the centroid of the flange cross-sectional area and therefore minimizes the seal point deflection.

A common rear flange attaches the booster and orbiter primary nozzles to the main chamber outer case. The primary nozzle is fastened to the outer rear flange of the conical shell section with 120 0.190-in. diameter bolts. The bolt circle diameter is sufficiently large to permit the required assembly clearance between the outer contour of the rear section of the chamber liner and the forward flange of the primary nozzle. The flange is an undercut flange, designed to withstand maximum seal, gimbal, maneuver, thrust, and the low internal pressure loads, whil fulfilling the maximum allowable leakage requirements of paragraph 3.7.12, CEI Specification CP2291. Inverted toroidal seals, developed by P&WA, are used at the front and rear flanges of the outer case. During Phase B 250K engine testing, no indications of leakage were observed at the high pressure flanged joints which incorporated these seals.

After unbolting the primary nozzle, access to the 48 bolts retaining the rear transpiration cooled liner is achieved and the transfer of the common powerhead to either a booster or orbiter engine is easily performed.

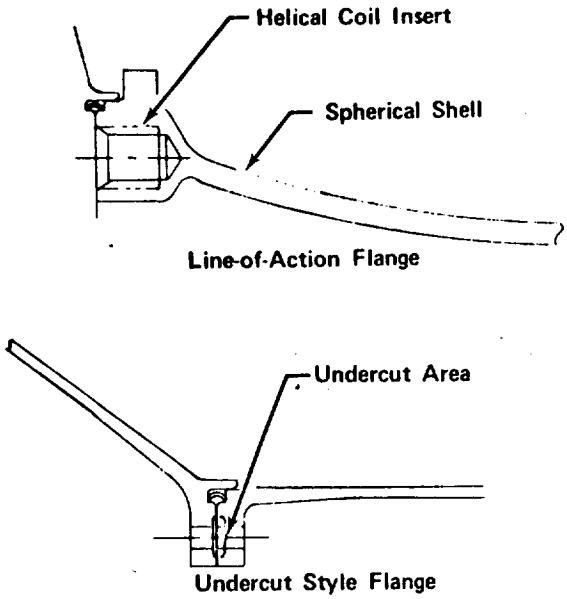

Figure V-24. Line-of-Action Flange Reduces Weight FD 46350

In addition to being the primary structural member between the main chamber injector and the primary nozzle, the outer case provides coolant distribution flowpaths to the chamber liners and serves as a mount for attaching the chamber liner sections, as shown in figure V-14.

d. Gimbal Actuator Brackets - PUNCH LOADS MINIMIZED BY TANGENTIAL ATTACHMENT

Gimbal actuator loads are transmitted to the case circumferentially tangent to a relatively rigid section of the outer case to minimize punch loads. The engine is gimbaled by two actuators 90 deg apart. Each actuator is attached to the engine by means of a clevis welded to a four-legged bracket, which in turn is welded to the main chamber outer case. The four-legged bracket concept was selected because it avoids excessive point loading by distributing the gimbal loads about the relatively rigid areas of the case. It is also a lightweight means of placing the gimbal actuator attach points at the locations specified in the Interface Control Document. The bracket legs are hollow tubes which are sized for a combination of buckling and bending loads. The front and rear legs of each bracket are butt-welded to lugs which are an integral part of the outer case as shown in figure V-25.

e. Chamber Liner Seals - RECIRCULATION PREVENTED BEHIND THE LINER WITH THE ADDITION OF PURGES

Hot combustion gases are prevented from entering the annular gap between the front chamber liner and the outer case by a piston ring seal with a hydrogen gas purge as a backup. As shown in figure V-4 , hydrogen gas purge and a spring washer seal are also used to prevent combustion gas recirculation at the annular gap between the rear chamber liner and the primary nozzle. Without these seals, hot combustion gases could recirculate behind the chamber liner causing a temperature rise in both the outer case and backwall of the chamber liner. The orifices in the outer case which control the 0.17 lb/sec flow of the purge gas are sized to prevent excessive pressure buildup behind the chamber liners when the engine shuts down.

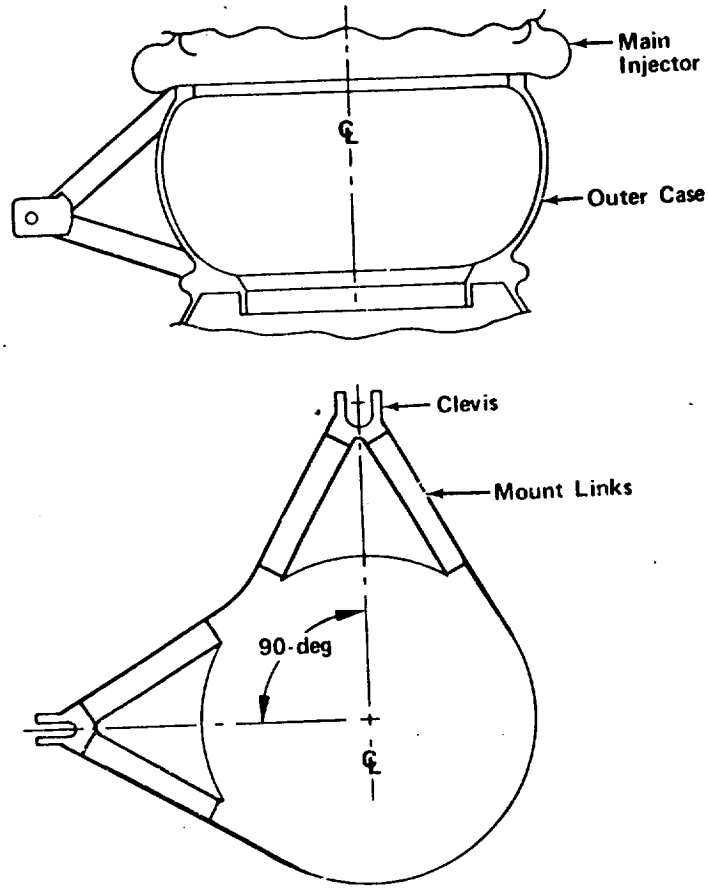

Figure V-25. Gimbal Mount Brackets Minimize Punch Loads FD 46363

During the Phase B 250K combustion tests on the etched copper wafer chamber, the chamber liner seals were eliminated because of a possible high pressure differential across the liners which could occur at an abort shutdown. Although the firing time was less than 30 sec, the temperature of the chamber liner backwall near the main injector stabilized near the predicted level of 1000°R. This indicated that the purge flow alone would be sufficient to prevent recirculation of the combustion gases; however, until additional testing is completed, the seals will be incorporated into the SSME main chamber configuration.

C. REQUIREMENTS

The requirements of the applicable paragraphs of CEI Specification No. CP2291 have been met as follows:

1. Components shall be designed to guarantee a minimum low cycle fatigue life as stated in paragraph 3.7.7.1.3.

   Compliance. The main chamber liner has a minimum low cycle fatigue life in excess of 1000 cycles.

2. The engine shall be capable of integrating a basic powerhead assembly with nozzles, the expansion contours of which are optimized for either booster or orbiter stage applications, as stated in paragraphs 1.2.b and 3.0.1.

Compliance. The rear chamber liner begins 0.5-in. downstream of the throat. The rear chamber liner contour, which differs for the booster and orbiter engine, was selected to provide optimum aerodynamic performance characteristics for the nozzle involved. The rear liner is easily removable from the basic powerhead.

3. Should chamber pressure disturbances occur, the amplitude of which is outside the allowable limit specified by paragraph 3.2.9.1, the major frequency components shall dampen within 1600 $\sqrt{f}$ milliseconds in accordance with paragraph 3.6.3.1.

   Compliance. The main chamber is capable of absorbing the incident energy at a frequency range from 10 Hz to 15,000 Hz within 1600 $\sqrt{f}$ milliseconds.

4. Materials known to be susceptible to embrittlement when exposed to gaseous hydrogen shall not be used in a configuration or application which will result in failure due to hydrogen embrittlement, as stated by paragraph 3.7.1.2.

   Compliance. The chamber liner is fabricated from copper and the outer case PWA 1052-1053. The life and strength of copper and PWA 1052-1053 is not affected by gaseous hydrogen.

5. Flight engines shall be equipped with capped or plugged measuring ports capable of accepting the high frequency pressure transducers used during the development program ports located within 1.24 in. downstream of the injector face spaced 135 deg apart (in accordance with paragraph 3.2.9.2).

   Compliance. Two capped ports capable of accepting "infinite tube" mounted Kistler dynamic pressure probes penetrate the outer case forward flange and are spaced 135 deg apart.

6. The capability of the engine to damp self-induced pressure oscillations shall be demonstrated (in accordance with paragraphs 4.25 and 3.2.9.2).

   Compliance. The torch igniter port can be used to mount a pulse gun as shown in figure V-22 for artificial pulsing during the development program. In addition, the center of the main chamber injector will have a bomb mounting capability.

7. External or internal leakage of engine propellants or fluids shall not occur in such a manner as to impair or endanger proper functions of the engine or vehicle all separable connections shall not exceed an allowable propellant gas leakage of 1×10^{-4} scc/sec of helium at

operating or leak check pressures (in accordance with paragraph 3.7.12).

Compliance. All separable connections or welded enclosures are designed to not exceed leakage requirements.

In addition to CEI Specification No. CP2291, the following are Pratt & Whitney Aircraft imposed requirements:

1. Hydrogen coolant shall be supplied at 3806.7 psia maximum pressure and 326.1°R temperature with the operating schedule in accordance with the design cycle.

   Compliance. The main chamber is designed to operate with hydrogen coolant at the specified pressure and temperature.

2. Hydrogen coolant shall be supplied at flow rates scheduled in the design cycle. The design point shall be 100% at a mixture ratio of 6.5. The flow rate at the design point shall be 5.25 lb/sec as shown in figure V-26.

   Compliance. The main chamber is designed to operate at the specified coolant flow rate.

3. The maximum chamber pressure shall be 3233.6 psia, in addition to 2.3% overpressure at the 109% thrust level.

   Compliance. The main chamber liner and outer case are designed to operate at the maximum chamber pressure, in addition to 2.3% overpressure at the 109% thrust level.

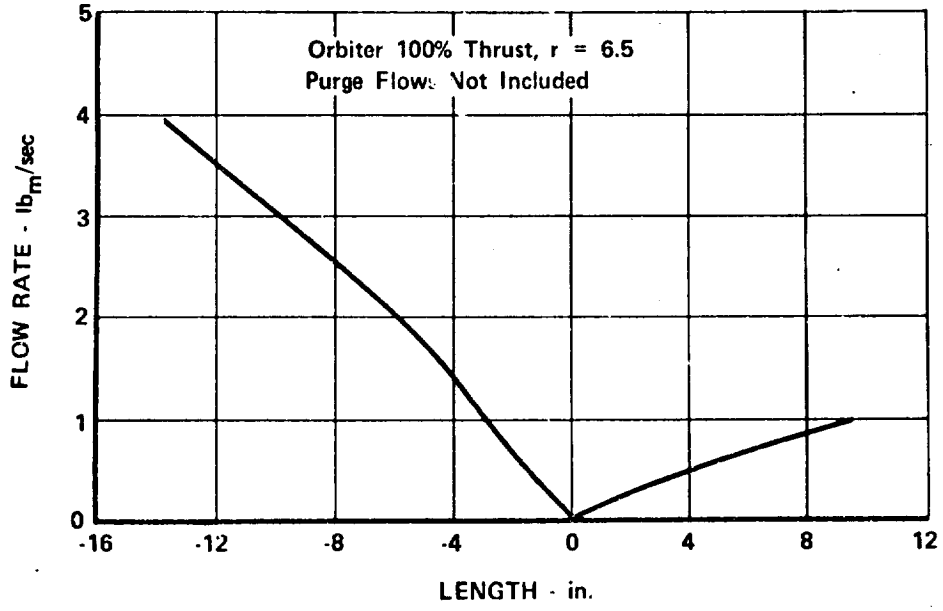

Figure V-26. Total Coolant Flow Rate vs Axial Length from Throat FD 52329

D. CAPABILITY

1. Transpiration Cooled Chamber

The CEI specification impulse performance and life requirements are exceeded. The SSME transpiration cooled main chamber design will provide in excess of four sec specific impulse margin over impulse performance requirements and will exceed the 400-cycle low cycle fatigue life by more than 100%.

The throat area can be increased 10% to provide thrust level growth. This increase can be accomplished by recontouring the chamber liner. No changes would be required in the outer case or other structural members as shown in figure V-27.

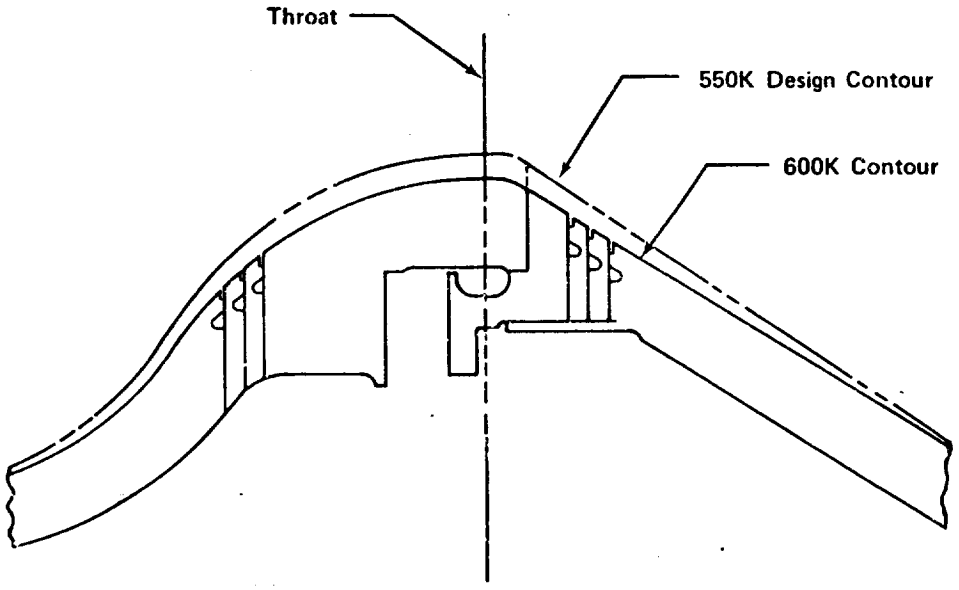

Figure V-27. Recontouring Transpiration Cooling Chamber Provides 10 Percent Increase in Thrust FD 46337

Growth potential of the main chamber can be accomplished by:

1. Increasing the chamber pressure for additional thrust, thereby increasing the heat flux to the wall. Transpiration cooling has a unique advantage over other types of cooling concepts in that it permits tailoring of coolant flow in any location within the chamber for any heat load caused by a change in thrust level. This change would not affect the cycle life of the chamber liner.

2. Increasing the chamber hot wall temperature by using a higher temperature material for the chamber liner wall would decrease the coolant flow rate, thereby improving performance.

3. Developing porous materials for the chamber liner which offer improvement in heat exchanger efficiency and coolant injection over the current wire mesh material would decrease the coolant flow rate, thereby improving performance.

2. Outer Case

The main chamber outer case is designed to meet the Structural Design Criteria, PWA FR-4449, and is limited by the 1.2 proof pressure test criteria. With improvements in material strength, the chamber pressure could be increased to provide thrust level growth.

E. SUBSTANTIATION

1. Transpiration-Cooled Liner

a. Chamber Liner Selection - COPPER WIRE MESH WAFER MINIMIZES TRANSPIRATION COOLANT FLOW

Copper wire matrix wafers were selected for the SSME transpiration-cooled main chamber liner design because of its improved internal wall heat transfer characteristics and a more uniform surface film distribution. The wire mesh wafer chamber utilizes a coolant flowpath from the circumferential distribution manifold to the inside diameter of the chamber, provided by the open pore area between the compressed woven wire matrix layers. The coolant flows through the woven wire matrix and is injected at low velocity into the chamber so that it tends to remain along the hot surface, rather than mix immediately with the hot gas stream, thereby reducing the heat transferred to the wall and enhancing the coolant film effect. The effective internal heat transfer coefficient is also enhanced by the high degree of turbulence associated with flow through the woven wire matrix. The detailed fluid thermal analysis of the woven wire mesh liner configuration may be referred to in Design Analysis For Transpiration Cooling, PWA FR-4463.

The two areas of improved performance are in the wall heat exchanger efficiency and the coolant film effectiveness. The wall heat exchanger efficiency, which accounts for the ability of the coolant to utilize its heat capacity to absorb the heat transferred to the wall, was increased due to five to 14 times more internal heat exchanger surface area being available. Increased film effectiveness of the coolant being transpired from the surface will be realized by the use of wire mesh due to more uniform coolant injection along the surface. Trade studies showed that a 50% reduction in cooling flows can be attained by utilizing a wire mesh wafer concept versus a photo-etched wafer concept. (Refer to Combustion Devices Trade Studies, PWA FR-4440.)

b. Wire Mesh Wafer Development - FABRICATION TECHNIQUES FOR SSME CHAMBER LINER ALREADY DEVELOPED

During the Phase B test program, P&WA worked closely with Aircraft Porous Media and Michigan Dynamics to develop the copper wire mesh material required for the SSME main chamber. Fabrication techniques have been developed which provide the required repeatable flow characteristics and the material properties approach those of solid oxygen free high conductivity copper with room temperature 0.2% yield strength in excess of 6200 psi. During the Phase B test program, P&WA developed fabrication techniques for sealing and restoring porosity of the wire mesh material. We have experimentally verified that the sealing technique used for the coolant feed holes is durable by thermally cycling several samples 100 times each. Complete sealing was retained throughout the tests.

c. Chamber Liner Material Selection - COPPER WIRE MESH WAFERS IMPROVE DURABILITY

An investigation to determine total performance characteristics between nickel and copper wire mesh material were conducted. (Refer to Combustion Devices Trade Studies, PWA FR-4440.) Because of nickel's higher allowable wall temperature, a 10% reduction in the total required coolant flow rate is possible compared to copper wire mesh. However, copper demonstrates better cycle life characteristics because its maximum wall temperature of 1900°R and thermal gradient are less severe than nickel's at 2500°R. Copper, which has a thermal conductivity five times that of nickel, will also dissiminate any local hot streaks more readily than nickel and is not embrittled by hydrogen. The cost of the copper wire mesh chamber is estimated to be 57% less than the etched copper wafer chamber for the SSME. This cost estimate is based upon the actual hardware costs of similar chambers fabricated during the Phase B test program.

With the above performance characteristics and based upon P&WA fabrication and test experience with copper, copper wire mesh was the material selected for the wafer design.

d. Durability - LOW CYCLE FATIGUE IS NOT A PROBLEM IN OUR POROUS TRANSPIRATION COOLED CHAMBER DESIGN

In addition to proven performance, the transpiration-cooled chamber concept permits the incorporation of design features which increase low cycle fatigue life. The thermal relief slots have demonstrated a reduction in thermal strain on chamber tests performed at the P&WA Florida Research and Development Center since their introduction in 1967.

To determine the low cycle fatigue capability of the wire mesh material, uniaxial bar test specimens were prepared. The specimens were loaded in a tension-compression cycle of constant strain until fracture occurred.

The testing was supplemented by NASA TM-X52270, "A Method of Estimating High Temperature Low Cycle Fatigue of Materials," to construct a strain versus life curve for the entire temperature range of the liner (to 1900°R). The curve produced, shown in figure V-29, shows life as a function of thermal strain and temperature.

P&WA's eight years of testing high pressure, high performance transpiration-cooled chambers have substantiated the inherent forgiveness of this cooling concept. During the recent Phase B testing, the baseline transpiration-cooled chamber was damaged due to insufficient cooling. The forgiveness of this cooling concept enabled the repaired chamber to be tested at 100% thrust with no degradation in impulse performance 83 hr after the damage was incurred.

e. Wafer Geometry - 0.300 IN. RADIAL THICK HEAT EXCHANGER MINIMIZES COOLING REQUIREMENTS

A primary wafer geometric parameter is the radial thickness of the heat exchanger. The most important considerations in establishing the heat exchanger radial thickness are the effect on coolant mass flux and wafer backside

wall temperature. The radial thickness must be sufficient to maintain the coolant mass flux near its minimum value. Figure V-29 shows the effect of the radial thickness of the wafer heat exchanger on the coolant mass flux. Beyond a certain value, increasing radial thickness has no effect on the coolant requirements of the heat exchanger; however, as shown in figure V-30, the wafer backside wall temperature is a strong function of radial thickness.

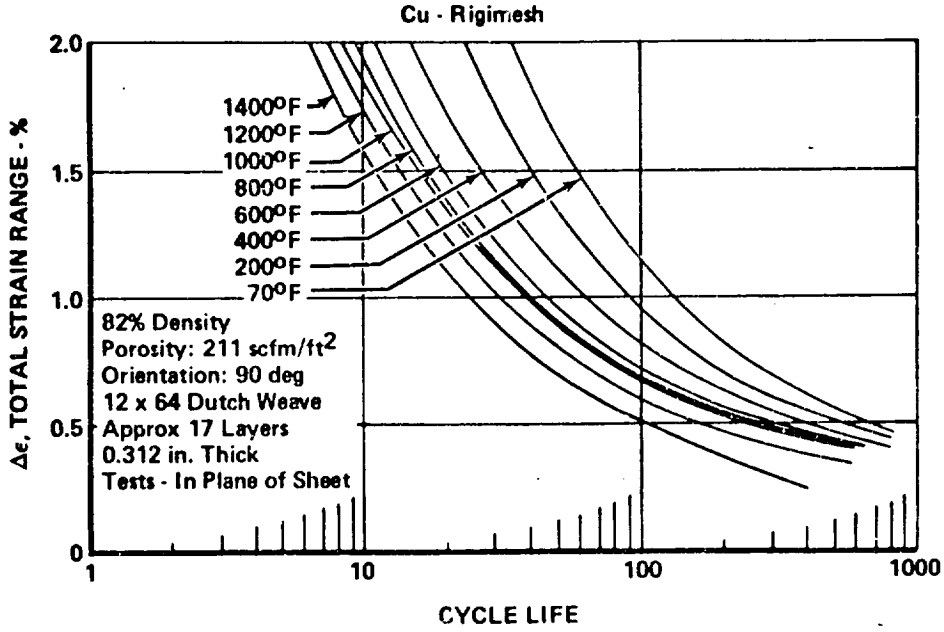

Figure V-28. Low Cycle Fatigue Design Curves FD 52412

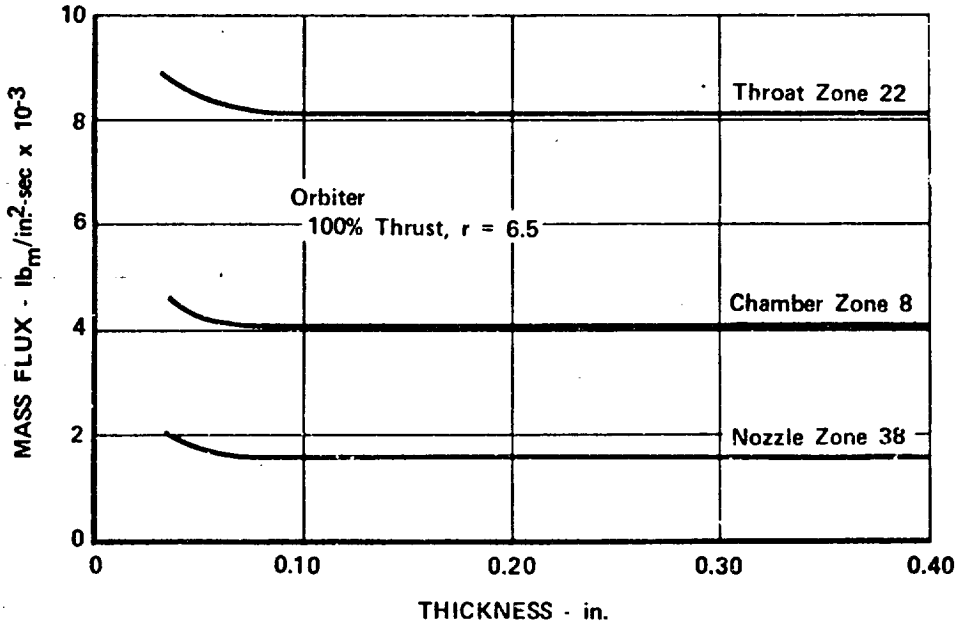

Figure V-29. Coolant Mass Flux vs Heat Exchanger Radial Thickness FD 46354

A minimum heat exchanger radial thickness of 0.300 in. was chosen because a thinner heat exchanger would require additional material on the heat exchanger outside diameter to compensate for the lower strength of the hotter

copper. Also, as radial thickness is decreased beyond 0.200 in., coolant mass flux requirements greatly increase. As radial thickness is increased, the liner diameter increases, thereby increasing the bolt circle diameter and the weight of the chamber housing. The transpiration-cooled chambers currently being tested during the Phase B 250K test program have minimum heat exchanger radial thicknesses of 0.300 in.

A wafer axial thickness of 0.25 in. was selected to maintain adequate coolant distribution characteristics while minimizing the number of wafers, thereby meeting the low cycle fatigue life requirement of 400 cycles and maintaining simplicity of manufacture.

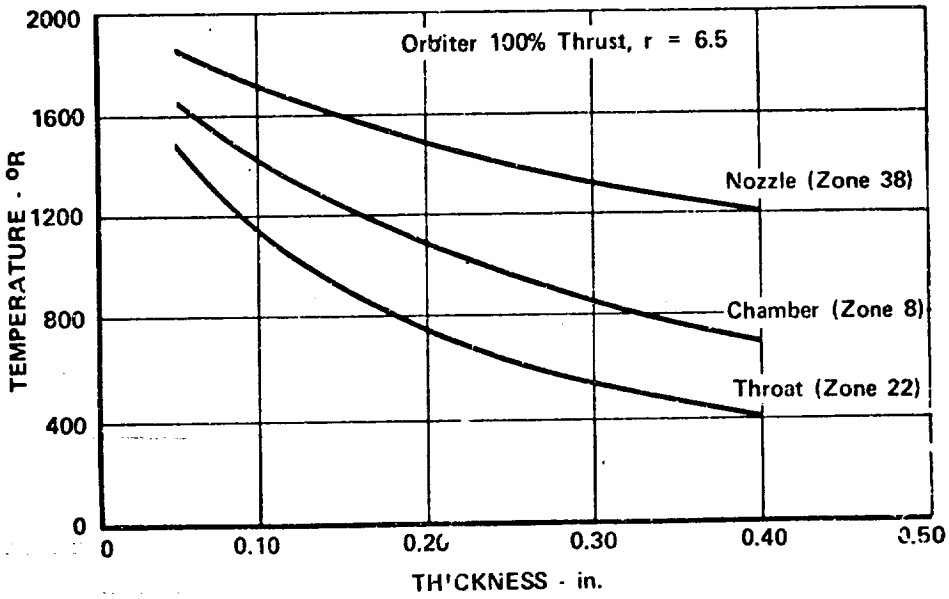

Figure V-30. Heat Exchanger Backside Wall Temperature vs Heat Exchanger Radial Thickness, Orbiter, 100% Thrust, Mixture Ratio = 6.5 FD 46355

f. Coolant Mass Flux - COOLANT MASS FLUX REDUCED

The coolant mass flux profile shown in figure V-31 is a reduction in the coolant mass profile demonstrated with a photo-etched wafer during Phase I testing of the 250K test program in 1967. The decrease in reduced chamber heat flux (that reaching the wall) in the 550K SSME below values for the 250K Phase I testing can be attributed primarily to (1) a lower combustion side film coefficient in the 550K engine due to its larger size, and (2) a physically improved liner heat exchanger in the 550K engine.

g. Chamber Surface Temperature - 1900°R HOT WALL BASED ON 250K EXPERIENCE

The design hot wall surface temperature is 1900°R which is approximately 550 deg below the melting point of copper. Selection of 1900°R as the design temperature for copper as shown in figures V-32 and V-33 is based on test experience at 250K thrust levels. The critical heat transfer parameters sensitivity to wall temperatures are shown in figure V-34.

As shown in figure V-35, lowering the hydrogen coolant temperature decreases the required flow rate to transpiration cool the chamber. The hydrogen coolant supplied from the primary nozzle regenerative heat exchanger is approximately 300° F. Analytical studies show that temperatures significantly below 300° F would require excessively small orifices.

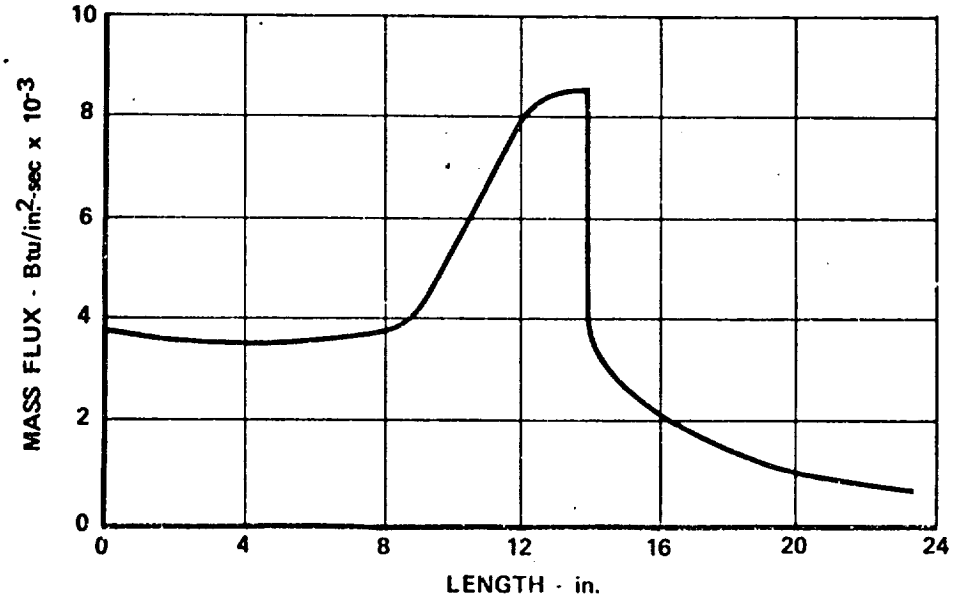

Figure V-31. Coolant Mass Flux vs Axial Length from Injector, 100% Thrust, Mixture Ratio = 6.5 FD 46356

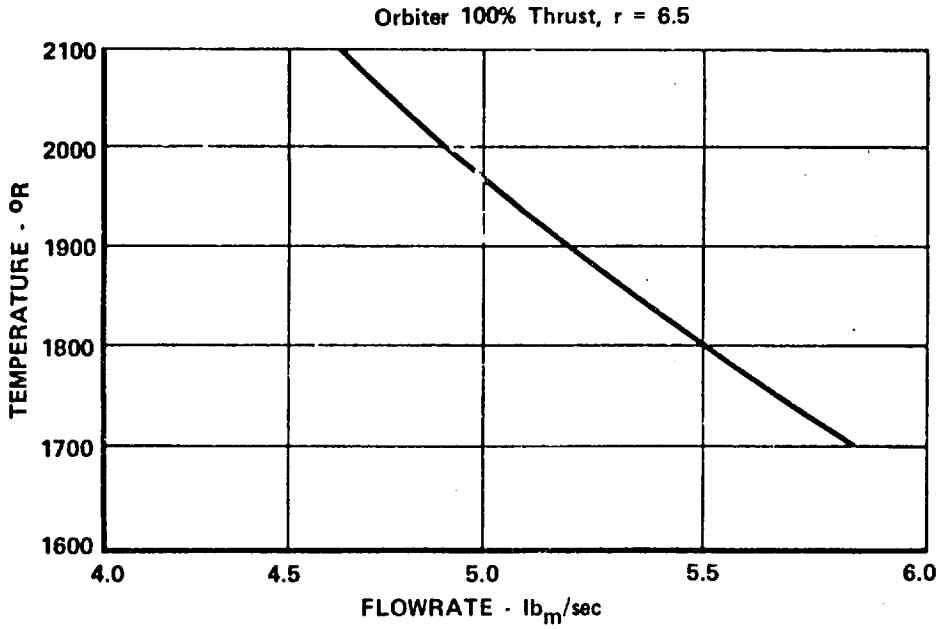

Figure V-32. Total Coolant Flow Rate vs Hot Sidewall Temperature FD 46353

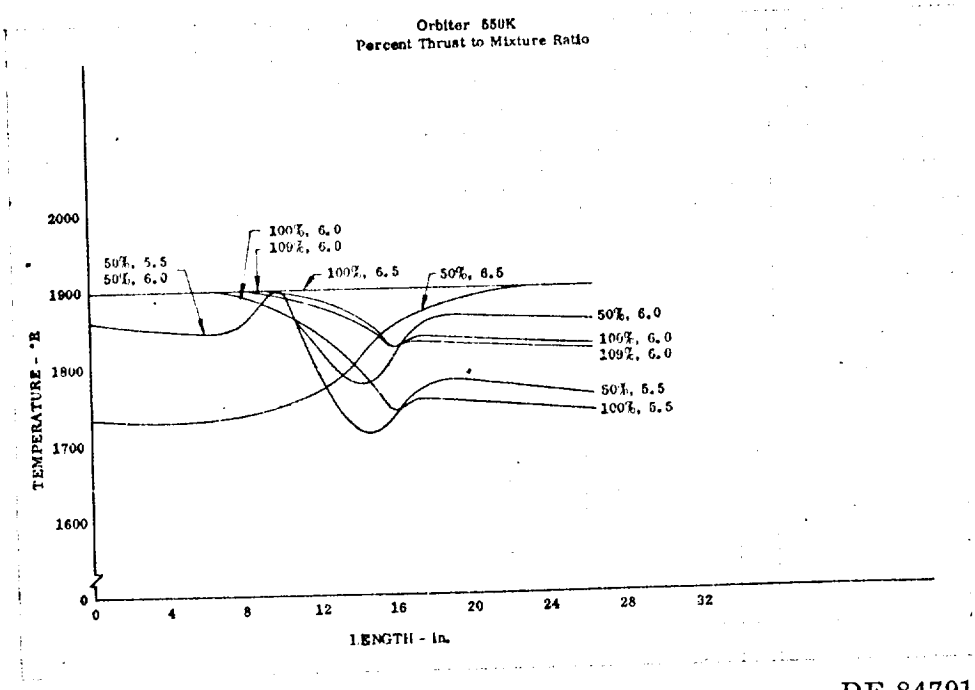

Figure V-33. Hot Sidewall Temperature vs Contour Length from Injector

DF 84791

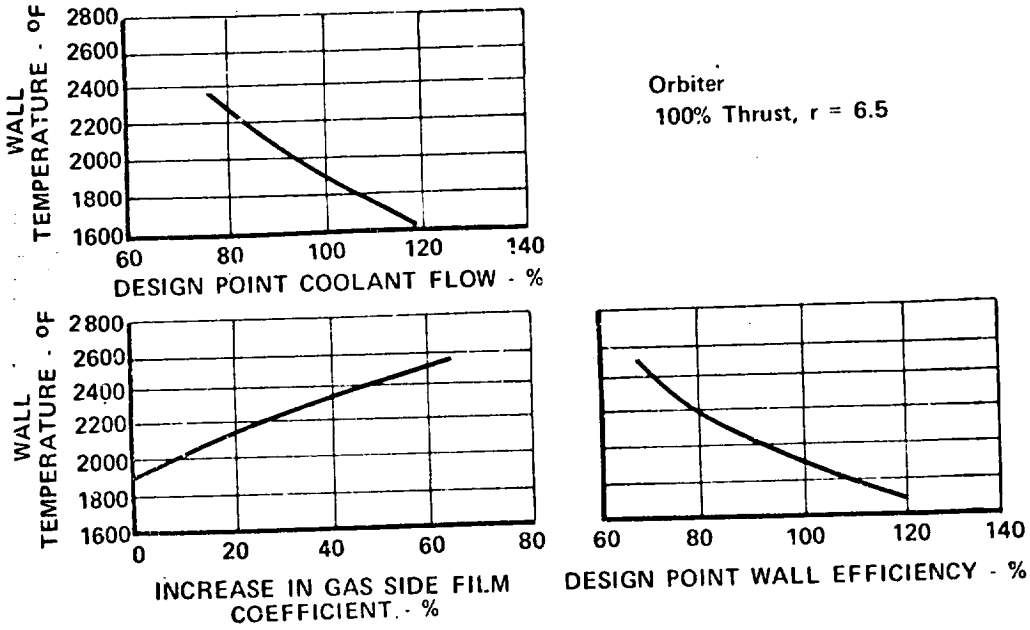

Figure V-34. Wall Temperature vs Heat Transfer Parameters

FD 46352

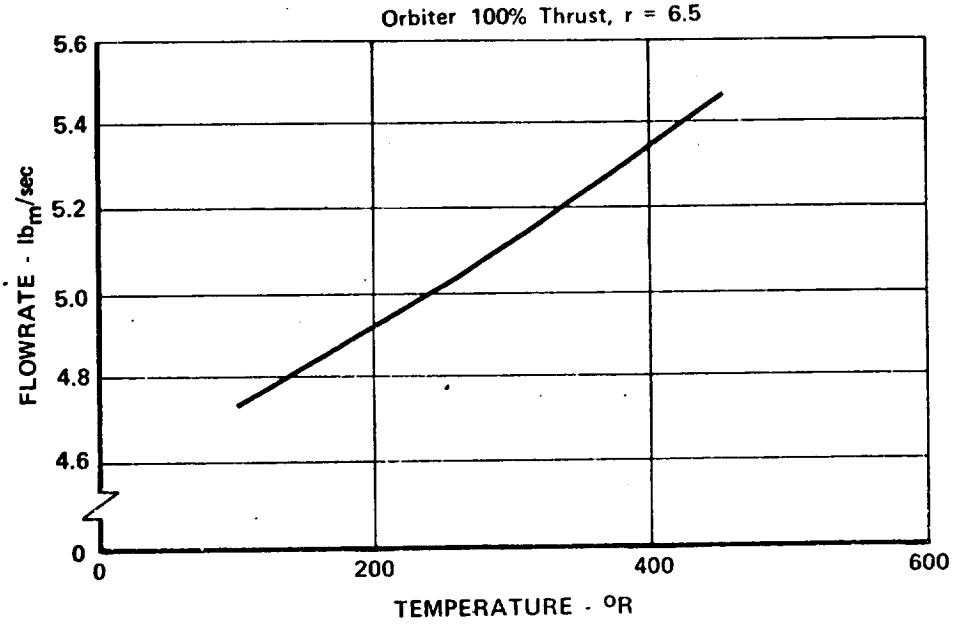

Figure V-35. Total Coolant Flow Rate vs Coolant Supply Temperature FD 46358

h. Coolant Filter - FILTERED ENGINE TRANSPIRATION COOLANT FLOW ENSURES UNRESTRICTED LINER COOLING

The transpiration cooling flow for the main chamber will be filtered by a semi-reverse flow centrifugal particle separator in the engine coolant supply system.

The semi-reverse-flow centrifugal separator utilizes fixes turning vanes on a contoured hub to induce swirl to the annular contour, and to flow swirl force the contaminants to the outer radius of the flowpath. The outer 43% of the flow containing the contaminants is ducted to the engine main case. The remaining flow is routed to the main chamber cooling liner. This separator is 100% efficient for particles 15 microns or larger. The efficiency for smaller particles is shown in figure V-36. This performance applies over the engine thrust range from 50% to 109%. These efficiencies are based upon data generated by P&WA for the U. S. Army Aviation Laboratories, Contract DAAJ02-70-C-0003.

The rigimesh liner has a mean pore size of 6 microns and a maximum absolute pore size of 20 microns. Therefore, the remaining particles in the flow will not be detrimental to chamber cooling effectiveness for the required life. If it was assumed that all the remaining particles 5 and 10 microns in size did not pass through the rigimesh and they evenly distributed themselves, after 7.5 hr at 100% thrust, they would fill only 18% of the available pore area at the inner surface of the chamber. This also does not account for flow re-distribution around restrictions through the thickness of the rigimesh liner.

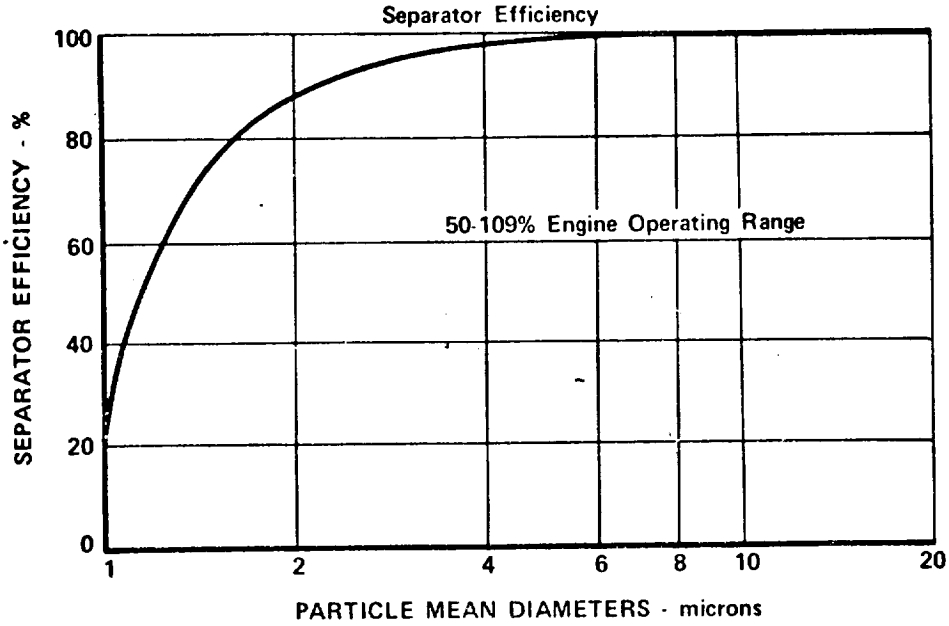

Figure V-36. High Efficiency Particle Separator Provides Clean Transpiration Coolant FD 52684

i. Chamber Contour - CHAMBER CONTOUR IS CONSISTENT WITH DEMONSTRATED HIGH PERFORMANCE CHAMBERS

The contour of the chamber liner is optimized for performance and is consistent with the chamber lengths, propellant "stay time," and contraction ratios P&WA has demonstrated on the chambers since 1963 on the RL10, 50K, and 250K hardware. Table V-1 shows the detail parameters as related to the hardware.

Table V-1. Main Chamber Contour Parameters

Engine \ Chamber Characteristics	Stay-Time (Milliseconds)	Chamber Length (in.)	Contraction Ratio
RL10A3-3	1.026	13.00	4.0:1
50K	0.940	13.00	3.0:1
250K	0.885	13.00	3.0:1
SSME 550K	0.977	13.83	3.0:1

The transpiration-cooled chamber design is based on eight years of combustion testing which is directly applicable to the requirements of the SSME. The results of 151 chamber firings at chamber pressures of 3000 psi in thrust ranges from 5000 to 250,000 lb have been used to design a safe and durable SSME main chamber.

2. Outer Case

The spherical shape of the outer case was chosen as the basis for the design concept of the main chamber because of its structural efficiency as a pressure vessel and because intersections with adjoining hardware may be easily stiffened with simple hoop rings, which take the discontinuity loads as pure tension.

The design concept and method of analysis have been substantiated by work performed on the main case. A discussion of the design evolution of the main case is presented in Section III of this document.

Studies conducted showed that a line-of-action flange at the case-injector interface would provide a minimum weight connection. The line-of-action flange reduces flange twisting by passing the shell load approximately through the centroid of the flange cross sectional area and therefore minimizes the seal point deflection. The line-of-action flange is used at the case-injector interface as shown in figure V-24. This flange concept has been demonstrated on the Phase B test program main case flanges.

Undercut flanges, shown in figure V-24, are used at the case-nozzle interface. The undercut flange is the minimum weight design for these applications because of relatively low pressure loads and large flange diameters.

3. Coolant Distribution

P&WA staged combustion testing during 1967 on the 250K chamber (Contract AF04(611)-10372) indicated that the main chamber configuration, shown in figure V-37, required improvement. These early chamber designs utilized the cavity between the chamber and outer case as a coolant manifold. This coolant manifold subjected the chamber liner to high external pressures and caused the chamber liner radial thickness to be sized for this buckling load.

The Phase B 250K test chamber and the SSME main chamber incorporate internal cooling passages which result in a chamber liner sized primarily by the heat exchanger and coolant distribution geometry. The weight savings on the 250K main chamber was 125 lb when the internal coolant distribution was incorporated onto the XLR129 engine design, currently being tested.

4. Impulse Comparison Testing

Impulse comparison testing is presently being conducted during Phase B comparing both regenerative and transpiration cooled chambers.

The 250K regeneratively cooled chamber is constructed of a one-piece copper alloy chamber liner, shown in figure V-38, with milled channels and an electroformed nickel closure. A copper alloy forging is cold worked to increase its tensile strength, after which the inner diameter surface is machined and 240 channels in the 250K chamber are milled into the outer diameter surface. A machining error in maintaining the correct wall thickness of 0.030 in. or a channel width of 0.050 to 0.080 in. could ruin the entire chamber liner. An outer nickel closure is electroformed over the copper liner, manifolds are attached by electron beam welding, and the assembly is heat treated before final machining of the flange surfaces.

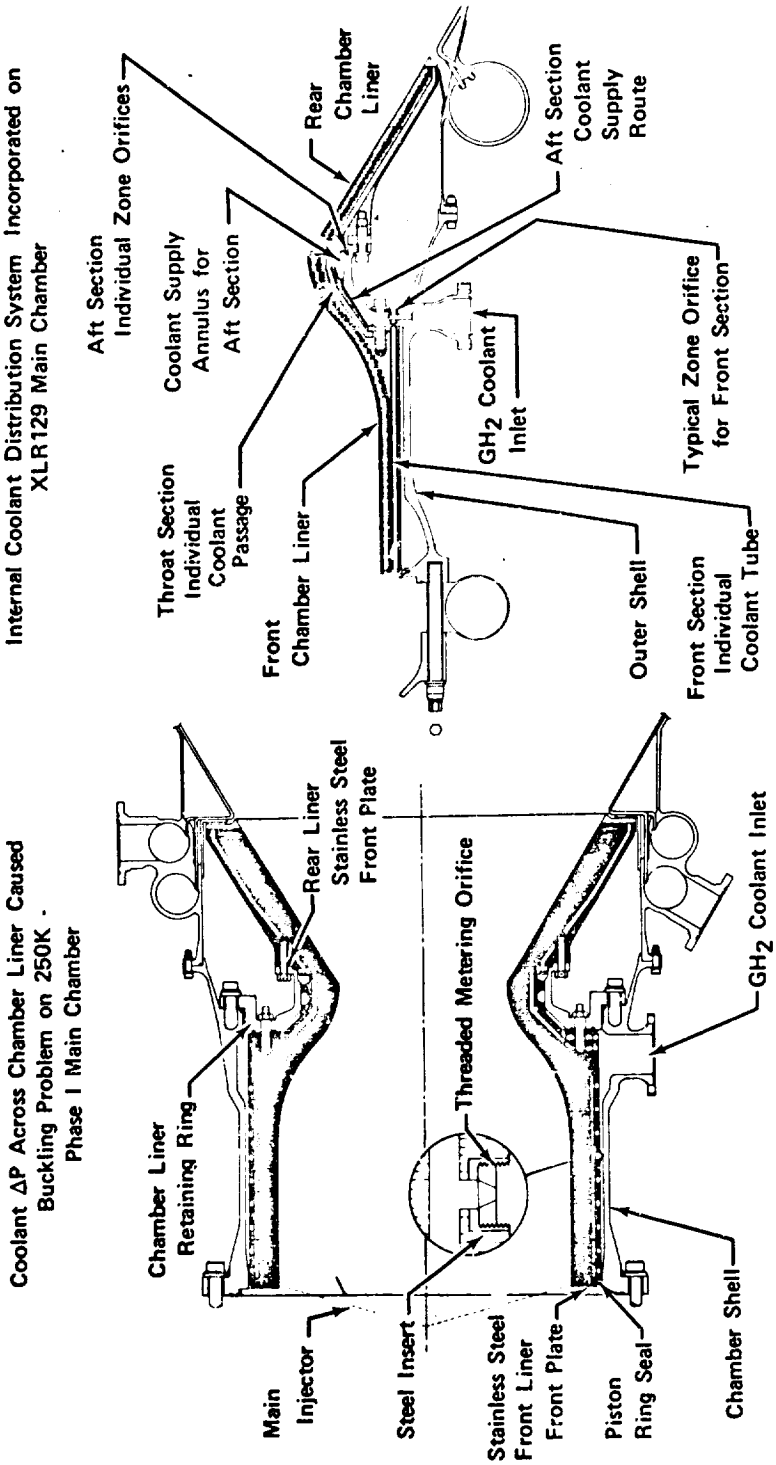

FD 46345

Figure V-37. 250K Cooled Chamber Coolant Distribution Configuration (Phase I and XLR129)

The 250K transpiration cooled chamber is fabricated from 1/4-inch thick copper wire mesh wafers and has a separable throat section as well as a divergent nozzle section. The forward chamber section is shown in figure V-39. Fabrication of the throat and divergent nozzle sections are presently being completed. Testing of this chamber will substantiate the SSME design cooling flows.

As a result of this testing a sound trade can be made of performance vs durability of the transpiration cooled chamber.

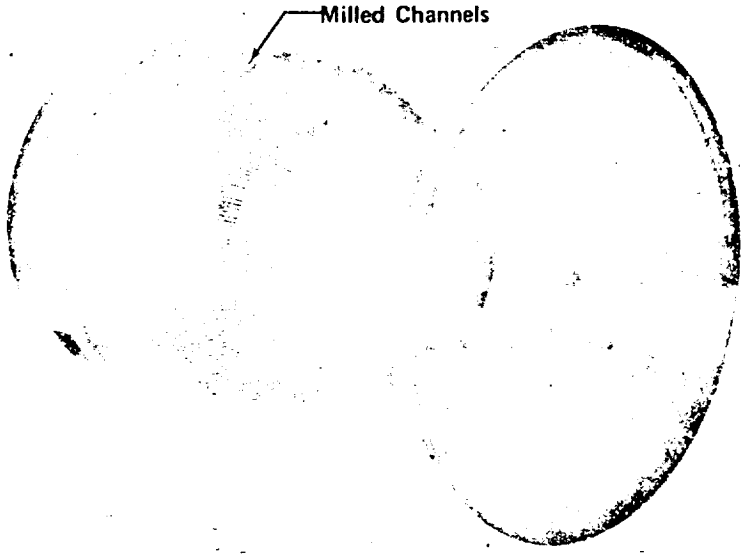

Figure V-38. Phase B-250K Regeneratively-Cooled Chamber FD 46330

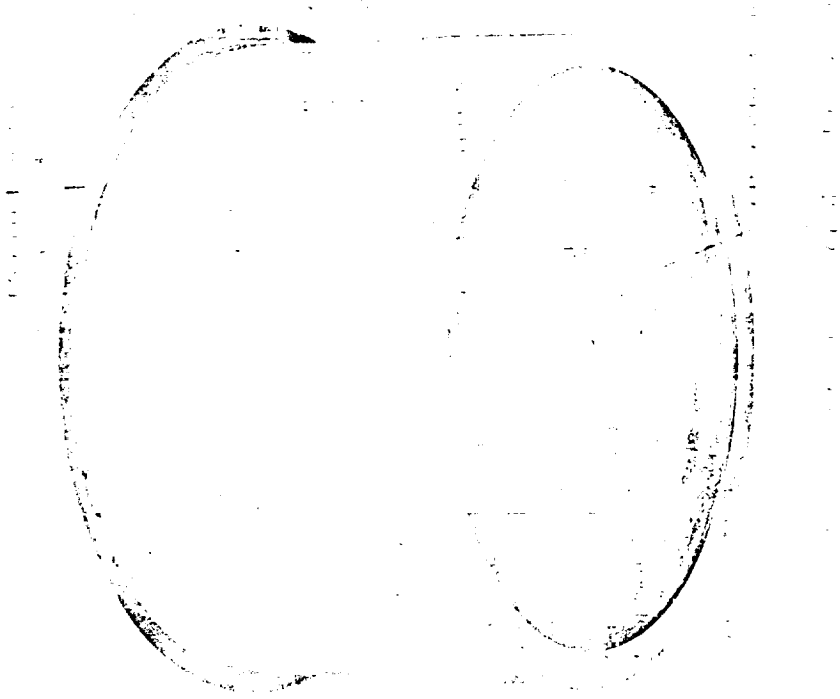

Figure IV-39. Phase B 250K Transpiration-Cooled Chamber Forward Section FE 106687

SECTION VI
TORCH IGNITERS

A. INTRODUCTION

Pratt & Whitney Aircraft has selected a common configuration continuous burning torch igniter for use in both the SSME preburner and main chamber. This significantly reduces development costs. The only mechanical design difference required for this physical commonality is sizing of the internal orifices.

The SSME torch igniter design is based on the result of continuous igniter development efforts since 1957 at P&WA's Florida Research and Development Center. Various ignition systems have been studied and tested, including hypergolic, pyrophoric, catalytic, and high energy capacitor spark igniters. The selected spark ignited, continuous burning oxygen-hydrogen torch igniter design evolved from these studies and a technology base utilizing experience and criteria obtained from torch igniters designed and tested for the successful RL10 and XLR129 engine programs.

The torch igniters are designed to provide system redundancy through use of dual spark igniters with separate exciters. The spark igniters ignite the torches, utilizing an oxidizer lead which provides a smooth and reliable ignition of the preburner and main chamber propellant gases.

The torch igniters have multiple altitude restart capabilities and the system does not require independent sources of propellant. Simplicity of operation is ensured by continuous burning of the torch igniter, eliminating the requirement for separate igniter valves.

Igniter flow rates are established by fixed area orifices. A tangential entry element is used to ensure that the oxidizer is completely atomized even during low fuel ΔP periods.

B. DESCRIPTION

As a result of the design effort to achieve commonality, one torch igniter configuration may be used for both the preburner or main chambers. Foolproofing installation of torch igniters is accomplished by pinning the main chamber igniter so it can be installed only in its respective flange. The only difference in the igniters is the internal orifices, which control the respective flow rates. The torch igniter consists of a cover, chamber, and a housing tube as shown in figure VI-1.

Figure VI-2 shows the location of the preburner and main chamber torch igniters. The discharge from the preburner torch igniter passes into the preburner duct at a distance of 2.750 in. from the preburner injector face. The discharge from the main chamber igniter passes into the main burner chamber at a distance of 2.300 in. from the main burner injector face.

The igniter for the preburner and main chamber is side-mounted which provides accessibility for inspection and service without major engine disassembly. Another attractive feature of side-mounted igniters is that upon removing an igniter assembly, internal inspection by a borescope of either the preburner or main chamber may be accomplished.

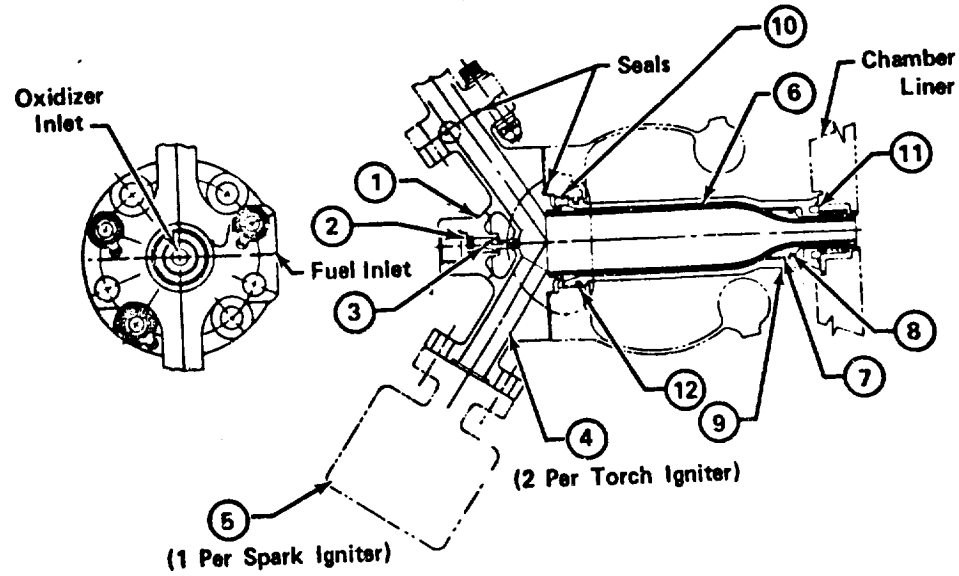

FD 46133

Figure VI-1. Common Torch Igniter for Preburner and Main Chamber

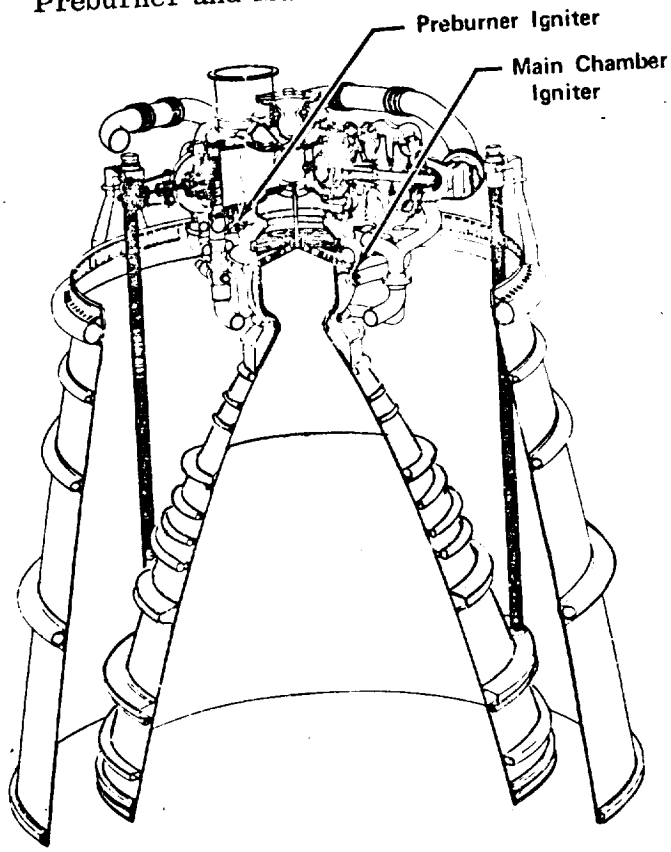

FD 52681

Figure VI-2. Igniter Location On the SSME

The igniter is shown in figure VI-1 with its salient features identified by numbers. The igniter cover, item 1 is the basic torch igniter structure with flanges for mounting the dual spark igniters and a braze attachment of the igniter chamber. The oxidizer orifice, item 2 and tangential entry oxidizer element, item 3 are presized and brazed into the cover. The igniter chamber, item 6 which is fabricated from oxygen-free copper (AMS 4602) is brazed into the bottom of the cover and a stainless steel (AMS 5646) piston ring holder, item 7 is brazed to the nozzle end of this chamber. The piston ring, item 8 bears circumferentially on the internal wall of the igniter housing tube to permit axial and transverse thermal growth of the igniter chamber. The housing tube, item 9 is fabricated from AMS 5735 and provides an annular passage for fuel coolant flow around the chamber. The igniter housing tube for the preburner and for the main chamber are threaded into their respective chambers. The housing tube has locking slots which mate with a locking ring in the igniter cover, item 10 to prevent loosening of the housing tube. At the threaded end of the housing tube, there is a cavity between the seal, item 11 and the threads. This cavity is pressurized by the coolant flow through a drilled passage in the housing. Pressurization of this cavity prevents back-leakage of hot combustion products into the cavity. A piston ring, item 12 at the igniter cover end of the housing tube, bears circumferentially against the flange, permitting unrestrained axial and transverse thermal growth of the housing tube. Figure VI-3 shows in more detail the torch igniter cover to chamber seal area and the sliding piston ring seal areas that accommodate differential thermal and pressure deflections of the torch igniter chamber and the preburner and main chamber.

- TORCH IGNITER CAN OPERATE SATISFACTORILY ON GAS OR LIQUID PROPELLANTS

The torch igniter system operates on propellants bled from the engine. The igniter can burn either gaseous or liquid propellants; this feature permits continuous operation without propellant valving. Torch igniter propellant and fuel coolant flowpaths are shown in figure VI-4.

- PREBURNER AND MAIN CHAMBER TORCH IGNITERS FED FROM COMMON PROPELLANT SOURCES

Previous design studies established XLR129 fuel and oxidizer igniter propellant tap-off locations. Cycle similarity led to retention of these for the SSME as subsequently verified by steady-state analysis, refer to PWA FR-4422, Torch Igniter Design Data. Fuel will be provided to each igniter from a tap-off location on the primary nozzle coolant supply line, just downstream of the fuel shutoff valve. Oxidizer will be provided to each torch igniter from a tap-off location in the preburner injector, just downstream of the preburner oxidizer shutoff valve.

Respective flow rates are controlled by presized orifices in each torch igniter. The fuel flow is split after it enters the fuel plenum of the torch igniter to provide torch combustion and cooling flow. Fuel is injected into the igniter chamber through an annulus former concentrically around the end of the tangential entry oxidizer element. This fuel then combines with the oxidizer and burns in the igniter chamber.

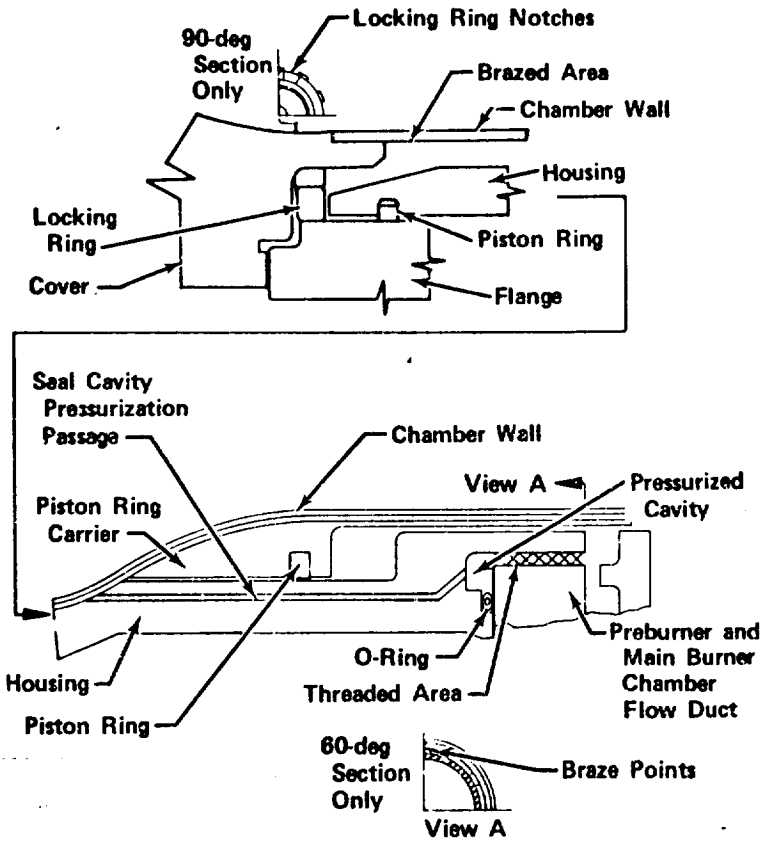

Figure VI-3. Preburner and Main Chamber Torch Igniter Assembly, Mounting and Sealing FD 46135A

- TANGENTIAL SLOT SWIRLER OXIDIZER ELEMENT ENSURES GOOD OXIDIZER ATOMIZATION AND HAS FLOW DISCHARGE COEFFICIENT SHIFT THAT TENDS TO CORRECT IGNITER MIXTURE RATIO FOR PHASE CHANGE

Oxidizer is injected into the igniter chamber through a tangential entry, self-atomizing element in series with an upstream orifice. This series orifice flowpaths provides nonadditive resistance during the startup phase when the oxygen is gaseous, and additive resistance in the liquid phase to control steady-state mixture ratios. In addition, testing show that the gaseous C_D of the tangential-entry element is 37% higher than the liquid flow C_D, further reducing the steady-state oxidizer flow rate. Refer to PWA FR-4422, Torch Igniter Design Data.

Tangential-entry elements provide finely atomized flow over a wide range of injection ΔP as shown in figure VI-5. The tangential entry of the flow into the element. As the flow exits the element, the velocity gradients within the vortex supply the forces required to atomize the liquid. The flow will be adequately atomized even during startup and shutdown transients, and the associated low injection ΔP conditions.

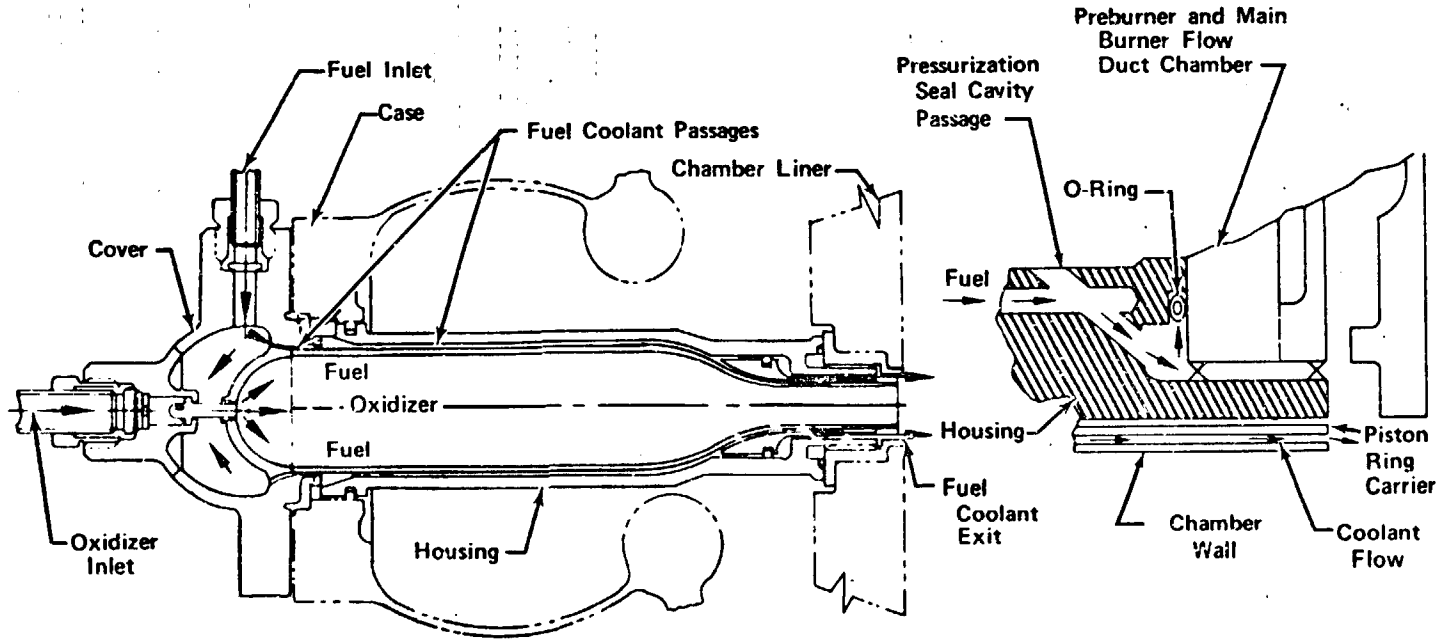

Figure VI-4. Preburner and Main Chamber Torch Igniter Propellant and Fuel Coolant Flow

FD 46136

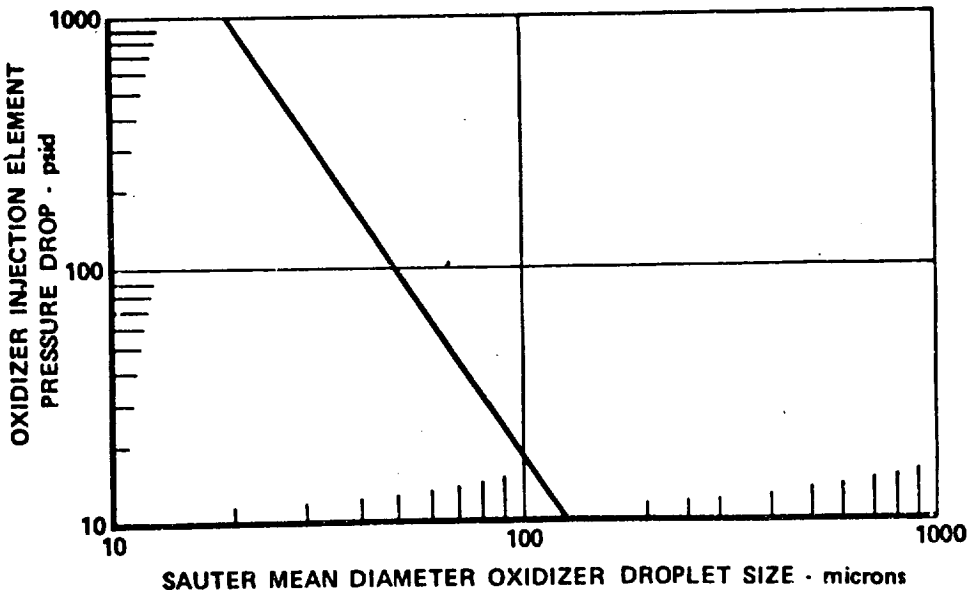

Figure VI-5. Oxidizer Droplet Size FD 52190

- FUEL COOLED IGNITER PROVIDED REQUIRED CHAMBER LIFE

The igniters fuel annulus has a radial gap of 0.014 for the preburner and 0.025 for the main chamber igniters. Fuel also flows through a series of controlled orifices around the periphery of the plenum into an igniter chamber coolant manifold. This manifold supplies coolant to a series of machined cooling passages and to control thermal gradients in the igniter chamber to cover braze area. After leaving these passages this flow cools the igniter chamber liner, thereby increasing the igniter chamber cycle life. A thorough stress and low cycle fatigue analysis was conducted on the chamber which revealed a predicted low cycle fatigue of approximately 7,000 cycles, well above the required 400 cycles (refer to PWA FR-4422, Torch Igniter Design Data).

The preburner and main chamber torch igniter steady-state operating characteristics and the conditions, just prior to and just after torch ignition are contained in PWA FR-4422, Torch Igniter Design Data.

C. REQUIREMENTS

The requirements of the applicable paragraphs of CEI Specification No. CP2291 have been met as follows:

1. All mechanical connect points shall be so configured by size and/or design to preclude inadvertent cross connections, as stated in paragraph 3.5.1.

   Compliance - The two connectors in the igniter cover are each of a different size.

2. Materials known to be susceptible to embrittlement when exposed to gaseous hydrogen shall not be used in a configuration/application that will result in failure due to hydrogen embrittlement, as stated in paragraph 3.7.1.2.

   Compliance - To avoid the possibility of hydrogen embrittlement, the cover is fabricated from AMS 5735. This material exhibits no degradation in a hydrogen environment.

3. Engine components shall be designed in accordance with special structural verification criteria and structural design criteria as specified by paragraphs 3.7.7.1.2 and 2.

   Compliance - The torch igniter is designed in accordance with FTDM 373, "Structural Design Criteria", which meets the requirements of the above paragraphs.

4. Structures and components shall be designed and tested to demonstrate a minimum low cycle fatigue life of 4 (on cycles), as stated in paragraph 3.7.7.1.3.

   Compliance - The igniter chamber liner is fabricated from oxygen-free copper (AMS 4602) because of its high conductive capability. To further increase the liner life, fuel is used as a coolant. A thorough stress and low cycle fatigue analysis was conducted on the liner and revealed a predicted low cycle fatigue of approximately 7000 cycles, which is well above the required 400 cycles.

5. The design shall permit ease of inspection and servicing with reasonable accessibility, as stated in paragraph 3.7.7.7.3.

   Compliance - The igniters are accessible for service. Inspections may be performed by a borescope through the spark plug tubes.

6. All orifice plates shall be designed to be noninterchangeable, as stated in paragraph 3.7.8.1.

   Compliance - All orifice plates are brazed into their respective igniters.

7. The allowable external leakage shall not exceed 1×10^{-4} sccs, as stated in paragraph 3.7.1.2.

   Compliance - Toroidal seals are used which exhibit less leakage than the allowable.

8. Flange designs shall feature no threaded or flared connection unless approved and minimum bolt circle diameter, nonlocking inserts, standard locknuts, etc., as stated by paragraph 3.7.13.1.

Compliance - All flanges are designed in accordance with FTDM 341, "High Pressure Flange Program", which meets the requirements of the above paragraph.

In addition to CEI Specification No. CP2291, the following ICD requirements shall be met:

Oxidizer and fuel tank pressure in the prestart and start conditions shall be 20 psia minimum, as stated in paragraphs 4.1.1 and 4.1.2.

Compliance - The igniter oxidizer and fuel orifices are sized to accommodate the conditions stated above.

In addition to CEI Specification No. CP2291 and the ICD, the following are Pratt & Whitney Aircraft imposed requirements:

1. The igniter design should utilize commonality where possible to reduce development costs.

   Compliance - This requirement has been achieved. One torch igniter can be commonly used in either the preburner or the main chamber, respective flow rates being controlled by orifices. Therefore, the only difference in the preburner and main chamber torch igniters will be their internal orifices.

2. The torch igniter shall be designed for continuous operation to eliminate the requirement for valving.

   Compliance - The igniter is designed structurally to withstand continuous operation. This has been accomplished by following designated structural design criteria. Also, the chamber liner is cooled with fuel to increase its cycle life.

3. The torch igniter shall be designed with the capability of sea level and altitude ignition.

   Compliance - Torch momentum and energy at sea level are sufficient for ignition. Lightoff propellant flow rates pressurize the chamber for altitude ignition. Oxygen lead ensures reliable ignition (refer to Trade Study PWA FR-4440, Liquid Oxygen Lead Versus Hydrogen Lead for Start).

4. The momentum of the torch igniter combustion products shall not damage the chamber (preburner or main chamber) wall opposite the torch or impinge on the wall adjacent to the torch.

   Compliance - Studies have indicated that chamber walls can withstand direct stoichiometric igniter torch impingement for over 30 seconds, as shown in figure VI-6. This is outside the range of the igniter steady-state mixture ratio and start transient duration. Studies further indicate that torch momentum is sufficient to keep the flame impingement from the

adjacent wall. Reduction of temperatures in this area is accomplished by fuel coolant flow past the nozzle end of the torch igniter and into the chamber.

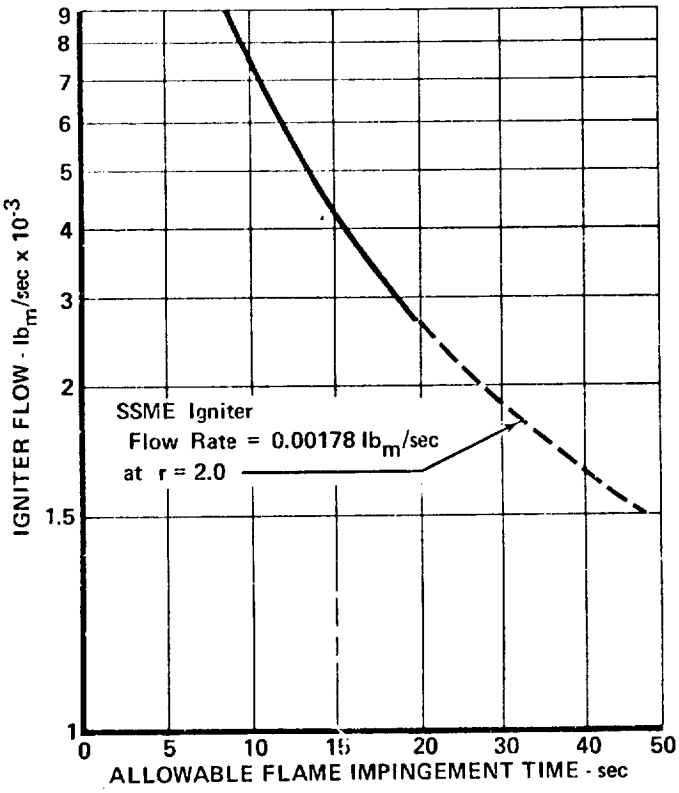

Figure VI-6. Igniter Flow Rate vs Allowable Flame Impingement Time for A Surface Temperature of 5700°R and Mixture Ratio = 8.0

FD 52280

D. DESIGN CAPABILITY

The sizing of the torch igniter chamber is a function of the propellant flowrate. The flowrate was increased so the chamber throat geometry could be increased for ease of manufacturing and cooling. This increase in propellant flowrate results in a torch energy release rate in excess of that required to ignite design starting flows. This excess energy therefore is achieved without penalty.

Due to design commonality, the main chamber igniter was sized to preburner conditions. Therefore, the main chamber igniter can operate at an increased combustor pressure at 42% without redesign.

The housing requires a drilled passage for fuel pressurization of the seal cavity. The wall thickness of the housing is increased to accommodate this passage, thereby enabling the housing capable of withstanding an 88% increase in operating pressure.

E. DESIGN SUBSTANTIATION

A study was performed to size the preburner and main chamber igniters to determine tap-off locations and steady-state operating conditions. Sizing the igniter included establishing the throat size, flow rate at ignition, and momentum of the torch products. The tap-off location determined whether separate valving was necessary and the steady-state conditions determined whether the igniter could be continuous burning. All of these items are interrelated.

To initiate a torch igniter design, it is necessary to determine the optimum tap-off location for the igniter propellants, considering conditions at ignition, during transients, and during steady-state operation. However, in the case of the SSME igniter, which was preceded by equivalent XLR129 igniter studies, it was unnecessary to repeat so comprehensive a tap-off location study (refer to PWA FR-4422, Torch Igniter Design Data).

- COMPREHENSIVE STUDY SHOWS SEPARATE IGNITER VALVES NOT REQUIRED FOR CONTINUOUS BURNING TORCH IGNITERS

Since the SSME and XLR129 cycles and flow schematics are very similar, it can be readily assumed that the optimum tap-off location for the igniters is in the primary nozzle coolant supply line immediately downstream of the fuel shutoff valve, and in the preburner injector immediately downstream of the preburner oxidizer valve. The selection of these tap-off locations for fuel and oxidizer ensures that no separate valves are required for the igniter and that the igniter/injector pressure drop and mixture ratio are acceptable (refer to PWA FR-4422, Torch Igniter Design Data).

- IGNITER THROAT SIZED TO CHOKE FOR ALTITUDE STARTS

The igniter throat size was established at 0.0952 $in.^2$, which was the same as that successfully tested during Phase I on the XLR129 torch igniter decreasing the throat size could not require increased propellant flow rates for pressurization of the igniter chamber for altitude ignition. The throat size could be decreased, but this would decrease the injector pressure drop and increase thermal stresses in the igniter throat wall.

- ENGINE STARTING IGNITER FLOWS STAY IN IGNITABLE REGION

During an altitude start, the unburned igniter propellant flow rate will cause choked flow at the igniter throat. The choked flow of the unburned propellants pressurizes the igniter chamber to values which can support combustion as shown in figure VI-7 and verified by RL10 altitude ignition test data. Previous experience with torch igniters shows that the igniter will initiate reliably at pressures below 1 psia with an oxygen lead. The design flows ensure a chamber pressure (2.25 psia) and mixture ratio (3.0) that are within the combustible region.

- TORCH IGNITER MUST PROVIDE SUFFICIENT ENERGY AND MOMENTUM FOR ENGINE IGNITION

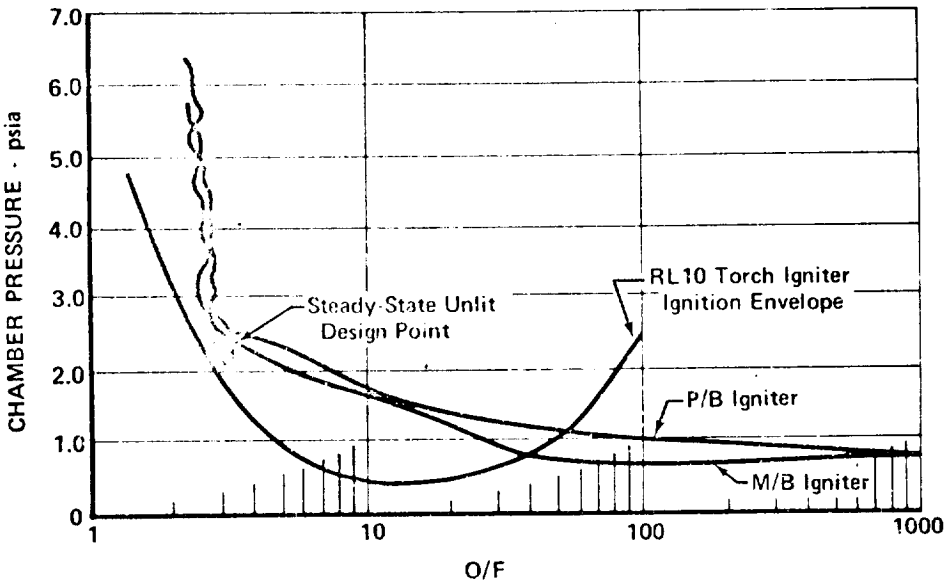

Figure VI-7. SSME Torch Igniter Lightoff Transient FD 52279

In addition to creating the necessary igniter chamber pressure, the propellant flow rate must be sufficient to release sufficient energy to ignite the preburner and main chamber at their respective starting flow rates. The SSME torch igniters are designed to have excess energy beyond that required to ignite the design starting flows. Therefore, starting flows can be increased without increasing the available torch energy. Figure VI-8 shows the igniter propellant flow at ignition versus the igniter pressure for a mixture ratio of 3.0.

Calculations show that the torch at altitude must supply energy at the rate of 1.59 BTU/sec at an igniter mixture ratio of 3.0, to ignite the propellants in the engine. The energy release rate of the torch propellant flow required for igniter chamber pressurization, for the present igniter configuration at altitude, exceeds this (1.59 BTU/sec) value by a factor of 30. Hence, since the ignition energy requirements at altitude are approximately 80 times higher than that required for sea level, the torch will supply sufficient energy at all flight conditions.

The burning igniter propellant momentum must be sufficient for the flame to extend sufficiently far across the preburner or main chamber cross section to interact with sufficient preburner or main chamber propellants to ignite the remaining propellants. The igniter flow momentum is also directly proportional to the burning igniter chamber pressure. Figure VI-9 shows the igniter flow momentum versus the igniter chamber pressure. The recommended minimum igniter propellant momentum is 1.5 ft-lb/sec^2 at sea level start. An igniter sized for an ignition pressure greater than 3.5 psia after ignition will ensure sufficient igniter momentum for an altitude start. The design flows result in a vacuum momentum of 21.4 lb_m-ft/sec^2 for the preburner igniter and 23.6 lb_m-ft/sec^2 for the main chamber igniter. As the back pressure to which the igniter is exhausting increases from zero in an altitude ignition to 14.7 psia for a sea level ignition, the igniter product momentum decreases to 8.3 lb_m-ft/sec^2 for the preburner igniter and 10.1 lb_m-ft/sec^2 for the main chamber igniter.

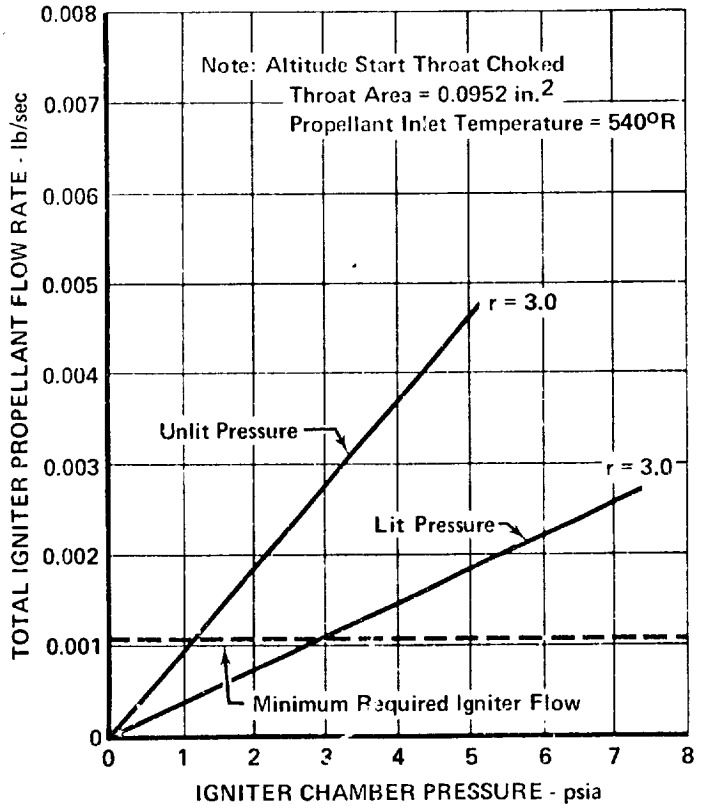

Figure VI-8. Igniter Chamber Pressures Created by Lit and Unit Propellant Flow Rates

The result of this study, verified by RL10 and XLR129 testing, shows that a torch igniter sized for altitude ignition at an igniter mixture ratio of 3.0 and an unlit igniter chamber pressure of 2.25 psia will satisfy the design requirements.

- SSME TORCH IGNITER DESIGN SUBSTANTIATED BY EXTENSIVE TESTING

The SSME torch igniter design has been substantiated by comprehensive testing of the RL10 and XLR129 igniters. The RL10 torch igniter which was a proposed configuration for the A3-3 engine, incorporated a wall-mounted spark plug which proved to be very durable and reliable throughout the RL10 torch igniter testing program. Altitude chamber tests of the RL10 torch igniter were conducted 714 times over wide ranges of flow and mixture ratio, for a total of 73,259 seconds. These data provided the ignition limits for design of the 250K igniter. The 250K torch igniter has been "Bench Tested" (firing of torch igniter only) 116 times for a total duration of 2670.5 seconds. This testing occurred over a range of mixture ratios from 0.5 to 3.0 and a temperature

range of 1300°R to 4600°R. Chamber tests (igniter firing chamber propellants at sea level) of the 250K igniter were initiated 209 times for a total duration of 2879 seconds. The RL10 torch igniter is shown in figures VI-10 and VI-11. The XLR129 torch igniter is shown in figure VI-12.

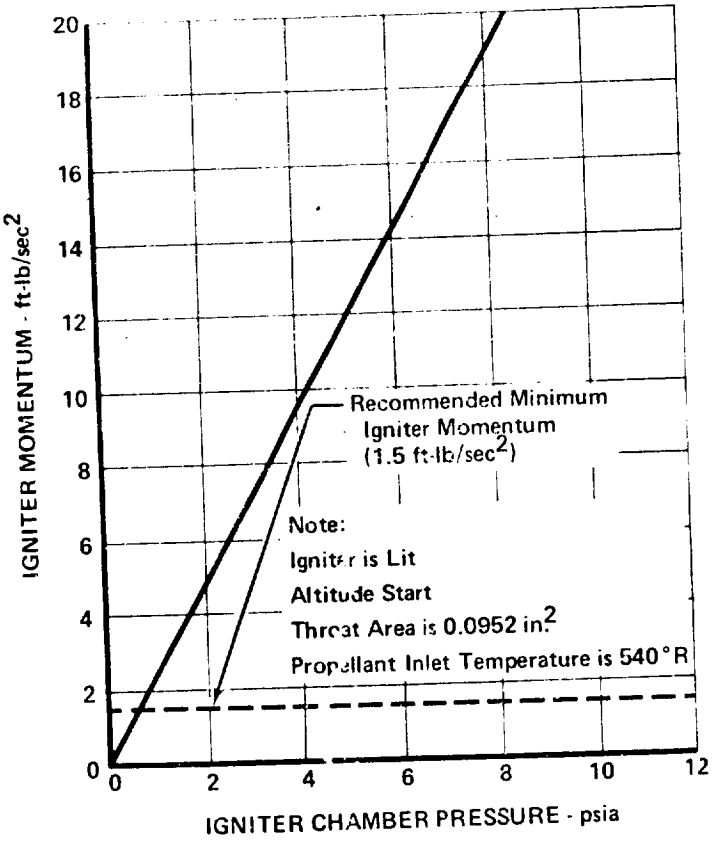

Figure VI-9. Igniter Propellant Momentum FD 52332

Figure VI-10. RL10 Torch Igniter FAE 51399

Figure VI-11. RL10 Injector and Torch Igniter FE 52233

Figure VI-12. XLR-129 Torch Igniter FE 97554

SECTION VII
NOZZLES

A. NOZZLE CONTOUR DESIGN

1. Introduction

The SSME nozzle contours were designed to provide the highest performance possible within the required envelope and cycle constraints. Geometric parameters that provide a general description of the SSME booster and orbiter nozzles are presented in figure VII-1. A tabulation of coordinates for the internal, physical (metal) contours of the supersonic portion of the nozzles is presented in table VII-1. These coordinates were used in the first iteration through the JANNAF methodology to define free stream edge conditions for the boundary layer analysis. Boundary layer displacement thickness distributions used during final nozzle design are presented in figures VII-2 and VII-3 for the booster and orbiter nozzles, respectively.

2. Description

The nozzle contour selections were made in the following manner. Preliminary nozzle selections were made using general performance and geometry maps generated by a P&WA method-of-characteristics bell nozzle design computer program (refer to "Digital Computer Programs for Rocket Nozzle Design and Analysis, Volume II, Bell Nozzle Design," Pratt & Whitney Aircraft Report, PWA FR-1021, prepared under Contract NAS9-2487 for the NASA Manned Spacecraft Center, 1964). A nozzle performance-geometry parametric study was conducted in combination with booster and orbiter cycle iterations to arrive at approximate nozzle designs which provided maximum specific impulse while meeting CEI specification geometry and thrust requirements. An important result of this study was the sizing of the throat area (A*) for both the booster and orbiter nozzle at 109.42 sq in. The parametric study yielded approximate nozzle designs and estimates of performance and permitted initiation of refined, final nozzle designs.

Throat flow conditions and the inviscid discharge coefficient for the desired combustion chamber geometry were calculated using the P&WA subsonic-transonic computer program described in "User's Manual for the Subsonic-Transonic Flow Deck (Deck IV)," Pratt & Whitney Aircraft Report, PWA FR-3465, Supplement II, prepared under Contract AF33(615)-3128, 1 October 1968. The discharge coefficient was calculated to be 0.9866 which compared favorably with a value of 0.982 obtained from empirical data in "Performance Characteristics of Compound A/Hydrazine Propellant Combination, Volume I - Technical Discussion," Rocketdyne Report TR-65-107, prepared under Contract AF04(611)-9573, May 1965. The close comparison of calculated and measured discharge coefficients substantiated the accuracy of throat flow conditions used for initiation of method-of-characteristics analyses in the final nozzle designs.

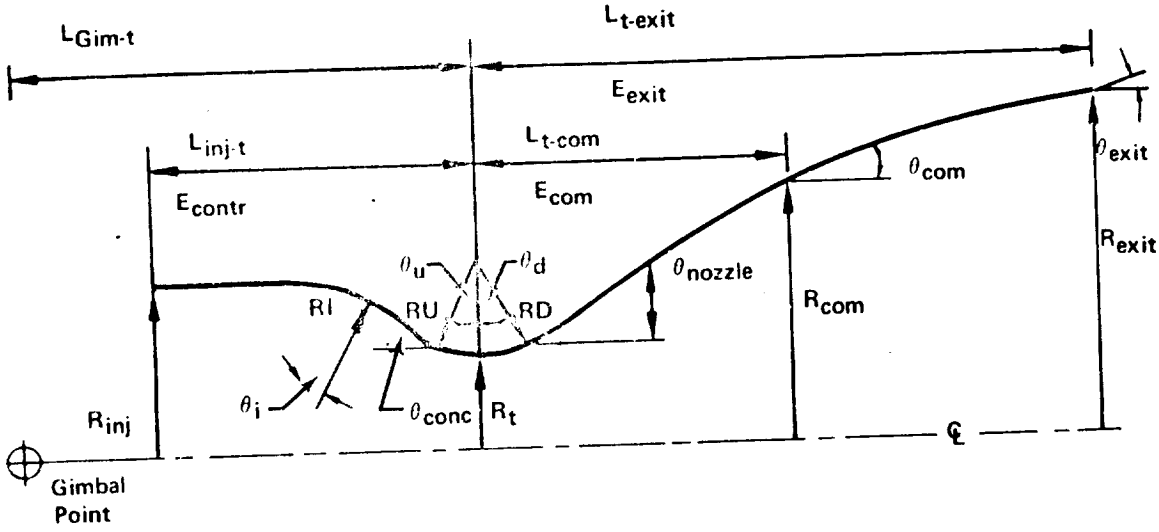

Booster

Radii, in.		Length, in.		Expansion Ratio, (-)		Angle, deg	
R_{inj}	= 10.240	L_{inj-t}	= 13.830	E_{contr}	= 3.011	θ_i	= 58.3
R_t	= 5.902	L_{t-com}	= 0.500	E_{com}	= 1.060	θ_{conc}	= 58.3
R_I	= 4.600	L_{t-exit}	= 100.050	E_{exit}	= 33.577	θ_u	= 58.3
R_U	= 4.540	L_{gim-t}	= 46.450			θ_d	= 27.3
R_D	= 0.661					θ_{nozzle}	= 27.3
R_{com}	= 6.077					θ_{com}	= 27.3
R_{exit}	= 34.198					θ_{exit}	= 5.9

Orbiter

Radii in.		Length, in.		Expansion Ratio, (-)		Angle, deg	
R_{inj}	= 10.240	L_{inj-t}	= 13.830	E_{contr}	= 3.011	θ_i	= 58.3
R_t	= 5.902	L_{t-com}	= 0.500	E_{com}	= 1.060	θ_{conc}	= 58.3
R_I	= 4.600	L_{t-exit}	= 221.050	E_{exit}	= 149.503	θ_u	= 58.3
R_U	= 4.540	L_{gim-t}	= 46.450			θ_d	= 27.3
R_D	= 0.661					θ_{nozzle}	= 27.3
R_{com}	= 6.077					θ_{com}	= 27.3
R_{exit}	= 72.160					θ_{exit}	= 6.9

Figure VII-1. Booster and Orbiter Nozzle Geometric Parameters FD 52428

Using approximate nozzle designs and wall temperature distributions estimated by heat transfer analyses, boundary layer growths throughout the combustion chamber and nozzles were determined using a modified version of the JANNAF Turbulent Boundary Layer Program. Boundary layer growth is relatively insensitive to minor variations in contour and Mach number distribution and this boundary layer analysis provided the displacement thickness distribution used in the final design. Displacement thickness was indicated to be slightly negative in the throat region, implying that the previously calculated non-viscous discharge coefficient should be increased. However, due to the probable increase in displacement thickness resulting from transpiration cooling flow, throat discharge coefficient was based on the data from "Performance Characteristics of Compound A/Hydrazine Propellant Combination, Volume I - Technical Discussion," Rocketdyne Report TR-65-107, prepared

under Contract AF04(611)-9573, May 1965 (CD = 0.982 for the SSME combustion chamber). This procedure for selecting discharge coefficient had been followed in the USAF 250K ADP Phase I program with satisfactory results. The displacement thickness distributions presented in figures VII-2 and VII-3 are based on a combination of the TBL calculated boundary layer and the design discharge coefficient of 0.982. Displacement thickness profile from the throat to the exit was faired to follow the general distribution shape calculated by TBL.

Table VII-1. Nozzle Contours

Orbiter Nozzle R_t = 5.902 in.		Booster Nozzle R_t = 5.902 in.	
X/R_t	R/R_t	X/R_t	R/R_t
0.0	1.0	0.0	1.0
0.25856	1.13532	0.30568	1.13627
0.58220	1.34975	0.57268	1.27836
1.01219	1.64898	1.07487	1.55711
1.52835	2.00725	1.46185	1.76982
2.28054	2.50903	1.88504	1.99464
3.14129	3.04813	2.34076	2.22632
4.31863	3.72291	2.82758	2.46134
7.16406	5.10701	3.61706	2.81412
10.93290	6.59493	4.48065	3.16088
13.26462	7.37202	5.41575	3.49836
16.13028	8.23044	7.49820	4.13298
23.69560	10.01243	9.85433	4.70257
30.93708	11.31005	12.47488	5.19648
37.45811	12.22713	15.34704	5.60986
		16.95256	5.79459

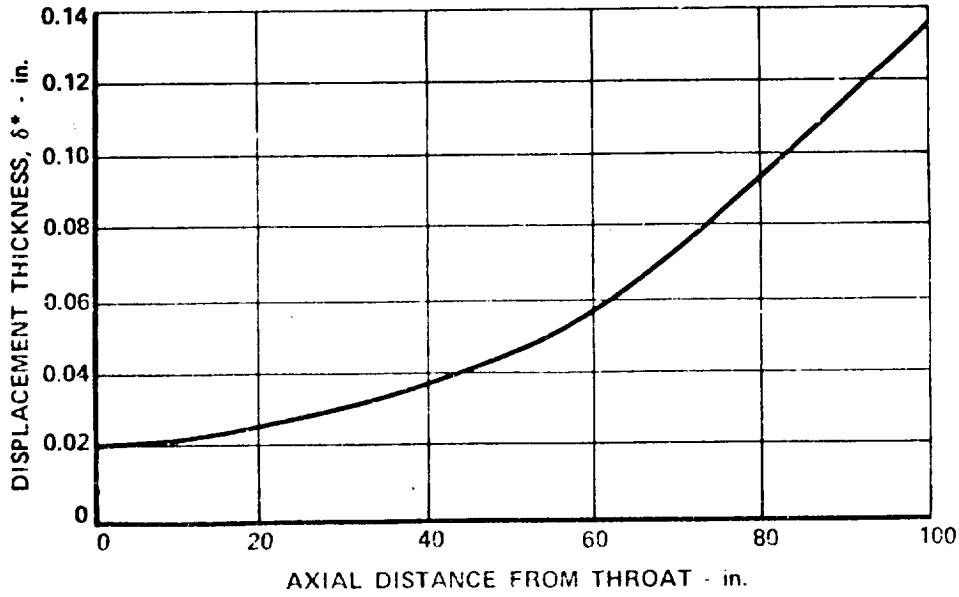

Figure VII-2. Booster Nozzle Boundary Layer Displacement Thickness FD 52682

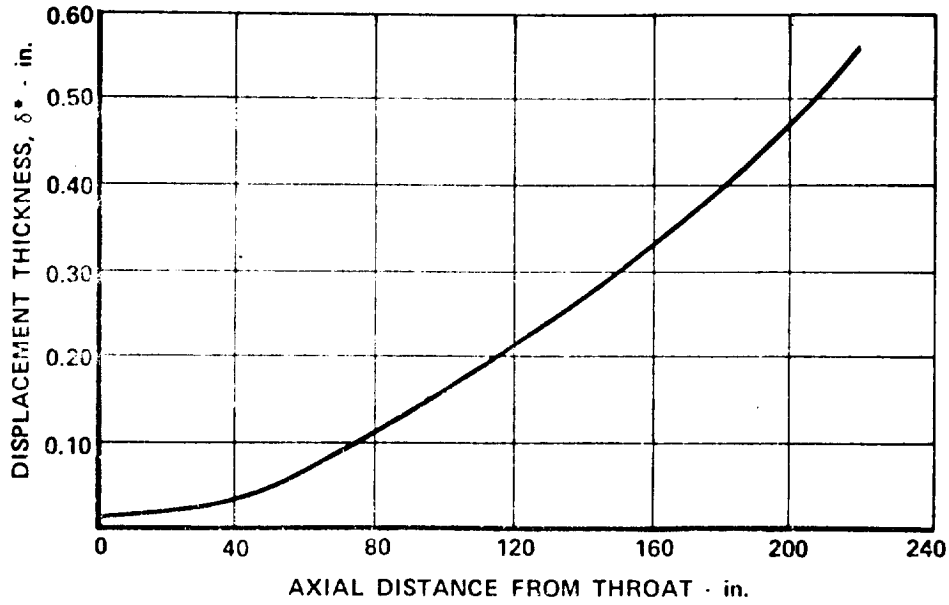

Figure VII-3. Orbiter Nozzle Boundary Layer Displacement Thickness FD 52683

Final aerodynamic designs were determined by use of the P&WA bell nozzle design computer program, assuming equilibrium flow, and accounting for variations between the booster and orbiter engines in injector mixture ratio, chamber pressure, and initial propellant enthalpies due to heat picked up during regenerative cooling by the hydrogen delivered to the injector. Start conditions for the method-of-characteristics solution were based on the subsonic-transonic analysis previously mentioned.

- STAGE MATCHED NOZZLE FROM THE THROAT INCREASES PERFORMANCE

The transpiration cooled combustion chamber liner extends downstream of the throat to an area ratio of 4.33. Prior to the nozzle contour being selected, a trade study was accomplished comparing performance of the orbiter engine with a common nozzle contour optimized for the booster used to the end of the transpiration cooled section with performance of the orbiter engine using an optimum contour nozzle from the throat. Specific impulse was approximately one sec higher with the uncompromised nozzle. Due to the extreme sensitivity of the space shuttle to specific impulse it was decided to break the nozzle very close to the throat and design the engines with optimum contours for both the booster and orbiter configurations.

The flexibility of the transpiration cooling technique permitted breaking of the contour at any desired location without undue design difficulties or weight penalties. Because the booster and orbiter powerheads are common, it was decided to provide a small circular arc (R_D = 0.661 in.) contour in both nozzle designs downstream of the throat. A break point 0.5 inches downstream of the throat was selected to preclude problems that might occur due to a contour mismatch if the break point was located at the throat. The circular arc region was included in the method-of-characteristics design analysis so that there would be no performance compromise due to the arc being included in the contour.

3. Requirements

The overall requirement of high performance was a primary consideration in the design of the nozzle contours. However, the nozzles also had to meet certain physical constraints.

The nozzle static lengths from the throat to the exit were set to meet the overall engine static length requirements specified in paragraph 3.3.1 of the CEI specification. Gimbal and powerhead lengths were established by the design requirements of these components and the remaining lengths available were used for the nozzles. Paragraph 3.3.1 also specifies maximum exit outside diameters. Wall thicknesses at the exit were established and the internal diameters were set to meet these requirements. In the case of the booster nozzle, a requirement also exists in accordance with table I of CEI specification CP2291 that the difference between sea level and vacuum thrust be 54K lb. This requirement set the booster nozzle inner diameter and it resulted in the outer diameter being less than the maximum allowed by paragraph 3.3.1.

A throat area (A*) requirement of 109.42 sq in. was used for the nozzles. This throat area was selected because it provides the thrust levels required per table I of CEI specification CP2291 with a chamber pressure of approximately 3000 psia.

4. Design Substantiation

The bell nozzle design computer program has been used in numerous aerodynamic nozzle designs, several of which have reached the hardware stage. The most notably successful were the RL10 and the USAF 250K high pressure ADP Phase I nozzles.

5. Design Capability

Because the break point for the common powerhead is located near the throat, the P&WA SSME has the capability of incorporating different nozzles with different area ratios and contours at some future time with a minimum of impact to the engine and with no compromise in nozzle performance.

Another feature of the P&WA nozzles, enhanced by the flexibility of transpiration cooling, is the ease of altering throat area, (either increasing or decreasing) with minimum of hardware modifications. Adjustment of engine throat area permits tailoring of the engine to meet future thrust or specific impulse growth requirements without drastic modifications to nozzle hardware or cycle adjustments. Preliminary analyses have indicated only minor chamber and nozzle performance losses for throat area increases up to 15%.

B. PRIMARY NOZZLE

1. Introduction

The primary nozzle designs are based upon demonstrated high pressure heat transfer and fabrication techniques.

Existing fluid flow and thermal design tools were updated and perfected by data developed during the XLR129, 250K Test Program. Tests were conducted using propellants, temperatures, pressures, and area ratios equivalent to the SSME design.

Fabrication methods are based upon procedures and techniques perfected during the fabrication of more than 300 RL10 engines and the high pressure 250K tubular regeneratively cooled nozzle. There has never been a flight failure of an RL10 engine.

Nozzle interchangeability and high efficiency are compatible with the transpiration cooled chamber.

Contours for both orbiter and booster regenerative nozzles are optimized because the transpiration cooled divergent nozzle cooling liner can be changed downstream of the throat.

2. Description

The one and one-half pass primary nozzle is designed to meet engine cycle requirements with lightweight tubular construction.

The primary function of the nozzle is to contain and direct the combustion gases and allow their shock-free expansion from an area ratio of 4.33 to area ratio of 78.38 (33.6:1 for the booster). A second function of the primary nozzle is to serve as a heat exchanger to condition the hydrogen for the transpiration cooled main chamber and case, and for supplying fuel to drive the low pressure turbopumps. A third structural requirement for the orbiter primary nozzle is to provide support for the extendible nozzle and its translating mechanism.

The primary nozzle configuration and flow schematic are shown in figures VII-4, VII-5 and VII-6, respectively.

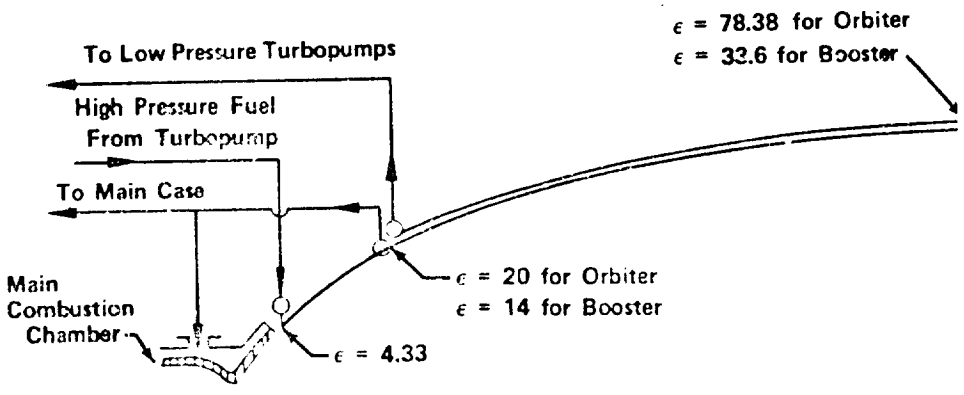

Figure VII-4. One and One-half Pass Regeneratively Cooled Nozzle Meets Engine Requirements FD 46215

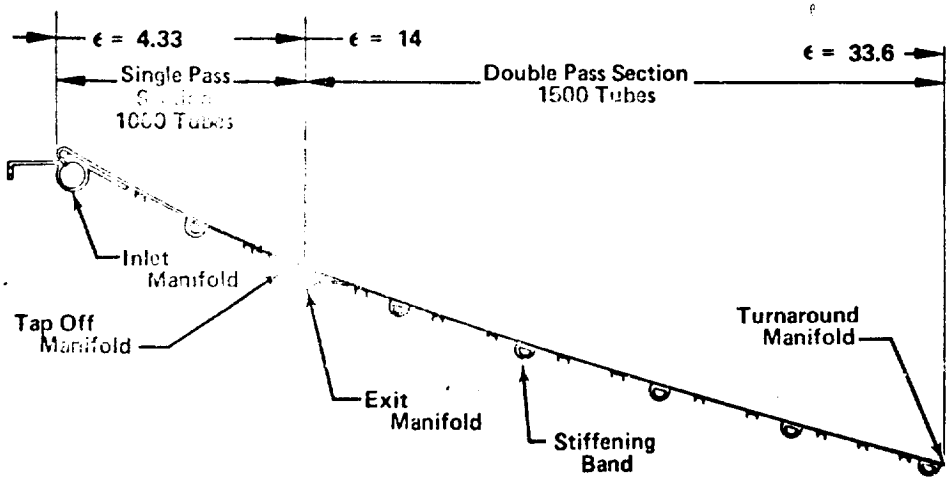

Figure VII-5. Booster Nozzle Configuration FD 46219

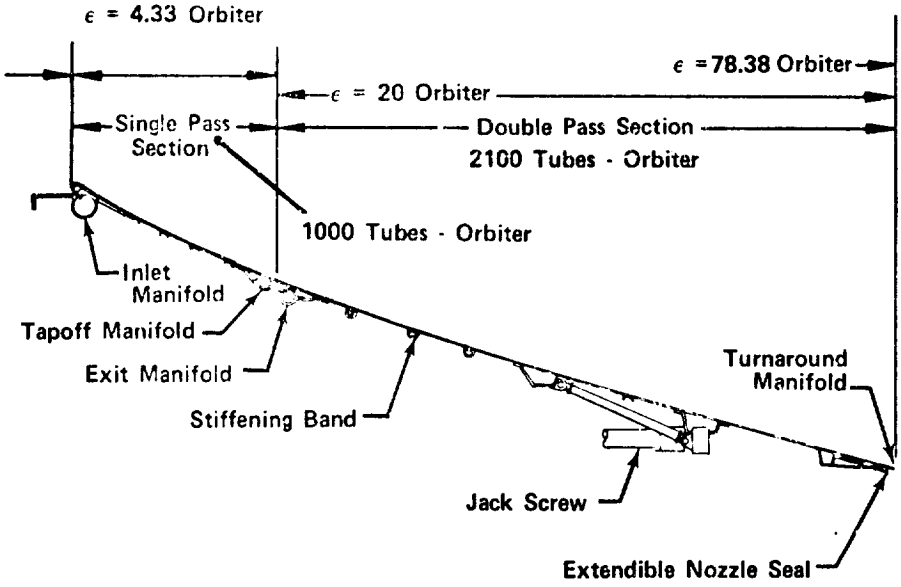

Figure VII-6. Orbiter Nozzle Configuration FD 46216

High pressure hydrogen from the main fuel pump is supplied to the nozzle heat exchanger at an area ratio of 4.33 and cools the nozzle to an area ratio of 20 for the orbiter nozzle and 14 for the booster nozzle. At this location approximately 25% of the total coolant flow is tapped off and used as coolant for the transpiration cooled liners of the main case and main combustion chamber. The remainder of the coolant continues to cool the nozzle to its exit at area ratio 78.38 and 33.6 for the orbiter and booster nozzle respectively. The turnaround manifold at the nozzle exit receives the coolant, reverses the direction of flow, and returns it to the exit manifold. After leaving the nozzle, the hydrogen is then used to drive the low pressure turbopumps.

a. Concept - PASS AND A HALF REDUCES COST AND WEIGHT

The single 1-1/2 pass heat exchanger design was selected over a previous design which consisted of a 1-1/2 pass heat exchanger for the low pressure turbopump supply, and a double pass heat exchanger for the transpiration supply. Studies made on the 415K engine showed a weight savings of 64 lb on the orbiter and 50 lb on the booster could be made by eliminating the double pass heat exchanger and extending the single 1-1/2 pass heat exchanger to the nozzle exit. This also resulted in lower fabrication costs by reducing the number of braze fixtures as well as reducing the total number of individual tubes from 4300 to 2400 for the orbiter nozzle and from 3500 to 2050 for the booster nozzle.

The regenerative nozzle tubes are shaped to form the nozzle contour prior to brazing. The tubular cross section at axial stations was determined by the cooling requirements at each location. Particular attention was paid to the cooling of the inlet region ($\epsilon = 4.33$) where tube low cycle fatigue life is the critical factor. Coolant pressure loss versus tube weight trade studies also were used to establish the internal geometry. Early studies showed that the total tube weight of the configuration which produced the lowest pressure drop of 250 psia would be 325 lb for the orbiter and 238 lb for the booster. By comparison, the heat exchanger design which uses a larger number of smaller diameter tubes would be 84 lb lighter for the orbiter and 52 lb for the booster, but the pressure loss would be increased to 370 psia, the minimum weight concept was selected for this design.

b. Manifolds - TAPERED MANIFOLDS REDUCE PRESSURE DROP AND WEIGHT

Any pressure drop in this heat exchanger represents a required increase in turbine inlet temperature, therefore, a number of provisions are incorporated to minimize pressure drop: (1) the inlet and exit manifold are tapered to maintain relatively constant velocity and avoid unwanted expansion and contraction flow losses, (2) the entrance and exit ports of the manifolds maintain a constant flow area to avoid flow pressure drops, (3) a minimum number of bends is used in the arrangement of the heat exchanger tubes and manifolds. The tapering of the manifolds not only decreases flow pressure losses, but also minimizes the weight of the manifolds. These manifolds are positioned in such a manner as to achieve the smallest possible mean torous.

The maximum stress point in the manifolds occurs where the entrance and exit ports are welded to the manifolds. This area has been strengthened to maintain the stresses below the 0.2% yield point for 1.2 proof pressure factor at the critical operating temperature. Flanges on the inlet and exit ports are of the cantilever design utilizing toroidal segment seals and meet the 0.002 in. maximum deflection criterion of the SSME Structural Design Criteria, PWA FR-4449.

c. Material - MATERIALS SELECTION PROVIDES HIGH STRENGTH AND LCF LIFE CAPABILITY

Inconel 625 was selected as the heat exchanger tube material. This selection is based on material section studies completed in the XLR129 250K program. To ensure brazing adjacent tubes, the sides of each are spanked

producing a minimum 0.030 in. flat braze contact area. The braze between tubes is inspected during fabrication to ensure that combustion products flowing in the nozzle do not leak to ambient or the backside of the tubes and the support jacket.

During fabrication, the tubes, bands, and manifolds are positioned in a special braze fixture. This entire assembly is then placed in a furnace for silver brazing. Braze repairs, if required, are made with a low temperature hand braze per AMS 2665.

Inconel 625 is used throughout the nozzle heat exchanger because it maintains thermal compatibility with the tubes, bands and manifolds during brazing and is the strongest of the nonhardenable nickel alloys. This material is easily welded, and it may be used after welding without any subsequent heat treatment. Visual inspection of the tube-to-manifold braze joints is possible because the manifold closure caps can be welded into place after the braze cycle.

d. Structural Support - COMBINATION OF JACKET AND BANDS PROVIDE NOZZLE STIFFENING

The extendible nozzle is attached to the orbiter primary nozzle through brackets, ballnut; jackscrews and then the bearing journal of the jackscrews. The 21,000 lb thrust of the extendible nozzle is added to the primary orbiter thrust load at a point 86 in. from the throat.

Figure VII-7 shows the accumulative thrust experienced by the primary nozzles caused by the axial pressure exerted on the nozzle walls, illustrated in figure VII-8.

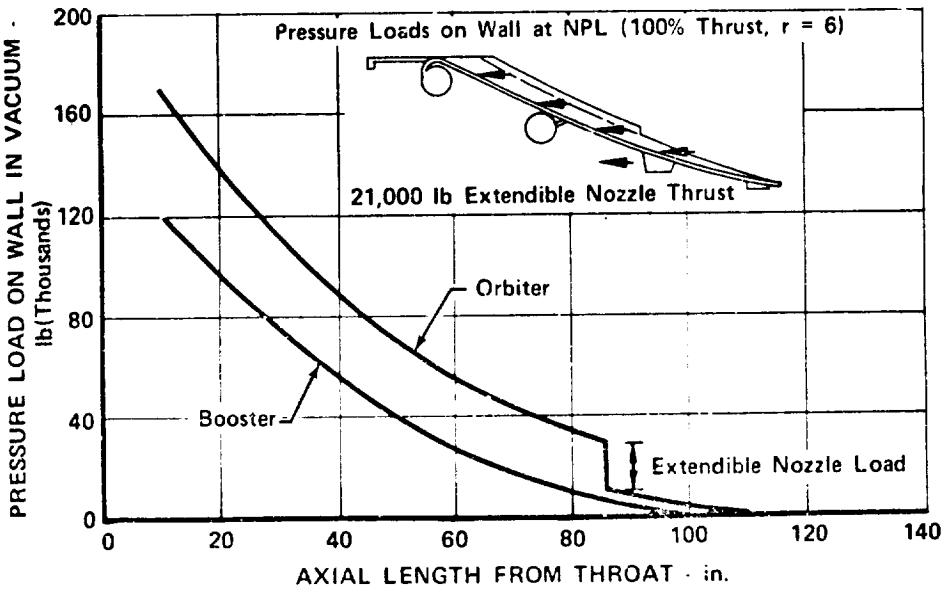

Figure VII-7. Primary Nozzle Also Transmits Extendible Nozzle Thrust FD 46217

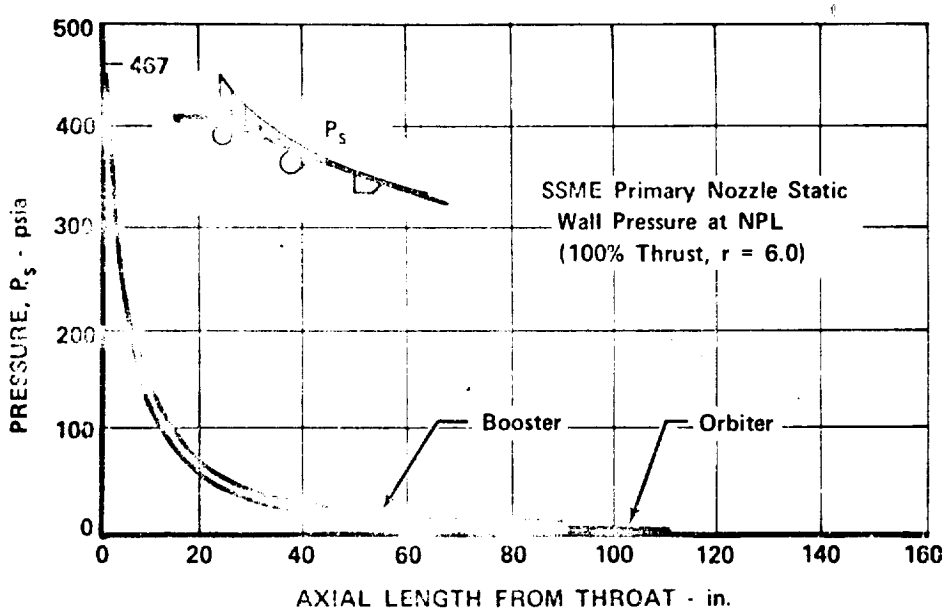

Figure VII-8. Nozzle Pressure Resulting from Shock Free Expansion FD 46218

The tubes, which form the nozzle contour, are treated analytically as though they possess no structural capability for supporting nozzle hoop loads. They are treated structurally as beams subjected to thermal stress due to the hot and cold wall temperature differential and bending stress due to the nozzle static wall pressure. In addition the logitudinal loads due to thrust, maneuver loads and gimbaling accelerations are considered, as shown in figure VII-9. Band locations are established by determining the "beam lengths" which limits tube stress to below the material yield strength at factors of safety of 1.1. A continuous jacket is used in the forward area of the booster/orbiter nozzles because the required band spacing becomes impractically close in this area. The band (or jacket) cross sectional area is sufficient to provide the required factors of safety on hoop stress at EPL nozzle pressure in vacuum. Band moment of inertia provides a 1.3 collapsing margin during nozzle overexpansion at sea level. A 1.3 natural frequency margin over known excitation sources is also provided. A computer program (Primary Nozzle Stiffening Program - 8065) has been developed which considers all loads, pressures, and temperature gradients. The output from the program gives the required band spacing, cross sectional area, and inertia.

The nozzle structure of large rocket engines must provide a strong and rigid structure where weight is at a premium. This task is further complicated by the fact that induced aerodynamic side loads are not readily predictable. The maximum loads seen by the nozzle are often developed during the start transients when conditions cause unsteady, unsymmetric flow separation. The structural design for the orbiter nozzle will withstand a 40,000 lb side load which is predicted to be adequate; however, if the induced side load should exceed this value during the development phase, it will be necessary to lengthen the sheetmetal jacket and modify the band spacing. Similarly, the booster nozzle was designed for 35,000 lb side load.

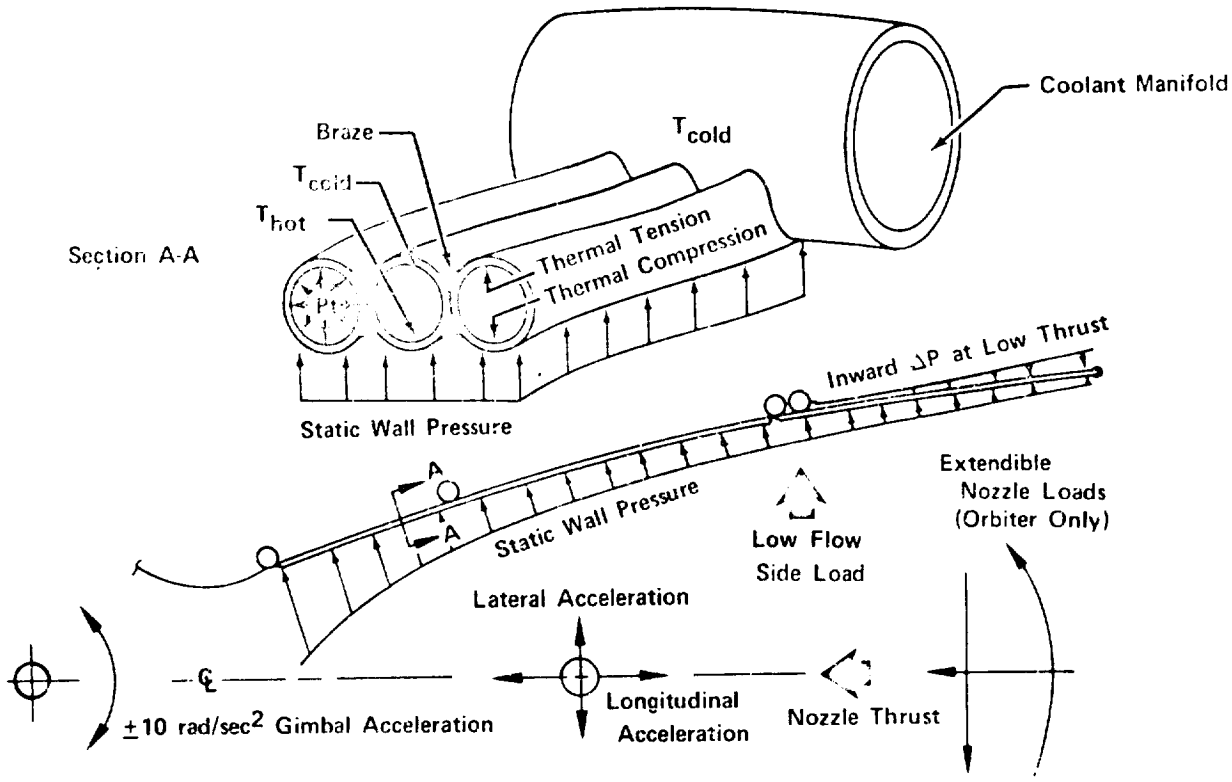

Figure VII-9. Nozzle Characterized by Complex Loading FD 52685

e. Thermal Protection - BANDS INSULATED TO WITHSTAND THERMAL ENVIRONMENT

During the boost phase of operation, the stiffening bands of the booster nozzle will see an environment of approximately 3000°R. The thermal protection selected for the booster nozzle bands consists of coating the 0.3 in. thick microquartz protected by a Hastelloy X facing sheet to limit the heat flux into the bands.

f. Interfaces - SEALS WITH PURGE BACKUP PREVENT RECIRCULATION

The forward end of the primary nozzle (figure VII-6) attaches to the rear flange of the main burner chamber with 120 MP35N 0.190 in. diameter bolts. This bolted flange is designed to withstand maximum seal, gimbal, maneuver, thrust, and internal pressure loads while fulfilling the maximum deflection criterion of 0.002 in. This flange is identical on both orbiter and booster nozzle to allow for interchangeability.

The clearance gap between the main burner liner and the forward end of the primary nozzle (area ratio 4.33) is kept minimal to prevent recirculation of combustion gas within this gap. Recirculation at this junction could cause an abrupt increase in tube wall temperature and thermal distress. Additionally an increase in tube wall temperature will occur if the combustion gases flow into the cavity behind the copper wafers. Therefore, a purge flow is supplied

to this cavity to prevent combustion gas "in flow." This purge flow protects the back wall of the copper liner and supplies film cooling for the heat exchanger tubes. A spring face seal between the heat exchanger and main burner copper liner is used to offer resistance and maintain a positive pressure in the cavity.

The spring face seal is a Belleville spring which is a conical sheet metal ring made of AMS 5537 (Haynes L-605). The seal is located between the aft end of the main combustion chamber and the forward end of the primary nozzle as shown in figure VII-10. The portion of the main chamber that bears against the seal is coated with a dry film lubricant in accordance with PWA 585-1H to prevent wear. The seal develops an initial seal load when compressed at assembly. If at any time, such as during engine abort, the pressure behind the copper chamber exceeds the nozzle pressure by more than 15 psi, the spring seal will deflect open and prevent buildup of high buckling pressure across the copper liner.

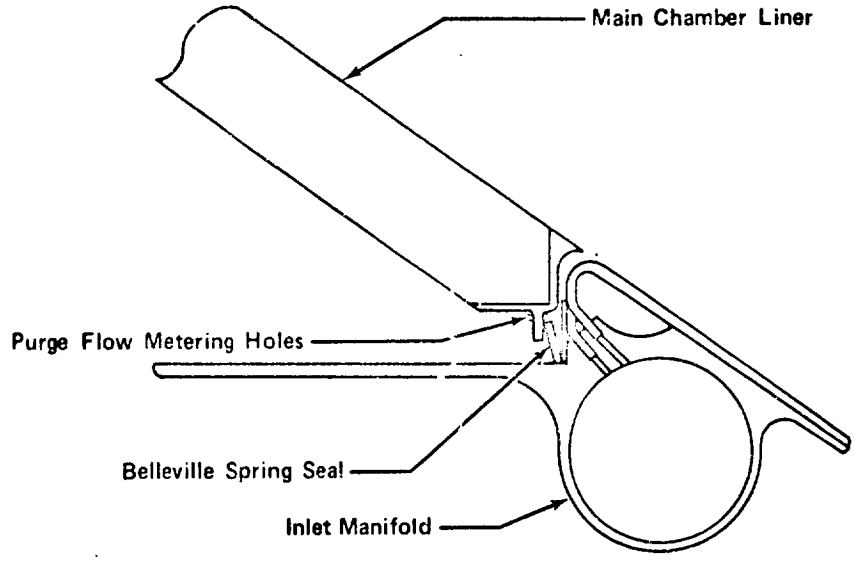

Figure VII-10. Primary Nozzle Seal Prevents Divergent Cavity Recirculation FD 52278

The function of the extendible nozzle seal is to contain the combustion gas at the primary nozzle/extendible nozzle interface. The seal is engaged by a ramp on the seal land when the extendible nozzle is translated into position. The seal is positioned such that it does not rub the extendible nozzle coolant passages during translation.

The seal consists of two-ply sheet metal ring with radial "keyhole" slots in each ply. The slots in each ply are positioned to seal the slots in the mating ply as shown in figure VII-11. Both plies are welded to a supporting ring for attachment to the primary nozzle. The assembly seals radially against a land on the extendible nozzle. The seal is cut radially in one place to simplify assembly and replacement, and the two plies overlap at this location to prevent a gross leak path. The seal assembly is riveted to the primary nozzle so that it can be readily replaced during overhaul.

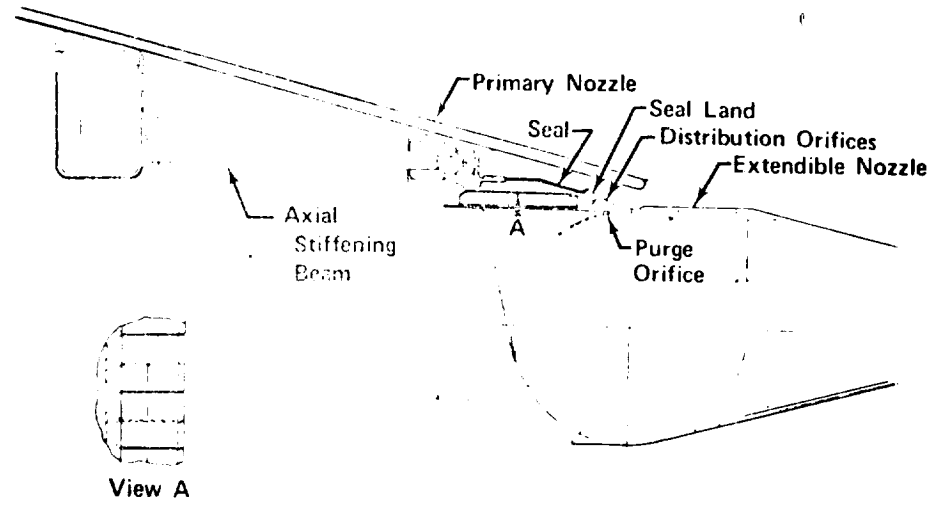

Figure VII-11. Spring Seal Prevents Extendible Nozzle Leakage FD 46221

The seal is designed to maintain engagement during radial deflection caused by tolerances, eccentricity, thermal expansion, and distortion of all related hardware. It is also loaded by internal pressure in such a way as to increase seal contact loading and reduce the maximum stress caused by radial deflection. Stresses under worst combined conditions are limited to ultimate strength/1.4 of the material.

A fuel purge coolant system is utilized to limit seal temperature to 1600°R. Hot leakage gas is diluted with 125°R fuel which is bled from orifice holes in the extendible nozzle distribution manifold at a location just downstream of the seal. The following list describes some of the seal parameters:

Material	Inconel 718
Thickness of one-ply	0.010 in.
No. of plies	2
Cantilever length	1.375 in.
No. of slots	240 (each ply)
Slot width	0.017 in.
Deflection capability	0.430 in. max
Pressure	5.11 psi max
Seal diameter	91.21 in.
Temperature of plies	1600°R max
Coolant flow	0.02 lb/sec approx.

Seals of this type have proven satisfactory through their use in turbojet engines. The J58 engine uses a similar seal in the afterburner section. A study of various seal concepts is presented in Combustion Devices Trade Studies, PWA FR-4440.

The turnaround manifold cross section at the exit of the primary nozzle has been kept as small as practical to minimize the step in the flowpath between the regenerative heat exchanger and the extendible nozzle. Like the other manifolds, the turnaround manifold meets the 1.2 proof pressure criterion.

In addition to the primary effort on the extendible nozzle seal design depicted in figure VII-11. Further effort will continue on an inflatable type seal made from Goodyear "Air Mat", a woven metal fabric coated with neoprene. (See figure VII-12.) The latter type seal offers several attractive features. It fills the void between primary and extendible nozzles and protects the extendible nozzle from hot gas impingement resulting from possible nozzle offset. Hot gases cannot recirculate to cause heating at the interface between the two nozzles. The seal tends to provide additional coolant if local leaks occur. It does not appear prone to damage, conforms easily to the mating surface, and is not dependent on combustion gas pressure to seal.

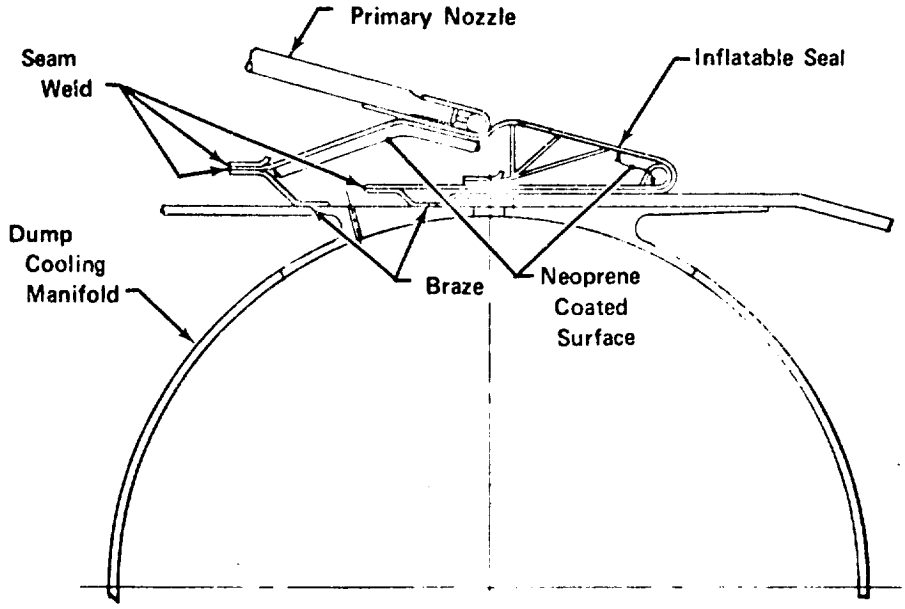

Figure VII-12. Transpiration Cooled Seal Has Added Features FD 46229

Certain drawbacks prevent incorporation of the inflatable seal as the primary design. More coolant is used than for the sheet metal seal, and the inflatable seal configuration does not lend itself to easy replacement. Perhaps more important than mechanical considerations are development and manufacturing problems. Special tooling is required for production of the inflatable seal which would result in dependence on a sole supplier. There is little previous experience available for such an application and hazards in cost, lead time, and development time have relegated the inflatable seal to a secondary but concurrent effort.

g. Extendible Nozzle Support - LIGHTWEIGHT LOAD DISTRIBUTION SYSTEM INCORPORATED

An important function of the primary nozzle is to provide support for the extendible nozzle. The rear thrust bearings for the jackscrew actuators are supported by a circumferential ring near the aft end of the nozzle as shown on figure VII-6.

The support ring has been sized to distribute the radial and tangential loads resulting from the extendible nozzle. The axial loads from the extendible nozzle are transferred to a stiffening ring located forward of the support ring. It is necessary to limit deflection of the jackscrew bearings supports. This system of rings and connecting rods proved to be the lightest method of providing support and limiting deflections. A circumferential ring at the aft end of the nozzle serves to stiffen the nozzle and provides an attachment surface for the extendible nozzle seal.

The available space at the nozzle exit limited the size of this ring. In order to obtain the stiffness required, the aft ring is connected to a second support stiffening ring by a system of axial shear webs. This system of axial webs and rings was sized to withstand the buckling loads that occur during sea level firing of the engine and to limit radial deflections of the extendible nozzle seal faces.

3. Requirements

The requirements of the applicable paragraphs of CEI Specification No. CP2291 have been met as follows:

1. The primary nozzle of both the orbiter and booster engines shall fit a common powerhead as stated in paragraph 1.26.

   Compliance - The forward flange on both nozzles is designed to fit the rear flange of the main chamber outer case. The main combustion chamber is also changed from the booster to orbiter configuration by interchanging the divergent section at a common flange on the chamber.

2. The orbiter engine shall be able to translate the extendible nozzle as stated in paragraph 1.2L.

   Compliance - The orbiter primary nozzle is designed to support the extendible nozzle and the translating mechanism by using a system of support rings and tie rods.

3. The orbiter engine shall be capable of being fired at sea level, including gimbaling with the extendible nozzle in the retracted position without the use of altitude test facilities or restrainer arms as stated in table I.

   Compliance - Stiffening bands are added to the nozzle to prevent buckling caused by the inward pressure differential of 12 psi. A buckling factor of 1.3 is used. A computer program is used to locate the bands and give the required areas and moments of inertia.

4. The engine shall be capable of starting at any altitude below 10,000 ft when fitted with the booster nozzle and at any altitude with the orbiter nozzle with the extendible nozzle retracted, in accordance with paragraph 3.2.1.

Compliance - The nozzle structure is designed to withstand buckling pressure from over-expansion of the exhaust gas and side loads due to unsymmetric flow separation.

5. When fitted with orbiter nozzle, the engine shall be capable of translating an extendible nozzle under the conditions stated in paragraph 3.2.10.1.

   Compliance - The orbiter primary nozzle is designed to support the translating mechanism and loads of the extendible nozzle. The support is accomplished by a system of support rings and tie rods meeting SSME Structural Design Criteria, PWA FR-4499.

6. Materials known to be susceptible to embrittlement when exposed to gaseous hydrogen shall not be used in accordance with paragraph 3.7.1.2.

   Compliance - Tests have shown that hydrogen does reduce the plastic strain capability of Inconel 625. The nozzle heat exchanger tubes are exposed to high pressure hydrogen but the tube wall temperatures on the coolant side are limited to 1100°R and strain rates are limited to 0.8%. These design limitations will give the required design life of 400 thermal cycles.

7. When fitted with the booster nozzle, the engine shall have a static length of 156 in. and exit diameter of 72 in. The engine with the orbiter nozzle shall have a retracted static length of 165.5 and diameter of 147 in. as required by paragraph 3.3.1.

   Compliance - The nozzles are designed using the envelope limits stated above. The orbiter primary nozzle exit diameter is determined by the exit area ratio of 77.0, which is the interface between the extendible and primary nozzle.

In addition to CEI Specification No. CP2291, the following are Pratt & Whitney imposed requirements:

1. Low pressure losses are desired for the heat exchanger since it provides power for the low pressure turbopumps.

   Compliance - A number of provisions are incorporated to reduce pressure drop: (1) the inlet and exit manifold are tapered to avoid unwanted expansion and contraction flow losses, (2) the ports into and out of the manifolds maintain a constant flow area to avoid flow pressure drops, and (3) a minimum number of bends is used in the arrangement of the heat exchanger tubes and manifolds.

2. The nozzle is fabricated using techniques developed during the RL10 and 250K programs.

   Compliance - Each of the 3100 tubes is identified by its flow characteristics and dimensions. The tube properties are indexed in a computerized library. Nozzle tubes are selected by the computer to optimize tolerance stackup and flow characteristics.

4. Capability

The primary nozzle provides for the aerodynamic expansion of the combustion gases. The contour is compatible with the engine cycle and accounts for the effects of sonic line distortion and boundary layer growth.

The regeneratively cooled booster and orbiter nozzles have been designed to meet but not exceed the yield and burst criteria and the 400 low cycle fatigue cycles required by CEI Specification CP2291. The low cycle fatigue life of the tubes could be increased 25% by an increase in coolant flow of 10%

The manifolds are designed to meet the yield and burst requirements of the CEI specification, 1.2 in yield and 1.5 in burst. The capacity of the manifolds can be increased by departing from present valves.

Both nozzles have bands to resist burst stress in certain areas and to resist buckling loads in other areas. The bands provide a safety margin on hoop stress of 1.1 in yield and 1.4 in ultimate. The margin on buckling is 1.3. The lowest natural frequency exceeds 10 cps.

The booster and orbiter nozzles have built in side load capacity due to other structural requirements. The nozzles can withstand the following side loads without permanent deformation:

Nozzle	Load
Booster	38,000 lb
Primary Orbiter	40,000 lb

A thermal low cycle fatigue program has been accomplished to optimize tubular, regeneratively cooled nozzle tube designs. Using a test rig, tube operating conditions are simulated by restraining one side of the tube as shown in figures VII-13 and VII-14. The side of the tube with the rigid bar is held at liquid nitrogen temperature (approximate temperature of cold-side of tube during operation) while the opposite side of the tube is being heated by an electrical induction heating element to a temperature approximating operation temperatures of the hot-side wall of the nozzle tube. The tube is pressurized to provide a predetermined stress level in the tubes. As the hot-side wall is heated, it tends to grow axially while it is being restrained by the opposite side of the tube, which grows shorter because of the liquid nitrogen temperature. The inside pressure is held constant as the heating element is cycled on and off. The cyclic frequency is selected so the hot-side wall temperature varies from liquid nitrogen temperatures to elevated temperatures that simulate engine operating wall temperatures. This causes hot-side plastic

deformation resulting in fatigue failure after repeated cycles. Low cycle fatigue tests were performed on various materials. Results all at equivalent hoop stress levels are shown in figure VII-15. Typical test results are shown in figure VII-16. Figure VII-17 is a typical temperature gradient predicted in the tubes near the coolant inlet manifold in the primary nozzle.

Figure VII-13. Induction Heated Tube FD 52696

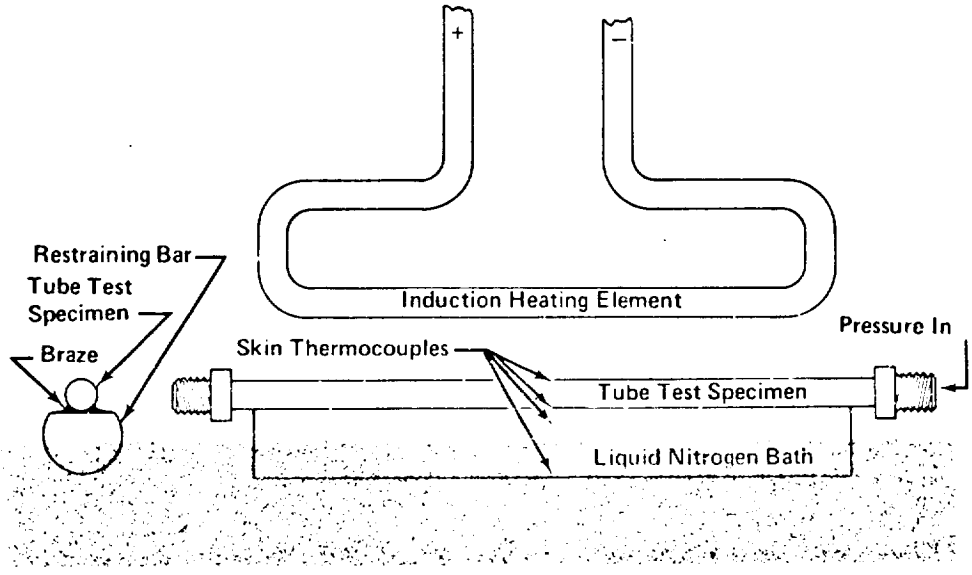

Figure VII-14. Schematic of Induction Heating FD 52687

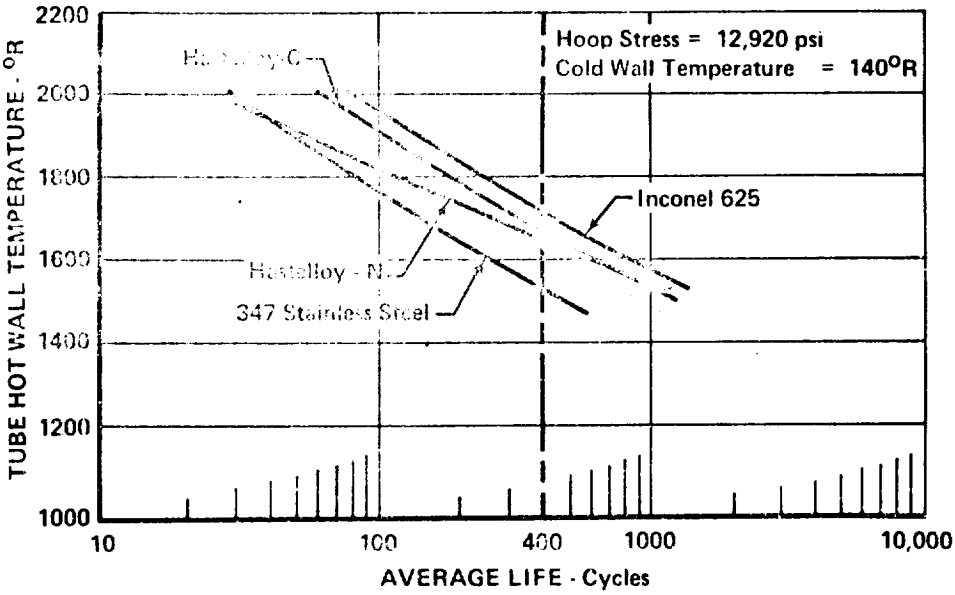

Figure VII-15. Thermal Low-Cycle Fatigue Life for Different Materials at Various Temperatures — FD 46225

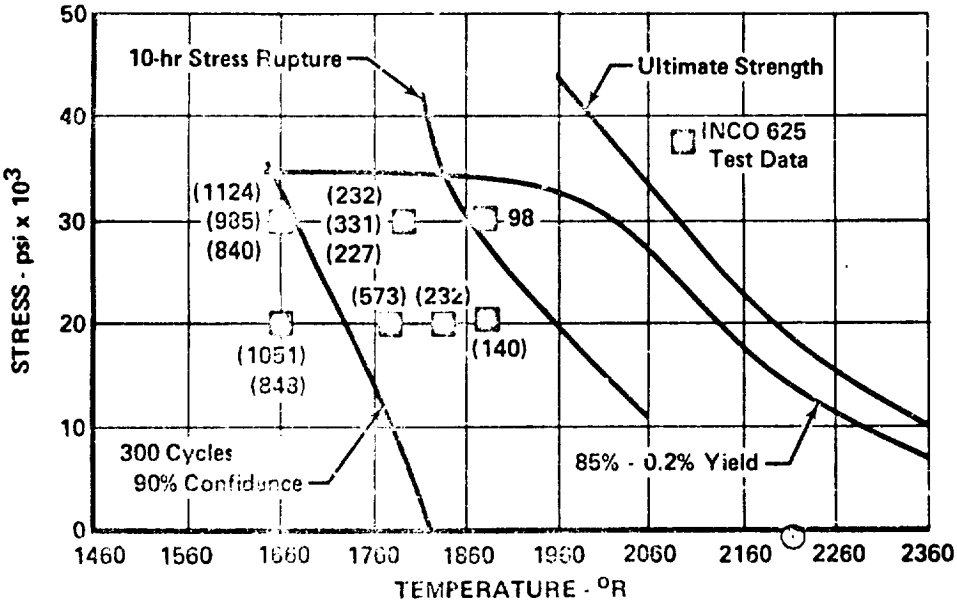

Figure VII-16. Low-Cycle Fatigue Test Results Predicted Thermal Gradient of Regenerative Tube Materials — FD 46227

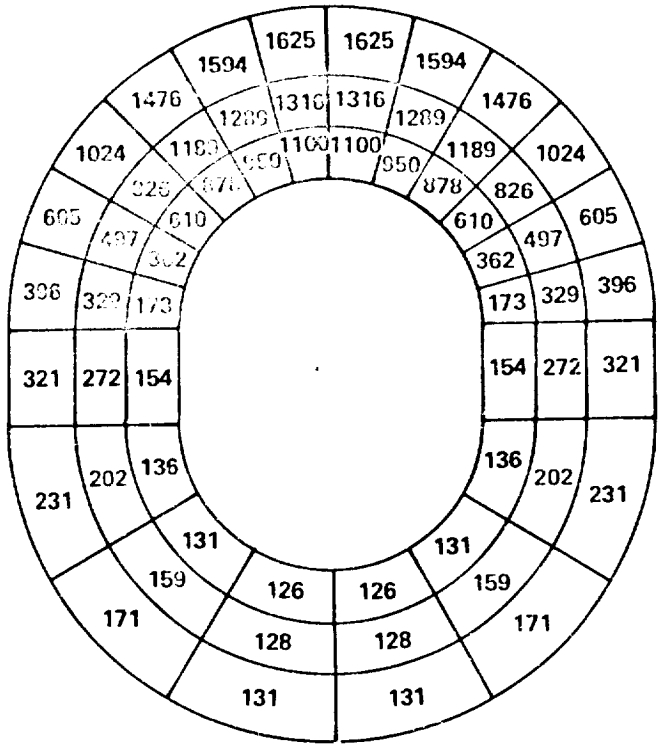

Figure VII-17. Nozzle Tube Nearest Throat (ϵ = 4.25) FD 46228

5. Design Substantiation

a. Background

During Phase I (Contract AF04(611)-11401), a two-pass regeneratively cooled nozzle was designed that extended from an area ratio of 4.75:1 to an area ratio of 20:1 and was fabricated of 668 AISI 347 tubes furnace-brazed together using pure silver brazing material. This nozzle had an AISI 347 continuous outer jacket that provided the required support for the primary nozzle loads and the loads imposed by the two-position nozzle and was fabricated in the same manner as described herein. The nozzle was tested in conjunction with the staged combustion tests performed during the Phase I program and recently during the 250K Phase B test program.

For the 250K Phase B tests, the primary nozzle is regeneratively cooled from an area ratio of 4.25:1 to 18.0:1. Thermal environments representative of those anticipated in the 550K SSME have been encountered during the last series of tests. During each of these tests, the heat picked up by the heat exchanger was within 20% of the predicted values.

b. Design Evolution

(1) Heat Exchanger Performance

The design of the pass and one-half regenerative heat exchanger is obtained by integrating heat transfer and fluid flow design techniques into an

analytical design approach. This is accomplished by:

1. Local heat balances across the tube wall
2. Summation of the coolant pressure loss
3. Summation of the coolant temperature rise.

The heat balance calculation through a tube cross section, as shown in figure VII-18, is determined by evaluating the combustion gas temperature, combustion side film coefficient, tube wall heat transfer, coolant film coefficient, and coolant temperature.

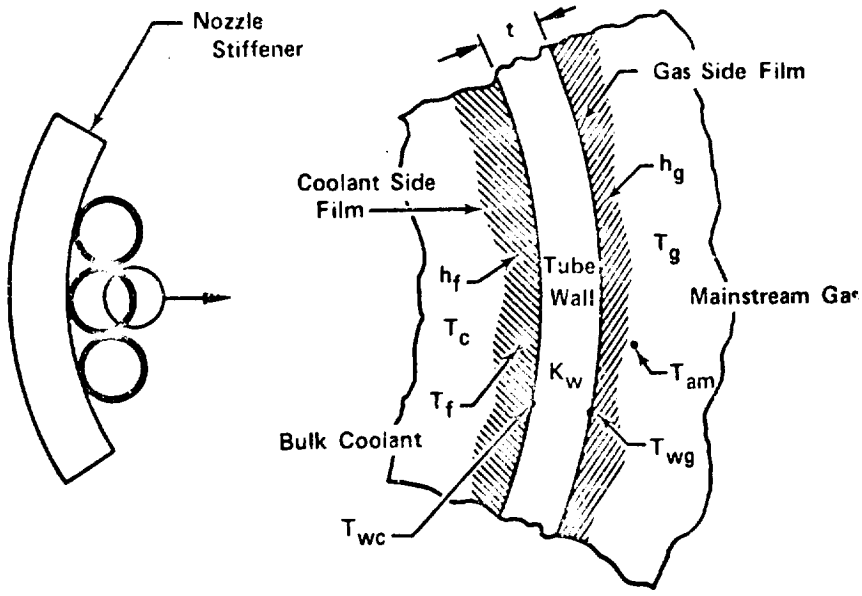

Figure VII-18. Heat Balance Calculation FD 46222

A representative plot of the combustion side film coefficient is shown in figure VII-19.

(2) Tube Wall Heat Transfer Calculation

The heat conducted through the tube wall is calculated using one-dimensional radial conduction assuming conductivity based on the average wall temperature:

$$R_w = \frac{ro}{k} \ln \frac{ro}{ri}$$

where:

R_w = wall resistance

r_o = tube outer radius

r_i = tube inner radius

k = wall thermal conductivity based on $T_{w_{ave}}$

$$T_{w_{ave}} = \frac{T_{wg} + T_{wc}}{2}$$

where:

T_{wc} = cold-side wall temperature

T_{wg} = hot-side wall temperature

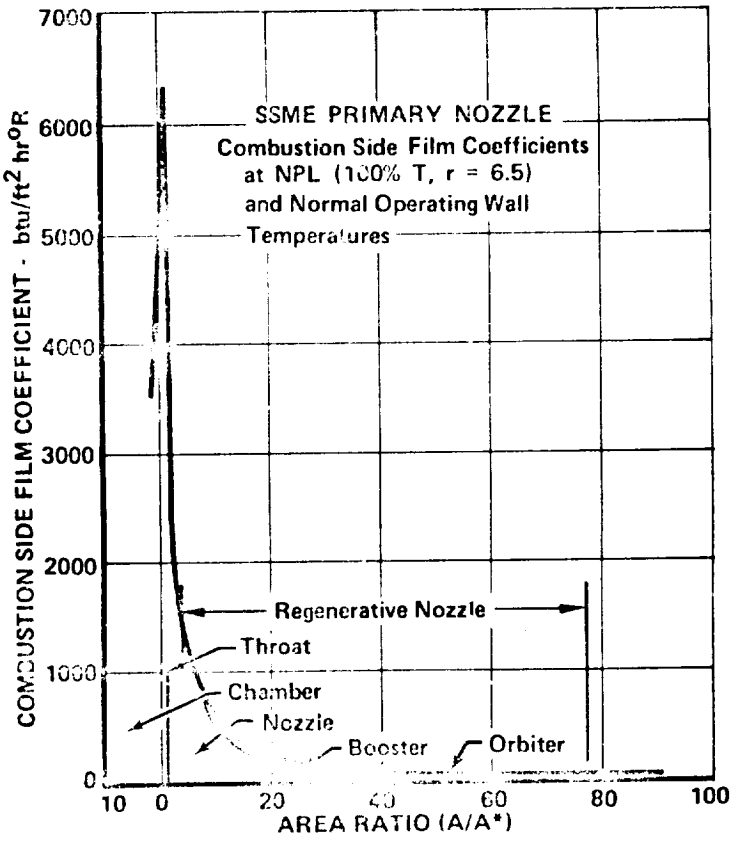

Figure VII-19. Combustion Side Film Coefficients for Orbiter Primary Nozzle FD 46223

(3) Coolant Film Coefficient

In calculating the heat conducted into the coolant, the coolant-side film coefficient is established using a Dittus Boelter film-temperature correlation.

(4) Combustion Gas and Film Coefficient

The combustion side gas temperature and film coefficient is evaluated using the Mayer integral boundary layer solution with an enthalpy driving potential, modified to reflect the results of the 250K staged combustion tests.

(5) Coolant Temperature

Using the preceeding analytical methods, a heat balance across the tube wall at each section is made to establish the hot and cold side wall temperature.

(6) Summation of Coolant Pressure Loss and Temperature Rise

The heat exchanger coolant pressure drop consists of losses associated with the following components:

1. Inlet manifold
2. Tubes
3. Turnaround manifold
4. Exit manifold

All of the components exhibit pressure losses involving the following mechanisms:

1. Momentum (area change) and heat addition
2. Friction
3. Turning

The regenerative nozzle is designed to a specific wall temperature to obtain 400 thermal cycles in its lower area ratio region, and it is designed to a specific stress margin in the higher area ratio region where the wall temperature is low. A high strength material is desirable to ensure light weight at the high area ratio end. A material to provide high thermal cyclic life is required for the low area ratio end. The maximum stress predicted for the nozzle at the higher area ratio is approximately 49,000 psi.

Several materials that provide the required stress margin have been considered as shown in figure VII-20. The tube material was selected by comparing the calculated stresses with the allowable stresses of candidate materials. The stress relative to the yield strength and thermal cycle life of the material is the governing criterion.

Subsequent design studies revealed that high pressure hydrogen could affect the low cycle fatigue life of Inconel 625, therefore, six additional tests were performed using hydrogen as the pressurizing gas instead of helium. A definite decrease in life was noted when hydrogen at 5000 psi was used as the pressurizing gas. The allowable strain rates for a 400 cycle life in an atmosphere free of hydrogen is approximately 1.36%. The effects of high

pressure hydrogen were found to reduce the allowable strain rates to 0.8%. The strain rates of the nozzle tubes are therefore limited to 0.8% in order to meet the engine low cycle fatigue requirements.

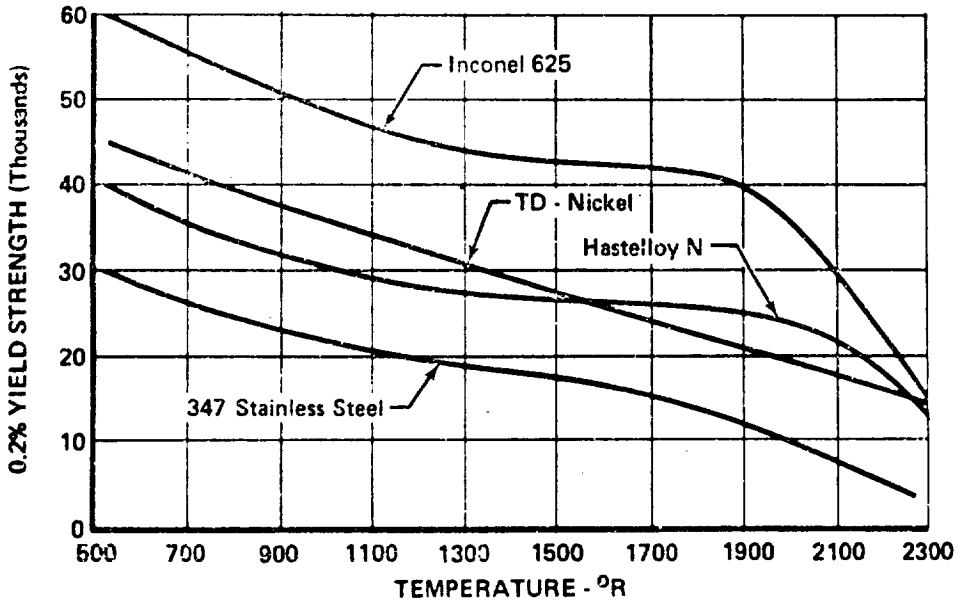

Figure VII-20. Material Yield Strength Comparison. FD 46226

SECTION VIII
EXTENDIBLE NOZZLE

A. INTRODUCTION

P&WA has selected a low pressure convectively cooled extendible nozzle with corrugated sheet construction for the SSME design. It is simple, lightweight, and less expensive to fabricate than regenerative or radiation cooled nozzles. It uses proven materials and manufacturing processes.

The assembled nozzle skirt and stiffening bands weigh about 1 lb/ft^2 as compared to 1.7 lb/ft^2 for a tubular nozzle and 1.9 lb/ft^2 for a radiation cooled nozzle.

P&WA first demonstrated the operating characteristics of an extendible nozzle with corporate funds during January 1967. In August 1967, a corrugated, convectively cooled skirt extension on an RL10A-3-3 thrust chamber was fabricated and successfully tested.

B. DESCRIPTION

The SSME extendible nozzle on the orbiter engine provides 15 sec increased specific impulse at altitudes above 165,000 ft and 27,000 lb extra thrust at NPL by allowing additional shock free expansion from an area ratio of 77.0 to 146.8. At altitudes below 150,000 ft, the nozzle is retracted providing a compact engine package in the orbiter vehicle.

The nozzle is fabricated from Inconel 625 and consists of a circumferential coolant distribution manifold, a smooth outer skin with circumferential stiffening bands and a corrugated inner skin. (See figure VIII-1.) The inner skin is resistance seam welded between corrugations to the inside surface of the outer skin, figures VIII-2 and VIII-3. The space between the inner and outer skins form longitudinal coolant passages. The nozzle is convectively (dump) cooled with low pressure, cryogenic hydrogen taken from the high pressure turbopump discharge and is orificed down to 186 psi before entering the coolant distribution manifold. The coolant manifold is 4.25 in. in diameter and has a 0.028-in. thick wall. It is brazed to the cylindrical portion of the nozzle skin at the forward end. Hydrogen at 116.8°R enters from the supply line and is distributed circumferentially about the nozzle through radial feed holes in the base of the manifold. There is one feed hole for each of the 1152 coolant passages. The mating holes in the outer skin are slightly larger than those in the manifold base to allow for misalignment at assembly.

During sea level and low altitude operation, the nozzle is retracted and coolant flow is not required. When the nozzle is extended and the orbiter engine is ignited, hydrogen coolant flows through the corrugated passages, is heated to 1620°R by the engine exhaust, and is ejected through small orifices at the exit producing 2662 lb additional thrust. These orifices are obtained by partially closing the end of each passage by means of a spherical dimple in the outer skin.

Material	Inconel 625
Outer Sheet	Smooth
Outer Sheet Thickness	0.014 Average
Inner Sheet	Corrugated
Inner Sheet Thickness	0.008 in.
Number of Corrugations	1152
Inlet Dia	104.52 in.
Envelope Dia	147.00 in.
Length	111.50 in.
Weight	596 lb

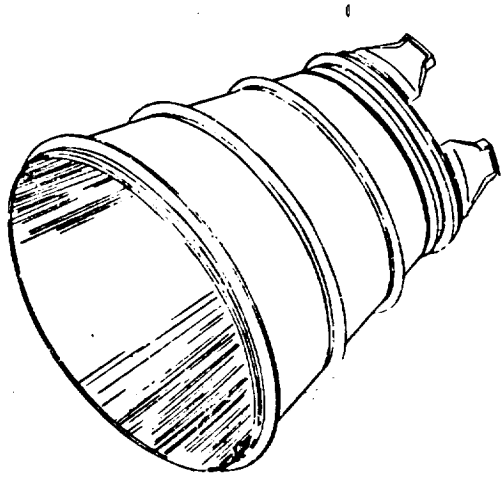

Figure VIII-1. Extendible Nozzle Design Features Corrugated Construction and Dump Cooling FD 46163

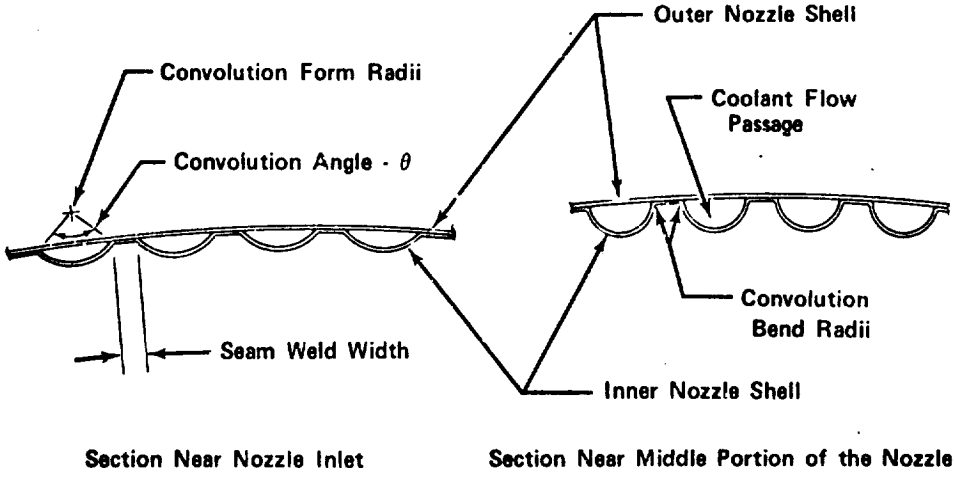

Figure VIII-2. Corrugated Nozzle Shell Configuration is the Key to Simple Lightweight Nozzle FD 46164

Three nozzle attachment brackets fabricated from Inconel 625 and 718 attach the extendible nozzle and coolant manifold assembly to the translation mechanism. Each bracket has the form of a truncated pyramid with its base curved to fair tangentially into the coolant distribution manifold. The top of the bracket is truncated and is faired into a rectangular flange that mates to one provided on the translation mechanism.

- DUMP COOLING PROVIDES A SIMPLE LIGHTWEIGHT DESIGN

Dump cooling the extendible nozzle was selected over regenerative cooling by carrying parallel SSME designs through system and structural analyses to determine weight, cost, performance, and reliability trades.

These trades are presented in Combustion Devices Trade Studies, PWA FR-4440. For the purpose of this trade study, coolant was obtained from the fuel high pressure turbopump discharge as in the baseline design. Coolant for the double pass regeneratively cooled nozzle was obtained from the primary nozzle fuel low pressure turbopump supply hex.

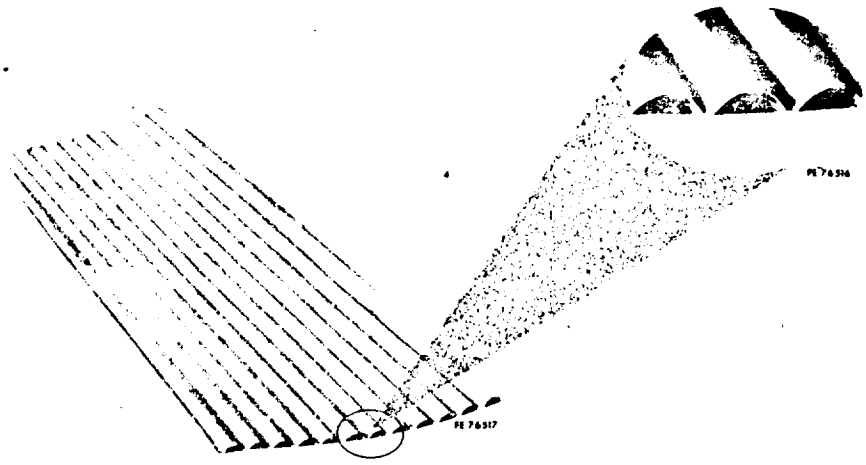

Figure VIII-3. Proved Fabrication Capability Demonstrated by Corrugation Sample Panel FD 52423

The trade study indicates that a full regeneratively cooled extendible nozzle is an attractive alternate for improving specific impulse. It compensates for extra weight by added payload if vehicle trades remain as they now exist. Unfortunately, the regeneratively cooled extendible nozzle increased engine weight by approximately 288 lb, engine cost by $140,000 and degrades system reliability because of required hot flex joints.

Dump cooling was also shown to be nearly 50% lighter and use 50% less coolant flow than a film/radiation cooled extendible nozzle. The nozzle was assumed to be film/radiation cooled at four stations along the nozzle wall using hydrogen from the fuel high pressure turbopump discharge. To maintain the same coolant flow rate as an equivalent dump cooled nozzle, it was determined that the wall temperature would have to reach 3160° F. Few materials can withstand this steady state temperature. Those that can are heavy, have a low stiffness to weight ratio, are difficult to fabricate, and may require an intensive development program.

By increasing the film/coolant flow rate, it is possible to lower the hot wall temperature to approximately 2600° F where Columbium may be substituted as the nozzle material. The coolant flow rate required to accomplish this is approximately 7.9 lb/sec.

The radiation cooled extendible nozzle skirt using Columbium was also found to weigh approximately 1.9 lb/ft^2. This assumes that the Columbium could be reliably coated to protect it from oxidation and that the hydrogen rich exhaust gases would not seriously degrade the Columbium. Both assumptions are high risk and not compatible with SSME philosophy.

- A CORRUGATED SHEET EXTENDIBLE NOZZLE IS SUPERIOR TO ONE CONSTRUCTED FROM TUBES

During engine operation the extendible nozzle receives little heat load compared to the primary nozzle. As such, a tubular heat exchanger similar to that found in the regenerative primary nozzle is not necessary.

Design studies showed that a dump-cooled extendible nozzle using a corrugated sheet is 100 lb lighter than one constructed from more costly, tapered tubes. The results also indicate: (1) the use of flat sheet stock allows for lower cost resistance welded fabrication method as compared to a tubular brazed method; (2) the corrugated sheet nozzle possesses greater axial stiffness because of greater coolant passage height; (3) the corrugated-sheet nozzle is lighter because of welded construction and eliminates needless double-wall thicknesses between tubes used in conventional nozzles; (4) the smooth outer surface of the nozzle facilitates stiffener attachment; (5) the area of the coolant flowpath, formed between inner and outer sheets, can be varied to match desired cooling flow velocity variations down the nozzle; and (6) hoop stress due to internal pressure is resisted by the cooled outer skin, whereas in tubular construction the hoop stress must be resisted by the braze between the tubes.

- INCONEL 625 IS SUITED TO THE EXTENDIBLE NOZZLE

Inconel 625 was chosen for the SSME extendible nozzle because of its good low-cycle fatigue properties at elevated temperatures, it high ductility at cryogenic temperatures (approximately 50% elongation at -320° F), good yield strength at maximum operating temperature (28,000 psi at 1450° F), and does not require heat treatment after bending or forming.

All available material candidates were studied for use in the extendible nozzle, comparing physical properties, mechanical properties, and ease of fabrication. The material selected required high strength at elevated temperatures and good ductility at both room temperature and elevated temperatures for easy forming and for high thermal cycle fatigue strength. Table VIII-1 provides a comparison between material candidates. Inconel 625 (AMS 5599) proved to be the most suitable for this application. Table VIII-2 lists its "A" value material properties.

- NOZZLE CORRUGATION PASSAGES DESIGNED FOR MINIMUM WEIGHT WHILE MAINTAINING DESIRED WALL TEMPERATURE

To optimize the performance of an engine using a lightweight dump-cooled extendible nozzle, it is necessary to design the heat exchanger to minimize the passage weight while maintaining the nozzle wall temperatures at levels required to ensure structural integrity through efficient coolant utilization. The design of the dump-cooled nozzle heat exchanger is optimized by integration of the heat transfer and fluid design techniques into an analytical design approach. This is accomplished by: local heat balances across the passage walls, summation of the coolant pressure losses, and summation of the coolant temperature rise.

Table VIII-1. Material Properties and Fabrication Considerations Favor Inconel 625

	Elongation, % Room Temperature	2000°R	0.2% Yield Strength at 2000°R (psi)	Weldability
Inconel 625 (AMS 5599)	50	*105	40,000	Good
Hastelloy X (AMS 5536)	37	20	22,000	Fair
Hastelloy N (PWA 1036)	45	12	22,000	Fair
Ni 200 (AMS 5533)	50	*110	3,600	Good
TD Nickel (PWA 1035)	12	2	20,000	Poor
Stainless Steel (AMS 5646)	50	35	10,000	Good

*International Nickel Data

Table VIII-2. Properties of Inconel 625 (AMS 5599) "A" Values

Density	= 0.305 lb/in.^{3}
Ultimate Tensile Strength at Room Temperature	= 120,000 psi
0.2% Yield Strength at Room Temperature	= 51,000 psi
0.2% Yield Strength at 1000°F	= 34,000 psi
0.2% Yield Strength at 1700°F	= 18,000 psi
Elongation at Room Temperature	= 30%

The local heat balance across the passage wall, illustrated in figure VIII-4, is determined by:

1. Evaluating the combustion side environment (T_{ADW}, hg)
2. Evaluating the heat conduction through the passage wall (T_1, T_2, T_3)
3. Evaluating the coolant side film coefficient (h_c)
4. Evaluating the coolant temperature (T_c)

The combustion side thermal environment is evaluated using the Mayer integral boundary layer solution with an enthalpy driving potential modified to reflect 250K staged combustion test results.

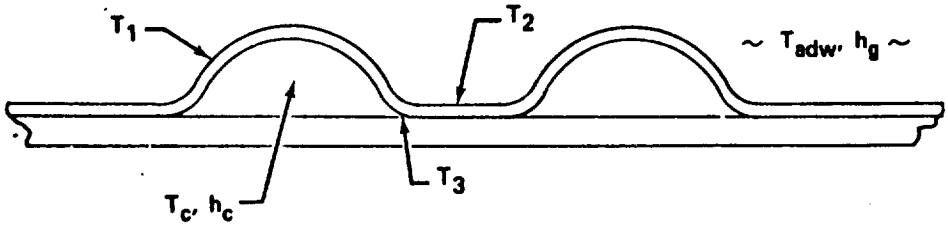

Figure VIII-4. Optimized Local Heat Balances Across Passage Walls Aids Nozzle Design FD 46167

The heat conducted through the passage walls is calculated using a two-dimensional nodal analysis. In calculating the heat conducted into the coolant, the coolant side film coefficient is established using experimentally verified forced convection correlations (Dittus-Boelter film temperature correlation) that have been derived for the particular region of coolant operation that account for the high wall-to-bulk temperature difference encountered during high heat flux conditions.

Using the preceding analytical methods, a heat balance across the passage walls at each section is made to establish the wall temperature.

The heat exchanger coolant pressure drop consists of losses associated with the inlet manifold and the coolant passages and involves the following mechanisms:

1. Momentum (area change)
2. Friction
3. Heat addition

The coolant passage pressure profile is set by the exit pressure.

The coolant temperature rise is obtained from the enthalpy rise that is obtained from the average heat input between incremental sections along the heat exchanger length.

The corrugated passage construction allows tailoring of the passage flow area along the nozzle length to obtain maximum coolant utilization, as shown in figure VIII-5, resulting in a low loss, lightweight design.

The selection of the maximum metal temperature (1910°R) as shown in figure VIII-6 during normal engine operation is due to a loss in Inconel 625 material properties above 1910°R. It also resulted from an evaluation of the required design margin to ensure that the metal temperatures would not exceed the heat treat temperature (2260°R) of Inconel 625. The probable variations in heat transfer are collectively considered to establish the required design margin.

The design point predictions of the analysis at the entrance and exit locations of the heat exchanger are shown in figure VIII-7. Note that the

coolant is discharged at high temperature thereby demonstrating its efficient utilization. (Temperatures shown are average temperatures.)

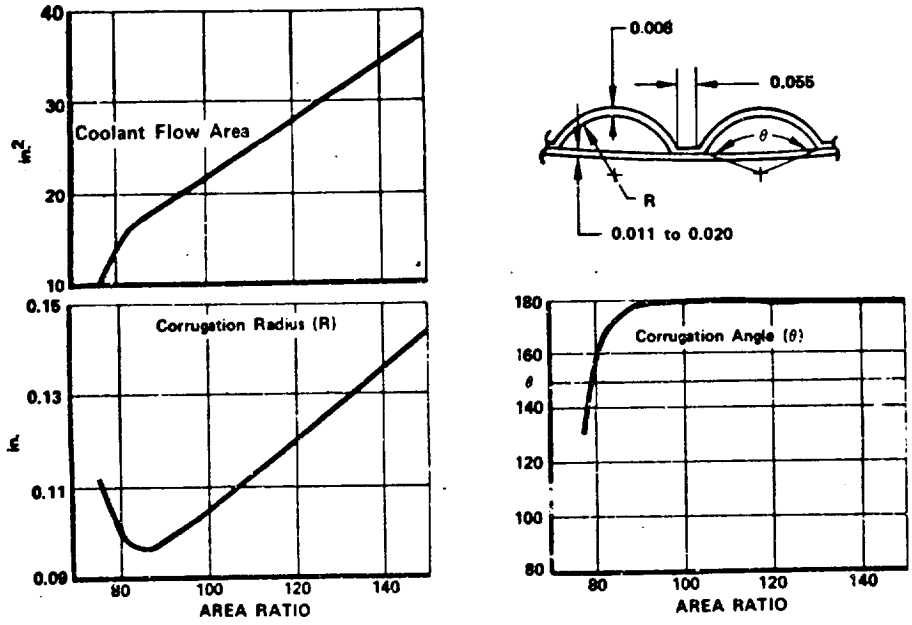

Figure VIII-5. Nozzle Corrugation Geometry is Tailored for Maximum Coolant Utilization FD 46168

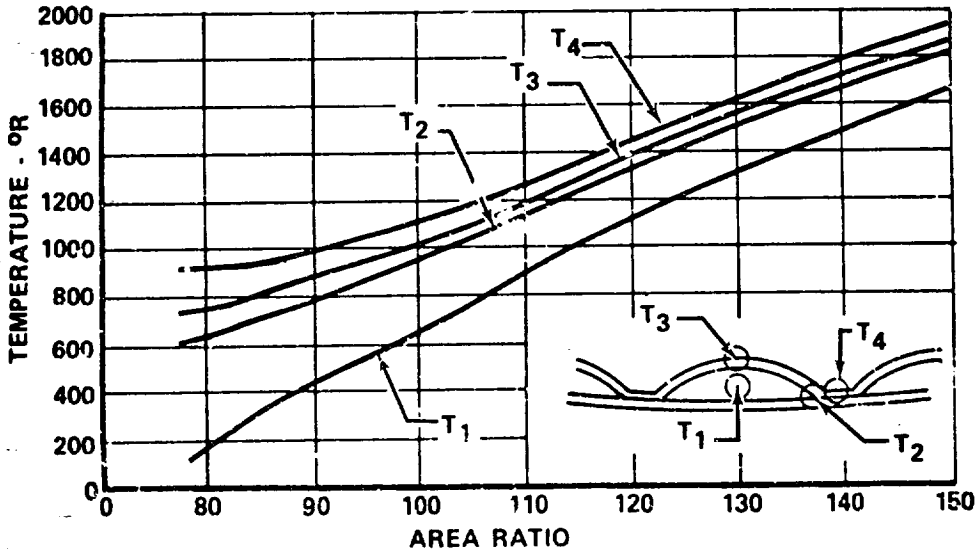

Figure VIII-6. Extendible Nozzle Temperature Profile Demonstrates Efficient Coolant Utilization FD 46169

After additional development, P&WA developed a gather forming technique that has been applied successfully to specimen panels. It results in an easily producible corrugated skin as shown in figure VIII-3. The fabrication sequence for the proposed SSME extendible nozzle is shown in figure VIII-8.

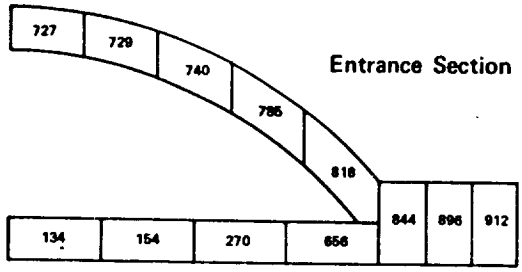

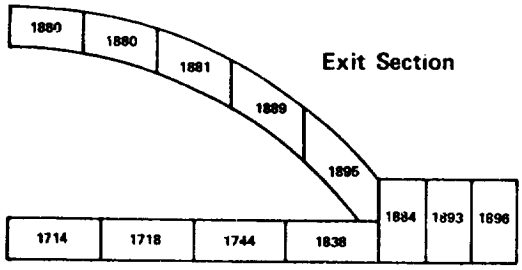

Figure VIII-7. High Temperature Coolant Discharge Demonstrates Efficient Nozzle Utilization FD 46170

Draw-Form-Clamp Sequence Produces Coolant Passages On Inner Panel

Inner Corrugated Panels and Outer Sheet Panels Are Sized and Resistance Welded to Form Subassemblies

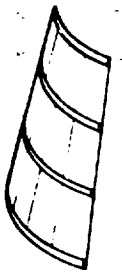

Four Subassemblies Are Butt-Welded Forming Six Sets of Panels With Brazed Reinforcing Band Segments

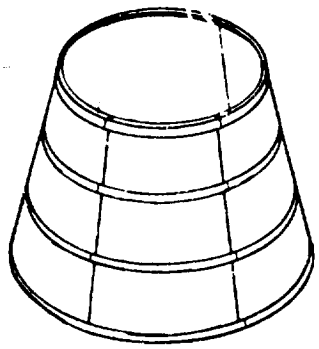

Six Panels Are Butt-Welded to Form the Basic Nozzle. Reinforcing Bands Are Spliced.

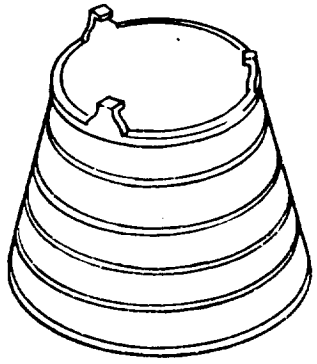

Coolant Manifold and Brackets Are Induction Brazed Completing the Nozzle

Figure VIII-8. Fabrication Sequence of the Extendible Nozzle FD 52282

- A LIGHTWEIGHT READILY FABRICATABLE STIFFENING BAND WAS SELECTED FOR THE EXTENDIBLE NOZZLE

In order to support loads from external pressure, gimbaling, maneuvering, vibration and nozzle axial thrust, it was required to design a band possessing the highest possible stiffness to weight ratio. Another criteria is that the band must not crimp prior to material yield.

Several candidate bands were optimized to determine the largest possible moment of inertia for a given band area. Figure VIII-9 demonstrates that a band of circular cross section is optimum since it supplies the highest stiffness to weight ratio. To provide braze area on this band, feet with thermal relief slots were incorporated on each side. The chosen stiffening band is shown in detail in figure VIII-10.

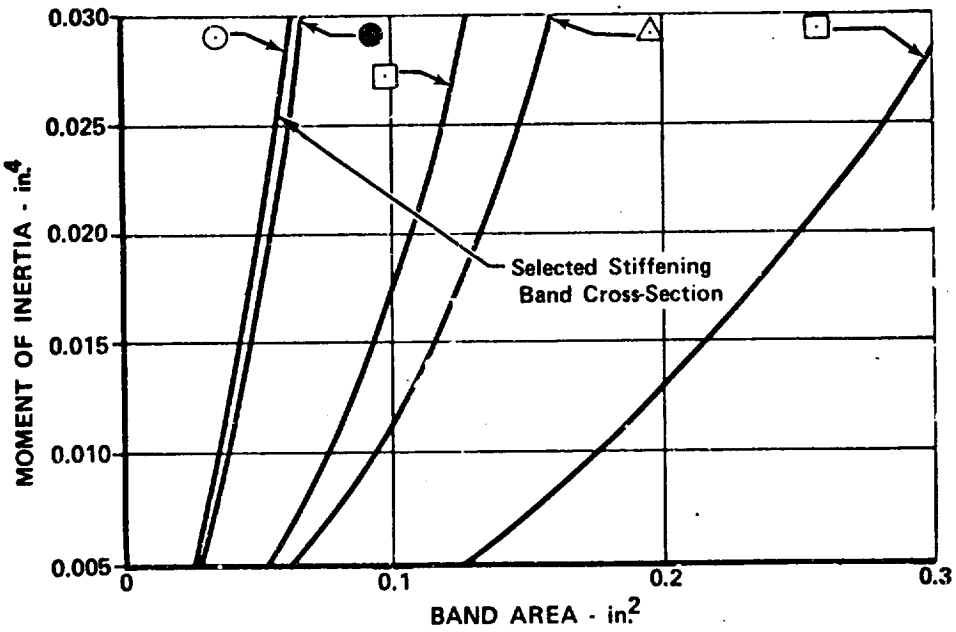

Figure VIII-9. Stiffening Band Selection is Optimized for Lightweight FD 47757

The circumferential stiffening bands are brazed to the external surface of the smooth outer skin. The stiffening bands are sized and spaced to prevent nozzle buckling during engine flight transient periods or altitude simulation testing.

- A LIGHTWEIGHT METHOD OF ATTACHING THE EXTENDIBLE NOZZLE TO THE TRANSLATION SYSTEM WAS DEVELOPED DURING THE XLR129 PROGRAM

Three mounting brackets attach the extendible nozzle and manifold assembly to the translation system assembly. This lightweight attachment method was developed during the XLR129 Rocket Engine Program. Each bracket, shown in figure VIII-11, has the form of a truncated pyramid with its base curved to fair tangentially into the coolant distribution manifold. The shell is formed from 0.027 in. sheet and 0.060 in. stiffness using Inconel 625.

The truncated top of the bracket is machined from Inconel 718, butt-welded to the stiffened shell faired into a rectangular flange that mates to one provided on the jackscrew ball-nut assembly.

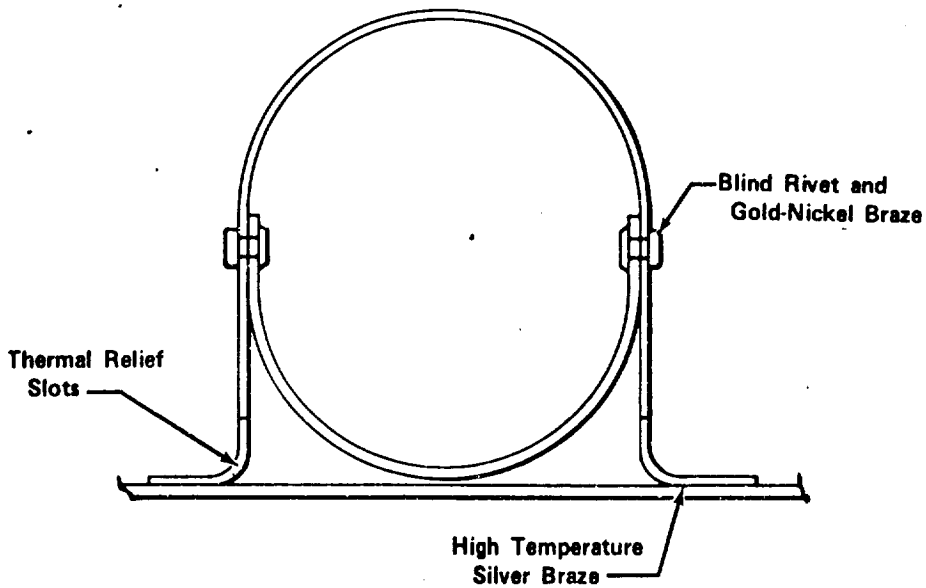

Figure VIII-10. Lightweight, Readily Fabricatible Stiffening Band FD 46166

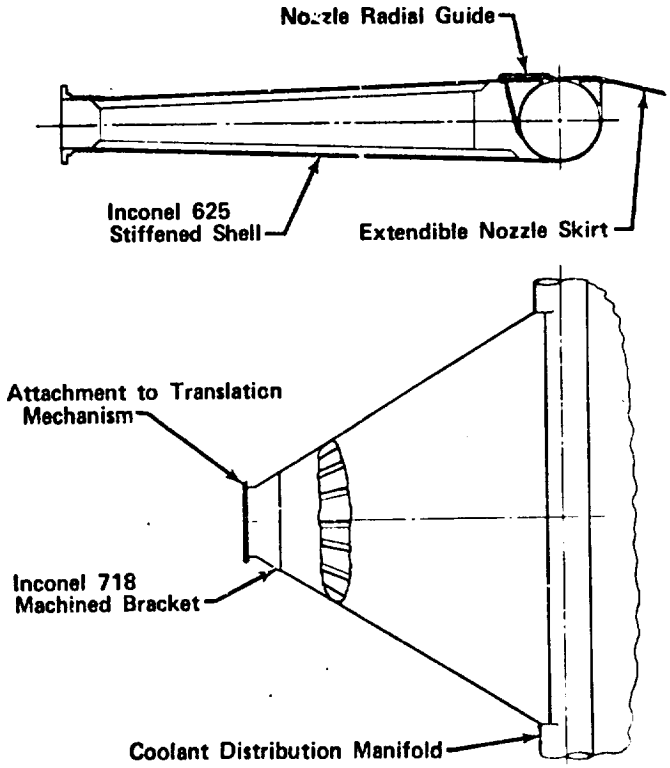

Figure VIII-11. Brazed Sheet Stringer Construction Results in a Lightweight Nozzle Attachment Bracket FD 52283

The mounting brackets straddle the coolant distribution manifold so that loads transmitted through their inner and outer walls are directed tangentially into the toroidal manifold shell. This tangential transition joint places the load on the manifold so that local bending at the point of application is minimized. Packaging limits each bracket to a 40 deg included angle on the coolant distribution manifold. Each bracket is sized to carry axial, flexural, and torsional loads imposed upon it during flight or altitude simulation testing.

- RADIAL GUIDES REDUCE NOZZLE WEIGHT

Radial guides prevent the primary and extendible nozzles from contacting while the nozzle is extended as shown in figure VIII-12. This allows the coolant distribution manifold to be sized as a stress and not a deflection limited structure resulting in a weight reduction of 58 lb.

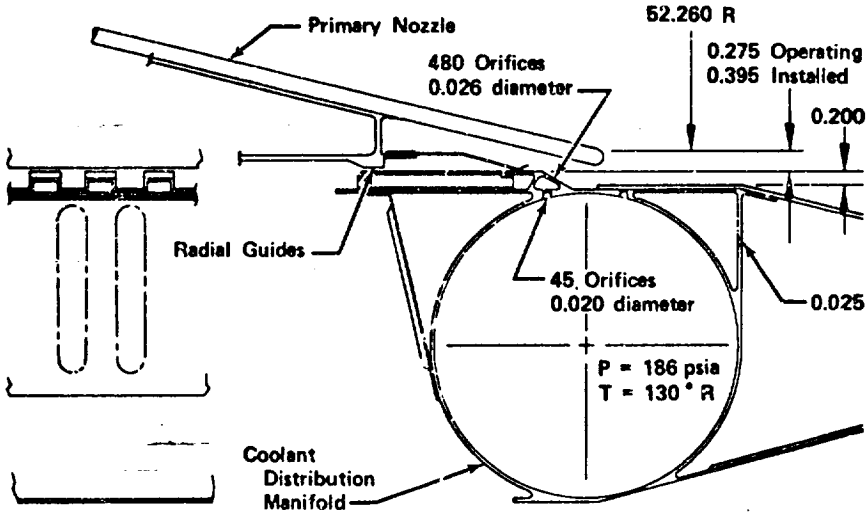

Figure VIII-12. Radial Guides Reduce Coolant Distribution Manifold Weight

FD 46162

1. Structural Analysis

a. Corrugation Thickness

The corrugated sheet thickness was calculated by determining the tensile stress on the seam weld that is produced by the coolant pressure at EPL in the corrugated passages. The sheet thickness selected prevents weld material stress rupture for 10 hr at T_{max} + 100 deg or yielding at emergency power. This method resulted in a corrugation thickness of less than 0.005 in. However, in order to avoid material handling and fabrication difficulties, the corrugation thickness was set at 0.008 in. This does not cause a weight penalty since the corrugated passages add to stiffening the nozzle to prevent it from buckling. Decreasing the thickness of the corrugated skin from 0.008 in. would have increased the number of stiffening bands required to prevent buckling. Thicknesses greater than 0.008 in. do not significantly reduce the number of bands required.

b. Outer Skin Thickness

The outer skin thickness was sized for EPL conditions and checked for an altitude shutdown engine transient occuring when the nozzle static wall pressure decreases rapidly and the corrugation coolant pressure and temperatures decrease more slowly. For both conditions, it is necessary to treat the outer skin as a fixed beam at operating temperature, with length equal to the corrugation width and a uniformly applied load equal to the coolant pressure. The tensile hoop stresses resulting from the static wall pressure were combined with bending stresses using the interaction equation described in SSME Design Structural Criteria, PWA FR-4449. This resulted in a stepped outer skin thickness of 0.011 to 0.018 in.

c. Axial Compressive Buckling Analysis

Having sized the nozzle skin, it is then necessary to determine if any circumferential stiffening bands are required to prevent axial compressive buckling. This is determined by computing the net compressive stress at each section of the outer skin. The net compressive stress is the difference between the thermal tension in the outer skin produced by the temperature difference between the hot corrugations and cooler outer skin and the compression produced by thrust, maneuver and gimbaling loads. In this analysis, the extendible nozzle experienced thermal tension in excess of compression at every section. Therefore, no stiffening bands were required for axial compressive buckling although bands are required for external pressure buckling and aerodynamic loads.

d. Compressive (Pressure) Buckling Analysis

According to the present CEI Specification, the extendible nozzle must be capable of extending at 110,000 ft minimum altitude. During a startup transient period, it is possible for a collapsing load to exist equal to the difference between the atmospheric pressure and the pressure inside the nozzle. To counteract this, the nozzle is designed to withstand 0.104 psi with a 30% margin.

This pressure buckling requirement does not present an undue hardship on the nozzle design, since the three intermediate stiffening bands required between the coolant manifold and exit band are also required to maintain the minimum required nozzle natural frequency of 10 cps.

e. Coolant Distribution Manifold

The coolant manifold located at the forward end of the nozzle is the primary structural member that transfers nozzle loads into the nozzle translation mechanism. Radial guides shown in figure VIII-12 enable the manifold to be sized as a stress, not deflection, limited member. (The guides prevent the primary and extendible nozzles from contacting.)

f. Nozzle Attachment Bracket

The three nozzle attachment brackets which attach the extendible nozzle and coolant manifold assembly to the translation mechanism are fabricated from Inconel 625 and Inconel 718 using a sheet stringer construction. The

0.060 in. stringers are crippling limited on the compression side and area limited on the tension side. The 0.027 in. sheet is sized from torsion considerations due to transverse loads. At the point of attachment to the coolant manifold, each attachment bracket spans 40 deg or approximately 38.23 in. of manifold circumference. This is necessary to spread the effect of concentrated reactions in the attachment brackets over the manifold, avoiding overstressing the nozzle skin beneath the attachment brackets.

g. Fracture Mechanics

The extendible nozzle coolant distribution manifold fracture mechanics analysis indicates that the proof factor of 1.2 is sufficient to ensure a component service life in excess of 400 cycles. Since the manifold wall thickness is sized by the local nozzle attachment bracket loads and not the coolant pressure, stress during the proof test is approximately 17,000 psi compared to an allowable value of approximately 67,000 psi.

h. Low-Cycle Fatigue

The SSME extendible nozzle has been designed for a minimum of 400 cycles. Areas of the nozzle where low-cycle fatigue failures due to thermal strain would be most likely are:

1. At low nozzle area ratios in the corrugated coolant passages where cryogenic hydrogen coolant produces a thermal gradient between the hot corrugations and cold outer skin. The thermal strain produced by the gradient in this area has been minimized by decreasing the coolant passage area locally which increases the flow velocity and decreases the corrugation temperature. The hot strain in the nozzle skin is approximately 25% of the strain required to produce failure in 400 cycles.

2. In the nozzle skin near the exit circumferential stiffening band due to the thermal response of the band which lags the nozzle skin during transient start and shutdown.

The total strain in this region consists of the thermal hoop and longitudinal strains produced by thermal lag, the thermal longitudinal strain produced by the hydrogen coolant and the strain produced by engine exhaust and nozzle coolant pressure. This strain system is reduced to an equivalent strain that exceeds 400 cycles.

i. Vibrations

Vibration of the nozzle during gimbaling can result in excessive deformation of the shell that could disturb nozzle flow and result in possible nozzle failure. The excitation is a combination of support bracket input loads, aerodynamic loads due to the expanding exhaust gases and acceleration of non-uniform mass distributions (tolerances) in the nozzle. Stresses and deflections cannot be directly determined as they depend on unknown excitation and damping. Therefore, the best design approach is to design the nozzle with a natural frequency exceeding the maximum required gimbaling frequency.

There are three natural frequencies which must be held above the maximum gimbaling frequency by a 1.3 margin: (1) minimum nozzle ring mode, (2) rigid body rocking laterally on the nozzle attachment brackets, and (3) rigid body bouncing axially on the attachment brackets.

1. Nozzle Ring Mode - This is the mode most likely to be excited by gimbaling. A survey of Space Shuttle Vehicle Contractors revealed that a minimum nozzle natural frequency of 10 cps would be desirable to ensure structural integrity.

   The nozzle natural frequency was found by using Deck 5883 which analyzes free vibration of rotationally symmetric shells. This deck is based on an analysis presented by A. Kalnis in the Journal of the Acoustical Society of America, Volume 36, July 1964. The program calculates the natural frequencies and mode shapes as well as stress resultants of symmetric or nonsymmetric free vibration of rotationally symmetric shells using linear bending theory.

   The extendible nozzle contour was simulated by six conical sections connecting points along the contour. The outer skin was simulated by isotropic shells of constant thickness and properties. The properties of each section were chosen at the hottest point within that section ensuring conversative results. The corrugated inner skin was simulated by orthotropic shells of constant thickness but different properties in the longitudinal and transverse directions. The nozzle stiffening bands were represented by rectangular rings sized to have the same area as the actual bands chosen to prevent pressure buckling in the altitude simulation facility. The band stiffnesses were simulated by adjusting the elastic modulus upward to yield the flexural (EI) stiffness of the actual bands.

   The coolant distribution manifold was assumed to restrain the nozzle shell in the radial and axial directions but did not provide any rotational restraint. The nozzle exit and free end of each stiffening band were completely unrestrained.

   The results demonstrate that the fundamental nozzle frequency is 13.2 cps, 32% higher than the most stringent vehicle requirement.

2. Rigid Body Rocking Modes - The axial stiffness of the nozzle attachment brackets must be sufficient to prevent rocking resonance due to gimbaling with at least a 1.3 margin on maximum gimbaling frequency.

   The natural frequency for this mode with three supports is:

$$f_n = \frac{1}{2\pi}\sqrt{\frac{3K_f R^2}{2\,I}}$$

where:

I = nozzle moment of inertia about its centroid

R = one half coolant manifold diameter

K_f = minimum flexural springrate of nozzle attachment bracket

The rocking resonant frequency was found to be 31.7 cps using the minimum flexural spring rate.

3. Rigid Body Bounce Mode - This frequency could be excited by nozzle pressure fluctuations or by gimbaling (centrifugal force excitation). A margin of exceeding 1.3 on gimbaling frequency is required.

The natural frequency for this mode with three supports is:

$$f_b = \frac{1}{2\pi}\sqrt{\frac{3\,K_a}{M}}$$

where:

K_a = axial springrate of nozzle attachment bracket

M = nozzle mass

C. REQUIREMENTS/COMPLIANCE

1. When fitted with the orbiter nozzle (skirt extended) and at altitude conditions in excess of 165,000 feet, the engine shall be capable of starting, within its service life to any power level between and including MPL and EPL, in accordance with paragraph 1.2.d and paragraph 4.1.7.c of the ICD and the applicable paragraphs of CEI Specification CP2291.

Compliance - Circumferential stiffening bands are spaced to prevent the nozzle skirt from buckling under a net external pressure of 0.104 psi with a 30% design margin. This corresponds to an altitude start at 110,000 feet that is nearly twice as severe as the loading condition at 165,000 feet.

2. The extendible nozzle shall be capable of gimbaling ±8 degrees with an angular velocity of 10 deg/sec under either firing or nonfiring conditions, with the nozzle extended or retracted. Excluding engine induced forces, the maximum angular acceleration shall not exceed 30 rad/sec^2. (In accordance with paragraph 3.1.4 and paragraph 4.4.2 of the ICD.)

Compliance - The gimbal angle, rate, and acceleration are not critical to the design for both operating and nonoperating conditions. The nozzle skirt stiffening requirements are based on the natural frequency and 110,000 feet altitude facility requirement. This exceeds the requirements of paragraph 3.1.4.

3. The extendible nozzle shall be capable of starting at any defined power level above 165,000 feet and at 110,000 feet in an altitude simulation facility, in accordance with paragraph 3.2.1.

   Compliance - The extendible nozzle is presently designed for 110,000 feet in an altitude simulation facility corresponding to a pressure load of 0.104 psi. This capability ensures successful operation at 165,000 feet where the combination of atmospheric and aerodynamic pressure loads is approximately 0.06 psi.

4. When fitted with the extendible nozzle and with engine not firing, the engine shall be capable of translating the nozzle at altitudes above 150,000 feet in accordance with paragraph 3.2.10.1 and paragraph 7.6 of the ICD.

   Compliance - The extendible nozzle is designed to withstand the 110,000 feet altitude facility requirement which is more severe than the aerodynamic sideload of 700 pounds at 150,000 feet, plus gimbaling and maneuver requirements.

5. When fitted with the orbiter nozzle at sea level and not firing, the engine shall be capable of translating in both the horizontal and vertical attitudes in accordance with paragraph 3.2.10.2.

   Compliance - The extendible nozzle is structually designed to exceed that required for ground handling loads of 2 g in any direction.

6. Hydrogen shall not be dumped into the base region during reentry or below 165,000 feet during ascent in accordance with paragraph 3.2.12 and paragraph 4.5 of the ICD.

   Compliance - Hydrogen is not required to cool the nozzle during reentry. During ascent, the hydrogen dump coolant is not required until the engines fire at altitudes above 165,000 feet.

7. The engine envelope shall be:

   277 inches with the orbiter nozzle extended

   165.5 inches with the orbiter nozzle retracted

147 ±. 125 inches in overall static diameter in accordance with paragraph 3.3.1 and paragraph 3.1 of the ICD.

Compliance - The extendible nozzle exit is 277 $^{+.00}_{-0.50}$ inches extended, 165±0.50 retracted and 147±0.125 inches in diameter. contracted, 147 ±. 125 inches in diameter.

8. The extendible nozzle shall be capable of withstanding 4.0 g handling load in any direction while installed in a handling frame without detrimental deformation. The nozzle shall also be capable of withstanding 2.0 g lateral acceleration during ground handling with the engine supported at its normal interface in accordance with paragraph (3.4.1.3).

   Compliance - Since the nozzle is designed to withstand an angular acceleration of 30 rad/sec during vehicle checkout, it is capable of withstanding the 4.0 g handling load without a handling fixture.

9. The extendible nozzle shall be capable of withstanding without degradation of reliability launch phase vibration, shock, acoustic, and aerodynamic loads, in accordance with paragraphs 3.4.3.3 and 3.4.3.2 and paragraph 7.6 of the ICD.

   Compliance - The natural frequency of the extendible nozzle is 13.2 cps. It will withstand the acoustic environment at sea level with the booster engines at EPL. The nozzle is also designed to withstand an external pressure load equal to the atmospheric pressure at 110,000 feet and aerodynamic loads of 700 and 400 pounds at 150,000 and 165,000 feet altitude respectively without degradation of reliability.

10. The acceleration load factors applicable to this engine shall be as indicated in table 2 and figure 4 of paragraph 3.4.5.4.

    Compliance - The extendible nozzle exceeds the acceleration load factors by 30% with a dynamic load factor of 5.

11. The engine reliability of the configuration must function without overhaul for 7.5 hours with a capability of (a) 100 starts to NPL or (b) 94 starts to NPL plus 6 starts to EPL, or (c) 6 EPL runs (in accordance with paragraph 3.6.1).

    Compliance - The extendible nozzle meets life requirements as shown in the structural analysis of the substantiation.

12. The extendible nozzle shall be designed to provide the following minimum factors of safety in accordance with paragraph 3.7.7.1:

    Minimum yield factor of safety is 1.10

    Minimum ultimate factor of safety is 1.40

Compliance - The extendible nozzle is designed in accordance with SSME Structural Design Criteria, PWA FR-4449, which meets these conditions.

In addition to CEI Specification CP2291, the following are Pratt & Whitney Aircraft imposed requirements:

1. The nozzle shall be thermally designed to NPL with a 25% margin and a mixture ratio of 6.5. This is the worst thermal condition.

2. The nozzle is dump cooled with 6.4 lb/sec of cryogenic hydrogen delivered to the coolant distribution manifold at 186 psia and 114.6°R.

3. The maximum allowable nozzle metal temperature is 1910°R (1450°F) which is determined from thermal and structural considerations.

4. The engine is structurally designed to EPL with a mixture ratio of 6.0. This is the worst structural condition.

5. The nozzle natural frequency is 10 cps. This determined the size of the nozzle stiffening bands.

6. The nozzle is fabricated using Inconel 625 from 24 corrugated panels which are butt-welded forming the nozzle shell.

D. CAPABILITY

1. The nozzle skin is stiffened to prevent buckling due to an external pressure of 0.104 psi with a 30% margin. This corresponds to engine start in an altitude simulation facility at 110,000 feet that is twice as severe as extending the nozzle at 150,000 feet or firing at 165,000 feet.

2. The gimbal rate and acceleration can be increased to 30 deg per second and 30 rad/sec^2 without nozzle weight increase. The gimbal angle can be increased without nozzle weight penalty.

3. The nozzle is designed with a natural frequency of 10 cps. This exceeds the most stringent vehicle contractor requirement by a design margin of 30%.

4. The nozzle's smooth outer skin is sized to limit its maximum stress to 90% of 0.2% yield at emergency power. The inner skin is oversized by a factor of two providing nozzle stiffening.

5. The nozzle is capable of withstanding twice the 2-g handling loads without a support fixture.

6. The extendible nozzle has been designed to be stress, not life limited. It is therefore capable of exceeding the 400-cycle CEI requirement by a large margin.

E. SUBSTANTIATION

1. Test Programs - THE EXTENDIBLE NOZZLE CONCEPT WAS DEMONSTRATED DURING JANUARY 1967

Under a 50K stages combustion test program, tests of a sheet metal water film cooled primary nozzle having an area ratio of 20:1 and a water film cooled sheet metal extendible nozzle having an area ratio of 60:1 (figure VIII-13) were conducted to obtain the following information:

1. Demonstration of the stability characteristics of an extendible nozzle when operated over a wide range of pressure ratios
2. Pressure ratio at which primary hot gas flow reattached to the inside wall of the extendible nozzle (which extended beyond the exit of the primary nozzle) when it was in the retracted position
3. Temperature and pressure distribution and their maximum levels reached in the nozzle during separated or reattached conditions
4. Effects of reattachment temperature and pressure during translation of the nozzle
5. Nozzle performance of an extendible nozzle in the extended or retracted position.

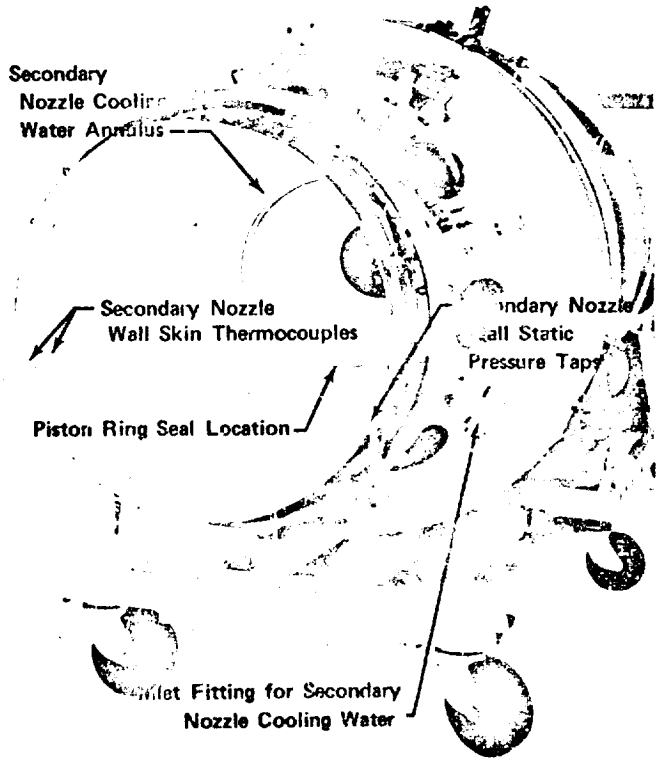

Figure VIII-13. Extendible Nozzle in Fixture FD 52422

In three hot firing tests with the extendible nozzle, the nozzle was successfully tested and was extended and retracted during the test. Test data indicated that the nozzle flow was stable up to the maximum operating level, the air being entrained around the annulus formed between the primary and extendible nozzle provided a uniform circumferential flow field that stabilizes the primary nozzle flow. The primary nozzle flow stream did not attach to the extendible nozzle wall until the nozzle was completely extended. At that time the rig was operating at a pressure ratio in excess of 175. Figure VIII-14 illustrates the test sequence of ramping the chamber pressure and translating the nozzle. The effect on the skirt static pressure is shown at a location approximately 2 inches upstream of the secondary nozzle exit plane. A manuscript of nozzle performance is shown in figure VIII-15 while the pressure ratio is varied and the nozzle translated.

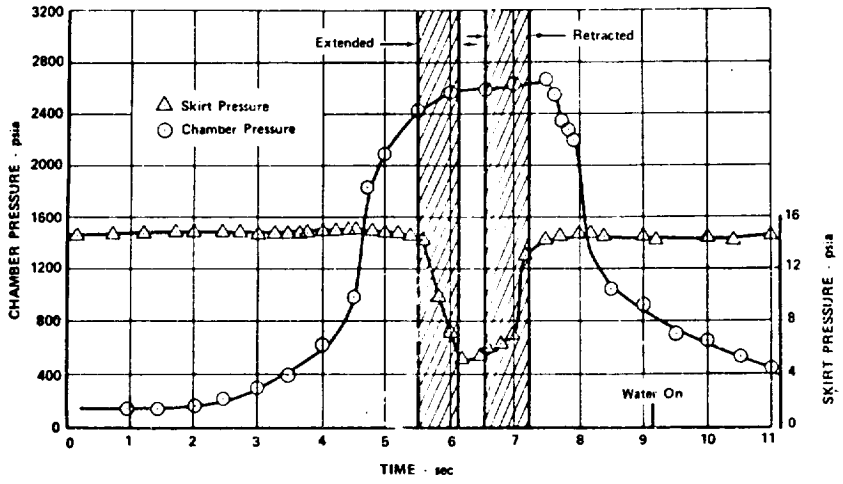

Figure VIII-14. 50K Extendible Nozzle Skirt Wall Pressure FD 52204

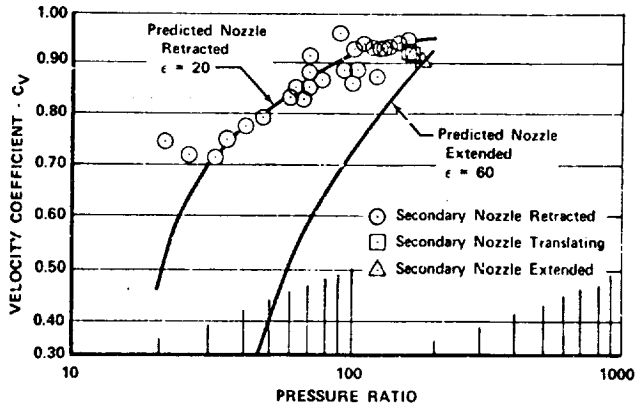

Figure VIII-15. 50K Extendible Nozzle Provides Stable Operation Over Wide Pressure Ratios FD 52203

The data from these tests confirmed that an extendible nozzle can provide stable operation over a wide range of pressure ratios, while providing improved nozzle performance at the low pressure ratios when the nozzle is extended, and with similar improved performance in the retracted position at high pressure ratios.

- AN EXTENDIBLE NOZZLE WAS TESTED AT 100% THRUST DURING SEPTEMBER 1967

A 250K stage combustion program was conducted to demonstrate the operating characteristics of the extendible nozzle. Nozzle hardware fabrication included one sheetmetal primary nozzle (ϵ = 20:1), one regeneratively cooled primary nozzle, and two sheetmetal extendible nozzle skirts (ϵ = 60:1). Eight tests were conducted at 100% thrust using the extendible nozzle (figure VIII-16) of which four tests were made using the regeneratively cooled primary nozzle, and four tests using the water film cooled sheetmetal primary nozzle.

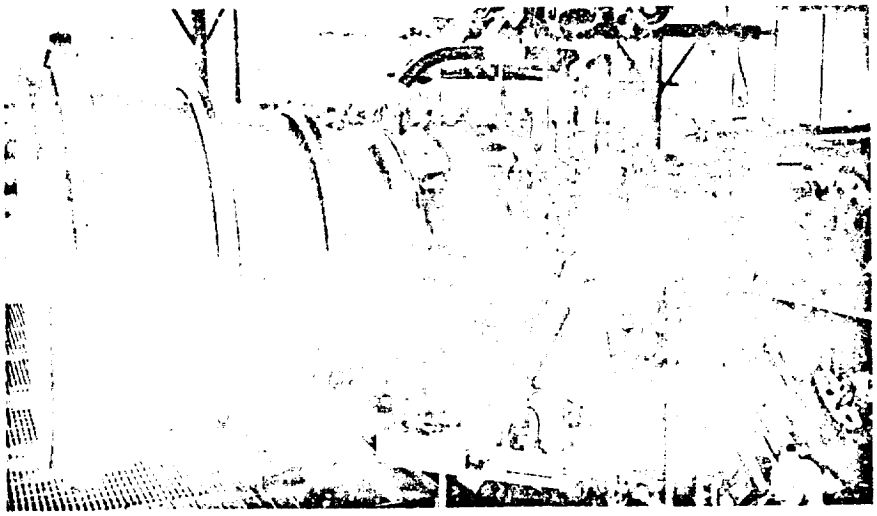

Figure VIII-16. Extendible Nozzle Is Test Proved FD 52425

- P&WA HAS FABRICATED AND TESTED A CORRUGATED DUMP-COOLED NOZZLE

A lightweight dump-cooled nozzle extension was fabricated and tested at P&WA during August 1967 as part of a 250K Demonstrator Program.

The dump-cooled extension nozzle was fabricated from 12 corrugated Inconel 625 panels with 0.008-inch wall thickness using explosive forming in a female Kirksite die. The panels were fitted to a 0.015-inch Inconel 625 cone and resistance welded to the cone between the corrugated coolant passage as shown in figure VIII-17. A manifold was brazed to the skirt using PWA 698 (gold-nickel) filler material. The assembly was leak checked, fitted to an RL10A-3-3 thrust chamber and successfully test fired.

This program was performed with company funds and demonstrated the feasibility of a lightweight dump-cooled nozzle extension. However, the forming technique was unacceptable because of material thinning and difficulty in holding tolerances between corrugations.

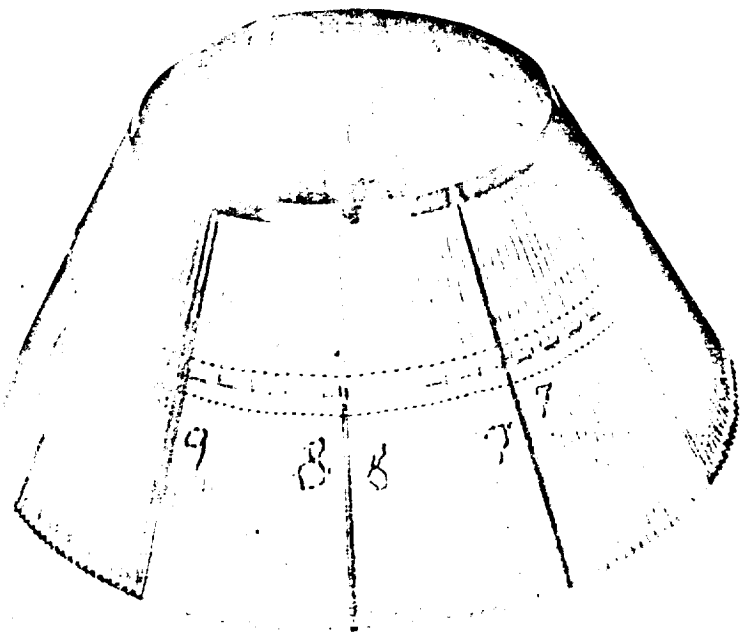

Figure VIII-17. Nozzle With External Corrugations Successfully Tested in August 1967 FE 7127-4

2. Fabrication Programs - THE SSME EXTENDIBLE NOZZLE USES PROVEN FABRICATION TECHNIQUES

An investigation of nozzle fabrication techniques was conducted during the XLR129 Rocket Engine Program to provide additional data and information to support the design of the extendible nozzle. Sample nozzle panels were fabricated to evaluate manufacturing techniques. The promising panels were subjected to hydraulic stress and thermal cycling tests to determine structural capability.

The first step in this fabrication study was to select a method to form the corrugated section of the assembly. Several techniques were considered, including explosive forming, hydrostatic forming, and die forming. The explosive forming method was used previously on the dump-cooled nozzle extension of an RL10 nozzle, but material thinning and difficulty in holding tolerances limited this method. From the two remaining methods, die forming was selected because it offered the highest degree of success. Figure VIII-18 illustrates the type of gather forming die selected to form the sample panel and low cycle thermal fatigue test samples. The corrugated sheets were joined to the flat sheets by resistance welding.

A die was fabricated to form corrugated panels 18-inch long and 16 corrugations wide. The corrugation height was varied from 0.293 to 0.350 inch over the 18-inch sample. The samples represented the nozzle inlet configurations where maximum thermal stresses occurred.

The first corrugated sheet formed with the die set resulted in corrugation heights 16.5% below the blueprint requirements. This was caused by material spring-back after forming. Future die sets for the actual nozzle will be

designed to compensate for this material spring-back to obtain required limits. Since this die set was for sample panels only, it was impractical to rework this particular set. To eliminate some of the spring-back in the samples, all the corrugated panels were annealed and then restruck with the forming die. This increased the corrugation height to within 5% of the blueprint requirements. The corrugated sheets were then resistance seam welded to flat sheet stock to make sample assemblies, as previously shown in figure VIII-3.

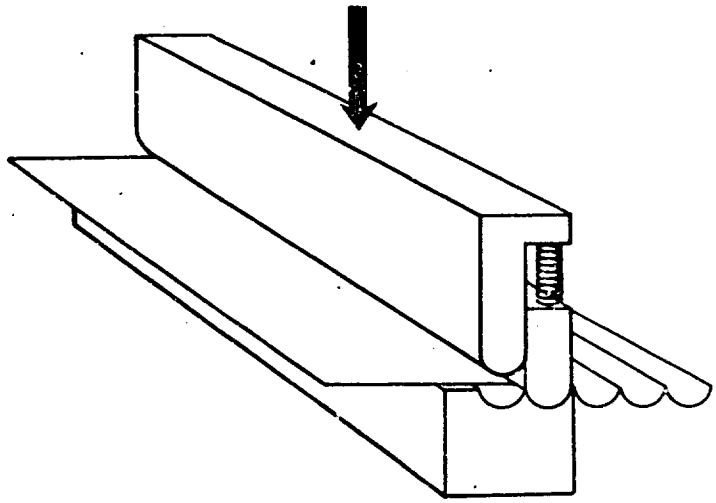

Figure VIII-18. Corrugation Fabricated by Die Forming FD 23215

3. Extendible Nozzle Detail Parts Testing - HYDROSTATIC PRESSURE TESTS PROVED CORRUGATED SKIN CAPABILITY

Figure VIII-19 illustrates the two-corrugation pressure test specimens fabricated for hydrostatic pressure testing. Several specimens were fabricated to prove the corrugated skin capability. Each corrugation was separately pressurized through fittings at one end of the corrugation. The opposite ends were welded closed. The first test specimen failed at 225 psig. The failure occurred at a spot tack weld that was outside the resistance weld width. The failure is depicted in figure VIII-20a sketch a. The next two specimens failed at 275 psig and 400 psig, respectively. Both specimens began to roll, as shown in figure VIII-20b sketch b. Both failed at the edge of the resistance weld, because of the sharp corner caused by the rolling of the assembly.

To investigate if rolling caused early failure, a specimen was tack welded along the edges (4 places both sides) to a 1/8 in. steel sheet. This specimen was pressurized to 380 psig before one of the four tack welds failed and caused a leak in the corrugation. This is shown in figure VIII-20c sketch c. The remaining tack welds on the No. 1 corrugation side held and the No. 2 corrugation did not lose pressure. This corrugation contained pressure until the remaining tack welds on the No. 1 side failed and the No. 1 corrugation folded up causing the No. 2 corrugation to fail next to the resistance weld. This indicated that the rolling had caused premature failures.

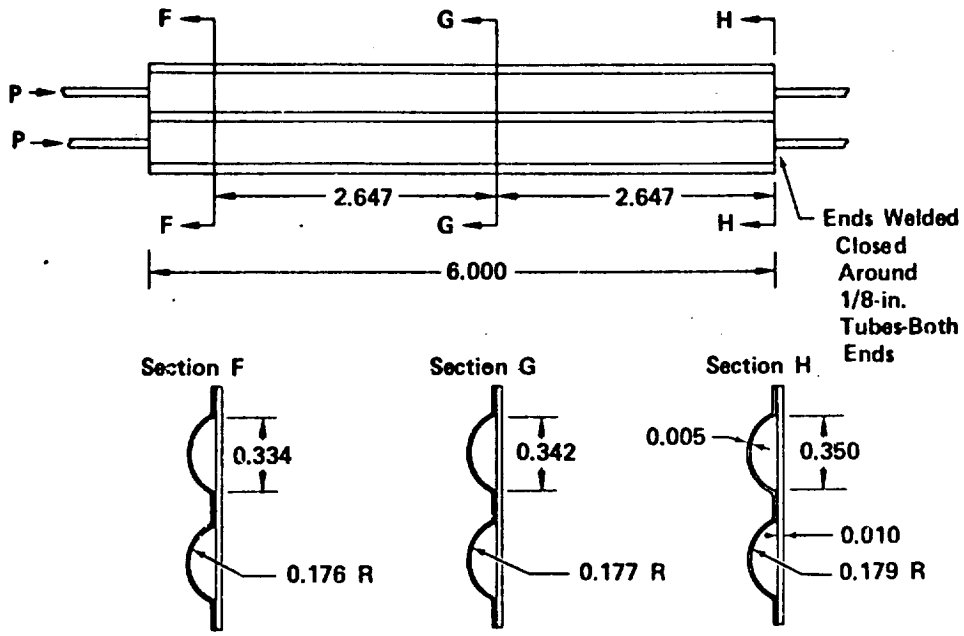

Figure VIII-19. Hydrostatic Test Samples Used to Substantiate Corrugated Sheet Capability FD 52419

The next specimen was seam welded on both sides to the 1/8 in. thick plate, as shown in figure VIII-20d sketch d. Both corrugations were pressurized to 1300 psig. One corrugation failed next to the seam weld at this pressure.

Because the extendible nozzle corrugations are designed to operate at low pressure, (186 psia maximum) it was concluded that the resistance welds between corrugations were adequate for supporting the operating internal pressure and that the corrugated skin itself was acceptable.

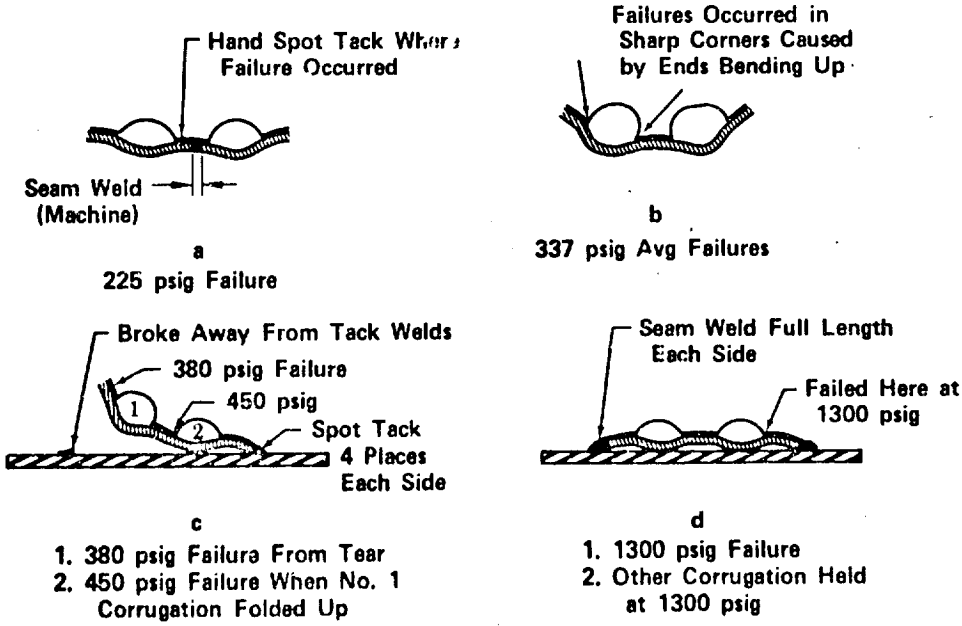

Figure VIII-20. Design Capability Proved by Failed Hydrostatic Test Samples FD 52420

- RESISTANCE WELD TESTS DEMONSTRATE DESIGN MARGINS

To determine the structural margins and the quality control required of the welds between the corrugations of the dump-cooled nozzle, pull tests of welded specimens were performed. Tensile test specimens were constructed by cutting Inconel 625 (AMS 5599) sheets into 1-in. wide strips 12 in. long. The two thicknesses were stacked and resistance welded 6 in. from the end giving a 1-in. length of weld to be tested. The two ends of the same thickness material were folded back and the load applied to these ends as shown in figure VIII-21a sketch a.

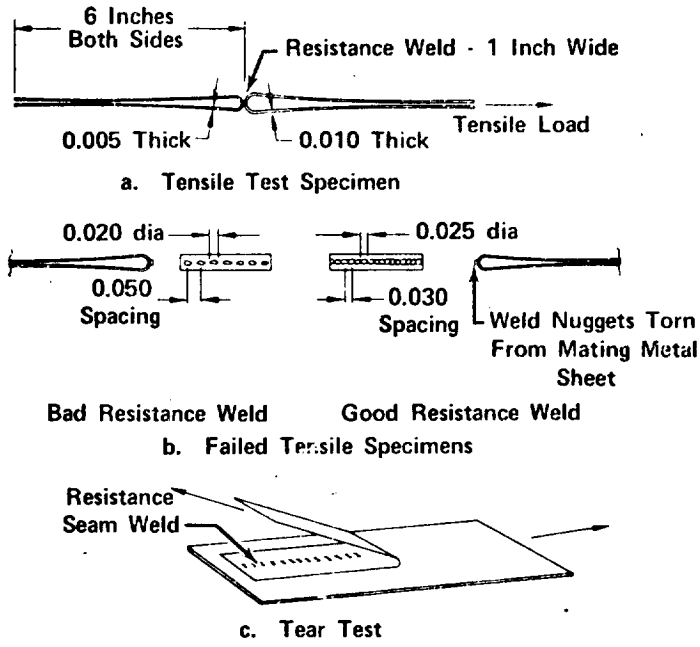

Figure VIII-21. Hydrostatic Test Samples FD 24995A

The initial tests were conducted with 0.005-in. thick Inconel 625 welded to 0.010-in. Inconel 625 with the following results:

Maximum Load, lb	
225	
218	184 lb average
125	

This early failure resulted because the weld nuggets were 0.050-in. apart (center-to-center) and the nugget diameter was 0.020 in. The nuggets should have overlapped as illustrated in figure VIII-21b sketch b. A second series of tests was conducted with better results.

Maximum Load, lb	
435	
302	357 lb average
336	

The weld nugget diameter was 0.025 in. and nuggets overlapped with 0.030 in. center-to-center distance.

The next series of tests was conducted with a thickness increase of one sheet from 0.005 to 0.010-in. thick. The second sheet remained 0.010-in. thick. Inconel 625 was the material.

Maximum Load, lb	
353	
599	
	423 lb average
343	
399	

The weld nuggets were 0.035 in. in diameter and nugget center-to-center distance was 0.030 in. resulting in a good overlapping seam weld. These tests indicated that the resistance weld joints were as strong as the parent material.

- THERMAL FATIGUE TESTING DEMONSTRATES THAT NOZZLE LIFE REQUIREMENT WILL BE EXCEEDED

Thermal fatigue testing was conducted during the XLR129 Rocket Program using a twin induction coil for heating, and copper fins brazed to the back of the fatigue samples and suspended in water for cooling. The test setup is illustrated in figure VIII-22.

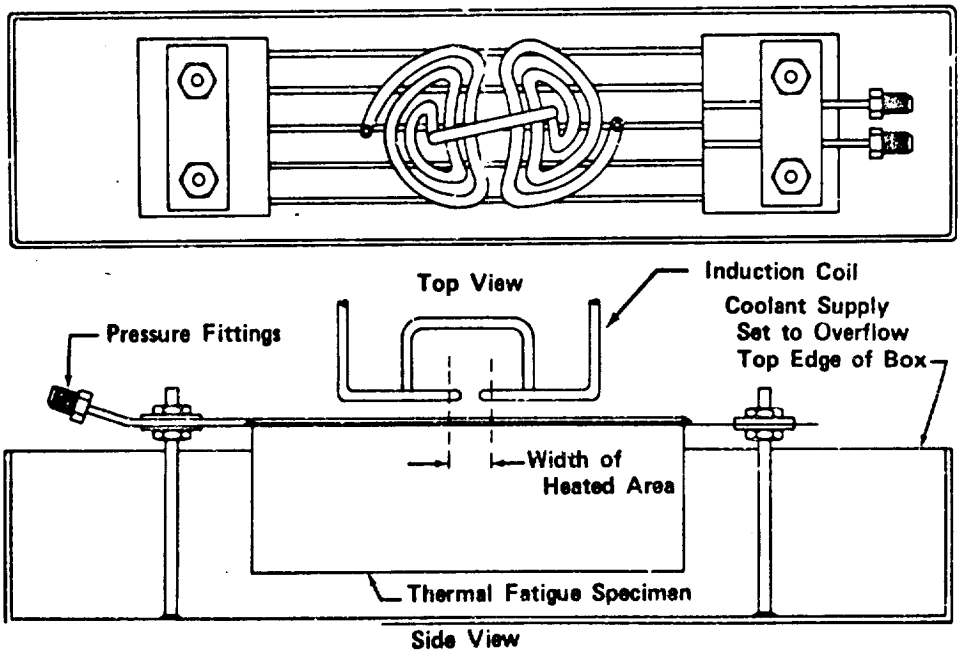

Figure VIII-22. Thermal Fatigue Cycling Setup FD 52421

The first 13 tests were conducted with thermal fatigue samples fabricated of 0.005-in. thick Inconel 625 (AMS 5599) corrugations resistance welded to 0.010-in. thick Inconel 625 (AMS 5599) sheet. Tests 14 through 21 were conducted with thermal fatigue samples fabricated of 0.010-in. thick Inconel 625 (AMS 5599) corrugations resistance welded to 0.010-in. thick Inconel 625 (AMS 5599) sheet. The results of testing with 0.005-in. thick corrugations is summarized in figure VIII-23 and for 0.010-in. thick corrugations in figure VIII-24. Since the thermal gradient of the SSME extendible nozzle is approximately 625 deg, it can be seen that the nozzle life exceeds the required 400 cycles.

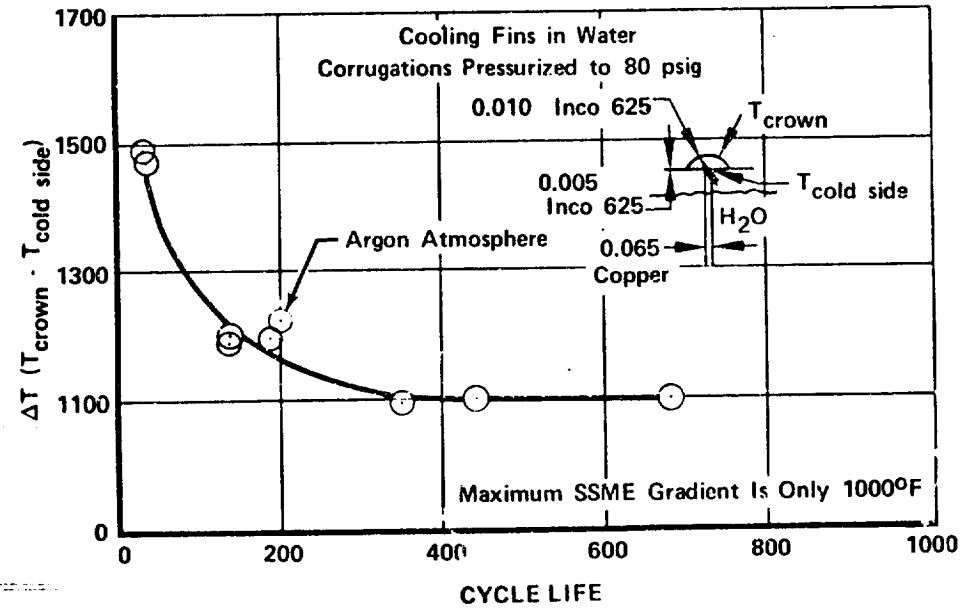

Figure VIII-23. Nozzle Cycle Life Assured For 0.005-Inch Thick Corrugations FD 51890

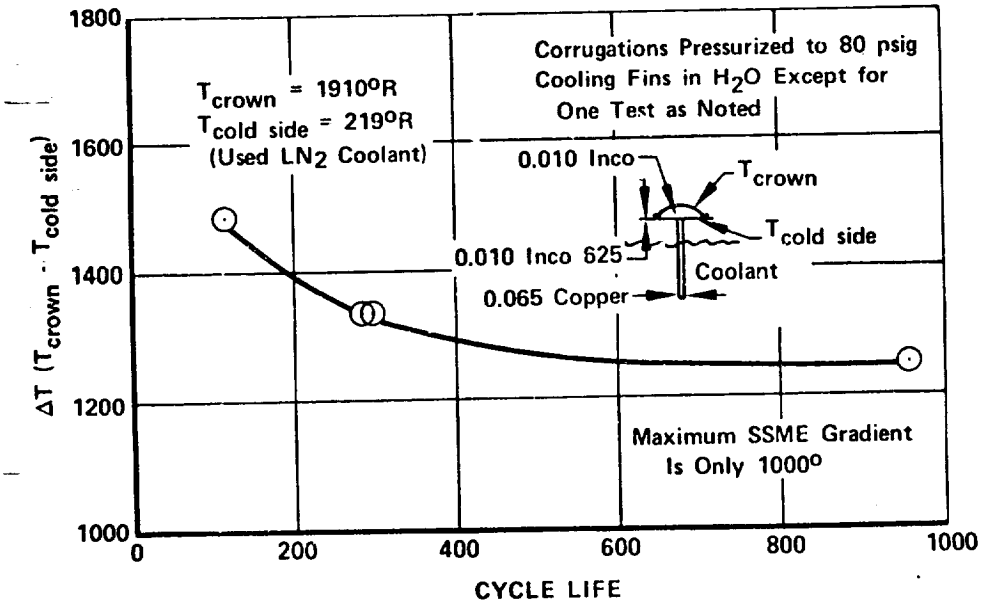

Figure VIII-24. 0.010-Inch Thick Corrugations Provide Increased Design Margins FD 51891

SECTION IX
COMBUSTION STABILITY

STABLE COMBUSTION SYSTEMS RESULT FROM DEMONSTRATED ACCURACY OF STABILITY ANALYSIS

The P&WA analysis of combustion system high frequency stability characteristics is based on the sensitive time lag theory. The double dead time theory presented in NASA TN D-3080, is used to evaluate low frequency combustion stability. During the design process the injectors and combustors were evaluated in terms of parameters which are common to both combustion stability and performance. The combustion system was then integrated by selecting that combination of component characteristics which provides designed-in high and low frequency combustion stability as well as performance. A detailed description of this method of integration is presented in FR-4471, Combustion Stability Analysis and Aids.

The high frequency combustion stability characteristics of the integrated design were evaluated by the sensitive time lag theory. This theory permits the dynamics of the injection-combustion process to be characterized by a time lag and an interaction index. Since a combustion system has only certain discrete frequencies at which the hot gas can oscillate in well defined modes, and since hot gas generation provides inherent damping, self-sustained oscillations can exist only if the combustion process is able to generate sufficient feed back energy at the proper frequency to drive the instability. The sensitive time lag represents the limited frequency range at which instability can exist and the interaction index represents the magnitude of the combustion energy feedback. High frequency combustion instability results when the sensitive combustion time lag is matched with one of the frequencies of the combustion chamber, and the combustion process is so highly sensitive that the chamber damping effects are not sufficient to offset combustion feedback.

P&WA's approach to the design of stable combustion systems is to provide extremely short ignition delay time and a rapid combustion rate that reduces the sensitive combustion time lag so that it can only match a combustion chamber frequency sufficiently high that the combustion process is not sensitive to it. In addition the damping process is augmented in the design by the distribution, size and number of injection elements as well as by control of combustion chamber axial pressure gradient. The correlation of these design features with combustion system stability characteristics is given in PWA FR-4471, Combustion Stability Analysis and Aids. Stability margin is provided through the use of a porous material in the design of the liners that protect the walls of the combustion chambers. The porous liners act as absorbing devices for dynamic pressure oscillations and exhibit excellent acoustic damping characteristics, thereby ensuring significant stability margin. This bonus capability is provided without compromise to performance. Included in PWA FR-4471 is the method of design analysis for these liners as well as the results of the analysis.

Figure IX-1, A and E present the results of the high frequency combustion stability analyses of the SSME preburner and main chamber designs. They show that both designs exhibit excellent high frequency combustion stability characteristics. The engine operating region lies well outside the shaded stability limit curves for both preburner and main chamber, indicating that high frequency combustion instability is highly unlikely in either combustion system. The first longitudinal

mode in the preburner and the tenth tangential mode in the main chamber are the most sensitive to spontaneous instability; however, both are well away from the combustion regions. For a more detailed description of the high frequency combustion stability characteristics of the SSME see PWA FR-4471.

The accuracy of this method of analysis for predicting the high frequency combustion stability characteristics of high pressure staged combustion engines is demonstrated in figure IX-1, B and F.

Data from XLR129 preburner testing and 250K staged combustion testing were used to calculate the theoretical high frequency combustion stability characteristics of the XLR129 preburner and 250K main chamber. Calculations were based on the same sensitive time lag theory used for the SSME. The theoretical analysis predicted the XLR129 and 250K combustion systems to be stable, as shown in figure IX-1, B and F. The accuracy of the prediction is verified by the stable combustion demonstrated during XLR129 and 250K engine testing. The theory agrees with the observed stability of the testing, substantiating this method of analysis for SSME combustion systems. The analysis of the SSME combustion systems indicates more stability margin than the XLR129 or 250K, as shown by the greater distance between the operating region and the shaded stability limit curves.

Low frequency combustion stability characteristics are described by an analog simulation of the propellant supply system and the combustion process. This analog computer program is based on the double dead time theory presented in NASA TN D-3080, TN D-4005, and TN D-4564. Propellant supply line dynamics, injector manifold flow dynamics and injection pressure drop characterize the propellant supply system. The combustion process is represented by an oxidizer vaporization delay time, analogous to the sensitive combustion time lag used in the high frequency analysis, and characterized by an ignition delay time which is a function of oxidizer droplet size and fuel injection temperature.

This program was developed during early 250K preburner testing for use in correcting low frequency combustion instability that occurred in a boiler plate preburner at 20% thrust. The instability was self limiting and was not observed above the 25% thrust level. The analog computer analysis succeeded in matching both the amplitude and frequency of the observed test stand instability, and showed that the instability resulted from coupling of the oxidizer vaporization delay with secondary oxidizer injector dyanmics. The analysis also indicated that reducing the oxidizer secondary manifold volume by 20% would result in a stable system. Subsequently, the XLR129 engine preburner injector configuration was designed with a reduced oxidizer secondary volume, and testing demonstrated that the low frequency combustion instability had been eliminated, as shown in figure IX-1, D.

The low frequency combustion stability characteristics of the SSME preburner is shown in figure IX-1, C. The results of this analysis show that the preburner design will not experience low frequency combustion instability and that it has considerable stability margin. The main chamber analysis is not shown because the combination of high fuel injection temperature and 25 micron LO_2 droplets produces such a short ignition delay time, and consequently such a high damping ratio, that low frequency combustion instability is precluded.

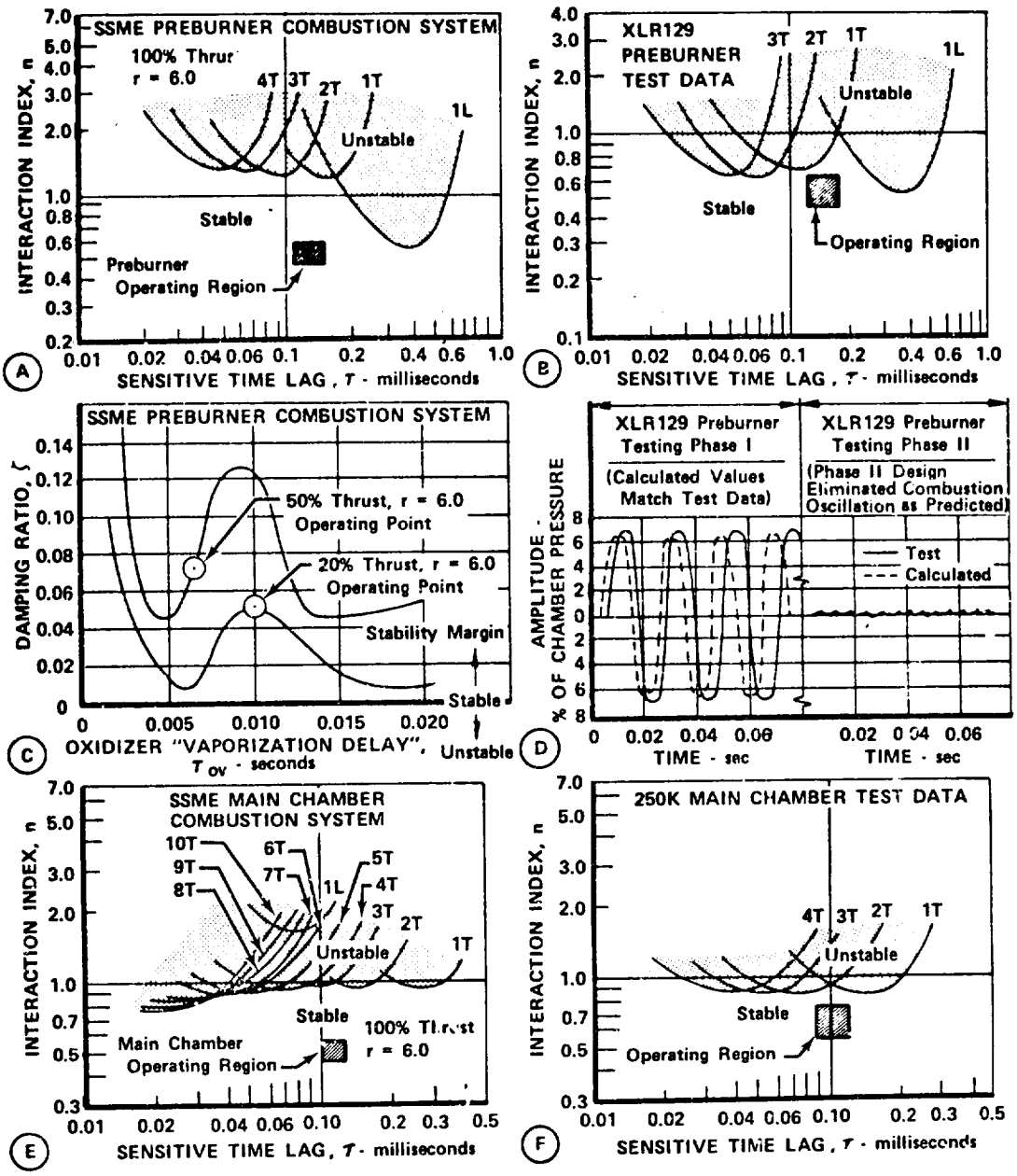

Figure IX-1. Demonstrated Accuracy of Stability Analysis Gives Designed-In Combustion Stability to SSME

FD50318

A complete presentation of the SSME low frequency combustion stability analysis is given in PWA FR-4471, Combustion Stability Analysis and Aids.

COMBUSTION STABILITY WILL BE EVALUATED THROUGH PERTURBATION TESTING

The SSME combustion system has been designed for stable combustion to confirm the design concepts; the engine will be perturbation tested during both development and production. Pulsing and measuring provisions have been designed into all engines without performance penalties.

Perturbation testing will be accomplished by detonating a small explosive charge within the combustor during operation to generate an instantaneous overpressurization that can trigger possible modes of instability. Dynamic instrumentation will record the growth or decay of these oscillations. A comprehensive program of perturbation testing is planned for Phase C/D. (Refer to PWA FR-4099, Program Development Plan.) It will evaluate the effects of charge size, location and engine operating conditions on engine stability.

Directional (pulse gun) and omnidirectional (pulse bomb) perturbation devices will be used for the preburner and main chamber. Pulse guns will be used primarily for radial or tangential modes while pulse bombs will be used for all modes. The pulse gun design will be the same as was successfully used during the 250K Phase I program.

The flight engines are designed to accept, without modification, the same pulsing devices used during development. The pulse guns are flange mounted through the chamber liners with the barrels flush with the liner inner walls. The pulse bomb and its extension system are mounted through the main injector face replacing the borescope plug as shown in figure IX-2. Neither of these mounting designs compromises engine performance.

The preburner and main injectors have two dynamic pressure transducers each, mounted at the outer injector periphery and coupled to the chambers through nonreflective "infinite" tubes. Pulsing and measuring provisions for the SSME are described in greater detail in PWA FR-4471, Combustion Stability Analysis and Aids.

The planned perturbation testing will assure that the SSME is stable and remains stable throught its 7-1/2 hour, 100 mission lifetime.

PREBURNER COMBUSTION STABILITY ENSURED BY MATCHED INJECTOR AND COMBUSTOR DESIGNS

The SSME preburner combustion system has been designed for both combustion stability and stability margin. The designs of the injector and combustion chamber are matched to provide high and low frequency combustion stability at the most demanding points in the engine cycle, steady-state operation with 95°R fuel and transient operation with 70°R fuel. The use of porous absorbing liners gives stability margin without a weight or performance penalty.

A decrease in fuel injection temperature normally has a destabilizing influence because the ignition delay time is increased and the axial static pressure gradient in the combustion chamber becomes more severe. The SSME preburner combustion system design avoids these destabilizing effects by matching injector and combustion chamber design characteristics so that a short ignition delay time and a uniform axial static pressure gradient result, allowing stable combustion.

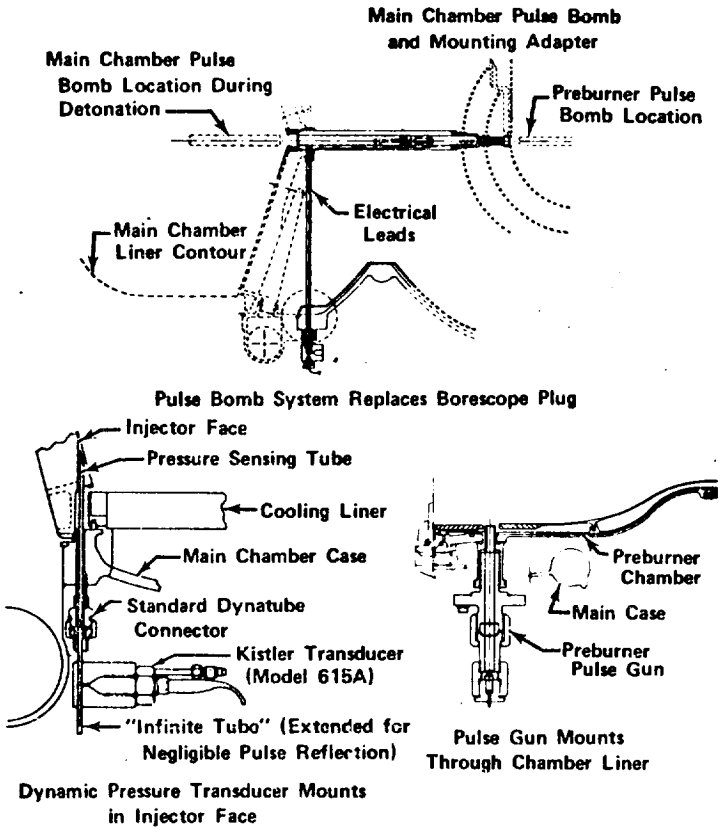

Figure IX-2. Stability Rating Capability Provided Without Performance Losses FD 50449

The use of an injection momentum ratio ≥ 4 and oxidizer atomization to 36 microns results in an ignition delay time of 0.16 milliseconds with cold fuel. Uniform distribution of injected propellants and a combustion chamber Mach number of 0.06 provide a uniform static pressure gradient in the combustion chamber. These criteria were used in the design of the 50K and 250K preburners to provide stable combustion with 55°R fuel temperature in the 50K and 95°R fuel temperature in the 250K preburner. Figure IX-3 is an empirical correlation from P&WA testing with cold fuel which relates injection momentum ratio, fuel temperature and combustion chamber velocity to combustion stability limits. The operating range of the SSME preburner design is shown to be well within the stable region of the correlation.

The use of a porous woven wire matrix material in the design of the combustion chamber liners provides these liners with high acoustic damping characteristics. This results in a substantial stability margin, as shown in figure IX-4. Absorption of 70% of dynamic pressure oscillations for all preburner acoustic modes is provided with no significant cost, weight or performance penalty since liners are a design requirement to reduce the thermal gradients in the cooled structural chamber wall for good LCF life.

To assure low frequency combustion stability, the preburner propellant supply system design is correlated with the combustion process. By use of an analog computer simulation, the propellant feed lines and injection manifolds

are designed to prevent coupling of the combustion process with the propellant supply system to avoid the resultant low frequency combustion instability.

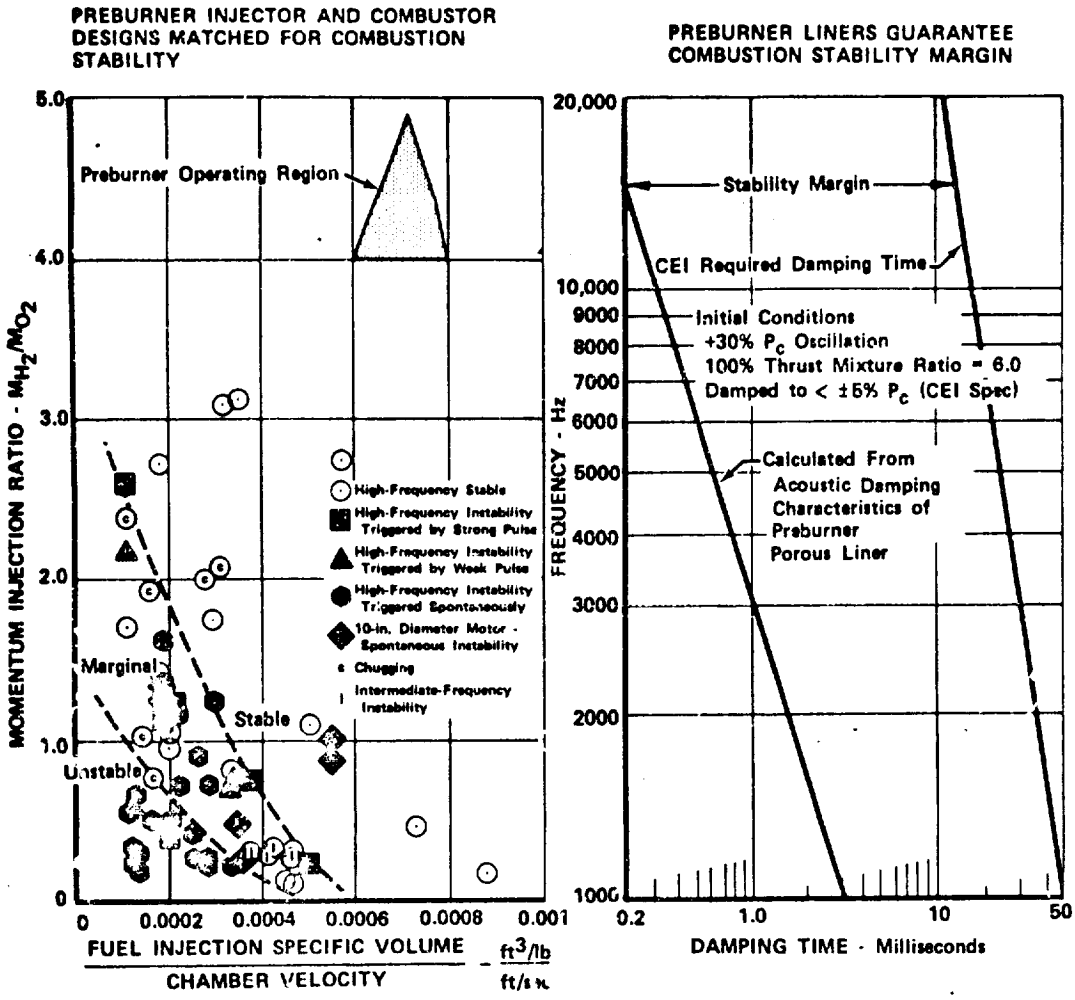

Figure IX-3. Preburner Injector Combustion Stability Data FD50319

A complete description of the SSME preburner combustion system design and stability analysis is given in PWA FR-4471, Combustion Stability Analysis and Aids.

COMBUSTION STABILITY OF MAIN COMBUSTOR ASSURED WITHOUT WEIGHT OR PERFORMANCE COMPROMISE

An extremely short ignition delay time and a rapid burning rate assure the main combustor design both combustion stability and high preformance. The short ignition delay times require a very high chamber frequency to couple with it. Since the combustion process is not sensitive to high frequencies there is no energy feedback mechanism and combustion instability cannot occur. In addition, the porous transpiration cooled main chamber liner provides significant stability margin without compromise to cooling effectiveness, weight or performance.

The combination of hot fuel injection and oxidizer atomization to 25 micron droplets results in an ignition delay of 0.09 milliseconds and a propellant reaction time of 0.45 milliseconds. This results in a required coupling frequency of approximately 10,000 Hz. High frequency combustion stability is assured because the combustion process cannot couple with the proper chamber frequency. High combustion performance is also realized due to the rapid combustion rate which allows maximum utilization of the combustion chamber volume. Additional high frequency stability is provided by the uniform propellant distribution resulting from the use of radial spraybars and the large number of classed oxidizer injection elements.

The combination of high oxidizer injection pressure drop, hot fuel injection and finely atomized oxidizer also provide low frequency combustion stability. The high oxidizer pressure drop combined with the high fuel pressure drop across the turbines serves to isolate the main chamber from the preburner and prevent coupling of pressure oscillations between the preburner and main chambers.

Since the main chamber liner is porous, it acts as a stability aid by providing 68% absorption of dynamic pressure oscillations over the range of main chamber acoustic frequencies. This significant amount of stability damping margin is gained without any loss of liner cooling effectiveness or compromise to weight or performance.

The specifics of the SSME main chamber combustion system stability analysis are included in PWA FR-4471, Combustion Stability Analysis and Aids.